

Antimicrobial Activity of Synthetic Analogues of Human β-Defensins

By

Hanieh Ijakipour

A thesis submitted to
the University of Birmingham
for the degree of
DOCTOR OF PHILOSOPHY

School of Metallurgy and Materials
College of Engineering and Physical Sciences
University of Birmingham
March 2023

UNIVERSITY OF
BIRMINGHAM

University of Birmingham Research Archive

e-theses repository

This unpublished thesis/dissertation is copyright of the author and/or third parties. The intellectual property rights of the author or third parties in respect of this work are as defined by The Copyright Designs and Patents Act 1988 or as modified by any successor legislation.

Any use made of information contained in this thesis/dissertation must be in accordance with that legislation and must be properly acknowledged. Further distribution or reproduction in any format is prohibited without the permission of the copyright holder.

© Copyright by HANIEH IJAKIPOUR, 2021

All Rights Reserved Word count: 25000

ABSTRACT

The emergence of antibiotic resistant bacteria calls for the advancement in a new class of drug and drug discovery. Antimicrobial peptides (AMPs) have been shown to have a broad spectrum of activity against pathogens such as bacterial, viral, and fungal infections. Although this class of molecules shows a broad spectrum activity, they often show poor bioavailability and stability *in vivo*. The key to resolve such complex problems is to either design an antimicrobial peptide that does not show degradation pattern or by performing post-synthesis modifications such as cyclisation or N-terminal acetylation or to design a peptide that when degraded retains its antimicrobial activity.

To design an effective antimicrobial peptide with a broad spectrum activity against Gram-positive and Gram-negative bacteria, Human Beta Defensin 1 (hBD1) and Human Beta Defensin 3 (hBD3) were chosen as reference sequences. These peptides were chosen due to the lack of research done on Beta defensins and their broad spectrum of activity against a variety of pathogens. The rational behind the design of peptides was to remove the Cysteine residues in the original sequence of the defensins to ease the synthesis process, the sequences were then shortened by removal of uncommon amino acids in the sequence of antimicrobial peptides found in ACP database. The sequences were then modified to show a minimum similarity of 40% to the original antimicrobial sequence.

To assess the activity of these peptides they were tested against different bacteria and the results determined that HBD-mod8 based on hBD1 showed comparable

antimicrobial activity to the positive control (antibiotic) against different bacterial species. To asses the stability and cytotoxicity of this peptide, it was tested against human serum and human Hela cells. To find the motif responsible for the activity of this peptide an alanine scan was set-up determining the motifs that were crucial for the activity of this peptide. Results showed the degradation of the peptide into a smaller fragment was the key in the antimicrobial activity and it showed a non toxic effect towards the human cells.

DEDICATION

I would like to dedicate this thesis to my loving father and mother. Without their undying support I would not have been able to do anything close to what I have been able to achieve.

ACKNOWLEDGMENTS

My PhD journey has been a hard one but I am thankful for having gone through it and I have many people to thank for helping me get through this difficult journey.

First and foremost I would like to thank my father, if it was not for him I would not have been able to be where I am and I am forever in indebted to him. Secondly, I would like to thank my two supervisors Prof Artemis Stamboulis for accepting me as a PhD student and providing me with the opportunity to do one and Dr Sarah A Kuehne, who helped me navigate my PhD the best she could and if it was not for her I do not know what would have come of my PhD.

Thirdly I would like to thank my partner Arash Azizilord who stood by me through all the hard times and held my hand as I passed through to the other side. Having him at times was the only thing keeping me grounded. It is also time to give A special thanks to my sisters Parinaz, Parimah and Pirayeh for always being there for me when I needed them.

I would also like to give thanks to my colleagues at the university for making this PhD possible. I would like to give a special thanks to Dr Richard Sheridan that extended the support that I needed to continue in my journey. I would like to thank Dr Christopher Williams at the Department of Chemistry for all his knowledge and help on the mass spectrometry instruments. He was a joy to work with and I was able to learn many important lessons from him. I am thankful to Alexander Antropenko for all his help with purification of all the peptides and Ben Hewitt for all his help in the cell culture labs and all the people who helped me in the School of Dentistry and accepted me with open arms. I would also like to thank Dr Maryam Esmaeili for

helping me in Robert Atkins building and allowing me to use her biological hoods.

I would like to thank Marc Bruggeman, Christos Softas and Iman Jassim for helping me navigate through this journey and see it to the finish line.

When life gets you down

JUST KEEP SWIMMING

Dory, "Finding Nemo"

Contents

Page

1 Introduction and Literature Review **1**

1.1 Antibiotic Resistance 2

1.2 Antimicrobial Peptides - AMPs 3

1.3 A brief history of Antimicrobial Peptides 4

1.3.1 Cationic Antimicrobial Peptides - CAPs 6

1.4 Defensins 8

1.4.1 Alpha Defensins - α-Defensins 9

1.4.2 Beta Defensins - β-Defensins 11

1.4.3 Theta Defensins - θ-Defensins 13

1.5 Mechanisms of Antimicrobial Peptides 14

1.5.1 Membranolytic Mechanisms 14

1.5.2 Non-Membranolytic Mechanisms 16

1.6 Activity of Antimicrobial Peptide 18

1.6.1 Bacterial, Viral and Fungal Activity 20

1.6.2 Anticancer activity 23

1.7 Limitations of Antimicrobial Peptides 24

1.8 Antimicrobial Peptide Design 25

1.8.1 Antimicrobial Peptide Databases 27

1.9 Application of Antimicrobial Peptides 28

1.10 Introduction to the hypothesis 30

1.10.1 Aims and Objectives 31

2 Materials and Methods **32**

2.1 Materials 33

2.1.1 Peptide synthesis 33

2.1.2 Peptide Characterisation 33

2.1.3 Antimicrobial Studies 34

2.1.4 Cell Culture Studies 34

2.2 Peptide Synthesis 35

2.3 Peptide Characterisation 40

2.3.1 Liquid Chromatography-Mass spectrometry(LC-MS) 41

2.3.2 Preparative HPLC 43

2.3.3 Matrix-Assisted Laser Desorption/Ionization-MALDI-TOF . . . 44

2.3.4 Circular Dichroism-CD 45

2.3.5 Peptide Stability 47

2.4 Antimicrobial Studies 47

2.4.1 Minimum Inhibitory Concentration-MIC 48

2.4.2 Antimicrobial Resistance studies 50

2.5 Cell Culture Studies 50

2.5.1 Cell Viability 50

2.6 Molecular Dynamic Simulations 51

2.7 Statistical analysis 52

2.7.1 Prediction models 52

2.7.2 Antimicrobial analysis 53

3 Antimicrobial Peptide Design **54**

3.1 Design Strategy 55

3.1.1 Sequences of potential antimicrobial peptides based on hBD1 . . 56

3.1.2 Structure of potential antimicrobial peptides based on hBD1 . . 58

3.1.3 Sequences of potential antimicrobial peptides based on hBD3 . . 64

3.1.4 Structure of potential antimicrobial peptides based on hBD3 . . 66

4 Characterisation **71**

4.1 Peptide Purification 72

4.1.1 Introduction 72

4.1.2 Results 72

5 Secondary Structure **89**

5.0.1 Introduction 90

5.1 Peptides based on hBD1 90

5.1.1 Results 90

5.1.2 Discussion 93

5.2 Peptides based on hBD3 97

5.2.1 Results 97

5.2.2 Discussion 102

5.3 Alanine substitution of peptide HBD-mod8 and the impact on structural conformation 103

5.3.1 Introduction 103

5.3.2 Results 103

5.3.3 Discussion 104

5.4 Molecular dynamic simulation of HBD-mod8 in POPC and DMPG/DMPC 108

5.4.1 Introduction 108

5.4.2 Results 108

5.4.3 Discussion 109

6 Biological characterisation **113**

6.1 Microbiology 114

6.1.1 Bacterial viability for hBD1 analogous 114

6.1.2 Bacterial viability for hBD3 analogous 122

6.1.3 The effect of alanine substitution on the activity of HBD-mod8 against Gram-positive and Gram-negative bacteria 128

6.1.4 Development of bacterial resistance against HBD-mod8 138
6.2 The effect of HBD-mod8 and its alanine substitutes on the viability of HeLa cells. 142

7 Human Serum Analysis **146**
7.1 Serum Analysis 147
7.1.1 Introduction 147
7.1.2 Results 147
7.1.3 Discussion 160

8 Discussion **163**

9 Conclusions and future works **171**

References **175**

A Characterisation **203**

B Structure **225**

C Biological Characterisation **252**

List of Figures

1.1 Differences between the connectivity of disulfide bridges in α-, β- and θ-defensins where, the superscript of Cysteine residues shows the relative proximity of the Cysteine residue from N-terminus. 8

1.2 Structure of Human α-defensin 1 produced by VMD software from data extracted from PBD database. 10

1.3 Sequence alignment result of all six α-defensins where the blue indicates positively charged residues and the red indicates anionic residues [52]. . 11

1.4 Sequence alignment result of β-defensins 1-4 only where the blue indicates positively charged residues and the red indicates anionic residues [52]. 13

1.5 Membrane dependent mechanisms of activity exerted by different antimicrobial peptides. 15

1.6 Non membrane dependant antimicrobial activity through signalling the adaptive immune system through inflammation and infection. AMPs have chemotaxis ability to towards iDC, monocytes/Pre-DCs, PMNs, modulation of lymphocyte activity and/or proliferation, alteration of the local cytokine environment, direct iDC activation via TLR4, or generation of primed iDC with enhanced antigen uptake and presentation capacity [90]. Dots represent antimicrobial peptides 17

1.7 Comparison of Gram-negative, Gram-positive and eukaryotic membrane bilayer. 19

1.8 Venn diagram representing the numbers of overlapping and non-overlapping sequences between different databases. 28
1.9 Structure of hBD1 on the left and hBD3 on the right hand side. Both structures share a pattern of double β-sheet and an α-helix at the N-terminus. 30

2.1 Removal of Fmoc from the N-termini of amino acid using a strong base. [167] 36
2.2 Coupling of the first amino acid to the rink amide resin using DIC and Oxyma pure [170]–[172]as activator and base respectively 38
2.3 Cleavage procedure from the solid support [174] 40
2.4 Peptide purity levels and their applications[176] 41
2.5 Illustration that shows the formation of elliptical shape as opposed to a direct circle changing the way the light is calculated 46
2.6 Plate streaking using different bacteria with a sterile loop. 48
2.7 Arrangement used for the 96 well plate to avoid cross contamination and determine the OD at 600nm. 49
2.8 Molecular dynamic simulation steps performed using Gromacs. 52

3.1 Percentage of 20 natural amino acids in antimicrobial peptide based on their abundance in 3579 peptides found in ADP3 databases [197] 56
3.2 Phylogenic tree of the hBD1 peptide series showing their parentage similarity and their relationship. Figure produced through Clustal Omega [201] showing the relationship between each sequence in the series of peptides based on hBD1 where the percentages shown are representative of the peptide alignment to the original hBD1 sequence and to each other respectively found through alignment using the ADP database. . 58

3.3 Multiple sequence alignment results for the peptides based on hBD1. The sequence at the top of the first point of comparison. Figure produced using Mview Clustal Omega [201] showing the consensus sequence between each peptide and the original sequence. Red residues are positively charged, Green residues are hydrophobic, Blue residues are negatively charge, Yellow residues are cysteines. Cov = coverage referring to the aligned positions in a sequence that contain actual residues representing the percentage of aligned amino acid sequence, Pid = Percent measuring the similarity between aligned residues in the sequences. It is calculated through determination of the percentage of positions in the alignment where the amino acids are identical across all sequences. . . . 59

3.4 Showing the secondary structure of peptides based on hBD1 as well as their amino acid frequency represented in a logo format, where the height of the symbol represents relative frequency of each residue, the overall height of the stack represents at each position reflects the level of conservation and the width of the symbol shows the degree of uncertainty at that position. The peptides are represented through a Newribbon for the structure represented by magenta for alpha helical, blue for turns and white for other types of structures. Residues are coloured by their type in both logos and their structure where non-polar residues are in (white/black), basic residues, acidic residues and polar residues. These figures were produced using Seq2Log [202] which calculates the frequency of each amino acid at each position using a frequency matrix showing the distribution of each residues at each position and I-TASSER [203] constructs a three-dimentional model of the peptide through fragment assembly and ab initio modelling to generate three dimensional models. The models were visualised using VMD [204]. 63

3.5 Phylogenic tree of the hBD3 peptide series showing their percentage similarity and their relationship. Figure produced using Clustal Omega [201] showing the relationship between each sequence in the series of peptides based on hBD3 where the percentages shown are representative of the peptide alignment to the original hBD3 sequence and to each other respectively found through alignment using the ADP database. 65

3.6 Multiple sequence alignment results for the peptides based on hBD3. The sequence at the top marks the first point of comparison. Figure produced through Mview Clustal Omega [201] showing the consensus sequence between each peptide and the original sequence. Red residues are positively charged, Green residues are hydrophobic, Blue residues are negatively charge, Yellow residues are cysteines. Cov = coverage referring to the aligned positions in a sequence that contain actual residues representing the percentage of aligned amino acid sequence, Pid = Percent measuring the similarity between aligned residues in the sequences. It is calculated through determination of the percentage of positions in the alignment where the amino acids are identical across all sequences. 66

3.7 Showing the secondary structure of peptides based on hBD3 as well as their amino acid frequency represented in a logo format, where the height of the symbol represents relative frequency of each residue, the overall height of the stack represents at each position reflects the level of conservation and the width of the symbol shows the degree of uncertainty at that position. The peptides are represented through a Newribbon for the structure represented by magenta for alpha helical, blue for turns and white for other types of structures. Residues are coloured by their type in both logos and their structure where non-polar residues are in (white/black), basic residues, acidic residues and polar residues. These figures were produced using Seq2Log [202] which calculates the frequency of each amino acid at each position using a frequency matrix showing the distribution of each residues at each position and I-TASSER [203] constructs a three-dimentional model of the peptide through fragment assembly and ab initio modelling to generate three dimensional models. The models were visualised using VMD [204]. 70

4.1 Comparison between the purity of the peptides based on hBD1 before and after purification step on LC-MS showing HBD-mod1, HBD-mod2, HBD-mod3, HBD-mod4, HBD-mod5, HBD-mod6, HBD-mod7, HBD-mod8. 77

4.2 Comparison between the purity of the peptides based on hBD3 before and after purification step on LC-MS showing the peptides HBD3-mod1, HBD3-mod2, HBD3-mod4, HBD3-mod5, HBD3-mod6, HBD3-mod7. . . 81

4.3 Comparison between the purity of the peptides based the alanine scanning of HBD-mod8 peptides before and after purification step on LC-MS. 88

5.1 Summarised version of the secondary structure of peptides based on hBD1 including HBD-mod1, HBD-mod2, HBD-mod3, HBD-mod4, HBD-mod5, HBD-mod6, HBD-mod7 and HBD-mod8 in PBS and SDS. The summarised version shows only the percentage of helix, strand and unordered in the structure of each peptide where helix is a combination of helix1 and 2, strand is a combination of strand 1 and 2 and unordered is a combination of turn and unordered. All the datapoints displayed in Figure B.2 represents a culmination of 3 measurements taken from the same peptide in each condition. The measured values are θ which is the machine unit used by the CD instrument. The percentage of unordered secondary structure is highly prevalent in all peptides in PBS but this percentage is reduced in SDS for HBD-mod1, HBD-mod2 , HBD-mod7 and HBD-mod8, where the percentage of helix has increased considerably in these peptides by approximately, 1.5-, 3-, 6- and 1.5-folds respectively. 92

5.2 Expanded version of the secondary structure percentages of peptides based on hBD1 that shows the helix 1, helix 2, strand 1, strand 2, turn and unordered portion of each peptide in two different condition on PBS and SDS shown side by side for better comparison. The highest percentage of secondary structure in most peptides in this series can mostly be attributed to turn and unordered in PBS with the exception of HBD-mod8 where the percentage of helix and unordered were similar before the addition of SDS. These figures were produced by the measurement of polarised light that has a specific finger print that can be attributed to different structure types. The analysis was performed through Dichroweb. 96

5.3 Summarised version of the secondary structure of peptides based on hBD3 including HBD3-mod1, HBD3-mod2, HBD3-mod3, HBD3-mod4, HBD3-mod5, HBD3-mod6, HBD3-mod7 and in PBS and SDS. The summarised version shows only the percentage of helix, strand and unordered in the structure of each peptide where helix is a combination of helix1 and 2, strand is a combination of strand 1 and 2 and unordered is a combination of turn and unordered. All the data points displayed in Figure B.3 represents a culmination of 3 measurements taken from the same peptide in each condition. The measured values are θ which is the machine unit used by the CD instrument. The percentage of unordered secondary structure is highly prevalent in all peptides in both PBS and SDS and that the buffer that the peptide resides in does not effect its structure drastically. 98

5.4 Expanded version of the secondary structure percentages of peptides based on hBD3 that shows the helix 1, helix 2, strand 1, strand 2, turn and unordered portion of each peptide in two different condition on PBS and SDS shown side by side for better comparison. There is no clear pattern between different peptides and their corresponding structures but the turn and unordered structures seem to be the most prominent in comparison to the rest of the structures. Although the percentage of unordered structure spikes in SDS. 102

5.5 Secondary structure of HBD-mod8 alongside its alanine substitutes expressed in the percentage of helix, strand and unordered that were calculated by combining helix 1 and 2, strand 1 and 2 and turn and unordered respectively. These peptides were all tested in 5 different conditions in PBS, SDS, DPC, LPS and LTA. Showing a clear change in the strctureu from PBS to SDS and with LPS and LTA showing very similar results just as with SDS and DPC. 107

5.6 Molecular dynamic simulation showing the difference in the conformation of HBD-mod8 in 1-palmitoyl-2-oleoyl-sn-glycero-3-phosphocholine (POPC). Produced using a combination of Charmm-gui membrane builder and Gromacs through 10ns of equilibration. The NVT mass distribution was also calculated through Gromacs NVT which shows the distribution of the peptide within the bilayer through mass density consideration and constant temperature and pressure. The molecules in Water, Lipid tail and the peptide is shown in the black circle to the side of (a). 110

5.7 Molecular dynamic simulation showing the difference in the conformation of HBD-mod8 in Dimyristoylphosphatidylglycerol/Dimyristoylphosphatidylcholine (DMPG/DMPC). Produced using a combination of Charmm-gui membrane builder and Gromacs through 10ns of equilibration. The NVT mass distribution was also calculated through Gromacs NVT which shows the distribution of the peptide within the bilayer through mass density consideration and constant temperature and pressure. The molecules in Water, Lipid tail and the peptide is shown in the black circle to the side of (a). 112

6.1 The effect of peptides as well as their differing concentrations on *S. aureus* survival with its corresponding antibiotics (Vancomycin) as control. (a)-(f) shows the 2-fold dilutions of peptides based on hBD1. The overall mean percentage of bacterial growth values for each peptide was used to calculate the p-values are 68(±25), 86, 96, 15, 85, 105, 122, 82 and 76 for antibiotic and HBD-mod1 to HBD-mod8, respectively. The p-value between HBD-mod1, HBD-mod2, HBD-mod3, HBD-mod4, HBD-mod5, HBD-mod6, HBD-mod7, HBD-mod8 and the control is 0.008, 0.000, 0.017, 0.000, 0.000, 0.000, 0.13* and 0.97* respectively. * shows favourable non significant difference 117

6.2 The mean values for each peptide used to calculate are 68(±9), 105, 103, 95, 97, 100, 103, 102 and 69 for Antibiotic and HBD-mod1 until HBD-mod8, respectively. The p-value between HBD-mod1, HBD-mod2, HBD-mod3, HBD-mod4, HBD-mod5, HBD-mod6, HBD-mod7 and the control was 1.0×10^{-13} and between HBD-mod8 and the control was 1.0*. At $500\mu M$, HBD-mo8 with p-value 7.5×10^{-5} ** and it shows a better activity than antibiotic it also shows similar activity to the antibiotic with p-value of 1.0* at concentration of $250\mu M$. * shows favourable non significant difference / ** shows favourable significant difference 119

6.3 The effect of peptides based on hBD3 as well as their differing concentrations on *S. aureus* survival with its corresponding antibiotics (Vancomycin). The overall mean percentage of bacterial growth values for each peptide used to calculate the p-values are 41(±9), 30, 76, 75, 74, 79, 97 and 87 for Antibiotic and HBD3-mod1 until HBD3-mod7, respectively. The p-value between HBD3-mod1 and the control was 0.06*, between HBD3-mod2, HBD3-mod3, HBD3-mod4, HBD3-mod5, HBD3-mod6, HBD3-mod7 and the control was, 1.2×10^{-13}. HBD3-mod1 no significant difference with p-value of 0.9* at $31\mu M$ * shows favourable no significant difference 124

6.4 The effect of peptides as well as their concentrations on *P. aeruginosa* survival with its corresponding antibiotics (Polymixin B) as control showing the 2-fold dilutions of peptides based on hBD3. The mean values for each peptide used to calculate the p-value are 24($\pm$5), 37, 62, 129, 127, 79, -106, 88 for Antibiotic and HBD3-mod1 until HBD3-mod7, respectively. The p-value between HBD3-mod1 and the control is 0.02 and 1.2×10^{-13} between HBD3-mod2, HBD3-mod3, HBD3-mod4, HBD3-mod5, HBD3-mod6, HBD3-mod7 and the control. All values show a significant difference between their activity against *P. aeruginosa* and the peptides meaning none of the peptides show an overall activity similar to the antibiotic tested with HBD3-mod1* and HBD3-mod2* showing favourable significance Although the antibiotic is included in every graph it was only tested at its critical MIC found in the literature and was not tested at different concentration. * shows favourable no significant difference 126

6.5 The effect of alanine substitution on antimicrobial activity of HBD-mod8 against *S. aureus*. According to the statistical analysis HBD-mod8, shows significant difference when compared to the activity of vancomycin with a p-value of 0.002. Similarly, 3HBD-mod8, 13HBD-mod8, 14HBD-mod and 15HBD-mod8 also show a significant difference when compared to the activity of vancomycin with the p-values of 5.2×10^{-5}, 0.001, 3.9×10^{-5} and 6.8×10^{-5}. On the other hand 10HBD-mod8 and 11HBD-mod8 show an activity comparable to that of the antibiotic with mean value of 49($\pm$14) and p-values of 1 and 0.9 respectively. 130

6.6 The activity of alanine substitution on the activity of HBD-mod8 against *P. aeruginosa*. According to the statistical analysis HBD-mod8, shows no significant difference with the activity of the antibiotic as previously shown with a p-value of 1 against *P. aeruginosa*. 1HBD-mod8 also shows comparable activity to that of Polymixin B with the p-value of 0.2. On the other hand 4HBD-mod8 shows a better activity than the antibiotic with a p-value of 0.005 and the mean value of 9% which is also larger than the mean value of the antibiotic at 33(±8)%. The other peptides all show a significantly different activity when compared to the activity of the antibiotic with mean values smaller than the mean value of the antibiotic. 132

6.7 The activity of alanine substitution on the activity of HBD-mod8 against *E. coli*. According to the statistical analysis the majority of the peptides show no significant difference when compared to the activity of the antibiotic at 14(±6)%. 1-2HBD-mod8, 6-9HBD-mod8, 12-13HBD-mod8 and 15HBD-mod8 all show a significant difference when compared to the activity of the antibiotic ciprofloxacin with mean values below that of the antibiotics. 134

6.8 The heatmap of the effectiveness of each peptide based on their p-value as well as the mean percentage of bacterial growth Each colour is representative of the effectiveness of the peptide against each bacteria. The colour Green is indicative of an effective peptide with either a larger mean value in comparison to HBD-mod8 or a mean value similar to that of the HBD-mod8. Colour Yellow is indicative of significant different values that could be caused by a larger mean value which called favourable significant different or lower mean value called unfavourable significant difference. Colour Red is indicative of unfavourable significant difference. The two heatmaps should be considered together for the result interpretation. 137

6.9 Resistance cycles of HBD-mod8 against *S. aureus*. The cycles were repeated until a percentage of bacterial growth had reached 90% is reached. It can be seen that *S. aureus* continues its growth pattern for 15 cycles against HBD-mod8 before becoming full resistance. 139

6.10 Resistance cycles of HBD-mod8 against *P. aeruginosa*. The cycles were repeated until a percentage of bacterial growth had reached 90% is reached. It can be seen that *P. aeruginosa* continues its growth pattern for 16 cycles against HBD-mod8 before becoming full resistance. . 140

6.11 Resistance cycles of HBD-mod8 against *E. coli*. The cycles were repeated until a percentage of bacterial growth had reached 90% is reached. It can be seen that *E. coli* continues its growth pattern for 19 cycles against HBD-mod8 before becoming full resistance. 141

6.12 The effect of HBD-mod8 and its alanine substitutes on HeLa cells. This figure was produced using three repeats of each peptide in three different wells on three different plates and the combination of the results produced the standard deviation lines shown in black after 24 hour incubation of cells with the peptides and the results were shown for MTT assay after 4 hour incubation. The data was normalised to show a 100% cell viability as the maximum amount so other values were reduced. . . 144

7.1 LC-MS data showing the degradation of the peptides with alanine substitutions based on HBD-mod8 in the most prominent peak found through chromatography. Using this methodology the most active motif of the peptide after degradation can be found through combination of this results and microbiology analysis of the activity of each peptide. These figures were produced using the MassLynx, and the peaks were identified manually. 159

8.1 Correlation between the log activity of the peptides based on beta defensins and the percentage of helix 1. It shows an upward trend where with the increase of helix 1 content of the peptide structure, the activity of the peptide also increases. The line of best fit is also shown to have a negative intercept in both instances. It can be seen that the percentage of helix 1 content of peptides based on hBD3 is much lower than hBD1. 166

8.2 Heatmap of culmination of the data showing the importance of a large structural change in the overall cytotoxicity of the peptides. 168

A.1 Amino acids key. (Web: https://www.compoundchem.com/2014/09/16/aminoacids).204

A.2 The blank run for the peptides based on hBD1 and hBD3 on LC-MS. . 205

A.3 The blank run for the alanine scan of the peptides based on HBD-mod8 on LC-MS. 205

A.4 Serum control 205

A.5 LC-MS chromatograms of HBD-mod8 and its alanine substituted peptides showing differences between the peptide in serum and peptide in water. it can be seen that some peptides in these series do not show a difference in peak compared to the control but it is clear that for most of these chromatograms the peptide in question is degraded and the spectrum data shown in section7.1 is indicative of these discrepancies. . 213

A.6 MALDI-TOF data for the fragmentation of HBD-mod8 and its corresponding alanine substitutions. 224

B.1 Showing the varying absorbance patterns in CD qualitatively. This has been used by Dicroweb to produce the percentage results that is presented in section 5 226

B.2 Showing the secondary structure of peptides based on hBD1 produced from CD in PBS and SDS representing an anionic environments to show the helical conformational change. All graphs were produced from the instrument software by reading the absorbance of the peptide and they are shown in the y-axis and wavelength shown in x-axis. 229

B.3 Showing the secondary structure of peptides based on hBD3 produced from CD in PBS and SDS representing an anionic environments to show the helical conformational change. All graphs were produced from the instrument software by reading the absorbance of the peptide and they are shown in the y-axis and wavelength shown in x-axis. 231

B.4 Showing the secondary structure of peptides based on alanine scan of HBD-mod8 (HBD-mod8-4HBD-mod8) produced from CD in PBS, SDS, LPS, LTA and DPC representing an anionic environments and mimicking bacterial membrane for Gram-negative and -positive bacteria respectively to show the helical conformational change. All graphs were produced from the instrument software by reading the absorbance of the peptide and they are shown in the y-axis and wavelength shown in x-axis.236

B.5 Showing the secondary structure of peptides based on alanine scan of HBD-mod8 (5HBD-mod8-9HBD-mod8) produced from CD in PBS, SDS, LPS, LTA and DPC representing an anionic environments and mimicking bacterial membrane for Gram-negative and -positive bacteria respectively to show the helical conformational change. All graphs were produced from the instrument software by reading the absorbance of the peptide and they are shown in the y-axis and wavelength shown in x-axis. 241

B.6 Showing the secondary structure of peptides based on alanine scan of HBD-mod8 (10HBD-mod8-14HBD-mod8) produced from CD in PBS, SDS, LPS, LTA and DPC representing an anionic environments and mimicking bacterial membrane for Gram-negative and -positive bacteria respectively to show the helical conformational change. All graphs were produced from the instrument software by reading the absorbance of the peptide and they are shown in the y-axis and wavelength shown in x-axis. 246

B.7 Showing the secondary structure of peptides based on alanine scan of HBD-mod8 (15HBD-mod8-19HBD-mod8) produced from CD in PBS, SDS, LPS, LTA and DPC representing an anionic environments and mimicking bacterial membrane for Gram-negative and -positive bacteria respectively to show the helical conformational change. All graphs were produced from the instrument software by reading the absorbance of the peptide and they are shown in the y-axis and wavelength shown in x-axis. 251

C.1 The effect of peptides as well as their differing concentrations on *S. aureus* survival with its corresponding antibiotics (Vancomycin) as control. (a)-(f) shows the 2-fold dilutions of peptides based on hBD1. The overall mean %bacterial death values for each peptide was used to calculate the p-values are 32, 14, 4, 15, 11, -5, -22, 18 and 24 for antibiotic and HBD-mod1 to HBD-mod8, respectively. The p-value between HBD-mod1, HBD-mod2, HBD-mod3, HBD-mod4, HBD-mod5, HBD-mod6, HBD-mod7, HBD-mod8 and the control is 0.008, 0.000, 0.017, 0.000, 0.000, 0.000, 0.13* and 0.97* respectively. Figure (b): HBD-mod8 at concentration $250\mu M$ has better activity than the antibiotic with higher mean %bacterial death and p-value of 9.9×10^{-5}**. * shows favourable non significant difference / ** shows favourable significant difference . 253

C.2 The effect of peptides as well as their differing concentrations on *P. aeruginosa* survival with its corresponding antibiotics (Polymixin B) as control. (a)-(f) show the 2-fold dilutions of peptides based on hBD1. . . 254

C.2 The mean values for each peptide used to calculate are 33, -5, -3, 5, 3, 0, -3, -2 and 31 for Antibiotic and HBD-mod1 until HBD-mod8, respectively. The p-value between HBD-mod1, HBD-mod2, HBD-mod3, HBD-mod4, HBD-mod5, HBD-mod6, HBD-mod7 and the control is the same value of 1.0×10^{-13} and between HBD-mod8 and the control is the value 1.0*. Figure (a) shows that HBD-mo8 with p-value 7.5×10^{-5} ** shows a better activity than antibiotic and figure (b) shows HBD-mod8 has a similar activity to the antibiotic with p-value of 1.0*. * shows favourable non significant difference / ** shows favourable significant difference 255

C.3 The effect of peptides as well as their differing concentrations on *S. aureus* survival with its corresponding antibiotics (Vancomycin) as control. (a)-(f) show the 2-fold dilutions of peptides based on hBD3. The overall mean %bacterial death values for each peptide used to calculate the p-values are 59, 70, 24, 25, 26, 21, 3 and 16 for Antibiotic and HBD3-mod1 until HBD3-mod7, respectively. The p-value between HBD3-mod1 and the control was 0.06*, between HBD3-mod2, HBD3-mod3, HBD3-mod4, HBD3-mod5, HBD3-mod6, HBD3-mod7 and the control was, 1.2×10^{-13}. Figure (e) shows HBD3-mod1 no significant difference with p-value of 0.9* at $31\mu M$ * shows favourable no significant difference. 256

C.4 The effect of peptides as well as their concentrations on *P. aeruginosa* survival with its corresponding antibiotics (Polymixin B) as control. (a)-(f) shows the 2-fold dilutions of peptides based on hBD3. The mean values for each peptide used to calculate the p-value are 76, 63, 38, -29, -27, 21, -6, 12 for Antibiotic and HBD3-mod1 until HBD3-mod7, respectively. The p-value between HBD3-mod1 and the control is 0.02 and 1.2×10^{-13} between HBD3-mod2, HBD3-mod3, HBD3-mod4, HBD3-mod5, HBD3-mod6, HBD3-mod7 and the control. All values show a significant difference between their activity against *P. aeruginosa* and the peptides meaning none of the peptides show an overall activity similar to the antibiotic tested. Although the antibiotic is included in every graph it was only tested at its critical MIC found in the literature and was not tested at different concentration. 258

C.5 The effect of alanine substitution on the activity of HBD-mod8 against *S. aureus* at all concentrations. In this figure the effect of all different concentrations was shown on each substituted peptide and its projected activity on the bacteria. It can be seen that at lower concentrations most of the peptides in the series do not hold their activity. This is not the case with 13HBD-, 14HBD- and 15HBD-mod8 show higher level of activity in the lower concentrations when compared to the rest of the peptide in this series. 259

C.6 The effect of alanine substitution on the activity of HBD-mod8 against *P. aeruginosa* at all concentrations. In this figure the effect of all different concentrations was shown on each substituted peptide and its projected activity on the bacteria. According to this figure HBD-mod8 shows the best activity across the board and it stays active until the concentration of $63\mu M$. 10HBD-mod8 shows large standard deviation bars meaning each time this analysis was performed this peptide showed varying results. 260

C.7 The effect of alanine substitution on the activity of HBD-mod8 against *E. coli* at all concentrations. In this figure the effect of all different concentrations was shown on each substituted peptide and its projected activity on the bacteria. The activity of the peptide across the whole series of substitutions is shown to have minimal effect on the activity against *E. coli* where they are mostly equally as active as HBD-mod8. With the expiation of 6HBD-mod that only shows a comparable activity at the highest concentration. 261

C.8 The resistance pattern of *S. aureus* towards HBD-mod8 at all concentrations. In this figure the pattern of bacterial resistance was shown for all peptide concentrations. It is evident that this bacteria build resistance towards the peptide immediately after the first cycle however the peptide is still able to remove the bacteria to a certain extent. Until cycle 15 in which the peptide stops being active against the bacteria showing 0% bacterial death at all the concentrations. It was also observed that this peptide works best at its highest concentration. 262

C.9 The resistance pattern of *P. aeruginosa* towards HBD-mod8 at all concentrations. In this figure the pattern of bacterial resistance was shown for all peptide concentrations. The resistance build up is more uniform with this bacteria showing a more cohesive pattern with a downward trend as the number of cycles increase across all concentrations. 263

C.10 The resistance pattern of *E. coli* towards HBD-mod8 at all concentrations. In this figure the pattern of bacterial resistance was shown for all peptide concentrations. Even with the activity of this peptide against *E. coli* being notable the resistance cycles were not so clear in the trends they display. With the highest concentrations showing very little change in activity level as the resistance build up. The lower concentrations for this peptide show very poor activity against the resistance. 264

C.11 Bar Chart displaying untouched cell viability data. 265

List of Tables

1.1 Antimicrobial peptide classification. 4

2.1 Gradient conditions as a percentage of organic and inorganic solvents used with two different LC systems coupled with Mass spectrometry . . 43

2.2 Gradient conditions as a percentage of organic and inorganic solvents scaled for the larger column on the Prep-HPLC system 44

2.3 Antibiotic final concentration used as a positive control. 48

3.1 List of potential antimicrobial peptides based on hBD1 with their corresponding molecular weight (MW), number of amino acid residues (AA number) and charge. 57

3.2 List of potential antimicrobial peptides based on hBD3 with their corresponding molecular weight (MW), number of amino acid residues (AA number) and charge. 64

7.1 Alanine(Ala, A) substitution of HBD-mod8 shown alongside the molecular weight of the sequences. A key for amino acid figure A.1 one letter word and their structure can be found in appendix A 148

7.2 Fragmentation pattern of alanine substituted HBD-mod8 peptides against human serum. 160

Abbreviations

ACN	Acetonitrile.
ADP	Antimicrobial Peptide Database.
AdV	Human Adenovirus.
AMPs	Antimicrobial Peptides.
AMR	Antimicrobial Resistance.
C.F.U	Colonie Forming Units.
CAMP	Collection of Anti-Microbial Peptide.
CAPs	Cationic Antimicrobial Peptides.
CCL	Chemokine ligand.
CCR	Chemokine receptor.
CD	Circular Dichroism.
DBAASP	Database of Antimicrobial Activity and Structure of Peptides.
DCM	Dichloromethane.
DCs	Dendritic cells.
DEFA	Defensin A gene.
DEFB	Defensin B gene.
DEFT	Defensin T gene.

DIC	N-Ethyldiisopropylamine.
DIEA	N,N-Diisopropylethylamine.
DMEM	Dulbecco's Modified Eagle Medium.
DMF	N,N-Dimethylformamide.
DMPC	Dimyristoylphosphatidylcholine.
DMPG	Dimyristoylphosphatidylglycerol.
DMSO	Dimethyl sulfoxide.
DPC	Dodecylphosphocholine.
DRAMP	Data repository of antimicrobial peptides.
E. coli	Escherichia coli.
ERK	Extra-cellular–regulated Kinase.
ESI	Electro spray.
FA	Formic acid.
FBS	Fetal Bovin Serum.
Fmoc	Fluorenylmethoxycarbonyl.
gp120	Envelope glycoprotein 120.
hBD	Human β Defensin.
HIV-1	Human Immunodeficiency Virus 1.
HMMS	Hidden Markov Models.
hNP	Human Neutrophil or Human α Defensin.
HPLC	High Pressure Liquid Chromatography.
HPV	Human Papillomavirus.
iDC	Immature Dendritic Cells.

IgA	Immunoglobulin A.
IgG	Immunoglobulin G.
IL-1β	Interleukin-1β.
IL-8	Interleukin-8.
LC-MS	Liquid chromatography–mass spectrometry.
LCPs	Lysosomal Cationic Proteins.
LF	Lethal Factor.
LPS	Lipopolysaccharide.
LTA	Lipoteichoic acid.
MALDI-TOF	Matrix-assisted laser desorption/ionization mass spectrometry.
MAPK	Mitogen-activated Protein Kinases.
MDS	Molecular Dynamic Simulation.
MHB	Muller Hinton Broth.
MIC	Minimum Inhibitory Concentration.
MRP	Multi-drug Resistance Associated Protein.
MW	Molecular weight.
NADPH	Reduced nicotinamide adenine dinucleotide phosphate.
OD	Optical Density.
P. aeruginosa	Pseudomonas aeruginosa.
PBS	Phosphate Buffered Saline.
PC	Phosphatidylcholine.

PDA	Photodiode-Array Detector.
PG	Phosphatidylglycerol.
PMBC	Peripheral Blood Mononuclear Cell.
PMNs	Polymorphonuclear Leukocytes.
POPC	1-palmitoyl-2-oleoyl-sn-glycero-3-phosphocholine.
Prep-HPLC	Preparative High Pressure Liquid Chromatography.
PS	Phosphatidylserine.
QSAR	Quantitative Structure-Activity Relationship.
ROS	Reactive Oxygen Species.
S. aureus	Staphylococcus aureus.
S. mutans	Streptococcus mutans.
SDS	Sodium Dodecyl Sulphate.
SPPS	Solid Phase Peptide Synthesis.
TAAs	Tumor-Associated Antigens.
TFA	Trifluoroacetic Acid.
TIPS	Triisopropylsilane.
TLR4	Toll-Like Receptor 4.
TNF-α	Tumour Necrosis Factor-α.
TSA	Tryptic Soy Agar.
UPLC	Ultra High Pressure Liquid Chromatography.

Chapter One

Introduction and Literature Review

1.1 Antibiotic Resistance

Infections and infectious diseases in England cost the NHS an estimated £30 billion per year, and it has been estimated that a decrease of 1% in hospital admissions for a common infection would save £2.8 million per year. Although the cost of widespread Antimicrobial Resistance (AMR) is difficult to estimate, the emergence of AMR over the past decade calls for an increase in the demand for new antimicrobial agents that bypass this resistance [1]. With the discovery of penicillin by Alexander Fleming in 1928, the antibiotic era began, and was the reason for saving countless lives and enabling the effective control of bacterial infections. This breakthrough allowed the major discovery of most antibiotic classes. This peak in antibiotic insurgence has plateaued since the 1960s with a lack of novel antibiotic discoveries and the lack of interest from pharmaceutical companies to invest in the production of new antibiotics [2]. The emergence of AMR has been attributed to the overuse and misuse of these drugs in medicine and in agriculture. Measures such as the reduction of prescribed antibiotics have been implemented to reduce the growth of AMR, however other agents are needed for multi-drug resistant strains of microorganisms [3]. With the exhaustion of current antibiotics and the end of an era of new and emerging antibiotic production, the importance of other antimicrobial agents is more evident. It has been widely speculated that the economic burden of AMR would be catastrophic without any action taken to combat this resistance [4]. There are 43 new antibiotics under clinical trial most of which, are in the first and second stage of approval, and two of which are on the way to approval as a new drug application in the year 2020 [5].

1.2 Antimicrobial Peptides - AMPs

With the relative ease in the production of peptides in recent years, they are widely used as biological systems to model biochemical, and biophysical interactions and to model protein folding and interactions [6]. Antimicrobial Peptides (AMPs) are a class of peptides that exert antimicrobial activity towards an array of different organisms. They are representative of the primary host defence system against pathogenic compounds that have been conserved throughout evolution. AMPs are not only the first line of defence in mammalians but also the first line of non-specific innate defence in most multicellular organisms [7]. With the abundance of multi-drug resistant strains of bacteria and the lack of new antibiotics to fight these strains, the research on AMPs has attracted special attention. These peptides are a multi-functional class of drugs involved in the primary defence against bacterial, viral, and fungal infections, [8] wound healing, [9] and cancer cell targeting [10]. AMPs exert their antimicrobial effects based on a primary electrostatic attraction to the cell membrane of the foreign pathogenic compound. However, they can also combat infection by signalling the immune system to clear and prevent the growth of microorganisms, showing a synergistic effect with the adaptive immune system [11]. This synergistic effect, complicates the study of the antimicrobial effect of novel peptide sequences as these compounds show their effect in many different modes of action.

The wide range of antimicrobial activity shown by AMPs can be attributed to the existence of 20 different natural amino acids that lead to the production of variable sequences. However, these molecules are limited in terms of their secondary structure, especially when in contact with a cell membrane [12] as AMPs often change their structure upon interaction with the cell membrane of a microorganism [13]. Since pathogenic compounds have devoted most of their genetic coding to expressing complex regulating countermeasures to antibiotics, it is vital to understand the role and the mechanism of action of AMPs to be able to enhance the design of these novel peptides and in-

crease the antimicrobial effect on pathogenic compounds whilst reducing cytotoxicity and stability, all while focusing on the mechanism of action of these compounds.

1.3 A brief history of Antimicrobial Peptides

Antimicrobial peptides are a diverse group of compounds that can be divided into three distinct categories based on their amino acid sequences. Table 1.1 shows the different type of AMPs with their subsequent examples.

Table 1.1: Antimicrobial peptide classification.

Types	Primary amino acids	Example
Anionic peptides	Rich in glutamic and aspartic acids	Dermicidin, MaximinH5
Linear cationic α-helical peptides	Linear rich in arginine and lysine	Cecropins (A), Magninin (2), LL-37 from humans
Cationic peptides	Rich in proline, glycine, histidine, tryptophan, arginine	Indolicidin, Hymenopraecin, Abaecin
Anionic and cationic peptides	Cysteine-rich with disulphide bonds	Human Neutrophil or Human α Defensin (hNP), Human β Defensin (hBD)
Anionic and cationic peptides	Fragments of larger proteins	Lactoferricin from Lactoferrin

The first antimicrobial peptide to be discovered was Gramicidin, a non-ribosomal peptide, isolated by René Dubos from soil bacteria *Bacillus brevis* in 1939. This AMP showed bacteriostatic and bactericidal activity by inactivating the glucose dehydrogenases followed by a secondary lytic ability resulting in cell death in Gram-positive bacteria [14]. This study also concluded that the effect of Gramicidin was likely due to cellular structure or function, since, it only showed activity towards Gram-positive bacteria. Gramicidin was also the first therapeutic antimicrobial agent used for its wound-healing capabilities and it was commercially manufactured as an antibiotic [15].

Lyzozyme was believed to be the first antimicrobial agent since its discovery in the 1920s [16]; however, it was later revealed that lysozyme exerts its antimicrobial activity enzymatically, therefore it is classed as a different antimicrobial agent to antimicrobial peptides, that, are active against pathogenic compounds through non-enzymatic mechanisms [17].

The next antimicrobial peptide, Purothionin, was discovered in 1972. It was extracted from the wheat endosperm. This peptide was found to be inhibitory to a range of pathogens, from most Gram-positive bacteria to a limited number of Gram-negative bacterial species with varying Minimum Inhibitory Concentration (MIC) values. This study showed structural differences between the α and β Purothionin, proving that the antimicrobial activity of AMPs is structurally dependent [18]. In 1962 Bombinin was extracted from orange speckled frog *Bombina variegate* [19] and in the 1960s lactoferrin was isolated from cow's milk [20], marking the discovery of the first animal-derived AMPs.

With the denouement of the golden age of antibiotics, focus was given to Lysosomal Cationic Proteins (LCPs) extracted from guinea pig Polymorphonuclear Leukocytes (Polymorphonuclear Leukocytes (PMNs)) granules, thought to be responsible for termination of bacteria by neutrophils, mostly through oxygen-independent mechanisms. PMNs are activated as a result of inflammatory agents such as bacterial Lipopolysaccharide (LPS), cytokines, and complement factors. This activation leads to the adherence of PMNs to the vessel wall before exiting the blood vessel in an attempt to eliminate pathogens in affected tissues [21]. LCPs are a 25 kDa protein bundle, later identified to be a combination of Cathepsin G, neutrophil elastase, proteinase-3 and azurocidin or heparin binding protein [22]. The activity of LCPs were shown to be distinct from the activity of lysosomal enzymes and they were the most active antimicrobial fraction of PMNs granules owing to the arginine-rich sequence [23]. This study also made a link between the antimicrobial activity of LCPs and an electrostatic attraction with the anionic membrane of pathogenic organisms [24].

Neutrophils exert their effects as effector cells in regulating B cell immune responses by phagocytose with the arginine-rich [25] and cysteine-rich [26] sequence and destroy the pathogenic species through a two step system; first they use the Reactive Oxygen Species (ROS) generated from phagocyte Reduced nicotinamide adenine

dinucleotide phosphate (NADPH) oxidase and second they release hydrolytic granule proteins. Although, the redux reaction necessary for destruction of pathogens only occurs if the complete enzyme has been assembled during activation [27]. Overall, PMNs show three modes of action; firstly, due to their iron-binding domain they are able to bind iron and deprive the pathogen of this important compound, secondly, their limited proteolysis manifest through their N- or C-termini antimicrobial peptides, thirdly, equipped with antimicrobial effect, they are able to induce microbial death as an isolated entity [28].

From 1970s to 1980s several leukocyte-derived antimicrobial peptides were isolated from rabbits and human PMNs called defensins [29], [30]. This discovery was made possible upon testing the antiviral capabilities of these peptides [31]. Defensins provide their antimicrobial effect through a membrane active pore forming model. These peptides provide a broad antimicrobial activity and are known for their three conserved disulphide bridges between cystine residues [32]. Another class of important antimicrobial peptides were also isolated from the C-terminal of bovine, rabbit and human PMNs identified for their homology to the protease inhibitor, Cathelin called Cathelicidin [33], [34]. Indolicidin was also extracted from bovine PMNs but unlike cathelicidin, it does not require cleavage to exert their antimicrobial activity [35].

1.3.1 Cationic Antimicrobial Peptides - CAPs

As mentioned in Table 1.1 Cationic Antimicrobial Peptides (CAPs), are rich in positively charged and aromatic amino acids that promote a helical structure that includes turns. Combination of these positively charged amino acids and neutral amino acids as well as glycine, produces amphiphilic peptides that possess hydrophobic and hydrophilic side chains, forming unique structures that are also possible due to the ring stacking ability of aromatic amino acids often observed in CAPs [36].

The electrostatic attraction of antimicrobial peptides to anionic pathogenic membranes, suggests that most antimicrobial peptides are cationic in charge and are also amphiphilic, meaning they are able to penetrate into the cell wall and interact with both hydrophilic and hydrophobic parts of the membrane. Although the exact mechanism of action of antimicrobial peptide is unclear, the cationic and amphiphilic regions of AMPs are widely understood to be influential in the intensity of their direct microbicidal activity [37]. These positively charged peptides initially accumulate on the bacterial surface, largely based on initial electrostatic attraction to the anionic polymers, such as LPS and Lipoteichoic acid (LTA) on the membrane of Gram-negative and Gram-positive bacteria, respectively. This is followed by a subsequent pore formation and several other complex models including the *toroidal-pore* or *barrel-stave* mechanisms or detergent-like membrane solubilisation, the *"carpet-like"* mechanism all leading to the loss of cellular content [38]. It should be noted that, membrane interactions are not the sole mechanism of antimicrobial peptides and the homeostasis caused by the disruption of the pathogenic membrane is not the only cause of bacteria death [39].

1.4 Defensins

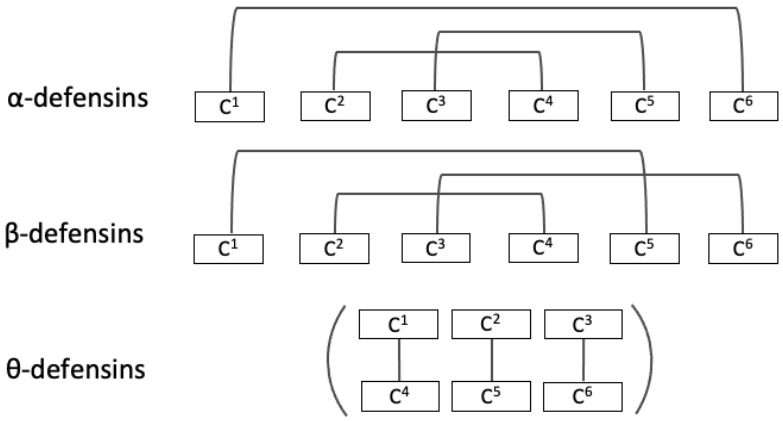


Figure 1.1: Differences between the connectivity of disulfide bridges in α-, β- and θ-defensins where, the superscript of Cysteine residues shows the relative proximity of the Cysteine residue from N-terminus.

Defensins are broadly microbicidal, cationic, 3-4 kDa, prepropeptides, classified based on the pattern of their three conserved disulfide bridges stabilising the β-sheet structure shown in Figure1.1 between six conserved Cysteine residues. Defensins are a part of innate immune system, with two main classes of human defensins identified; α-defensins and β-defensins. Additionally, another class of defensins identified as θ-defensins are found in non-human primates [40]. α-Defensins, originally called hNP, since they were extracted from human neutrophils or PMNs were the first defensins to be discovered. Human neutrophils ingest the invading microorganisms, namely bacteria, and control their division stoping proliferation [29]. Originally PMNs were found to exert their antimicrobial activity through oxygen dependent means where, oxygen induces the activation of phagocyte oxidase enzyme. This multicomponent enzyme reduces the molecular oxygen and forms oxygen radicals. PMNs main bactericidal mechanism was believed to be the generation of oxidative metabolites [27]. Although this was later debunked by the discovery of Lysozyme found in phagocytes and secreted from mucosal epithelia [41]. The discovery of Lysozyme led to the discovery of antimicrobial

cationic peptides with the aid of the advancements in chromatographic methodologies. Defensins were amongst the discovered polypeptides showing membrane related activity towards microorganism in a non-enzymatic manner [42].

1.4.1 Alpha Defensins - α-Defensins

Humans, express six different α-defensins including; hNP1-4 in the primary PMNs granules [43] and HD5-6 produced from the human Paneth cells and female urogenital tract [44], [45]. They show a broad spectrum activity towards a multitude of pathogenic microorganisms and fungi. Similar to penicillin, these peptides are only antimicrobial against growing cultures of bacteria. These peptides are effected by the physiological concentration of cations such as salt alongside serum/plasma components, namely, Albumin [32]. Precipitation and aggregation of α-defensins during the oxidative folding in formation of disulfide bonds due to the basic and hydrophobic nature of these peptides, dramatically reduces their overall yield [46].

Defensin A gene (DEFA) descended from Defensin B gene (DEFB), is usually outnumbered by the number of β-defensins and are much more scarce, only found in humans and mammals, where the number of β-defensin genomes ranges from 20-40, α-defensins have between 1-8 [47]. hNP1-3 are almost identical with the discrepancy at the N-terminal where an Alanine (Ala - A) is present in hNP1, absent in hNP2 and, changed to Aspartic acid (Asp - D) in hNP3. With proteolytic degradation as the cause of the absence of an Alanine or aspartic acid residue in hNP2, this peptide lacks its own gene, hence, there are only 5 genes encoding for α-defensins located on chromosome 8p23.1 in the human body. $5 - 7\%$ human PMNs proteins belong to hNP1-3, compared to hNP4 that is much less abundant in PMNs and it also shows a highly conserved sequence across all species that display this peptide unlike hNP1-3. Additionally, hNP4 has a higher cationic charge which could account for it's moderate

increase in antimicrobial activity [48]. As mentioned α-defensins are not only produced in PMNs but they are also consistently secreted in the human Paneth cells that were found in the lining of epithelial cells of the small intestines. HD5 and HD6 are able to recognise foreign microorganisms approaching the intestinal lumen and are able to bind to anything including themselves in a non-specific manner [49].

α-Defensins show a β-sheet core structure shown in Figure 1.2 stabilised by the disulfide bridges that superimpose the rigidity of these peptides thus, protecting them against their processing enzymes [50]. The α-defensins structure has been attributed to its three antiparallel β-strands where, $\beta 1$ and $\beta 2$ in every seven to eight residues, are connected with a β-hairpin, ending with two termini of variable lengths.

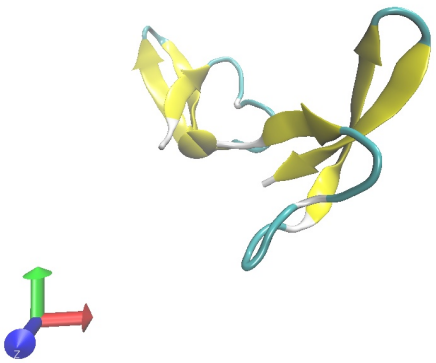


Figure 1.2: Structure of Human α-defensin 1 produced by VMD software from data extracted from PBD database.

The presence of disulfide bridges along with the single salt bridge between the Arginine (Arg - R) and Glutamic acid (Glu - E) residues, help restrain the structure. The proximity of the Cysteine (Cys - C) residues in the structure also follow a pattern with, the first two cysteine residues separated by one amino acid and the last two

adjacent to each other. The Cys residues along with the Arg, Glu and two Glycine (Gly - G) residues are amongst the conserved residues in α-defensins,[51] according to Figure 1.3.

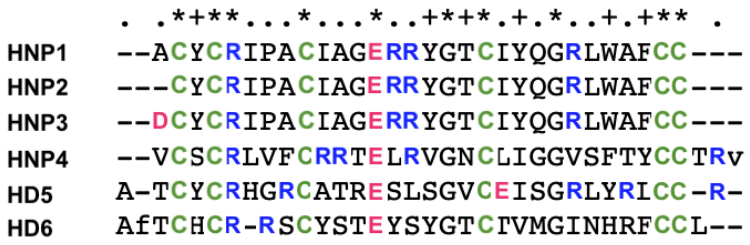


Figure 1.3: Sequence alignment result of all six α-defensins where the blue indicates positively charged residues and the red indicates anionic residues [52].
* Completely conserved residues/ + Partially conserved residues/ · Non-conserved residues

These conserved residues being the most rigid part of these sequences are, indispensable for the structure and function of α-defensins and its oligomerisation. Substitution of any of these conserved residues results in the disruption of proteolytic stability, folding properties and chemotactic activities of α-defensins.[50], [53], [54] The dimerisation and the ability for higher order multimerisation are among the important factors for the antimicrobial function of α-defensins through binding to glycoproteins and bacterial toxins [55], [56].

1.4.2 Beta Defensins - β-Defensins

The first identified β-defensin was found in the bovine trachea and bovine PMNs [12] and the first hBD, hBD1 was isolated from plasma filtrate in 1995 [57] followed by the discovery of hBD2 and 3 found from skin flakes of a psoriasis patient.[29] The subsequent hBD discoveries were done by the genome analysis of the available β-defensin sequences [58]. Unlike α-defensins, there are 40 potential coding regions dedicated to

β-defensins in the human body. DEFB are located in chromosomal region 8p21-p23 which includes the DEFA genes as well, suggesting a common ancestral origin between DEFB and DEFB1, DEFB4 and DEFB103 genes. Other chromosomal regions for DEFB genes are 6p12, 20p11.1 and 20p13 [59]. Most β-defensins have a common genomic organisation with two exons and one intron where the second exon codes for a pro-peptide [60], [61]. Although DEFB1 follows a different pattern of expression where, the first exon codes for the signal- and pro-peptide and the second exon codes for the mature peptide undergoing post transitional modifications and truncation that yields multiple forms of the peptide ready to be released. This gene also codes for the most telomeric β-defensins region within the chromosome [62]. DEFB105 is also expressed differently since it has three exons and two introns, encoding for a short signalling peptide, mature peptide and a small anionic pro-peptide, respectively [63], [64].

So far only four human β-defensins have been extensively studied with alignment shown in Figure 1.4. hBD1 is primarily expressed in the epithelial lining of the urinary [65] and respiratory tracts [66] and it was found that it shows promising antimicrobial activity in reduced conditions found in the body, but in it's oxidised form where the disulfide bridges are formed, it shows no antimicrobial activity except towards *Escherichia coli (E. coli)* [67].

hBD2 has been found, mainly, on the surface of the skin, the gastrointestinal and respiratory tracts similar to hBD1 and it is mainly secreted as a response to an inflammation [45], [68]. hBD3 is an exception in that it is, not only found in the epithelia, it has also been detected in heart, liver, fatal thymus and placenta at lower levels and it is shown that it is expressed in keratinocytes as a response to stimuli [63], [69]. hBD4 is mainly expressed in the testis, gastric antrum and in the epithelia of thyroid gland, lungs, uterus and kidneys. The production of hBD2, hBD3 and hBD4 are inducible by exposure to pathogenic compounds and cytokines [70]. This is especially true in the case of hBD2 which is highly expressed in normal epithelial cells

following contact with microorganisms or cytokine stimulation [67], [71].

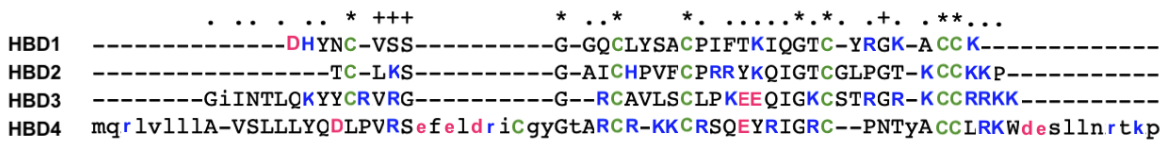


Figure 1.4: Sequence alignment result of β-defensins 1-4 only where the blue indicates positively charged residues and the red indicates anionic residues [52].
* Completely conserved residues/ + Partially conserved residues/ · Non-conserved residues

During an investigation on hBD3 peptides folding structure and the characterisation of their antimicrobial effect, it was concluded that hBD3 requires disulfide bridges for the initial attraction to the pathogenic compound, however, disulfide bridges are not necessary for it to exert its toxic mechanisms towards *E. coli* [72]. It was also shown that the introduction of D-amino acids abrogated the need for a disulfide bridge for exhibiting activity, likely due to the increase in the stability of the peptide when D-amino acids are introduced in the structure [73].

1.4.3 Theta Defensins - θ-Defensins

θ-defensin genes Defensin T gene (DEFT) arose from the mutation of DEFA gene [74] even though these peptides only exist in non-human species [75] These defensins show impressive antimicrobial and antiviral activity whilst maintaining low toxicity, made up of 18 amino acids taking a cyclic backbone formation. The presence of a premature stop codon in the inherited DEFT genes that renders its translation, is the reason for the lack of θ-defensin in humans and other invertebrates [76]–[78].

1.5 Mechanisms of Antimicrobial Peptides

The mechanism of antimicrobial peptide activity has been poorly understood due to the number of different ways they can exert their antimicrobial effect against pathogens. There are many variables that can effect this activity and that only complicates the study of AMPs further, leading to difficulty in designing reproducible methodologies in the laboratory. Variables such as; number of amino acids, secondary structure, peptide concentration, salt concentration, number of hydrophobic and hydrophilic amino acids present in the sequence of the AMPs and, the charge of the peptide can effect the mechanism of their activity [79]. Although studying these mechanisms is difficult, they have been extensively documented and can be divided into two types of interactions.

First, is membranolytic mechanisms where the peptide can either induce different types of membrane protrusion leading to cell content leakage [80]. This membranolytic mechanism, also includes insertion of AMPs inside the membrane without disrupting its structure and effect intracellular systems. Second, is non-membranolytic mechanism where AMPs effect the immune system and allow the presence of white blood cells in the site of infection or inflammation [54].

1.5.1 Membranolytic Mechanisms

Most AMPs are initially attracted to pathogens through electrostatic attraction to the negatively charged molecules on the membrane [79]. For example, defensins initiate activity towards pathogens through a "fatal attraction" towards the anionic microbial membrane due to their cationic nature, culminating in target cell death elicited mainly through microbial membrane disruption and leakage of cellular contents. These negatively charged biological molecules are normally not present in the outer layer of human cells and eukaryotes. Therefore AMPs are not normally attracted to normal human

cells [81].

Mechanisms which cause the leakage of cytoplasmic content and membrane rupture include, *toroidal* formation, *carpet* formation, and *barrel stave* formation. These have different ways in which they effect the bilayer but all ultimately lead to membrane disruption and bacterial inhibition. The schematic view of each of these mechanisms can be found in Figure 1.5.

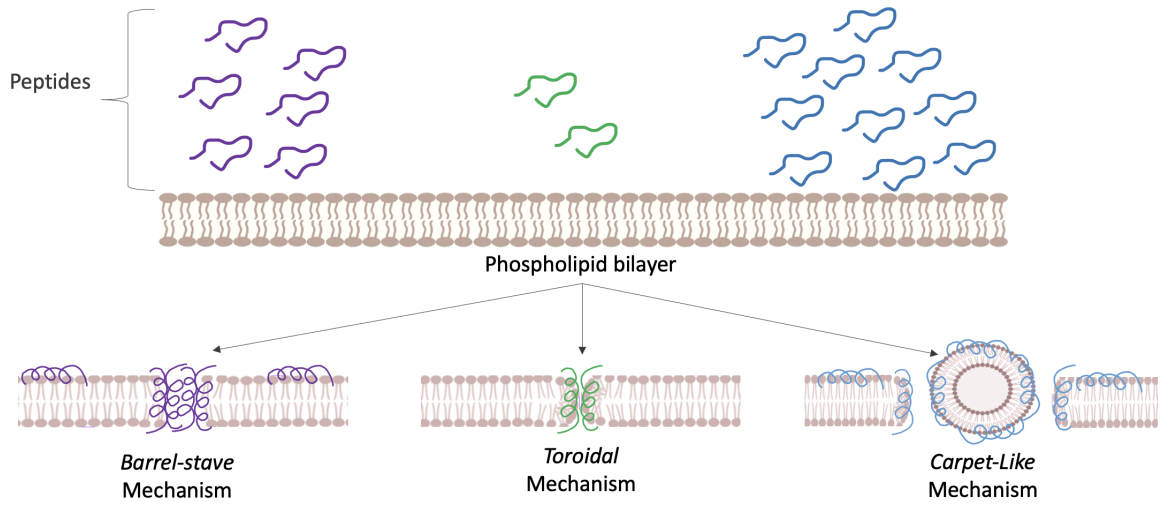


Figure 1.5: Membrane dependent mechanisms of activity exerted by different antimicrobial peptides.

As shown in this figure the *barrel stave* mechanism starts by the formation of a peptide assembly on the membrane as they insert and form a channel resembling an ionic channel within the membrane where the existing phospholipid molecules are replaced by the new peptides, hence, forming a water filled pore inside the membrane bilayer [82]. On the other hand, the *toroidal* mechanism, similar to *barrel stave*, requires the lodging of the peptide between the membrane but in this case the peptide rearranges the phospholipid bilayer and becomes a part of the membrane forming a channel-like structure around the curvature of the membrane as opposed to a pore by replacing the phospholipid molecules completely [83], [84] where the water core is lined by both the

inserted peptides and the lipid head groups [38]. The *carpet* mechanism differs from the two mechanisms, where, the peptide is able to attach parallel to the membrane and line it like a carpet [13]. Once the critical concentration of the peptide attached on the membrane surface is reached, hydrophilic residues face the polar lipid head groups and the hydrophobic residues face toward the lipid tails leading to the disintegration of the membrane and eventually the formation of micelles with peptides on the outside and the phospholipids on the inside [85]. This mechanism is not dependent on the peptide-peptide interactions and does not require the peptide length to span the full length of the membrane height to form a pore in the bilayer. Therefore, many antimicrobial peptides show this type of antimicrobial activity [38].

1.5.2 Non-Membranolytic Mechanisms

There is structural evidence, such as the similarity between the activity of L- and D-versions of the AMPs against the same pathogen, that explains the presence of non-membranolytic pathways that does not depend on the structure of the peptide. Instead it depends on targeting the pathogen's intracellular molecules or the cross talk between the peptide and the adaptive immune system [86]. According to numerous studies, α-defensins are able to communicate through different signalling pathways and warn the adaptive immune system regarding the presence of pathogenic microorganisms [87], [88]. Over numerous decades other species such as plants and fungi have survived using defensins and they lack an adaptive immune system, hence, it is apparent that the main mode of action for defensins is through membranolytic activities plus their ability to form net like structures that encapsulates foreign entities and the communication of defensins to the adaptive immune system is an ancillary service [49]. Additionally, some defensins interact with the nucleic acid and disrupt the production of proteins but do not show any membrane activity, supporting the idea that some AMPs show non-membranolytic activity displayed in Figure 1.6. Another hypothesis is the presence

of certain effector molecules that facilitate the permeabilisation of the membrane and the subsequent uptake of AMPs [89].

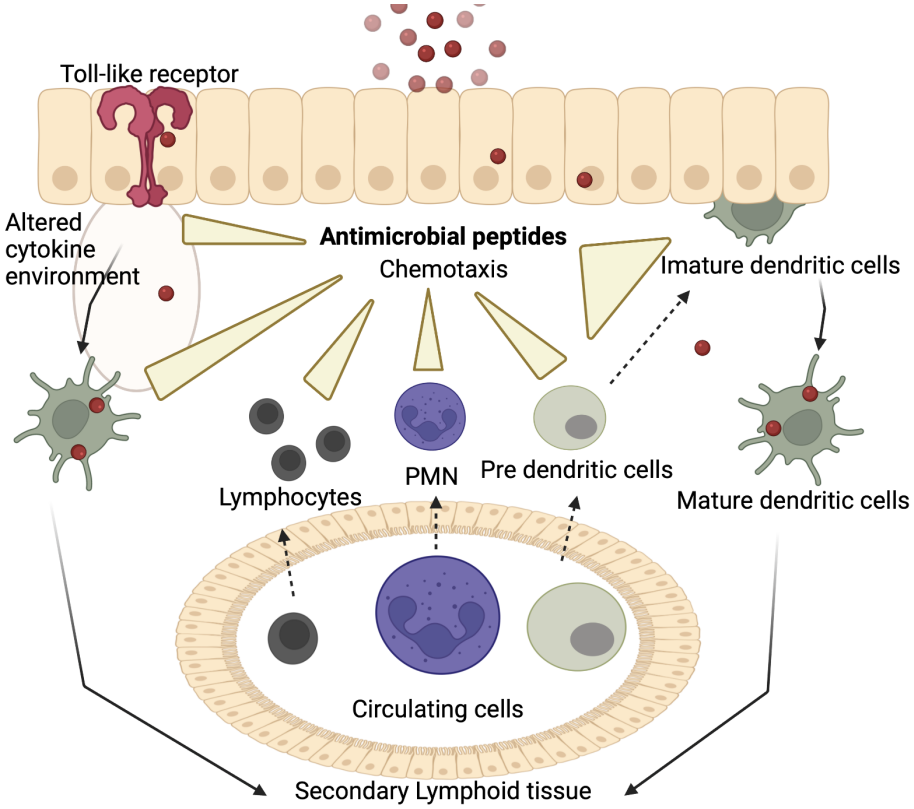


Figure 1.6: Non membrane dependant antimicrobial activity through signalling the adaptive immune system through inflammation and infection. AMPs have chemotaxis ability to towards Immature Dendritic Cells (iDC), monocytes/Pre-Dendritic cells (DCs), PMNs, modulation of lymphocyte activity and/or proliferation, alteration of the local cytokine environment, direct iDC activation via Toll-Like Receptor 4 (TLR4), or generation of primed iDC with enhanced antigen uptake and presentation capacity [90]. Dots represent antimicrobial peptides

The stabilised form of the disulfide bridge in hNP1-3 and HD5, is necessary for the neutralisation of bacterial toxins,[91] inhibition of Tumour Necrosis Factor-α (TNF-α) secretions by macrophages [92] and binding Envelope glycoprotein 120 (gp120) of Human Immunodeficiency Virus 1 (HIV-1) and bacterial cell wall Lipid

II, a membrane bound peptidoglycan precursor [93]. Their activity against Gram-negative bacteria is attributed to the disruption of bacterial membrane whilst they also exhibiting lectin-like activity towards glycosylated proteins. hNP1-3 deferentially modulate cytokine response of activated monocytes, through chemotaxis of human monocytes. This process enhances the TNF-α and Interleukin-1β (IL-1β) expression in addition to being a signalling molecule for iDC and naive human CD4 and CD8 T cells [94]. In addition, whilst enhancing systemic Immunoglobulin G (IgG) antibody responses, α-defensins do not effect Immunoglobulin A (IgA) response and provide a bridge between B- and T-cell interaction linking the adaptive and innate immunity [95]. The aggregation of defensins, in presence of bacterial toxins and binding to gp120 allows the dimerisation and formation of higher order aggregates in solution [96]. As DCs are important molecules for inflammation and allergy presentations, hBD1 shows a massive contribution to the progression of skin inflammation and allergies through chemotaxis towards DCs that increase antigen uptake and the production of mature DCs and or their activation through Chemokine receptor (CCR)6 and TLR4 [97].

1.6 Activity of Antimicrobial Peptide

Biological membranes are a mosaic combination of Proteins and Phospholipids, whilst Sterols and Glycerides also contribute to the surface topology and biochemical architecture of bio-membranes. The fundamental differences between mammalian and pathogenic membranes are attributed to the variation in: membrane composition and architecture; energetics such as transmembrane potential and polarisation; and structural features including the presence of Sterols, LPS and Peptidoglycan. Hence, the interaction of AMPs and more specifically defensins towards pathogenic cell membrane differs from the interaction with mammalian cells and the degree in which, antimicrobial peptides can differentiate between the two membranes is an important factor that

should be considered when designing a biological agent [98], [99]. Figure 1.7 shows the differences between the normal mammalian membrane and the bacterial membranes.

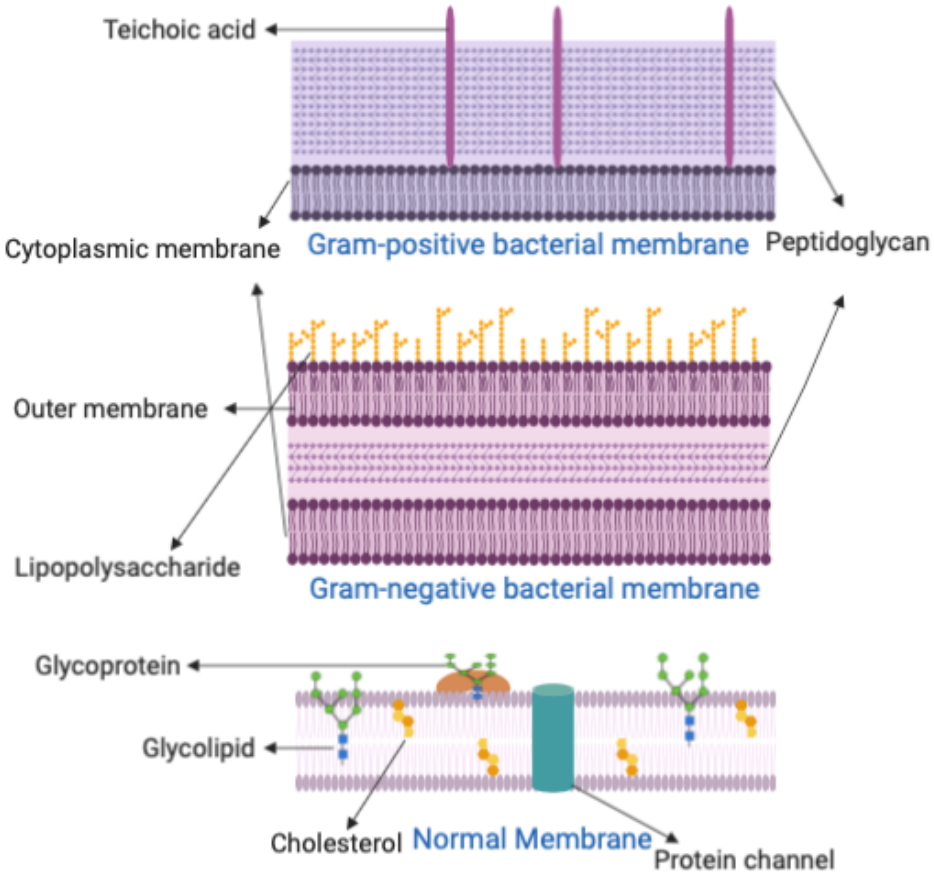


Figure 1.7: Comparison of Gram-negative, Gram-positive and eukaryotic membrane bilayer.

Although, these variations contribute to the difference in the antimicrobial activity of defensins against different cell types, they are not the sole reason for the attraction of these molecules to specific membranes. Defensins target cells based on interior complexities as well as membrane attraction and the idea of electrostatic attraction mainly through the outer membrane has been rendered obsolete [100]. Defensins chemoattract and lead to activation of different immune cells [81], [87], [94], [101], [102], they also regulate cytokine production [81], [92]. They interact with the complement system [81], and they promote wound healing via growth of epithelial cells

[81], [103]. Since AMPs adapted to perform their antimicrobial activity on pathogens through different countermeasures, it is difficult for the pathogens to develop immunity against these molecules. The development of immunity towards AMPs will only induce another pathway to fight against the pathogens.

1.6.1 Bacterial, Viral and Fungal Activity

The presence of Lipid II on the outer membrane of some bacterial species increases the activity of Nisin, a small amphiphilic antibiotic peptide, through liposomal leakage and disruption of peptidoglycan production leading to permeabilisation of the bacterial membrane [104]. Nisin can also displace the Lipid II from cell division and block cell wall synthesis [105]. The activity of HD5 and hNP1 against non-envelop viruses, Human Adenovirus (AdV) and Human Papillomavirus (HPV), is related to their hydrophobic core and more specifically the hydrophobic side chains on one side of the peptide only [106]. Although, prior to this revelation, the importance of Arg residues in the antiviral activity was highlighted [107]. The presence of Tryptophan(Trp-W) residue in hNPs also, plays one of the most important roles in the activity of this defensin. Substitution of Trp with an Alanine (Ala-A) residue significantly impacts the ability of hNPs to kill *Staphylococcus aureus (S. aureus)*, bind to gp120 and self aggregate and dimerise especially, since dimerisation disrupts the lipid bilayer [108], [109]. The binding and interaction between hNP1 and Lipid II, and the interaction between hBD1 and chemokine receptor, CCR6, show a different mode of action than their interaction with non-envelop viruses, indicating that the differences in the important residues show varying activity against different types of pathogens. On the other hand, hBD1 induces Chemokine ligand (CCL)20, a CCR6 ligand, release in Peripheral Blood Mononuclear Cell (PMBC), inhibits HIV infectivity by 50%[110] through indirect upregulation of hBD3, a known HIV-1 coreceptor CXCR4 antagonist [62].

Not all defensins, in a similar class, show the same mode of action to every pathogen and the reality of the anti-pathogenic action is much more complicated than the initial electrostatic attraction [111], [112]. The presence of disulfide bridges in HD5 induce the secretion of Interleukin-8 (IL-8) in the intestinal epithelial cells [81] and block the viral capsid assembly, inhibiting AdV infection [113]. Removal of disulfide bridges affect the activity of hNP1 and HD5 in a way that does not effect their activity against *E.coli* but it inactivates them against *S. aureus*, proving that they show different modes of action towards different bacteria [81], [113]. In contrast hBD3, with the net charge +11, shows toxic effect towards Gram-negative and Gram-positive strains of bacteria regardless of the presence of its disulfide bonds [81], [114]. The presence of hBD3 [115] and hBD4 help mast cell degranulation through activation of Mitogen-activated Protein Kinases (MAPK), p38, and Extra-cellular–regulated Kinase (ERK)1-2, promoting wound healing and inflammatory response [116]. β-Defensins appear to have a positive impact on catabolic pathways in articular cartilage formation leading to the breakdown of the extracellular matrix [117]. Defensins are able to bind to the host cell receptors and they play an important role in innate and adaptive immunity and in addition to the membrane and lipid binding activity, defensins, also bind to carbohydrates and nucleic acid. As an example by cross-linking the glycoproteins on the host membrane surface they prevent the attachment of influenza virus [118]. It has been reported that some cariogenic bacteria, including *Streptococcus mutans (S. mutans)*, are susceptible to human β-defensins and LL-37. This is also supported by the excess presence of β-defensins in children with dental caries presentation. Dental caries refers a condition where the presence of bacteria such as *S. mutans* causes tooth decay [119].

Many studies have shown that the L- and D-enantiomers of antimicrobial peptides provide the same activity and mechanism for the inhabitation of pathogens. L- and D-hNP1-3 show the same activity against *E. coli* where they stop the synthesis of DNA, RNA and proteins and render the colony production [96], [120]. Studies per-

formed on bacteria and *Candida albicans* [121] also show the same pattern with the L- and D-enantiomers of different AMPs [122]–[124]. On the other hand the D-hNP1 and D-HD5 showed lack of activity against *S. aureus*. The presence of a thick layer of peptidoglycan covered in LTA and the thin layer of peptidoglycan covered with an outer membrane with LPS on the outer surface in *S. aureus* and *E. coli*, respectively, can explain the [125] discrepancies between the two different experimental outcomes [126]. The initial attraction of cationic peptides to the anionic components of bacterial cells such as LPS and LTA is evident and it is the first point of contact and uptake for the peptides, however the subsequent antimicrobial activity in *S. aureus* is affected by chirality dictating that the first attraction does not necessarily induce antimicrobial effect and subsequent bacterial killing is effected further by other pathways and mechanisms of action [127]. Although AMPs have shown non specific affinity for different anionic membrane molecules α-defensins display a special affinity towards glycosylated molecules. Since most cell surface molecules are glycosylated and anionic, there is an enhanced affinity for these molecules to bind through highly reversible non-covalent means, dependent on relative affinity constant and diffusion-limited flow rates [128], [129].

Since AMPs adapted to perform their antimicrobial activity on pathogens through different countermeasures, it is difficult for the pathogens to develop immunity against these molecules. The development of immunity towards AMPs will only induce other pathways to fight against the pathogens [99]. The resistance of bacteria to the antimicrobial peptide and namely the presence or the absence of disulfide bridges in defensins, depend on many factors such as, the susceptibility of the bacteria itself, the testing conditions and the bacterial growth phase, presence of other metabolites and glucose [120].

1.6.2 Anticancer activity

Due to the presence and over expression of anionic molecules and the increased o-glycosylated mucins on the surface, the overall charge of cancer cells is negative [130]. Phosphatidylserine (PS) is an anionic immunosuppressive phospholipid molecule located in the inner membrane, whilst, the phospholipids and phosphatidylcholines are localised primarily on the outer membrane of normal eukaryotic cells. As a result of injury, apoptosis or hemostasis complement cascade is activated which allows the passage of PS to the outer membrane. This is mainly due to oxidative stress in the cell environment during apoptosis, that lead to the Ca^{+2} influx and low flippase activity [131], [132]. Although the presence of PS in the outer leaflet leads to phagocytosis via macrophages, the presence of the CD47 which, is over expressed in many cancer cells, inhibits tumour phagocytosis [125]. The over expression of CD47 on the outer membrane of myeloid leukaemia, breast cancer and prostate cancer cells will not only lead to escaping the phagocytosis but it also leads to escaping the immune surveillance that leads to poor prognosis and metastasis of the tumour cells [133].

As PS is an anionic molecule it leads to the attraction of CAPs, hence antimicrobial peptides are able to be used in defence against cancer cells not only through the initial electrostatic attraction to PS but also through their mechanisms to signal dendritic cells and aid with phagocytosis. DEFB1 promotes apoptosis of cancer cells through its assumed tumour suppressor abilities [134] and its absence in most tumour samples [135]. The under expression of hBD1 in prostate [134] and an exon mutation in the hBD gene clusters in colon [136] cancer have shown to be linked to poor prognosis and the growth of the cancer cells.

Although chemotherapy is the best course of action for many cancer types it is not the best way to go forwards due to its lasting side effects for the patients and its non-specific mode of action where it is as toxic to normal cells as is to cancer cells.

Some cancer cells can also develop resistance towards chemotherapeutic drugs through the presence of membrane associated proteins such as P-glycoprotein and the Multi-drug Resistance Associated Protein (MRP) turning into efflux pumps [130], [137]. The hydrophobicity of the AMPs has been linked to its activity towards the cancer cells and numerous research have shown that the relationship between the hydrophobicity and the therapeutic index is a bell curve rather than the proposed linear correlation meaning, as the hydrophobicity of AMPs reaches its threshold of effectiveness its therapeutic index decreases towards the cancer cells [138]. Antimicrobial peptides can be used in cancer therapeutics in different ways including: vaccines that mimic tumour antigens known as Tumor-Associated Antigens (TAAs) that can be recognised by T cells; tumour targeting with radioisotopes and cytotoxic drugs; and peptides that impact angiogenesis [139].

1.7 Limitations of Antimicrobial Peptides

Although antimicrobial peptides show a variety of different amino acid sequences, they are limited to having a few different structural paradigms. The complexity of these molecules and their attraction to different cell types highlights their multiple roles in host defence, showing a variety of use as a pharmaceutical agent. Issues with their pharmacokinetic abilities has been highlighted in the past that requires specific changes implemented in their sequence of amino acids to provide a higher pharmacokinetic ability for each application individually as opposed to being used for several purposes at once [10]. In addition, AMPs are easily hydrolysed and show poor transport capabilities across membrane barriers *in vivo* leading to poor tissue distribution which limits their clinical usefulness. Chemicals such as salt concentration [140], changes in the pH[141] and the presence of proteases or other plasma components [142] can also effect the function of the antimicrobial peptides significantly decreasing their antimicrobial

activity. The lack of bioavailability caused by insolubility and instability of peptides is related to their intrinsic physicochemical properties. This in turn causes potential toxicity to host cells, poor pharmacokinetic performance, and large scale production costs that lead to limitations that in turn effect the interest in these molecules as drug targets and negatively effect the research into antimicrobial peptides [143]. Additionally, limitation in the experimental designs such as, measurement of the hemolysis and or erythrocyte permeabilisation in which the cytotoxicity of the antimicrobial peptides are measured that are a poor representation of the actual cytotoxic capability of the peptides since these molecules show different activity *in vivo* and in contact with different cell types [100].

Despite the mentioned limitations, different modifications have been suggested to reduce the toxicity of AMPs whilst increasing its pharmacokinetic abilities [10], [144]. The use of un-natural amino acids has been suggested in previous research to help the stability of the peptide against hydrolysis. Another method to improve the pharmacokinetics abilities of AMPs is vector-mediated delivery of genes encoding membranolytic or apoptotic AMPs into the targeted pathogen. Conjugation of AMPs to homing peptides has also been suggested to reduce the toxicity and increase the pharmacokinetics abilities of AMPs [7]. Other useful ways to increase the effectiveness of AMPs include cyclisation, micelle formation [145], changes in chirality of the amino acid, and pegylation [146]. It is also important to choose a model that is more representative of the effect of peptide in vivo.

1.8 Antimicrobial Peptide Design

Strategies such as alteration of antimicrobial peptides via amino acid substitution can be employed to reduce its toxicity and increase the antimicrobial activity of the original AMPs. This strategy has been successfully used to produce peptides such as

bactenecin [86], polyphemusin [143] and, indolicidin [147]. Another strategy focuses on the truncation of already existing antimicrobial peptides to see the activity retention of the peptide which can then be used to find the effective sequence composition of a longer antimicrobial peptide and use the much smaller version of the peptide with similar antimicrobial activity, reducing production cost [148]. Although it is difficult to achieve antimicrobial activity with peptides shorter than 8 amino acids, examples such as the 6 residue bovine lactoferricin was shown to have equivalent antibacterial activity compared with the full-length 25-residue lactoferricin B peptide [28]. Other strategies such as removal of disulfide bonds of certain AMPs that display these bonds can be employed, however, they do not necessarily make use of them in their activity towards certain bacterial types. This is especially true in the case of α-defensin where the disulfide reduction or replacement of cysteine residues with alanine lead to loss of β-sheet core [49].

These strategies can be used but they are often time consuming and require many synthesis efforts to produce peptides that are not always showing the desired effect expected from the modification. Therefore other strategies are needed to find the most optimised sequence of a novel AMPs, focusing on the identification of sequence patterns, crucial residue positions and amino acid frequencies from known AMPs. This information is used to build a predication model to generate a library of AMPs based on already existing sequences [149]. All the prediction methodologies heavily depend on the sensitivity of the prediction model to minor changes in the sequence that can predict the small impact it can have on the antimicrobial activity [99].

Additionally, the most rational and widely used strategy is the Quantitative Structure-Activity Relationship (QSAR) model which, predicts the biological activity of the antimicrobial peptide using physicochemical descriptors found from their amino acid sequences [150]–[152]. Prediction of an active AMP sequence is also performed, using *de-novo* models based on the frequency and the position preferences of different

amino acid residues in a library of active antimicrobial peptides. Use of these methodologies can guarantee sequence diversity of the peptide library with a variety of different composition, tridimensional structures, and mechanisms of action whilst preserving the antimicrobial activity of the designed peptide [149]. Predictive models can be used to find the likelihood of the presence of a certain amino acids at each position. These can help determine the combination of amino acids in the correct position to have an antimicrobial effect and reduce the cytotoxicity behaviour of the subsequent peptide. The determination of the position of the amino acid can also help with determining the structure of the designed peptide [151], [153].

These methodologies can be further enhanced by including known amino acid residues that cause antimicrobial activity and help increase their broad spectrum activity. Residues such as Trp that help π-stacking with Proline (Pro - P) residues and Pro residues inducing turns in the structure of the peptide or residues that increase the cationic charge of the peptides such as Arg and Lys residues in pardaxin, magainin-II and, β-defensin was found to increase their antimicrobial activity [154].

1.8.1 Antimicrobial Peptide Databases

Different peptide libraries can be used to perform the *de-novo* design of AMPs. These libraries have all been curated towards a specific function of peptides but they are mostly consisting of peptide showing antimicrobial activity. Antimicrobial Peptide Database (ADP) is an original database released in 2003 and it is currently housing 3324 natural peptides with known sequence and activity towards different pathogens and cancer cells. It enables sequence alignment and prediction of peptide structures [155]. Data repository of antimicrobial peptides (DRAMP) is a manually edited open source database of 22407 different peptides and their subsequence sequences, structures, activities, physicochemical, patent, clinical and reference information opened in 2013. Similar to ADP

it allows for sequence alignment but it also predicts the activity of the peptides [156]. Collection of Anti-Microbial Peptide (CAMP) was created antimicrobial family studies and it contains 1386 AMPs with information regarding their conserved sequences captured as patterns and Hidden Markov Models (HMMS). This database also allows sequence alignment and provides information regarding the protein structure, activity, and target organisms plus it is linked to databases like UniProt and PubMed [157].

Database of Antimicrobial Activity and Structure of Peptides (DBAASP) is a manually-curated database designed to help the scientific community to design antimicrobial compounds with a high therapeutic index housing 18405 monomers. It provides information regarding the physicochemical parameter of the peptides and sequence alignment of *de-novo* designed peptides [158]. Figure 1.8 shows a Venn diagram of overlapping sequences between the databases.

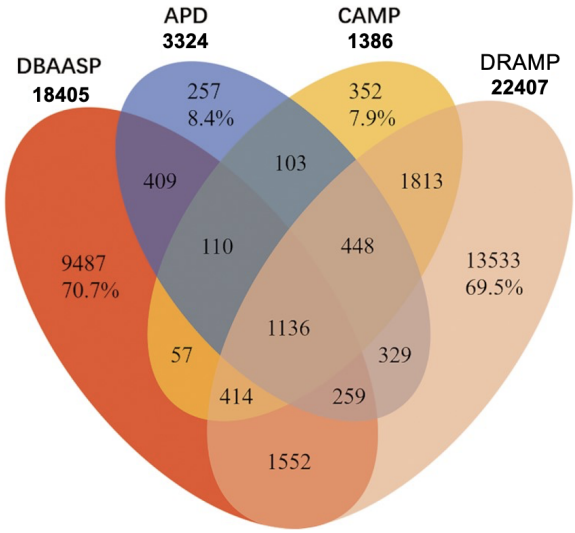


Figure 1.8: Venn diagram representing the numbers of overlapping and non-overlapping sequences between different databases.

1.9 Application of Antimicrobial Peptides

Peptides have many different uses in terms of their therapeutic capabilities. They can be used in hydrogels as a delivery method for therapeutics and wound dressing for their antimicrobial capabilities. Peptides encoded in DNA plasmids are able to target different pathogens and cancer cells alike. Surface coatings of metallic and

prosthetic implants such as catheters, hip, knee implants, and contact lenses, coated with antimicrobial peptides hinder biofilm formation, hence decreasing pre-implant infection on wounds [159]. Although expensive, AMPs can be used as sprays to disinfect different surfaces such as tooth surface for the treatment of dental caries. GERM CLEAN designed by Xiong. *et.al* was found to have impaired the attachment, biofilm formation, and acid production of *S. mutans* to the teeth [160].

Methods for the modification of different material surfaces include the physical and chemical modifications. Chemical modification refers to the conjugation of the antifouling agents on the surface of the material via a spacer. These agents are in a fixed position and they provide their effects based on the attachment of the bacteria. Advantages of using such mechanism is the presence of a clear structure adapted upon conjugation and the clear antimicrobial effect of these agents. Disadvantages include the presence of dead bacteria on the surface of the material and inability to reach the implanted area for removal of bacterial agents [161]. Physical modification refers to the formation of hydrogels and coating of surfaces with antimicrobial agents to release when needed and necessary into the implanted area. This modification can help to eliminate the bacteria agent and prevent the formation of biofilm on the surfaces before the attachment of bacteria and colonisation as well as escaping resistance mechanisms. On the other hand the mechanism of action of these modifications are not clear and they do not have a clear structure. A mixture of both could be helpful on a material surface to provide full immunity and help combat biofilm formation [162].

Peptides are widely utilised as model systems in biophysics due to their uniformity, purity, and compatibility with numerous physical and spectroscopic approaches. Production of peptide model systems provide useful information on the protein secondary structure through the break down of amino acid propensities and the affect they have on the formation of such structures [6], [163].

1.10 Introduction to the hypothesis

The the structure of the hBD1 peptide consists of two beta-sheets and an alpha-helix at the N-terminus [111] and there are many residues that are important for the activity of this peptide in chemotaxis and general attraction to pathogens through the electrostatic charges. hBD1 has also shown capabilities in dimerisation in their quaternary structure. It was shown in many of the studies that the presence of disulfide bridges could be diminished if only electrostatic attraction is desired as seen with hBD3 since cysteines are hypothesised to only be relevant for chemotactic capabilities, as is the case for hBD3 [110], [164]. Shown in Figure 1.9 is the structure of hBD1 and hBD3.

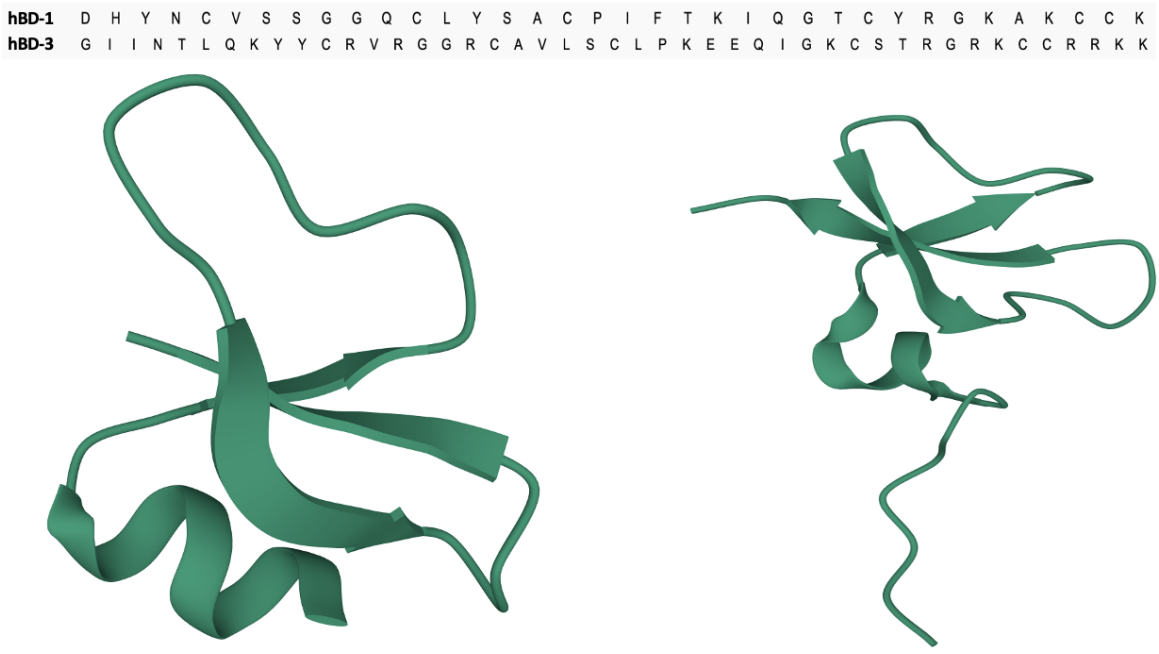


Figure 1.9: Structure of hBD1 on the left and hBD3 on the right hand side. Both structures share a pattern of double β-sheet and an α-helix at the N-terminus.

In this research the aim was to reduce the size of the sequence to overcome the production cost and increase the stability of the defensins; hBD1 and hBD3 [165]. The proposed methodology was to first remove the Cysteine residues from the sequence of

these peptides and truncate the whole sequence by the removal of amino acids so that the majority of the amino acids would still align to the original parent peptide. This hypothesis was formed due to the nature of the antimicrobial activity of these peptides in their oxidised form and the importance of disulphide bridges only as an initial point in the attraction of these peptides to pathogens.

1.10.1 Aims and Objectives

The aim of this thesis was to: Design peptides based on either hBD1 or hBD3 that shows broad spectrum antimicrobial activity whilst showing minimal cell toxicity.

The objectives for this thesis were: To ensure the designed peptide shows an alpha helical structure.

To ensure serum stability or retain of antimicrobial activity even after degradation.

To ensure the designed peptide shows antimicrobial activity across a wide spectrum of bacteria from Gram-negative to Gram-positive.

To ensure the designed peptide does not show cytotoxic effect. synthesise a peptide with a broad spectrum of activity against both Gram-positive and Gram-negative bacteria whilst showing minimal cytotoxincity and not to be effected and degraded by the serum presence in human blood.

To keep the antimicrobial activity of the original peptide intact or increase its activity with the change of its structure and amino acid sequence.

To successfully retain the antimicrobial activity of these peptides even after removal of the cysteine residues from the original sequence.

Chapter Two

Materials and Methods

2.1 Materials

2.1.1 Peptide synthesis

All N-terminals of the amino acids were protected with Fluorenylmethoxycarbonyl (Fmoc) groups and the side chain was also protected with proper protecting groups. Amino acids; Fmoc-Arg(Pbf)-OH, Fmoc-Gly-OH, Fmoc-Ala-OH, Fmoc-Lys(Boc)-OH, Fmoc-Trp(Boc)-OH along with Fmoc Rink Amide ProTide Resin (Loading 0.25 mmol/g) and Oxyma Pure(Ethyl cyano(hydroxyimino)acetate)) were purchased from CEM Microwave Technology and Fmoc-Tyr-OH, Fmoc-Ser-OH, Fmoc-Val-OH, Fmoc-Thr(tBu)-OH, Fmoc-Glu(OtBu)-OH, Fmoc-Ile-OH, Fmoc-Lue-OH, Fmoc-Asp(OtBu)-OH, Fmoc-Phe-OH, Fmoc-Gln(Trt)-OH, Fmoc-Pro-OH, Fmoc-Thr(tBu)-OH, Fmoc-Tyr(tBu)-OH along with the solvents and reagents used for Solid Phase Peptide Synthesis (SPPS) and cleavage components: Dichloromethane (DCM) ($\geq$ 99.8%), N,N-Dimethylformamide (DMF) ($\geq$ 99.8%), N-Ethyldiisopropylamine (DIC) (Biotech grade, $\geq$ 99.5%), Carboxyfluorescein (BioReagent, HPLC $\geq$ 95%), Piperidine (Biotech grade, HPLC $\geq$ 99.5%), Trifluoroacetic Acid (TFA) (HPLC grade, $\geq$ 99%) and Triisopropylsilane (TIPS) ($\geq$ 99%) were purchased from Fisher Scientific [Fisher Scientific, 2019]. The purity of all amino acids was above 98%. The anhydrous diethyl ether (Et2O) of HPLC grade for the precipitation of peptides was purchased from Fisher Scientific. The Phosphate Buffer Saline (PBS) pH7.4 used for the release studies and dissolving peptides was purchased from Sigma-Aldrich.

2.1.2 Peptide Characterisation

All solvents used for analytical chemistry were purchased from Sigma-Aldrich for HPLC grade solvents. This includes Water, Acetonitrile, Ethanol. Formic acid was purchased from Alpha Aesar [Alpha Aesar, 2022]. Dry ice was supplied via ice deliveries from

School of Chemistry and Dentistry [University of Birmingham]. For Circular Dichroism (CD) experiments the Sodium Dodecyl Sulphate (SDS) powder and Dodecylphosphocholine (DPC) were purchased from Sigma-Aldrich [Sigma-Aldrich, 2022] along with the LTA and LPS were purchased from Merk [Sigma-Aldrich, 2022]. For the peptide stability studies the RPMI1640 media was purchased from Sciencell [Biotrend, 2022] and the Human serum used was purchased from Merk [Sigma-Aldrich, 2022].

2.1.3 Antimicrobial Studies

The Muller Hinton Broth (MHB) and Tryptic Soy Agar (TSA) were purchased from Sigma-Aldrich [Sigma-Aldrich, 2022]. *E. coli* of ATCC 25922 strain, *Pseudomonas aeruginosa (P. aeruginosa)* of PA01 strain and *S. aureus* of 8325-4(SH1000) strain were used in this study supplied by the School of Dentistry [University of Birmingham]. The antibiotics used as a positive control for bacteria are Ciprofloxacin, Polymyxin B and Vancomycin respectively all purchased from Sigma-Aldrich. PBS was also made using Phosphate Buffered Saline (PBS) capsules purchased from Sigma-Aldrich [Sigma-Aldrich, 2022] with deionised water from MiliQ.

2.1.4 Cell Culture Studies

Epithelial HeLa cells used in this study were supplied by the School of Dentistry [University of Birmingham]. The cells were started from passage number 2 and they were split using Dulbecco's Modified Eagle Medium (DMEM) High Glucose, Fetal Bovin Serum (FBS), L-Gultamine, 0.25% Trypsin, 0.1% EDTA [-] Sodium Bicarbonate from Corning [Corning, 2022], and Penicillin-Streptomycin (5,000 U/mL) all purchased from Thermofisher Scientific [Thermofisher Scientific, 2022]. The CyQuant^{TM} MTT Cell Viability Assay kit purchased from Invitrogen to [Invitrogen, 2022] was used to determine the viability of the cells. PBS was also made using PBS capsules purchased

from Sigma-Aldrich [Sigma-Aldrich, 2022] with deionised water from MiliQ. The media used to perform the MTT assay was Gibco DMEM 1x, high glucose, HEPES, no phenol red [Gibco, 2022]. Sterile Dimethyl sulfoxide (DMSO) used as negative control was purchased from Sigma-Aldrich.

2.2 Peptide Synthesis

Solid Phase Peptide Synthesis SPPS uses amino acid building blocks mounted on a resin of choice based on solid phase peptide synthesis developed in 1960s.[166] This method includes 4 different steps starting with swelling of the resin of choice which is fastened with a linker (Number of linker measured by mmoles of linker per gram of beads) via immersion in an appropriate solvent. This, will increase surface area of the resin and insure that the linker groups on the resin are exposed to as many amino acids as possible, increasing the yield of peptide production.

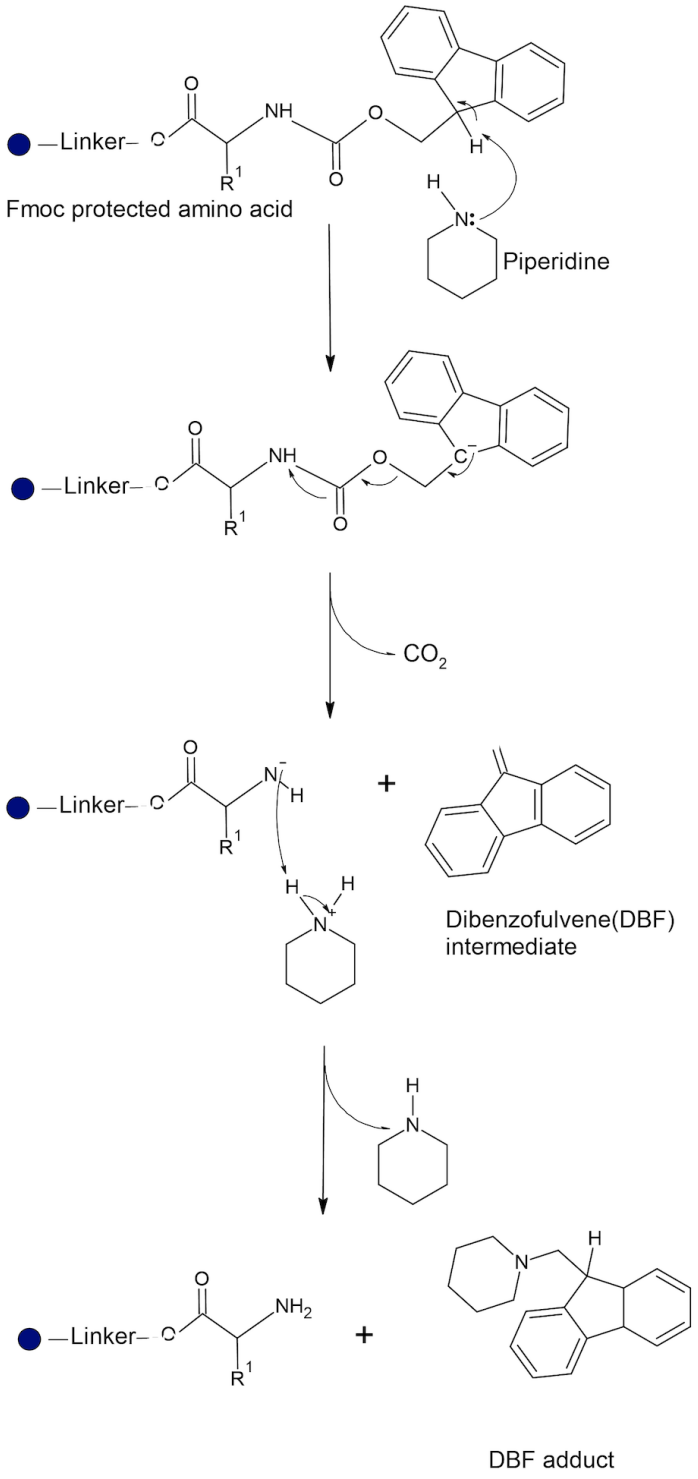


Figure 2.1: Removal of Fmoc from the N-termini of amino acid using a strong base. [167]

The amino acids in SPPS should be protected on the N-terminus, to prevent undesired side-chain reactions. Fmoc fluorescein is one of the common N-terminus protection groups shown in Figure 2.1 and the process in which these amino acids are used to perform SPPS is called the Fmoc/tBu SPPS. The cleavage of this protecting group can also aid in tracking the process of amino acid coupling using UV-Vis spectroscopy. In order to begin the process of SPPS the Fmoc group is removed from the protected resin. This process is called the deprotected step and it is usually performed using a base that allows the cleavage of Fmoc group from the N-terminus.[168] Once the amino acid is ready for reaction, the coupling reagent and its corresponding base are added to provide the basic environment needed for the amide bond formation. Once the peptide bond is formed between the amino acids and the resin according to Figure 2.2 and the uncoupled amino acids are washed away. Each peptide in this study was Fmoc deprotected with the last N-terminus in its free form. The cleavage from the

solid support is performed using a strong acid such as TFA [169].

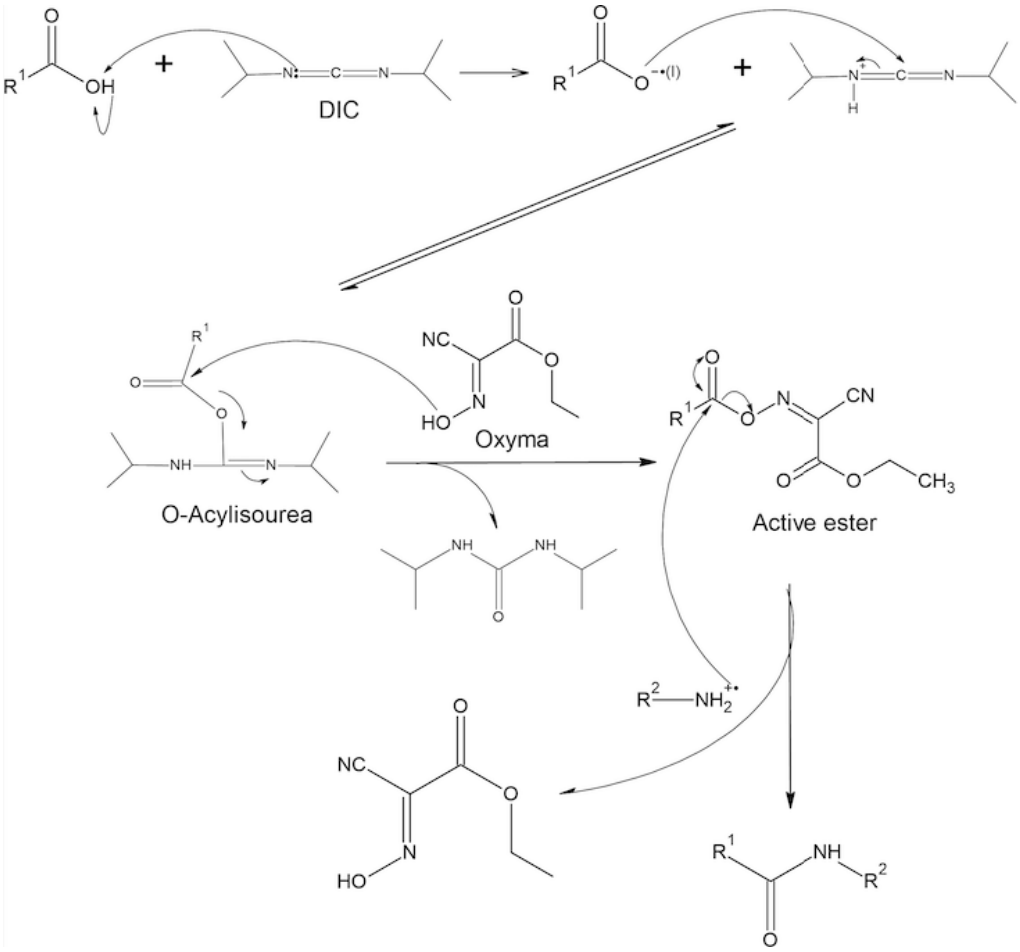


Figure 2.2: Coupling of the first amino acid to the rink amide resin using DIC and Oxyma pure [170]–[172]as activator and base respectively

The SPPS preparation of the peptides were performed using the Automated Microwave Peptide Synthesiser [CEM, 2019]. This instrument was equipped with a microwave, which allows for a more efficient synthesis by shortening the synthesis time due to the presence of microwave irradiation and the use of Nitrogen Gas in pressure addition by the idea of liquid displacement. The scale of production was set as 0.10 mmol. The resin used in this experiment was the Rink amide (200-400mesh) with the resin loading of 0.25 mmol/g. The synthesis was performed with DMF as the main solvent and the deprotection step was performed using 20% Piperidine in DMF whilst

the coupling was performed using CarboMax chemistry with DIC [173] as the activator and Oxyma Pure(Ethyl cyano(hydroxyimino)acetate) as the base. The program was set to perform deprotection, wash, coupling followed by two more washing steps for single coupling that lasted 4 minutes. There was a longer 8 minutes long coupling cycle designed for bulky amino acid residues where the coupling lasted 8 minutes and the remaining steps were the same the shorter coupling. For Arginine(Arg - R) residue the coupling was performed twice which accompanied a wash in between each addition of the coupling mixture. The single 4 minute coupling was performed on all amino acids and for the amino acids with the bulkier side chains such as, Tryptophan(Trp - W), Proline(Pro - P), Lysin(Lys - K) and Phenylalanine(Phe - F) the 8 minute long coupling was used.

Once the resin was removed from the reaction vessel the DMF was removed using vacuum filtration and washed with 3x7ml of DCM the solvents removed and the resin was washed with 2x7ml of cold diethyl ether to ensure the complete removal of DMF which prevents the cleavage process from continuing as normal. After the wash step the peptides are let to dry for one hour in a desiccator. The cleavage step was then performed using a cleavage cocktail of 95% TFA with 0.5% TIPS added as the scavengers to minimise the side chain interactions followed by the addition of 0.5% deionised water for 2 hours at $36°C$. The cleavage cocktail was removed through vacuum filtration and the filtrate was added to 4x50ml falcon tubes containing 20ml ice cold diethyl ether to pellet the cleaved peptides after placing the falcon tubes inside a refrigerated centrifuge for 10 minutes at 4400rpm speed. The cleavage procedure can be found in Figure 2.3.

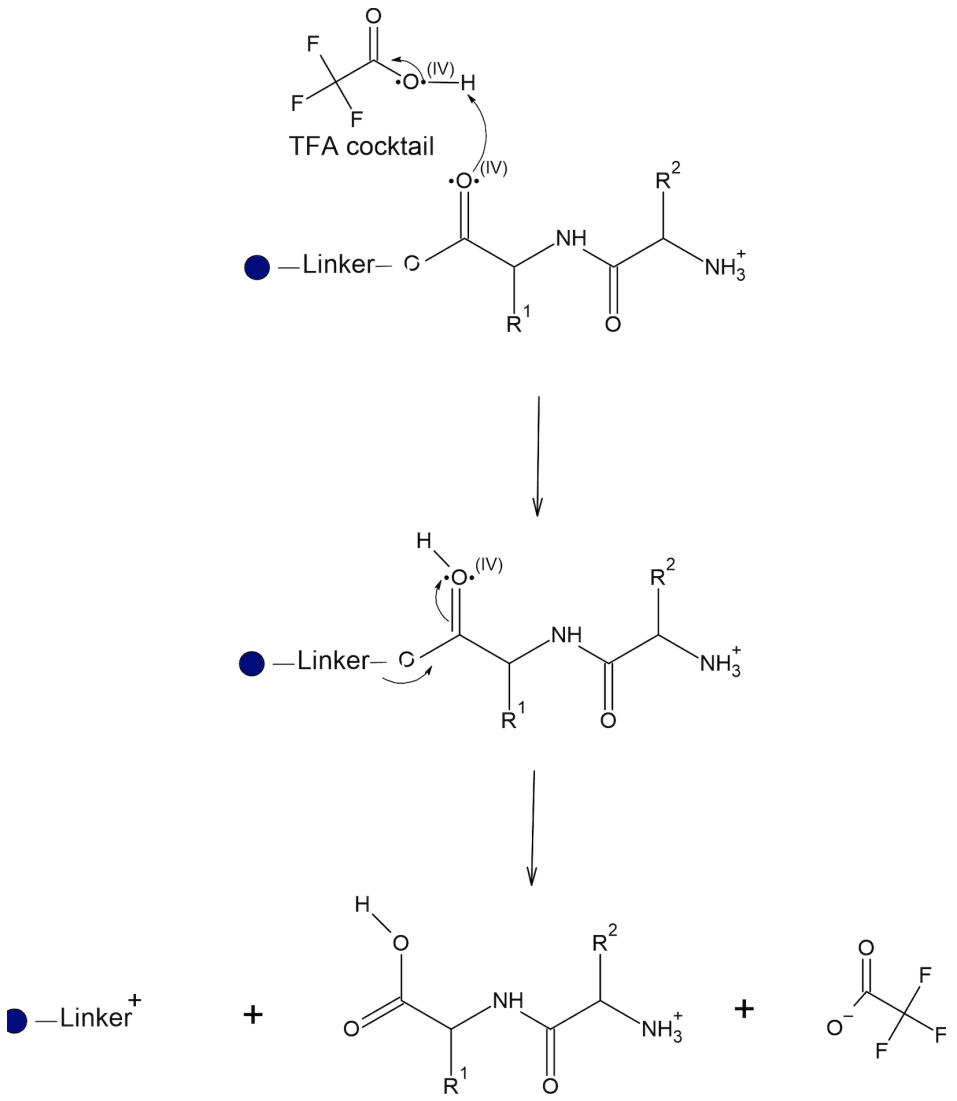


Figure 2.3: Cleavage procedure from the solid support [174]

2.3 Peptide Characterisation

The peptide yield and efficiency can be measured using different techniques but Liquid chromatography–mass spectrometry (LC-MS), the recommended technique, used to provide both the mass and the retention time of the peptide is a preferred technique for peptide analysis and determination of their purity. For the purpose of this research

a combination of LC-MS and Matrix-assisted laser desorption/ionization mass spectrometry (MALDI-TOF) is used to first determine the purity of the peptide prior to cleaning and after this step and second to find the retention time of the peptide to be used for the cleaning step with preparation High Pressure Liquid Chromatography (HPLC) [169], [175]. Peptide characterisation helps to find the purity and the efficiency of the synthesised peptides.

It is important to identify the purity of the peptides since there are three levels of acceptable purity when handling peptides. The peptides purities and their applications listed in Figure 2.4 can be used as a guid to decide the purity needed depending on the application. The purity of peptide is originally measured using a Reverse Phase LC-MS and the peptide is further tested using MALDI-TOF mass spectrometry and CD to perform structural analysis for the peptides.

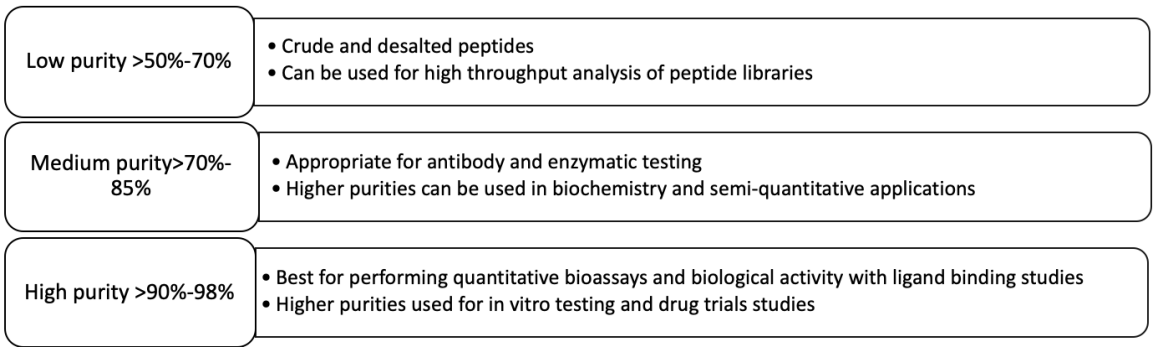


Figure 2.4: Peptide purity levels and their applications[176]

2.3.1 Liquid Chromatography-Mass spectrometry(LC-MS)

To find the retention time and quantify the peptides purity LC-MS is utilised. The instrument used was Waters SQD LC-MS [Waters, 2022], located in School of Chemistry, Mass Spectrometry Facility [University of Birmingham]. The methodology for LC-MS depends on the peptide's charge distribution, determinant of the polarity and

hydrophobicity of the peptide. Firstly the LC-MS was used in its HPLC format and when upgraded the instrument was paired with Waters Ultra High Pressure Liquid Chromatography (UPLC) system equipped with a Photodiode-Array Detector (PDA) detector in addition to the Electro spray (ESI) mass spectrometer [SQ2 detector with a Zspray] paired with the waters XSelect Peptide CSH C18 Column $130A^{\circ}$ of dimensions $2.5\mu m$ 2.1x100mm.

To get the retention time of the peptide and use it to estimate its retention time in Preparative High Pressure Liquid Chromatography (Prep-HPLC), a 50 minute run was utilised for HPLC and a 10 minute run for UPLC system with mobile phase composition of water+0.1% Formic acid (FA) and Acetonitrile (ACN) +0.1% (FA) with different gradient shown in tables 2.1a and 2.1b for HPLC and UPLC at $40^{\circ}C$ respectively. The combination in which the mobile phase and the stationary phase were chosen is important to the overall separation power provided by the instrument. Therefore, finding an optimal methodology for each peptide is essential. Peptides were prepared using 20% acetonitrile/water solvent to concentrations of 1mg/ml.

To find and identify the correct fraction eluted from the column, a combination of mass spectrometry and UV detection was employed. Since the mass spectrometer only plots the mass/charge ratio of the peptides against the strength of their signal, their overall Molecular weight (MW) of the peptide is divided by different positive charges in ESI+ mode. Since all peptides have a charge of more than 4+ this method was applied to all peptides synthesised in this experiment. Since all peptides have a Trp(W) residue incorporated in the sequence, the PDA detector allows the detection of peptides at 280nm absorption.

Table 2.1: Gradient conditions as a percentage of organic and inorganic solvents used with two different LC systems coupled with Mass spectrometry

(a) HPLC system

Time(min)	Water+0.1%Formic acid	Acetinitrile+0.1%Formic acid
0	95	5
0.1	95	5
30	5	95
40	5	95
40.1	95	5
50	95	5

(b) UPLC system

Time(min)	Water+0.1%Formic acid	Acetinitrile+0.1%Formic acid
0	95	5
0.1	95	5
6	5	95
9	5	95
10	95	5

2.3.2 Preparative HPLC

The peptides are purified on Agilent 1260 Infinity Prep-HPLC system in the School of Chemistry, Chromatography Facility [University of Birmingham]. To be able to translate the methodology used with the smaller column on the LC-MS system to the bigger XSelect Peptide CSH C18 OBD Prep Column $130A^{\circ}$ of dimensions $5\mu m$ 19x150mm on the Prep-HPLC system, Waters Gradient Calculator webpage for conversion of the methodologies between different column dimensions was used. The composition of the mobile phase was also kept constant between the instruments with water+0.1% FA and ACN +0.1% FA. The gradient shown in table 2.2 was used for all the crude peptides that were injected at 1mg/ml concentration dissolved in 20% acetonitrile/water solvent

injected at the maximum volume of 10ml due to the limitations in the volume of the loop used in conjunction with the instrument.

Table 2.2: Gradient conditions as a percentage of organic and inorganic solvents scaled for the larger column on the Prep-HPLC system

Time(min)	Water+0.1%Formic acid	Acetinitrile+0.1%Formic acid
0	95	5
0.3	95	5
24	60	40
30	60	40
31	95	5
40	95	5

The fractions collected were analysed on the MALDI-TOF instrument to determine the correct fraction is freeze dried and subsequently used for the biological analysis.

2.3.3 Matrix-Assisted Laser Desorption/Ionization-MALDI-TOF

In this methodology the Brukers Ultraflextreme Matrix Assisted Laser Desorption/Ionization mass spectrometry(MALDI-MS) [Bruker, 2022] located in the School of Chemistry, Mass spectrometry Facility [University of Birmingham] was used and the peptides were prepared by an addition of matrices that assist with the ionisation of the samples via crystal formation. In this experiment, matrix Dihydroxybenzoic acid (Super-DHB) was used purchased from [Fisher Scientific, 2019]. 10mg/mL of Dihydroxybenzoic acid was prepared by diluting in a 50:50 methanol:water solution [177]. The concentration of the samples were chosen as 10%v/v dilution by using 2 μl of the sample. A series of 1:10 dilutions were made to obtain the best concentration of the samples for the optimised crystallisation.

2.3.4 Circular Dichroism-CD

This instrument helps to measure and determine the structure of optically active and chiral molecules as linearly polarised light when passed through a circular dichroic sample will become elliptically polarised. ASCO-1500 series CD instrument School of Biosciences University of Birmingham was used to assess the conformation of the peptides in initially in two different conditions of SDS and PBS with pH of 7 and 7.4 respectively and 0.02mg/ml concentration for each peptide. For the later studies the experiments were expanded and the peptide conformations were analysed using LTA, LPS and DPC for better understanding of these different conditions and their effect on the structure of the peptides. A quartz cuvette with 1mm path length was used [178].

Peptides and proteins are one example of molecules that can be analysed with this instrument. CD employs the use of circularly polarised light which travels towards the sample and determines the structure by measuring the change between the right-circularly polarised light (l_R) and left-circularly polarised light (l_L) [179]. Different structures will have different affinity for either of the circularly polarised light and this affinity is detected by the photon detector. This detector will then provide a graph of the absorption of light which then accounts for the ability of chiral molecules to rotate the plane of polarised light of the D-line of sodium. The degree of ellipticity θ in millidegrees m° is the tangent of the ratio of the minor to major elliptical axis shown

in figure 2.5 [180].

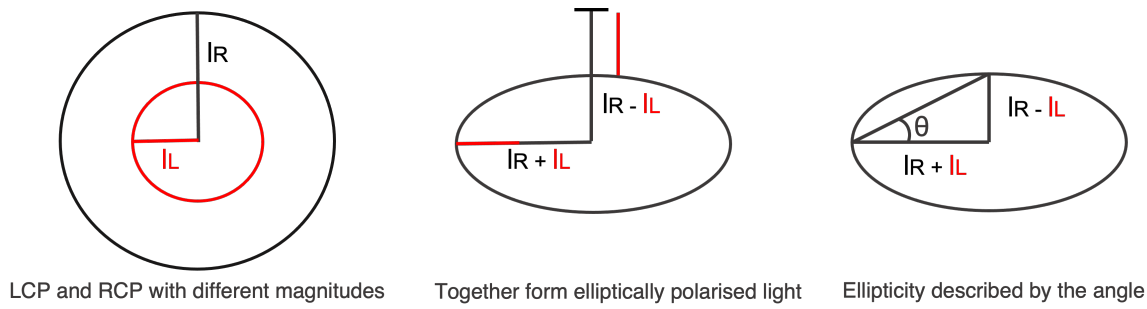


Figure 2.5: Illustration that shows the formation of elliptical shape as opposed to a direct circle changing the way the light is calculated

To be able to find the individual residue ellipticity that allows for the easier comparison between different proteins the mean residue ellipticity $[\theta]$ MR is calculated for which the mean residue concentration is needed. Figure 2.1[181] shows the equation for the calculation of this value that has been used throughout this experiment.

$$\begin{aligned}
[\theta] &= \theta \times \frac{0.1 \times MRW}{(C \times P) \times 3298^2} \\
[\theta] &= MeanResidueEllipticity(degrees cm^2 dmol^{-1} residue^{-1}) \\
\theta &= MachineunitinMillidegrees(mdeg) \\
Meanresidueweight(MRW) &= \frac{proteinmeanweight(Da)}{Numberofresidues} \\
P &= Cuvettelength(cm) \\
C &= PeptideConcentration(mg/ml)
\end{aligned} \tag{2.1}$$

2.3.5 Peptide Stability

The analysis was performed on the peptide that showed the most antimicrobial activity and its corresponding alanine substitutions. The stability was tested against the human serum which is the most comparable test to the bodily conditions that the peptides will encounter [182]. First the peptides were diluted using RPMI1640 media to a final concentration of $300\mu M$ stock that was then reduced to a final concentration of $20\mu M$ when added to human serum. Before the addition of the peptides, the media was supplemented with 25% serum that was warmed through for 15 minutes at $37°C$.

Once the supplement serum was warmed through, $70\mu l$ of the peptide was added to 1ml of the serum supplement and left for 1 hour at $37°C$ for the reaction to complete. $100\mu l$ of the solution was then added to 96% ethanol, cooled to $4°C$ for 15 minutes and spun on eppendorf centrifuge at 18000g for 2 minutes to pellet the serum and take the supernatant for analysis. The pellets were then suspended in de-ionised water to be analysed on LC-MS and MALDI-TOF according to their methodology mentioned in section 2.3.3 2.3.1.

2.4 Antimicrobial Studies

To be able to study the antimicrobial activity of the peptides their MIC was determined. Here MIC refers to the minimum inhibitory concentration in which there is visible loss of growth of bacteria in the presence of the peptide. To have a suitable representation of the antimicrobial activity of these peptides three different bacteria are chosen, *E. coli* to take into consideration the bacteria present in the lower intestine and the gut [183], *S. aureus* to represent a Gram positive bacteria that is common on implant surfaces as it is found on the skin and the upper respiratory tract [184] and *P. aeruginosa* to represent a commonly studied bacteria in all of antimicrobial studies due to their ability

to show resistance to commonly used antibiotics and additionally for their ability to create biofilms and therefore render the antibiotics useless for their defence [185].

2.4.1 Minimum Inhibitory Concentration-MIC

The frozen stock of bacteria supplied by the School of Dentistry [University of Birmingham] was streaked shown in Figure 2.6 on a Tryptic Soy Agar (TSA) agar plate and left in the incubator at $37°C$ with a supply of 5% CO_2 for 24 hours for the formation of single colonies.

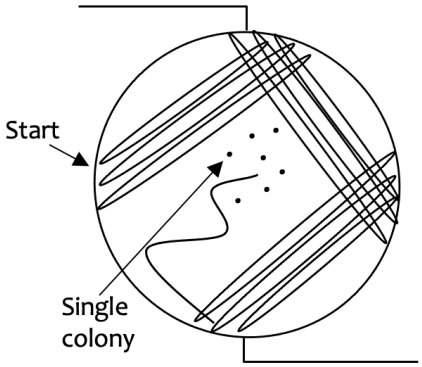


Figure 2.6: Plate streaking using different bacteria with a sterile loop.

Antibiotics used as positive control for each bacteria were Ciprofloxacin [186] for *E. coli*, Polymixin B [187] for *P. aeruginosa* and Vancomycin [188] for *S. aureus*. Each antibiotic stock was made using sterile water and the powder after which the stock was filtered using a $0.45\mu m$ sterile filters. The stock antibiotic was then diluted on the day of the experiment to their corresponding MIC shown in table 2.3.

Table 2.3: Antibiotic final concentration used as a positive control.

Antibiotic	Target bacteria	Concentration in the 96 well plate
Ciprofloxacin	*E. coli*	$3\mu M(1\mu g/mL)$
Polymixin B	*P. aeruginosa*	$1.8\mu M(2mg/L)$
Vancomycin	*S. aureus*	$1.3\mu M(2\mu g/mL)$

To be able to perform the MIC assays, two single colony were taken and grown in 10ml of MHB at $37°C$ on a shaking incubator and after 18-24 hours, the overnight culture was diluted to an Optical Density (OD) at 600nm of 0.1 [2×10^9Colonie Forming

Units (C.F.U)]. These bacteria were used as inoculum for the 96 well plates. The peptides were diluted to a final concentration of $500\mu M$ using MHB to keep the solvents consistent. These peptides were then used to perform a 2-fold dilution until a final concentration of $16\mu M$ is reached and the 96 well plate was then filled in 1:1 ratio with the inoculum and the different concentration of peptides, shown in Figure 2.7. Similarly, the antibiotics and broth were also added to the plate in a 1:1 ratio to the inoculum as positive and negative control respectively. The plates were left in a shaking incubator at $37°C$ and after 18 hours of incubation the OD at 600nm was measured using a ELx800 microplate reader [Bio-Tek ,2022].

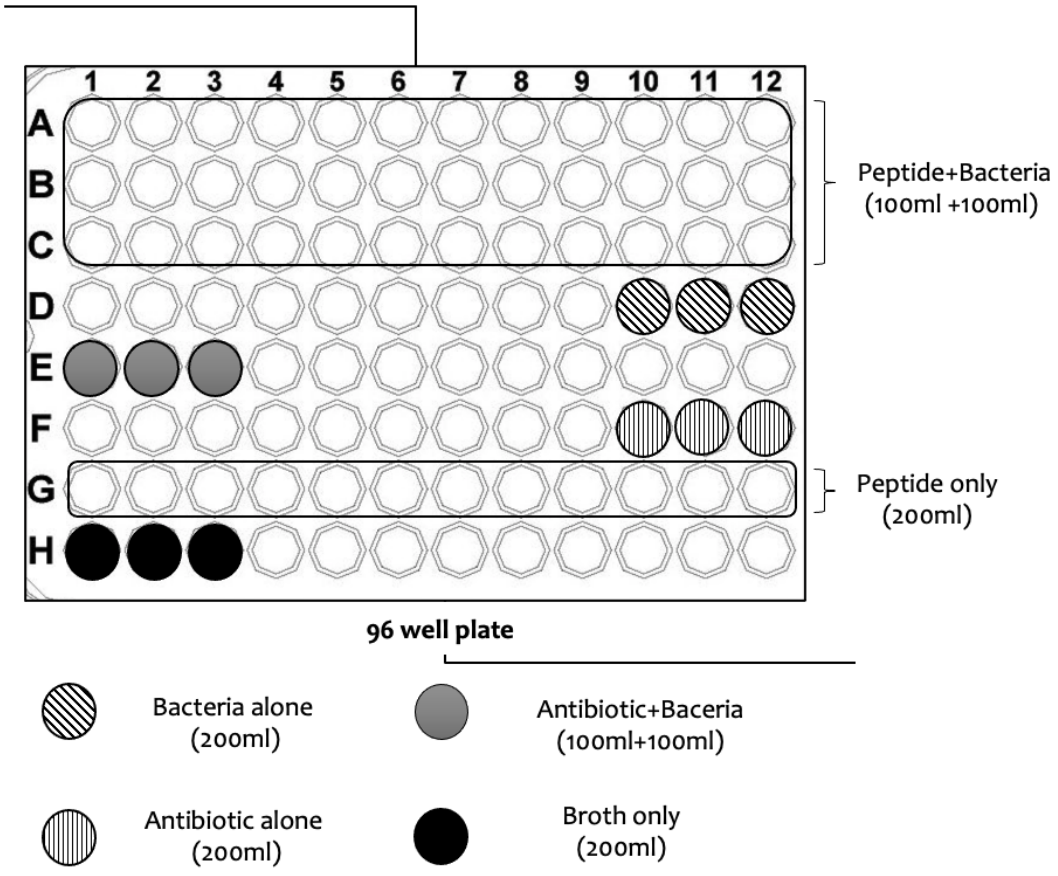


Figure 2.7: Arrangement used for the 96 well plate to avoid cross contamination and determine the OD at 600nm.

2.4.2 Antimicrobial Resistance studies

In addition to the determination of the MIC values for each designed peptide, the resistance of each bacteria was tested against the most active antimicrobial peptide. The experiment was performed using the same technique as mentioned in subsection 2.4.1 in 96 well plates but the inoculum chosen was taken from the well that showed minimal bacterial growth and not a full inhabitation of bacterial growth. This inoculum was measured and the OD_{600} was adjusted to 0.1 to keep a consistent inoculum concentration per experiment. The experiment was repeated in cycles until antimicrobial resistance was observed.

To assess the presence of only the desired bacteria each time the inoculum was plated and observed for colony integrity. If infection was observed the experiment was repeated from the last non infected plate from a frozen batch of inoculum.

2.5 Cell Culture Studies

Cell culture studies were performed in the School of Dentistry, University of Birmingham. HeLa cells supplied by the school were used due to their epithelial nature and extensive documentation when dealing with antimicrobial peptides [189]–[191]. To find the toxicity of the designed peptides the viability of the cells

2.5.1 Cell Viability

First the DMEM media was supplemented with 10% FBS, 5% of Penicillin-Streptomycin and 5% L-Glutamine. To start the cells from the frozen passage II stock supplied, the stock was defrosted and immediately centrifuged at 1000RPM for 3 minutes to pellet the cells. Once the supernatant was removed the cells were resuspended in 1ml of sup-

plemented media and were added to a flask containing 14ml of fresh media and allowed to grow at $37°C$ under 5% CO_2 to reach $80-90\%$ confluency. The cells were then trypsinised using 0.25% Trypsin to be used in the 96 well plates. The cells were allowed to grow at different concentrations to assess the signal of the MTT assay at different number of cells per well to find the optimum cell number per well and concluded to include 100,000 cells per well for the cytotoxicity experiments.

The experiments were then started with the trypsinised cells added to each well of a 96 well plate, incubated at $37°C$ under 5% CO_2 overnight to reach confluency per well. The plates were then removed from the incubator and washed with PBS and the media was replaced with the peptides, diluted with DMEM starting from $500\mu M$ to $16\mu M$ and left in the incubator overnight. The CyQuant MTT kit was used by dissolving the MTT reagent in 1mL of PBS and once the DMEM media was removed from the wells, $50\mu L$ of the MTT reagent along with $50\mu L$ of fresh un-supplemented DMEM media without phenol red was added to each well and incubated for 4 hours. Once the plate was removed from the incubator, $100\mu L$ of SDS dissolved in $5\mu L$ of PBS was added to each well and incubating for an additional 4 hours. The plates were observed using a ELx800 microplate reader [Bio-Tek ,2022] and the OD was measured at 570nm. Media alone was used as positive control and DMSO was used as negative control. There was also the MTT reagent alone as a control of the kit integrity.

2.6 Molecular Dynamic Simulations

To aid in the better understanding of the interactions between the different membranes and the peptides, some of the peptides were chosen in the order of their activity and Molecular Dynamic Simulation (MDS) was used to model this interaction. I-Tasser [192] was used to first model the peptide structure in free form and without the presence of any membrane. The membranes were then constructed using

Charmm-gui [193] online membrane builder tool with the presence of the peptide. The resulting membrane peptide combination were then minimised and equilibrated through 5000 and 50000 steps respectively and simulated for 10ns using Gromacs [194]. The steps for the simulation are shown in Figure 2.8 1-palmitoyl-2-oleoyl-sn-glycero-3-phosphocholine (POPC) and Dimyristoylphosphatidylglycerol (DMPG)/ Dimyristoylphosphatidylcholine (DMPC) where used to model zwitterionic mammalian membrane and bacterial membrane, respectively [195], [196] .

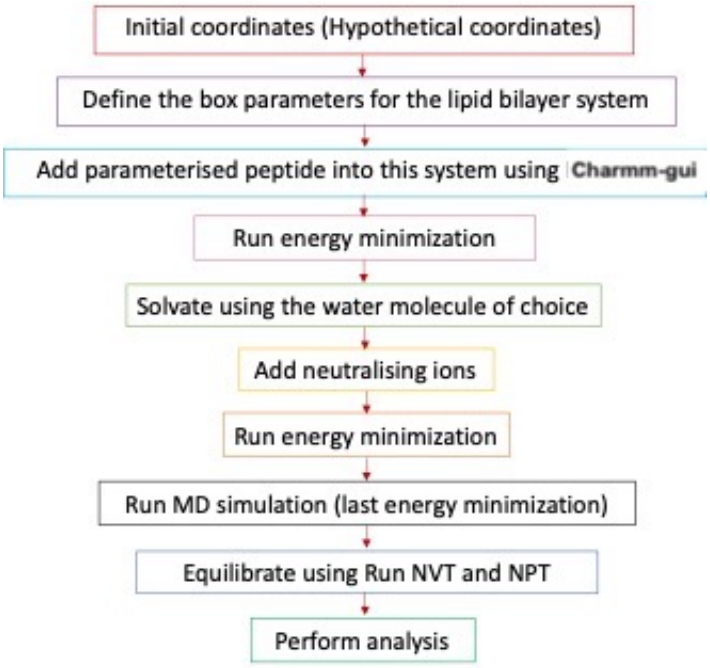


Figure 2.8: Molecular dynamic simulation steps performed using Gromacs.

2.7 Statistical analysis

2.7.1 Prediction models

The predicted structures were constructed through I-TASSER software that uses a combination of methodologies to compile a three-dimensional structure for the pep-

tides. The method used within the software includes threading the sequence of the peptide into a database of known protein structures to determine similar structures snd templates with similar folds. It involves aligning the sequence to the template found through the initial search and construction of secondary structure based on this similarity. Through model generation the identified template structure is used to generate an initial three-dimensional structure through fragment assembly. Through energy minimisation and spatial restraints the fragments are refined and recombined to produce initial models. Side chain packing and loop modelling techniques are also employed to enhance accuracy. After this step a series of models are produced and I-TASSER provides ranking of the models based on their similarity percentages to the specific protein sequence and the top ranking models are selected as prediction models.

2.7.2 Antimicrobial analysis

To find the significance of the antimicrobial activity of the peptides designed a One Factor ANOVA test was used with Dunnett's and Tukey HSD. This methodology was employed to test the significance of the antimicrobial activity as a whole without the consideration of the concentration and to later test the effect of concentration on the activity of the peptides against the bacteria. If the p-value was below 0.05 with mean value of inhibition higher than the positive control the results were favourably significant. All figures were produced using Matplotlib in Python.

Chapter Three

Antimicrobial Peptide Design

3.1 Design Strategy

To begin the process of peptide design that show antimicrobial activity against a variety of bacterial species, several criteria were implemented to ease the process of synthesis and to increase the likelihood of antimicrobial activity in the designed sequences based on hBD. These criteria were executed by the reduction of sequence length between 20-22 amino acids long and the removal of the Cysteine (Cys - C) residues from original sequence to ease the synthesis process and reduce the complication of side disulfide bridge formation during peptide interactions with other peptides and the bacteria. According to previous research hBD1 and hBD3 maintain their antimicrobial activity in the reduced form without the formation of the disulfide bonds [72]. Hence it was hypothesised that the removal of Cys residues from the sequence would not have an effect on the antimicrobial activity of the new designed sequences. Additionally, alpha helical peptides have shown a consistent antimicrobial activity throughout the literature so the aim of the modifications were to ultimately achieve an alpha helical structure [185]. The sequence and choice of amino acid in each position was also influenced by the alignment of the designed sequence to the original parent sequence of, hBD1 or hBD3, to find the percentage of alignment, avoiding a random design of de novo antimicrobial peptides.

To achieve these incentives, the Cys residues were removed from the original sequence and replaced with the most abundant amino acid residues in those positions found in known antimicrobial peptides shown in Figure 3.1 and the sequences were shortened by the removal of the least abundant residues found in antimicrobial peptides from the original sequence. These sequences were then aligned using 3 different database of (ADP3 [197], DBAASP [198] and, CAMP [199]). All the peptides shown aligned to their corresponding parent peptide and those that did not show alignment were discarded.

As shown in Figure 3.1 Tryptophan (Trp - W) is not a common amino acid found in antimicrobial peptides, however, in this study it was incorporated in most sequences due to the ease of detection as a result of its ring structure as well as its known toxic effect on pathogens. However, the addition of Trp residue was kept to a minimal due to its toxic effects towards mammalian cell lines attributed to its cell penetrating ability [200].

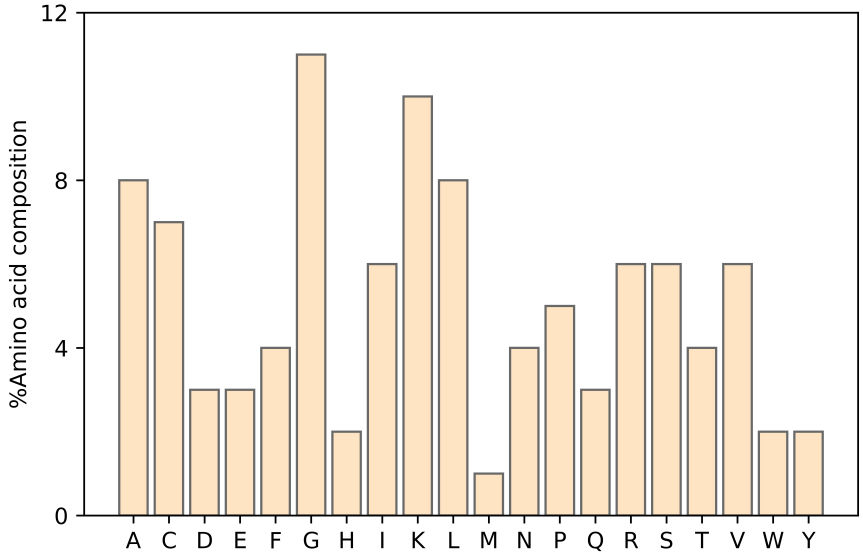


Figure 3.1: Percentage of 20 natural amino acids in antimicrobial peptide based on their abundance in 3579 peptides found in ADP3 databases [197]

3.1.1 Sequences of potential antimicrobial peptides based on hBD1

Table 3.1 shows the sequences designed based on hBD1. Each line includes the sequence, molecular weight, charge and the hydrophobicity of each design as well as the original sequence that the peptides are based on in the first row of the table.

Table 3.1: List of potential antimicrobial peptides based on hBD1 with their corresponding molecular weight (MW), number of amino acid residues (AA number) and charge.

Peptide Name	**Sequence**	**AA number**	**Charge**	**Hydrophobicity**(%)	**MW** (g/mol)
Original HBD1	DHYNCVSSGGQCLYSACPIFTKIQGTCYRGKAKCCK	36	+4	36	3977
HBD-mod1	DSGQARKPIFTKIYRGWRKIAK	22	+6	32	2620
HBD-mod2	DYSLYAPIFTKIRGTYRGKAK	21	+4	29	2449
HBD-mod3	GGLYAPIFTKIRGTYRGKAKK	21	+6	29	2326
HBD-mod4	GLGDKLAKGKAKGLGWKIAK	20	+5	40	2039
HBD-mod5	GLGDKLAKGKWKTYRGKAKK	20	+7	25	2234
HBD-mod6	GLGPKLAKGKWKTYRGKAKK	20	+8	25	2215
HBD-mod7	GLGPKLAKIKWKTYRGKAKK	20	+8	30	2272
HBD-mod8	GLGPKLAKIFTKWKTYRGKAK	21	+8	33	2392

According to this table HBD-mod1 and HBD-mod8 share a very similar hydrophobicity profile to the original hBD1 sequence. HBD-mod1-3 were designed to align to the original hBD1 sequence and according to Figure 3.2 they show a similarity ranging from 43% to 55% for both HBD-mod2 and -mod3. As these sequences were the first three designed peptides they show a strong similarity to the original sequence, sharing a consensus sequence of 'PIFT' and 'YRGKAK' according to Figure 3.3 with the original hBD1. HBD-mod4 on the other hand, shows the least similarity to the original sequence showing a strong hydrophobic sequence with only 24% similarity to the original sequence with only the amino acid Glycine (Gly - G) as a consensus. This is due to the design of this peptide, which was a culmination of most frequent amino acid residues for each position observed in antimicrobial peptides found in different databases and literature.

Using HBD-mod4 as a starting point for the rest of the peptides in this series, HBD-mod5 and HBD-mod6 were designed to align to both hBD1 and HBD-mod4 to achieve an antimicrobial peptide that shows abundant amino acids at each position whilst maintaining its similarity to the original hBD1. Therefore HBD-mod5 and -mod6 both show 35% similarity to the original sequence with 'YRGKAK' as the main

consensus sequence. In an effort to increase the alignment percentage to the original

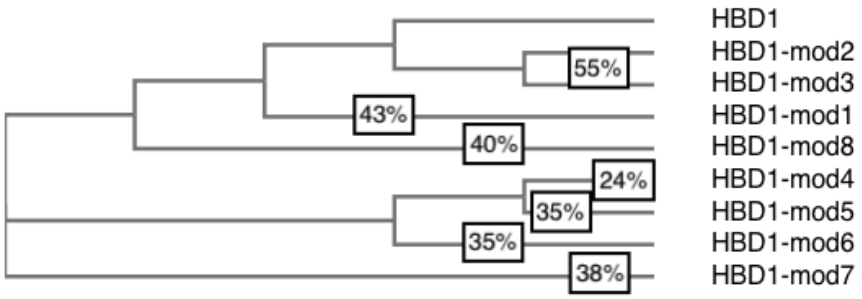


Figure 3.2: Phylogenic tree of the hBD1 peptide series showing their parentage similarity and their relationship. Figure produced through Clustal Omega [201] showing the relationship between each sequence in the series of peptides based on hBD1 where the percentages shown are representative of the peptide alignment to the original hBD1 sequence and to each other respectively found through alignment using the ADP database.

hBD1 the sequence of these two peptides was further refined to align 38% and 40% to hBD1 for HBD-mod7 and -mod8, respectively. The weakest similarity was shown to be between the sequence of HBD-mod4 and hBD1, due to the lack of consensus sequence with the original peptide sequence. It can also be seen that HBD-mod5 and HBD-mod6 are the most similar to HBD-mod4, as they were designed by the combination of HBD-mod4 and hBD1.

3.1.2 Structure of potential antimicrobial peptides based on hBD1

Figure 3.4 shows the structure of each peptide with their corresponding amino acid frequency compared to other antimicrobial peptides in each position. These Figures display the structure of the peptides as well as its compositional hydrophobicity depending on the amino acid in each position where the white show non-polar amino acids, blue shows basic residues, red shows acidic residues and green shows the polar

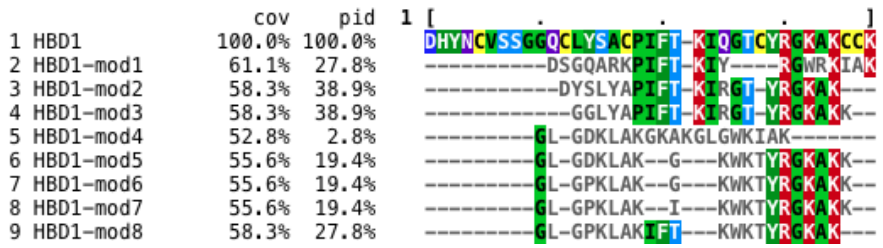


Figure 3.3: Multiple sequence alignment results for the peptides based on hBD1. The sequence at the top of the first point of comparison. Figure produced using Mview Clustal Omega [201] showing the consensus sequence between each peptide and the original sequence. Red residues are positively charged, Green residues are hydrophobic, Blue residues are negatively charge, Yellow residues are cysteines. Cov = coverage referring to the aligned positions in a sequence that contain actual residues representing the percentage of aligned amino acid sequence, Pid = Percent measuring the similarity between aligned residues in the sequences. It is calculated through determination of the percentage of positions in the alignment where the amino acids are identical across all sequences.

amino acids. On the other hand, the structure is highlighted by magenta for alpha helical, beta sheets are coloured yellow and pale blue shows turns and white shows all other structures.

In order to find the most antimicrobial peptide, the refinements were not only done to increase the percentage of alignment towards the hBD1 original sequence shown in Figure 3.2 but to also increase the alpha helical structure of the final designed peptide as shown in Figure 3.4a and 3.4o for HBD-mod1 and HBD-mod8, respectively.

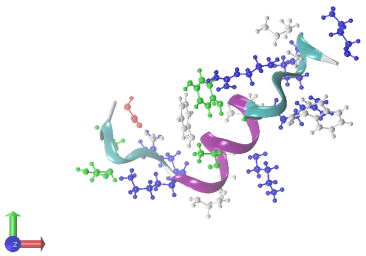
Although HBD-mod2 and -mod3 both aligned strongly to hBD1 their structure did not form an alpha helix according to Figure 3.4c and 3.4e, respectively showing a structure with the combination of a coil and β-sheet. Since the sequence of HBD-mod4 3.4g showed the least similarity to the original sequence and its structure retained a combination of all three structures including the alpha helical portion through the use

of 'GDKLAK' . This motif was repeated in all other sequences following this peptide to achieve the same alpha helical point in all the following sequences.

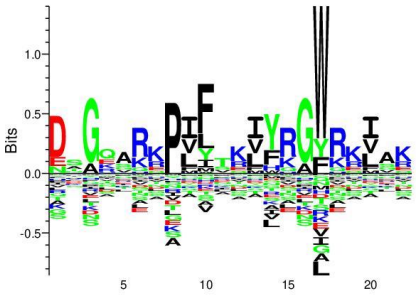
The change from this motif to 'GPKLAK' in the sequences of HBD-mod6, Figure 3.4k, and -mod7, Figure 3.4m, reduced their portion of their structure to a non alpha helical proportion, which was further refined by continuation of the motif 'IKW' in HBD-mod7 and the sequence of 'IFIKW' in HBD-mod8 that allowed the alpha helical structure to return. This motif was copied partially from the 'PIFIKI' motif of HBD-mod1 shown in Figure 3.4a which also showed an alpha helical portion in the overall structure. In fact HBD-mod1, -mod3, -mod2 and -mod8 share the 'IFT' motif with the original hBD1.

The logos in Figure 3.4 show the conserved nature of each amino acid at each position through the size of the amino acid where the larger the size the more conserved the amino acid in that position. Additionally, these figures show other conserved amino acids in the position which helps with choosing other amino acids for the following sequence of the series.

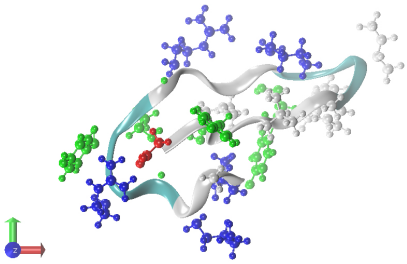
W shows the most conserved profile since it is the largest amino acid when compared to the rest. This amino acid was shown in all of the sequences in Figures 3.4h-3.4p. Other amino acids of note according to the logos are Phenylalanine (Phe, F) in Figure 3.4f that was removed from the sequence for the following sequences but later added to the last sequence of the series HBD-mod8 in Figure 3.4p. The last G in the sequences of HBD-mod2, -mod3, -mod5, -mod6, -mod7 and, -mod8 also shows a conserved nature between all of the logos. Proline Pro, P in the forth position was also conserved according to Figure 3.4l, 3.4n and 3.4p.



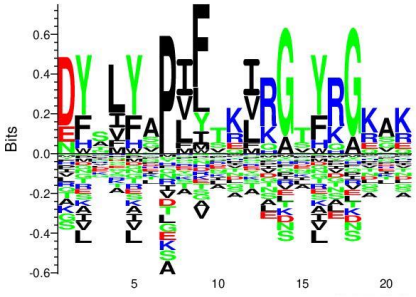
(a) HBD-mod1



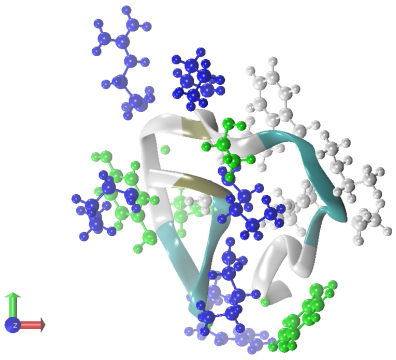
(b) HBD-mod1-logo



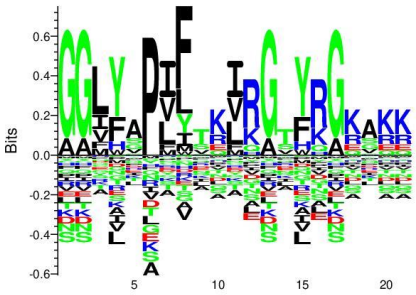
(c) HBD-mod2



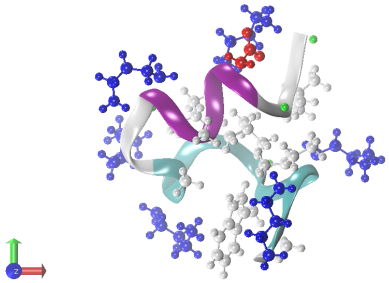
(d) HBD-mod2-logo



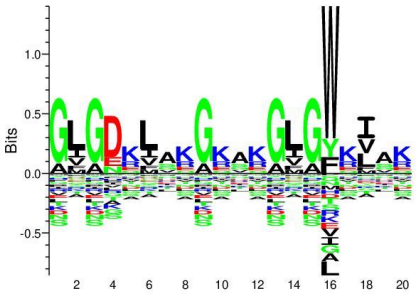
(e) HBD-mod3



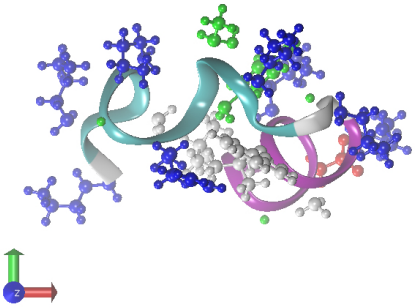
(f) HBD-mod3-logo



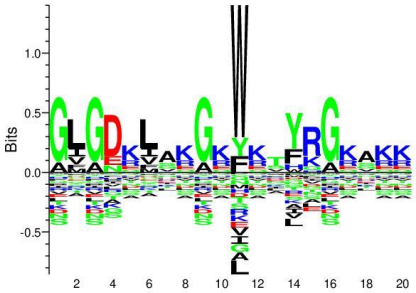
(g) HBD-mod4



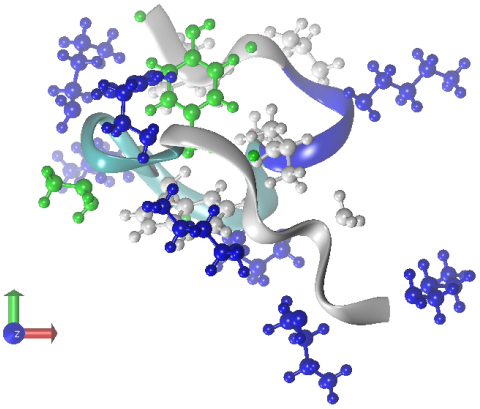
(h) HBD-mod4-logo



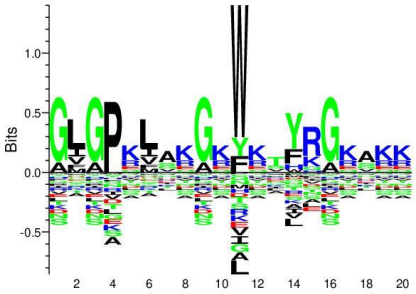
(i) HBD-mod5



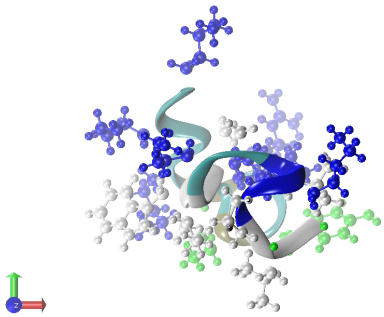
(j) HBD-mod5-logo



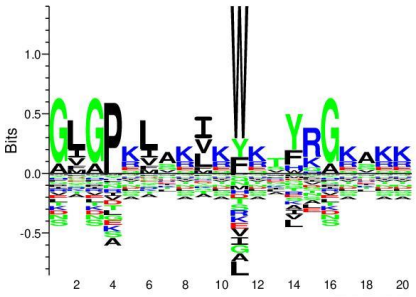
(k) HBD-mod6



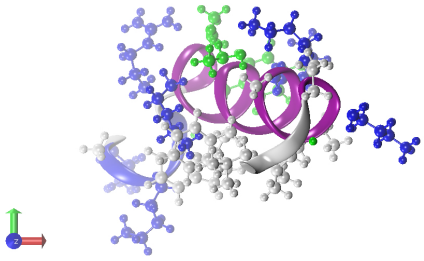
(l) HBD-mod6-logo



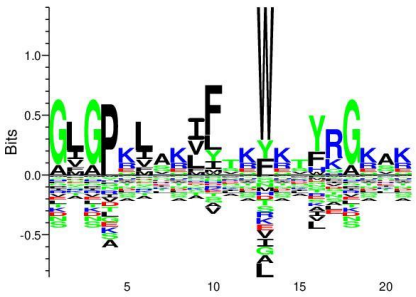
(m) HBD-mod7



(n) HBD-mod7-logo



(o) HBD-mod8



(p) HBD-mod8-logo

Figure 3.4: Showing the secondary structure of peptides based on hBD1 as well as their amino acid frequency represented in a logo format, where the height of the symbol represents relative frequency of each residue, the overall height of the stack represents at each position reflects the level of conservation and the width of the symbol shows the degree of uncertainty at that position. The peptides are represented through a Newribbon for the structure represented by magenta for alpha helical, blue for turns and white for other types of structures. Residues are coloured by their type in both logos and their structure where non-polar residues are in (white/black), basic residues, acidic residues and polar residues.

These figures were produced using Seq2Log [202] which calculates the frequency of each amino acid at each position using a frequency matrix showing the distribution of each residues at each position and I-TASSER [203] constructs a three-dimentional model of the peptide through fragment assembly and ab initio modelling to generate three dimensional models. The models were visualised using VMD [204].

3.1.3 Sequences of potential antimicrobial peptides based on hBD3

Table 3.2 shows the sequences designed based on hBD3. Similar to table 3.1 this table shows the sequences, molecular weight, charge and the hydrophobicity of each sequence designed as well as the original sequence. In this peptide series all the designed peptides were based on the original sequence hence the higher similarity percentages than those observed with the peptides based on hBD1.

Table 3.2: List of potential antimicrobial peptides based on hBD3 with their corresponding molecular weight (MW), number of amino acid residues (AA number) and charge.

Peptide Name	**Sequence**	**AA number**	**Charge**	**Hydrophobicity**(%)	**MW** (g/mol)
Original HBD3	GIINTLQKYYCRVRGGRCAVLSCLPKEEQIGKCSTRGRKCCRRKK	45	+10	33	5161
HBD3-mod1	GGRAWLPKWIGKWTRGRKRKK	21	+8	29	2566
HBD3-mod2	GGRALPKWIGKWTRGRKRKK	20	+8	25	2380
HBD3-mod3	GGRALPKQIGKWTRGRKRKK	20	+8	20	2322
HBD3-mod4	GGRALPKEQIGKWTRGRKRKK	21	+7	19	2451
HBD3-mod5	GGRALPKEEQIGKWTRGRKRKK	22	+6	18	2580
HBD3-mod6	GGRALPKWIGKWTRGRKRRKK	21	+9	24	2536
HBD3-mod7	GGRALPKWIGKWSTRGRKRRKK	22	+9	23	2623

The most similarity in this series of peptides was observed between HBD3-mod4 and -mod5 at 47% with hBD3. These peptides showed a positive charge of 7 and 6, respectively, followed by the lowest percentage hydrophobicity compared to the rest of the peptides in the series based on hBD3. HBD3-mod7 showed the second highest similarity to the original sequence at 44%, with a relatively large positive charge as well as percentage hydrophobicity of 23. This peptide seems to be the best candidate for antimicrobial activity. HBD3-mod1, -mod2 and mod6 all show varying levels of similarity as well as hydrophobicity compared to the original sequence not showing notable differences between each peptide.

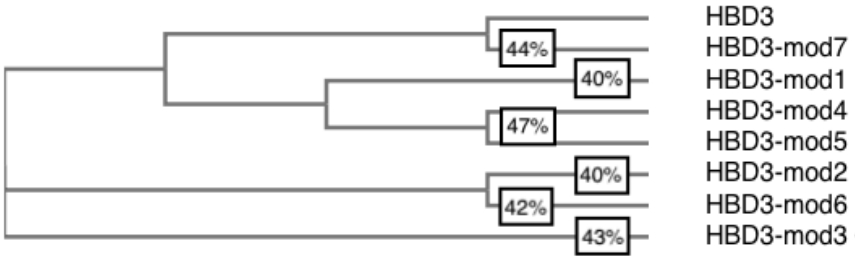


Figure 3.5: Phylogenic tree of the hBD3 peptide series showing their percentage similarity and their relationship. Figure produced using Clustal Omega [201] showing the relationship between each sequence in the series of peptides based on hBD3 where the percentages shown are representative of the peptide alignment to the original hBD3 sequence and to each other respectively found through alignment using the ADP database.

Figure 3.6 shows the consensus sequences shared between each peptide and the original hBD3 sequence. the consensus motif that is shared between HBD3-mod4 and -mod5 is 'LPKEEQIGK' with the difference of first Glutamic acid (Glu - E) residues which is only included in HBD-mod5. This consensus is repeated in HBD3-mod6 and mod7 with the removal of the 'KEEQ' motif, where 'STRGRK' is repeated in HBD3-mod7.



Figure 3.6: Multiple sequence alignment results for the peptides based on hBD3. The sequence at the top marks the first point of comparison. Figure produced through Mview Clustal Omega [201] showing the consensus sequence between each peptide and the original sequence. Red residues are positively charged, Green residues are hydrophobic, Blue residues are negatively charge, Yellow residues are cysteines. Cov = coverage referring to the aligned positions in a sequence that contain actual residues representing the percentage of aligned amino acid sequence, Pid = Percent measuring the similarity between aligned residues in the sequences. It is calculated through determination of the percentage of positions in the alignment where the amino acids are identical across all sequences.

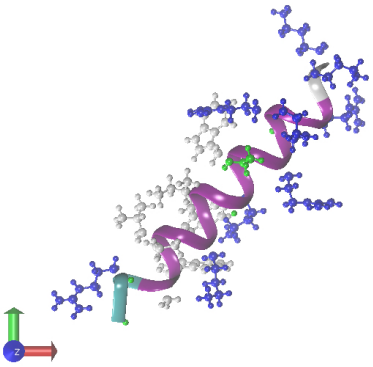
All the peptides in the series share the motif 'LP' and 'IGK' with the original sequence. Although the 'RK' motif is repeated in all but HBD3-mod1, -mod4 and -mod5, this motif is the same as 'RKCCRRKK' of the original sequence with the 'CC' removed for ease of sequencing on HBD3-mod6 and -mod7.

3.1.4 Structure of potential antimicrobial peptides based on hBD3

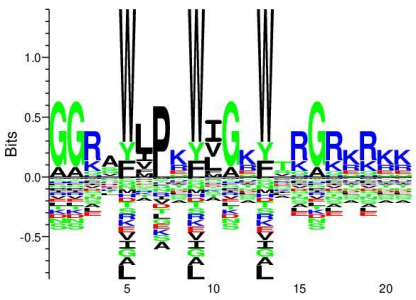
Figure 3.7 shows the structure of each peptide in the series based on hBD3. Similar to Figure 3.4 this figure shows both the structure of the peptide as well as its residue logo showing the wight of each amino acid per position. The peptides are displayed through the secondary structure as well as their amino acid type, where the white show non-polar amino acids, blue shows basic residues, red shows acidic residues and

green shows the polar amino acids. On the other hand, the structure is highlighted by magenta for alpha helical, beta sheets are coloured yellow and pale blue shows turns and white shows all other structures.

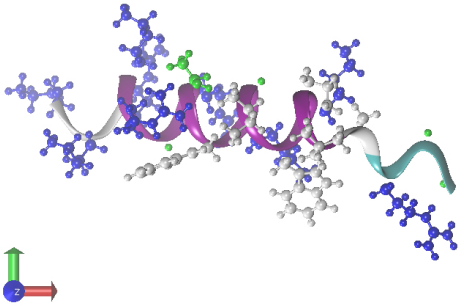
HBD3-mod1 in Figure 3.7a shows a majority alpha helical structure with W being the most prominent amino acid residue in this structure according t o Figure3.7b. Since W is shown in the literature to increase the cell penetration ability of the peptides one of these residues was removed in HBD3-mod2, Figure 3.7d, which changed the structure from a majority alpha helical structure to a combination of turns and other types of secondary structures. As seen through the alignment results the structure of HBD3-mod4 and -mod5 shown in Figures 3.7g and 3.7i respectively clearly show this similarity with very similar structural proportion of helical, turn and others which is owed to their similar sequences differing by the removal of E according to Figure 3.7h and 3.7j.



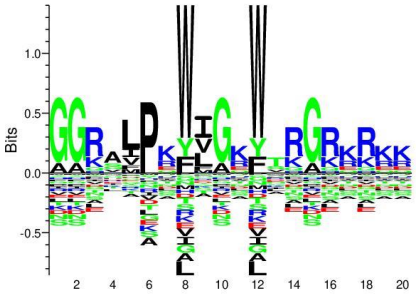
(a) HBD3-mod1



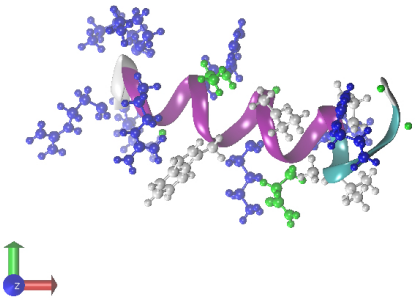
(b) HBD3-mod1-logo



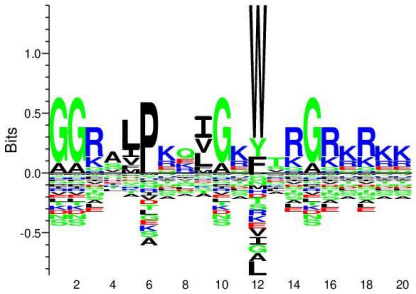
(c) HBD3-mod2



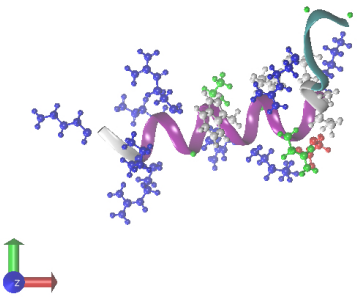
(d) HBD3-mod2-logo



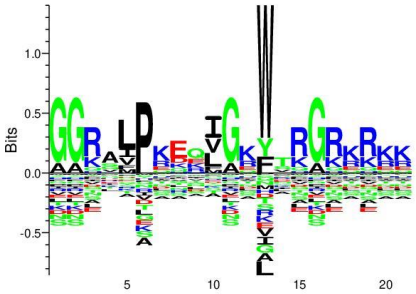
(e) HBD3-mod3



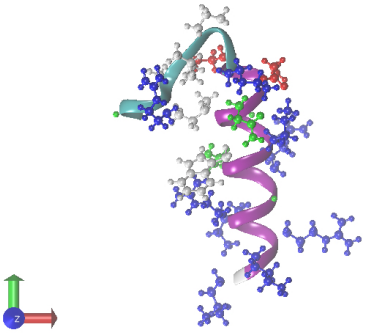
(f) HBD3-mod3-logo



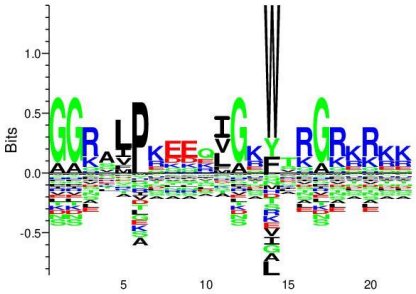
(g) HBD3-mod4



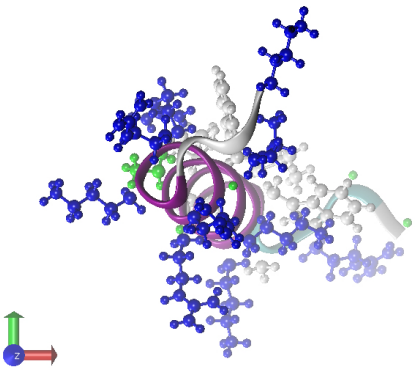
(h) HBD3-mod4-logo



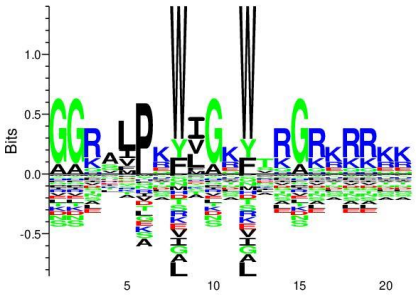
(i) HBD3-mod5



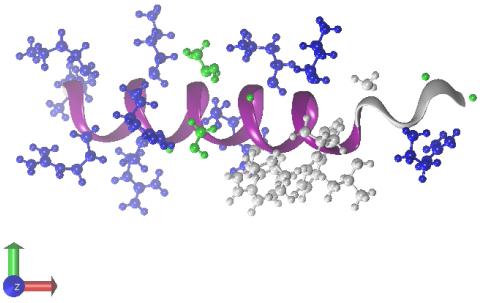
(j) HBD3-mod5-logo



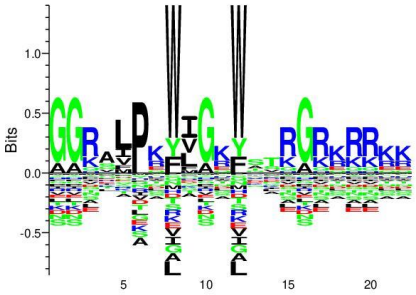
(k) HBD3-mod6



(l) HBD3-mod6-logo



(m) HBD3-mod7



(n) HBD3-mod7-logo

Figure 3.7: Showing the secondary structure of peptides based on hBD3 as well as their amino acid frequency represented in a logo format, where the height of the symbol represents relative frequency of each residue, the overall height of the stack represents at each position reflects the level of conservation and the width of the symbol shows the degree of uncertainty at that position. The peptides are represented through a Newribbon for the structure represented by magenta for alpha helical, blue for turns and white for other types of structures. Residues are coloured by their type in both logos and their structure where non-polar residues are in (white/black), basic residues, acidic residues and polar residues.

These figures were produced using Seq2Log [202] which calculates the frequency of each amino acid at each position using a frequency matrix showing the distribution of each residues at each position and I-TASSER [203] constructs a three-dimentional model of the peptide through fragment assembly and ab initio modelling to generate three dimensional models. The models were visualised using VMD [204].

Chapter Four

Characterisation

4.1 Peptide Purification

4.1.1 Introduction

In order to find the purity of each peptide and to use the data to perform the purification step on the HPLC system, the peptides where first analysed through LC-MS where the chromatogram shows the purity of the peptides prior to purification and allows for the identification of the peak that belongs to the peptide to be collected in the purification step. Once the peaks were identified, the LC-MS method was modified to ensure the elution of the peptide on the preparative-HPLC system so that the correct peak was collected. The collected peptides were then concentrated and analysed further on the LC-MS and MALDI-TOF to verify the peptide and its purity.

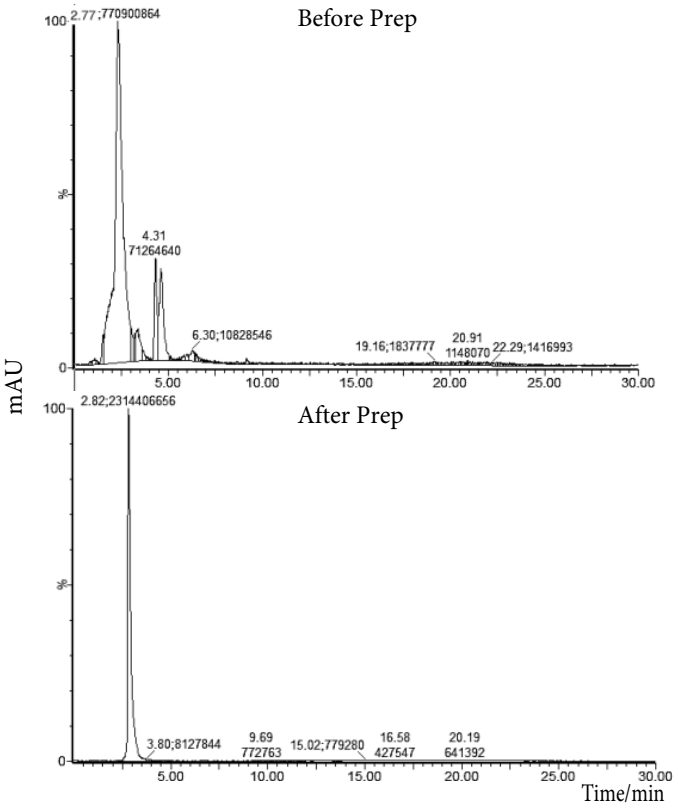
4.1.2 Results

Figure 4.1 and figure 4.2 show the LC-MS results before and after purification for the peptides based on hBD1 and hBD3 respectively, with their design shown in chapter 3.

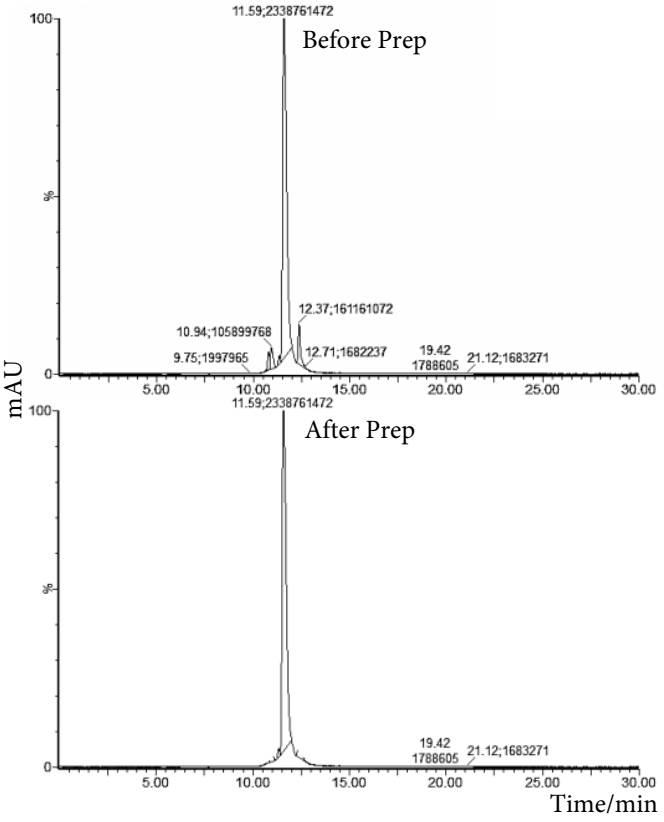
According to these graphs the peptides all show a purity of $\geq 90\%$ after purification. The purified peptides were used in all the experiments mentioned in this thesis such as the microbiology and serum stability studies. It can also be seen that all peptides show a small eluted peak at 20-22 minutes which belongs to the residual peptides that were previously cleaned but were not eluted properly from the column and they were also present in the blank run included in appendix A. Although, these blanks were subtracted from the final results they were not fully removed from the graphs due to software difficulties. Note that the initial analysis was done on the peptides for 30 minutes only but the blank sample was allowed to run until 40 minutes.

Figures 4.1a-4.1h show the LC-MS data for HBD-mod1-HBD-mod8 and Figures

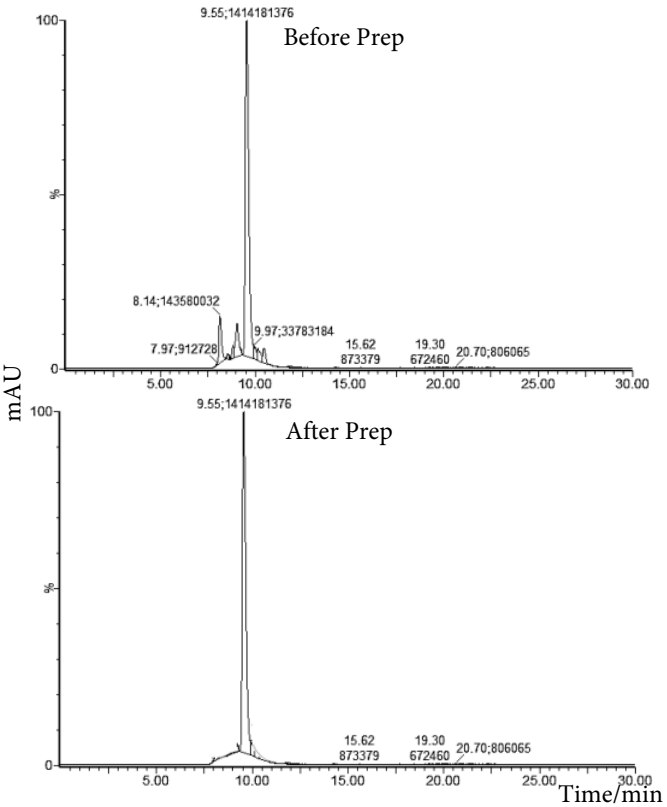
4.2a-4.2g show the data for HBD3-mod1-HBD3-mod7.



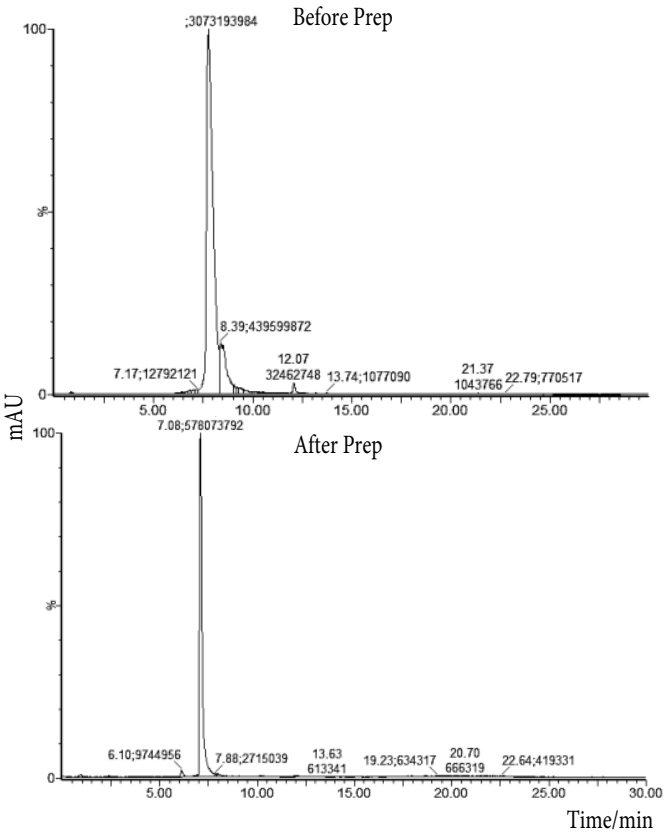
(a) HBD-mod1



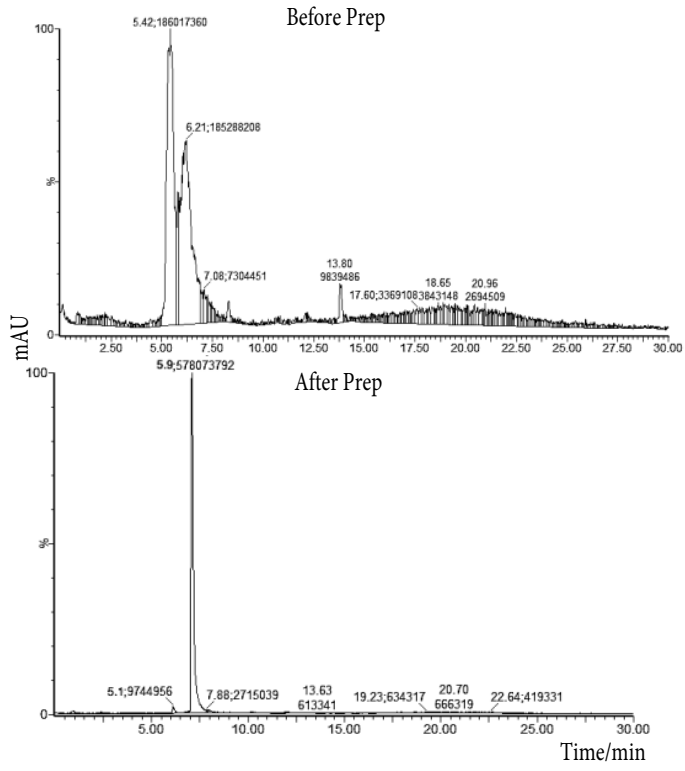
(b) HBD-mod2



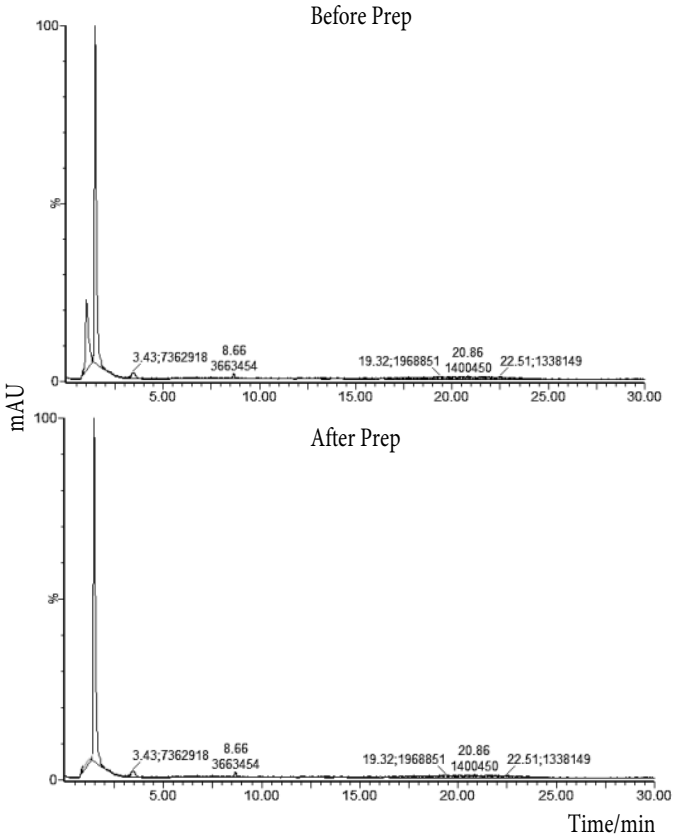
(c) HBD-mod3



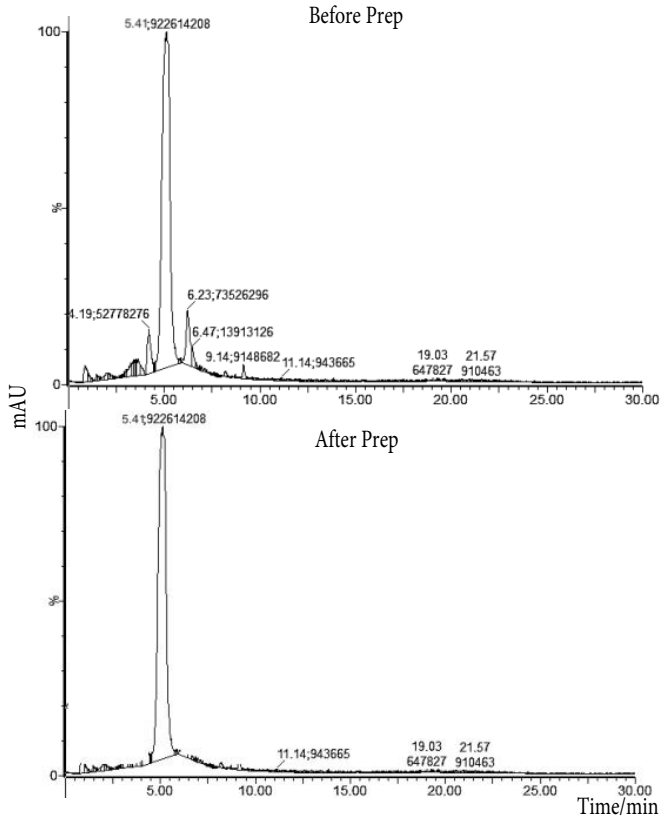
(d) HBD-mod4



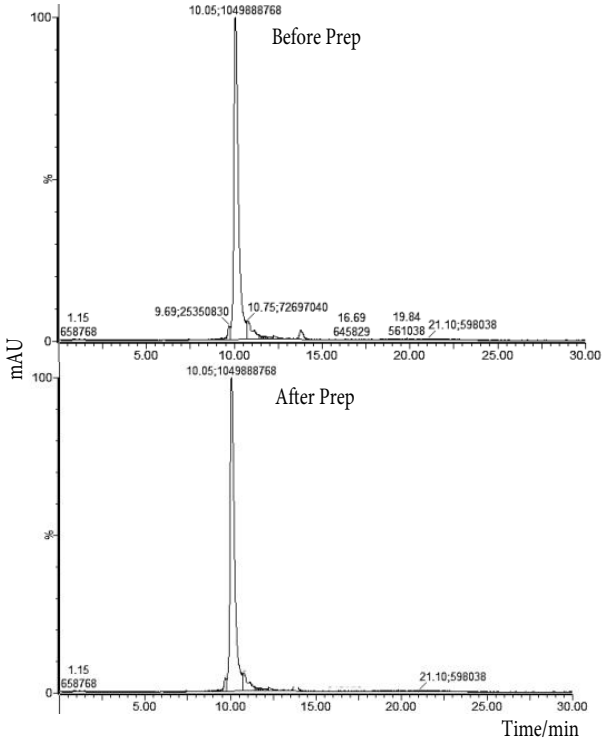
(e) HBD-mod5



(f) HBD-mod6

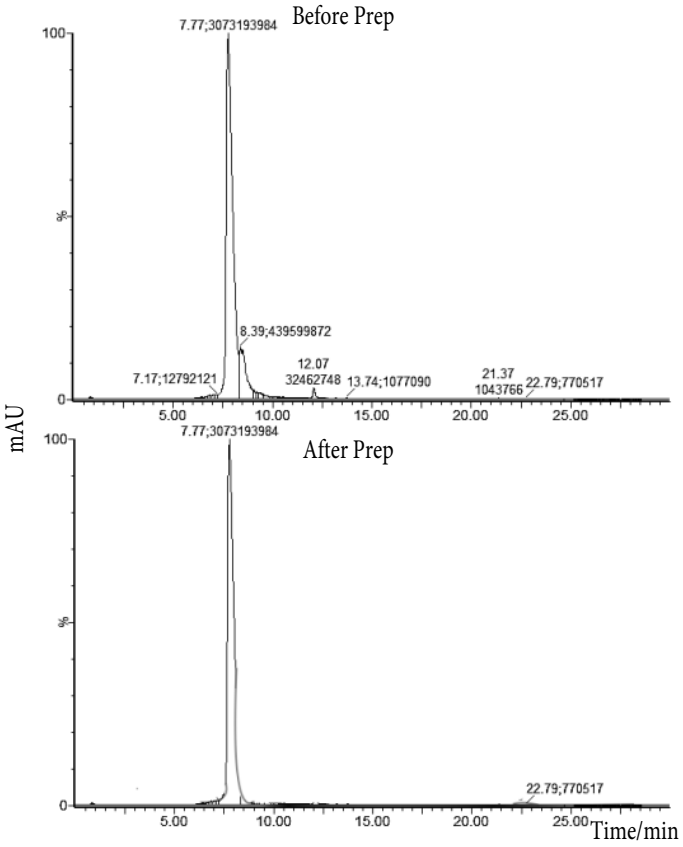


(g) HBD-mod7

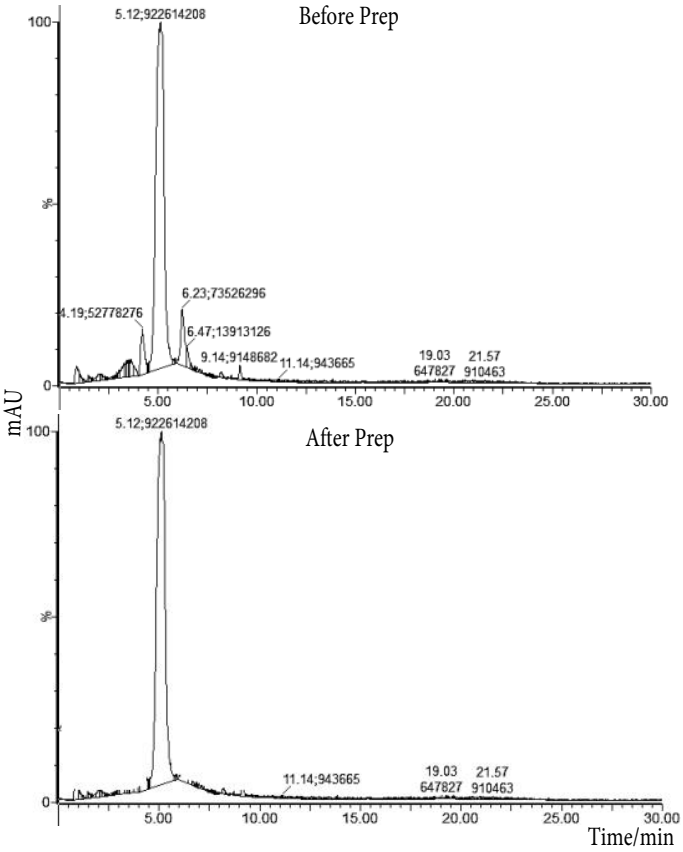


(h) HBD-mod8

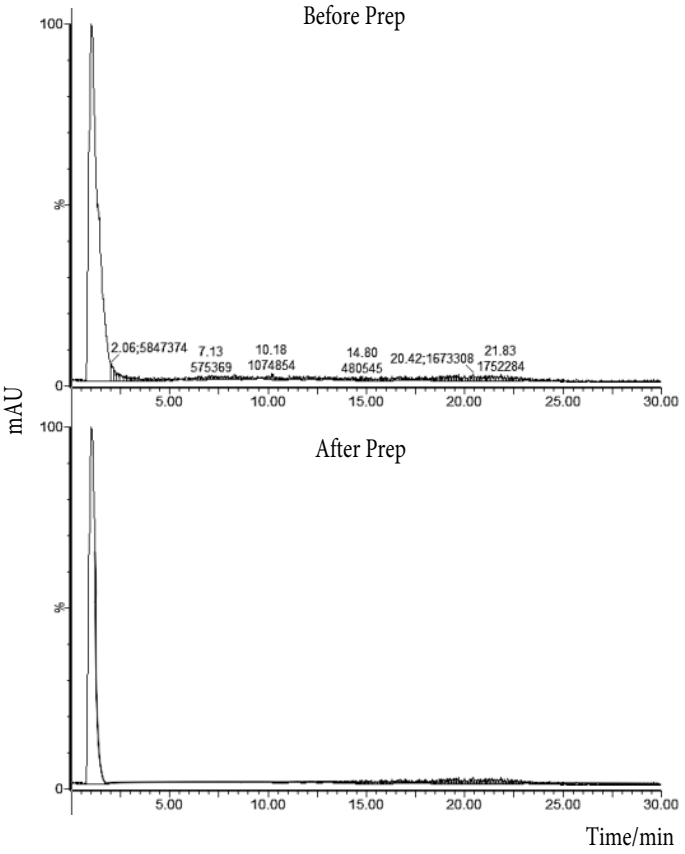
Figure 4.1: Comparison between the purity of the peptides based on hBD1 before and after purification step on LC-MS showing HBD-mod1, HBD-mod2, HBD-mod3, HBD-mod4, HBD-mod5, HBD-mod6, HBD-mod7, HBD-mod8.



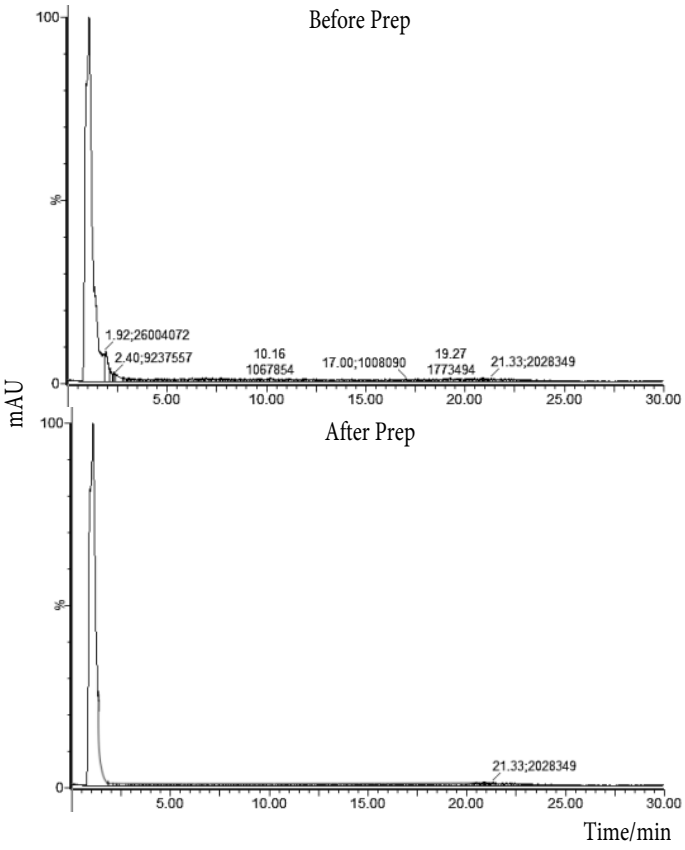
(a) HBD3-mod1



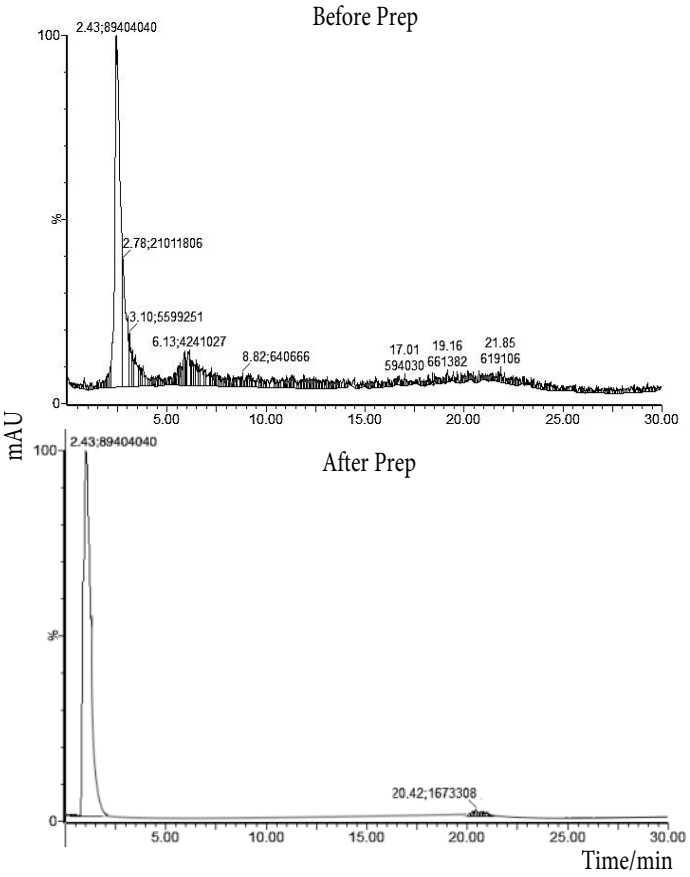
(b) HBD3-mod2



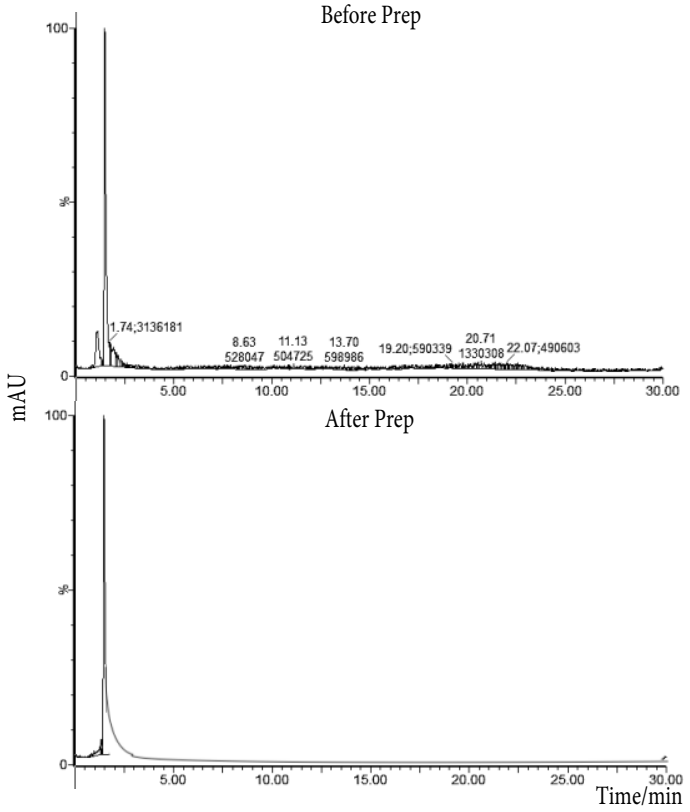
(c) HBD3-mod3



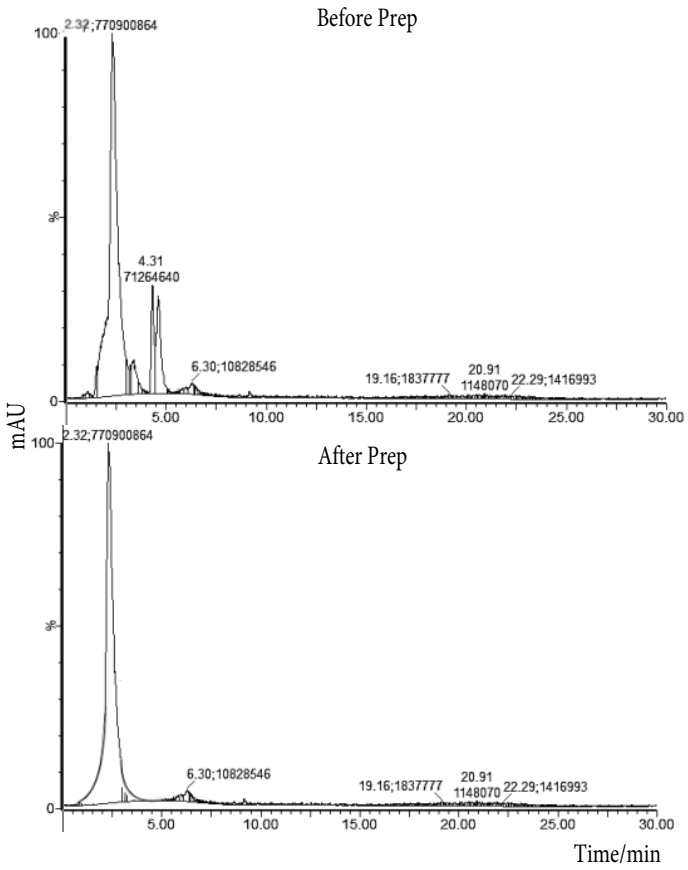
(d) HBD3-mod4



(e) HBD3-mod5



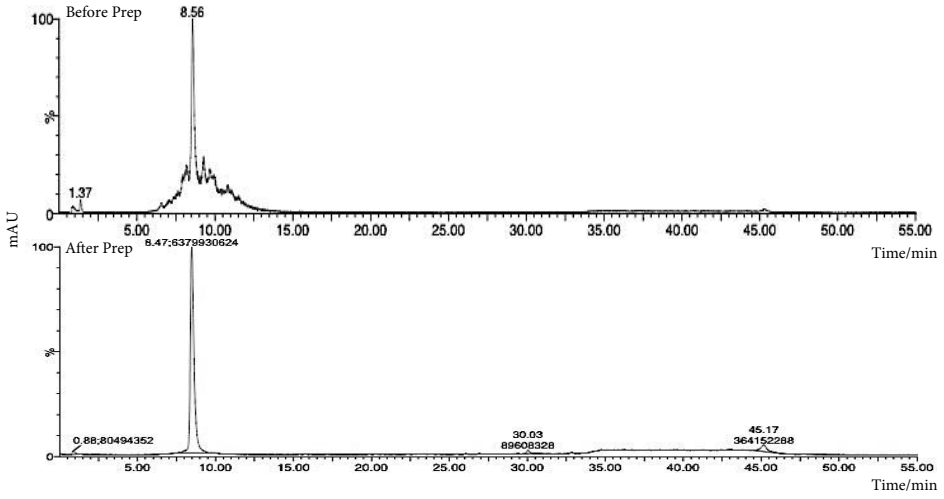
(f) HBD3-mod6



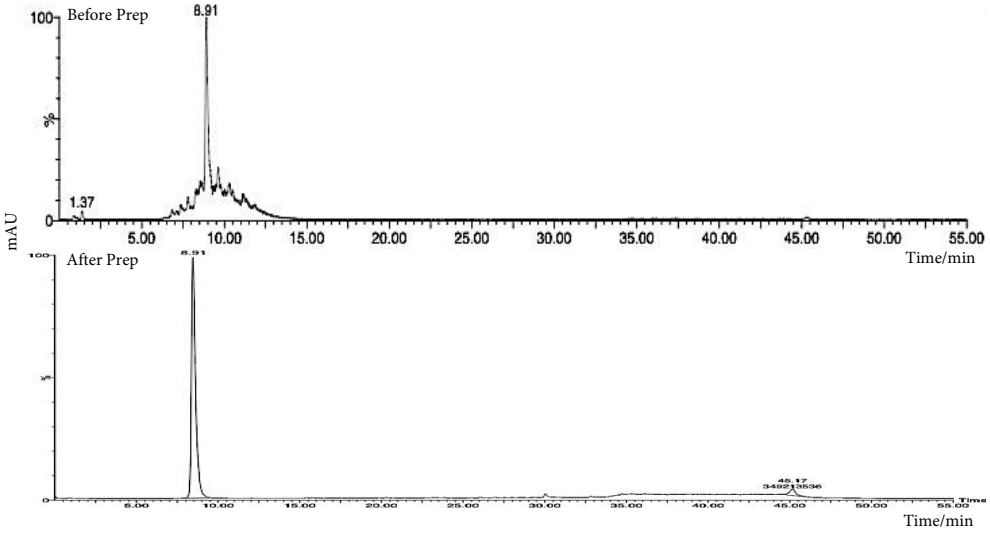
(g) HBD3-mod7

Figure 4.2: Comparison between the purity of the peptides based on hBD3 before and after purification step on LC-MS showing the peptides HBD3-mod1, HBD3-mod2, HBD3-mod4, HBD3-mod5, HBD3-mod6, HBD3-mod7.

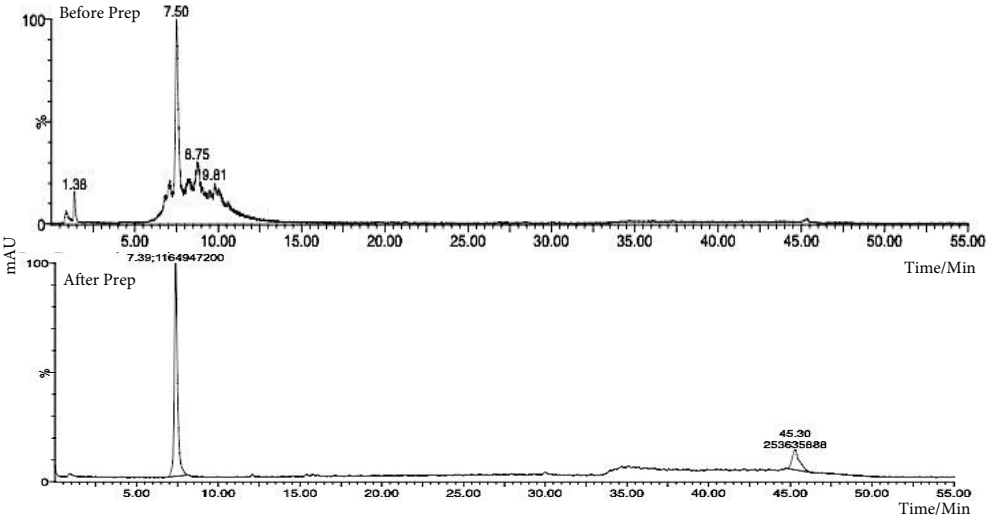
Following the determination of the most antimicrobial peptide sequence, the sequence was taken and an alanine substitution was done on the corresponding sequences. The result of the purification on these peptides can be seen in Figures 4.3. The final concentration of these peptides were near 90%. The use of alanine substitution has become a common approach for studying the influence of individual residues on the structure and antimicrobial activity of peptides. By replacing side chain residues with methyl groups, this method effectively identifies the specific side chains responsible for secondary structure formation and functional activity [205]–[207].



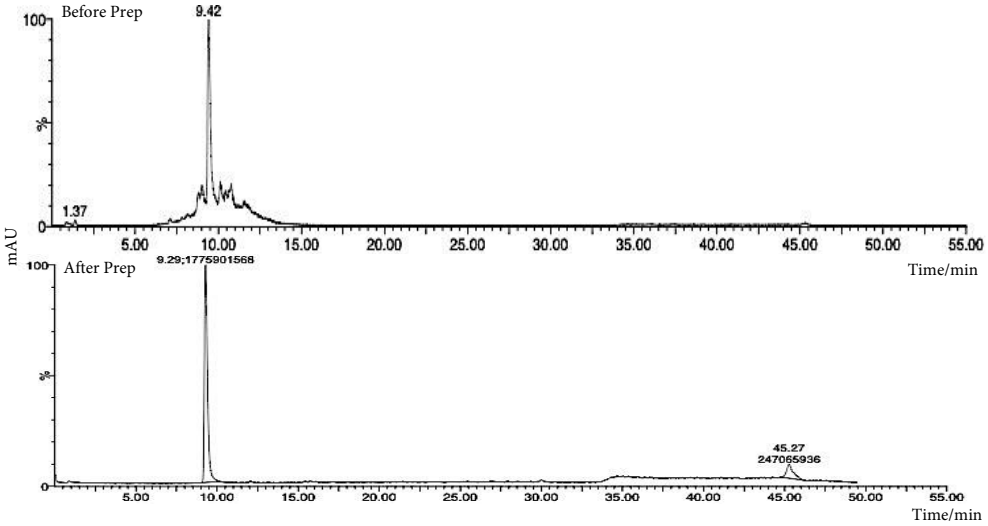
(a) HBD-mod8



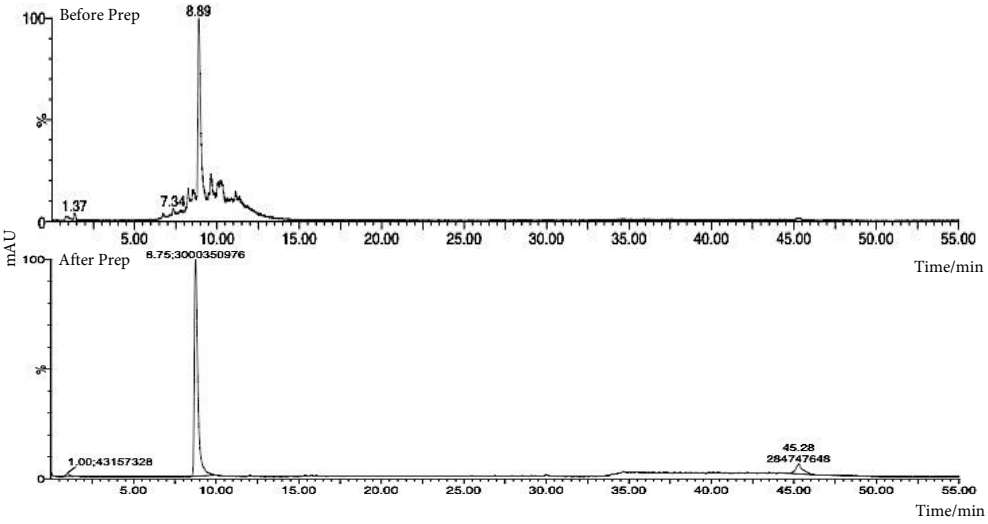
(b) 1HBD-mod8



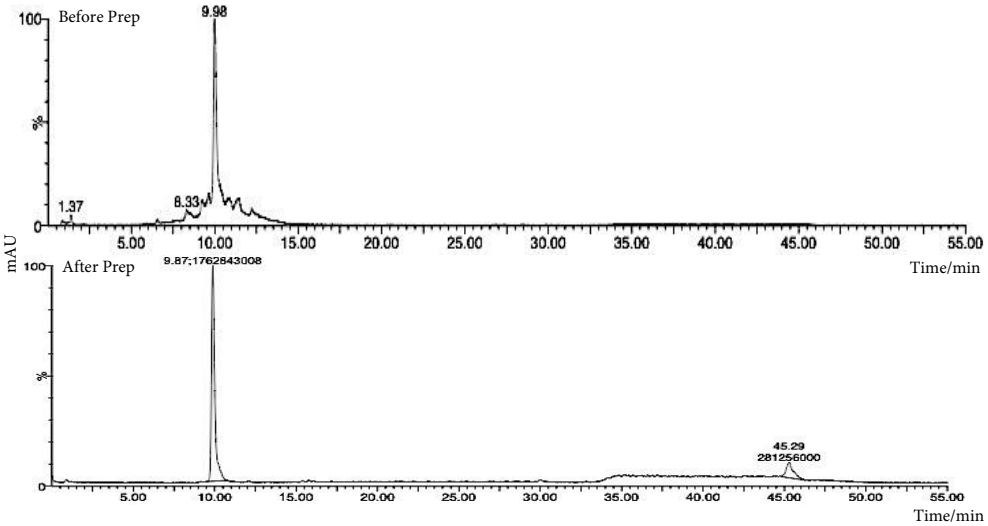
(c) 2HBD-mod8



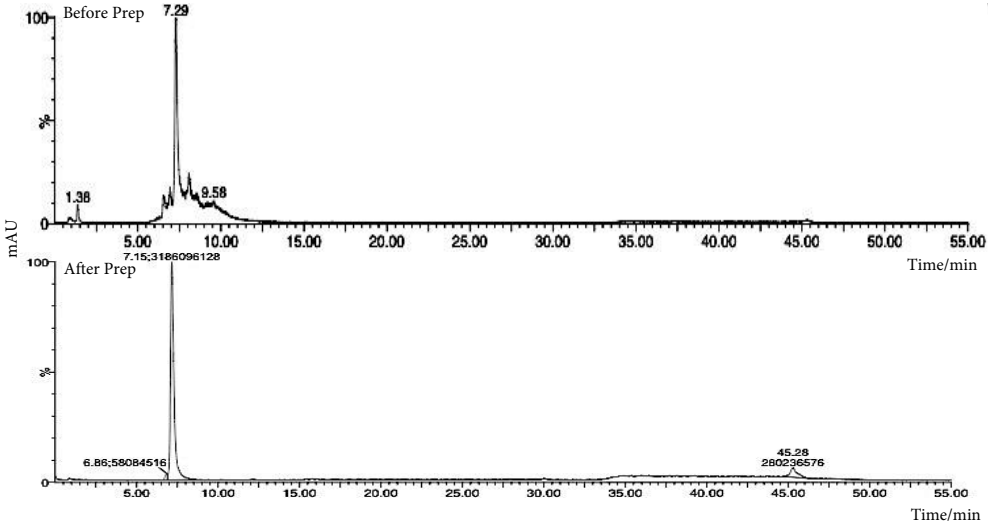
(d) 3HBD-mod8



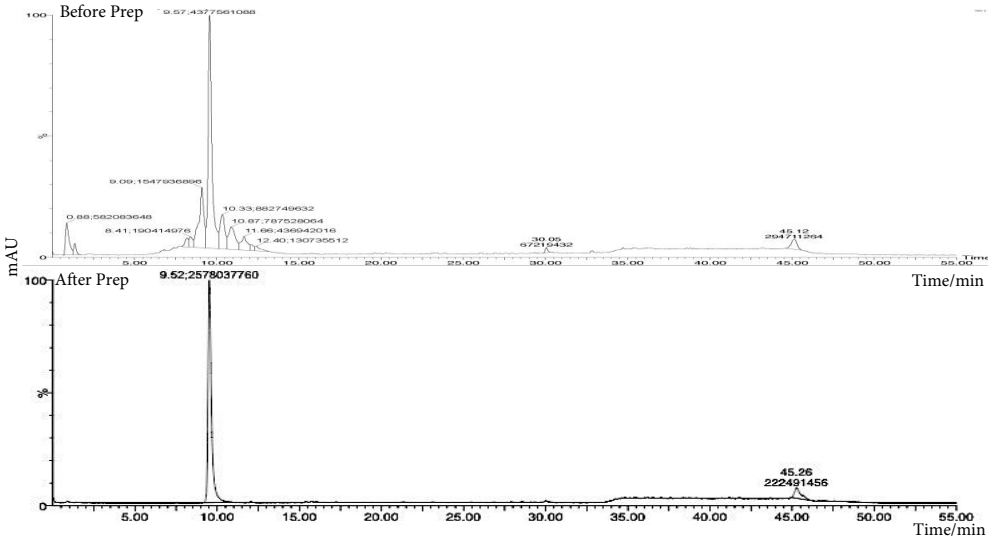
(e) 4HBD-mod8



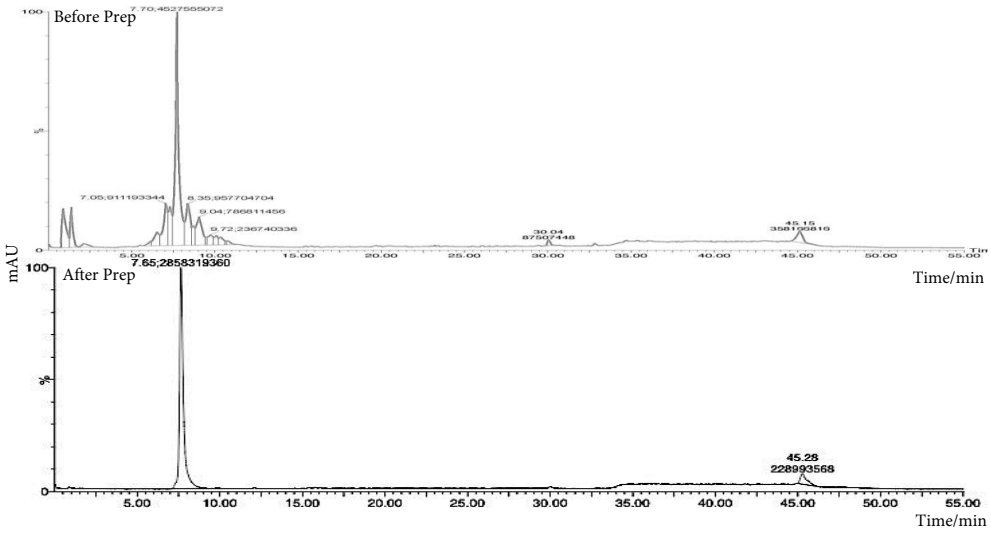
(f) 5HBD-mod8



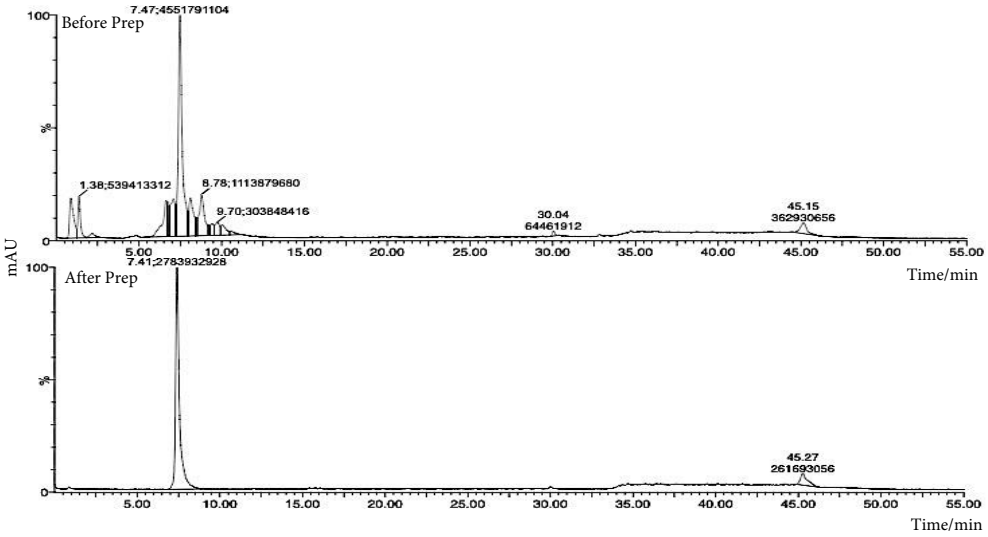
(g) 6HBD-mod8



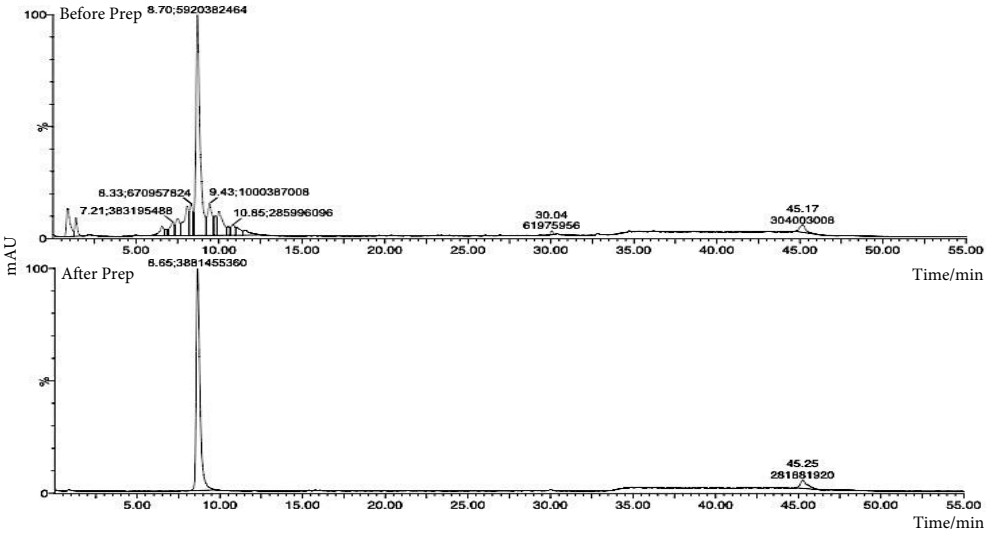
(h) 7HBD-mod8



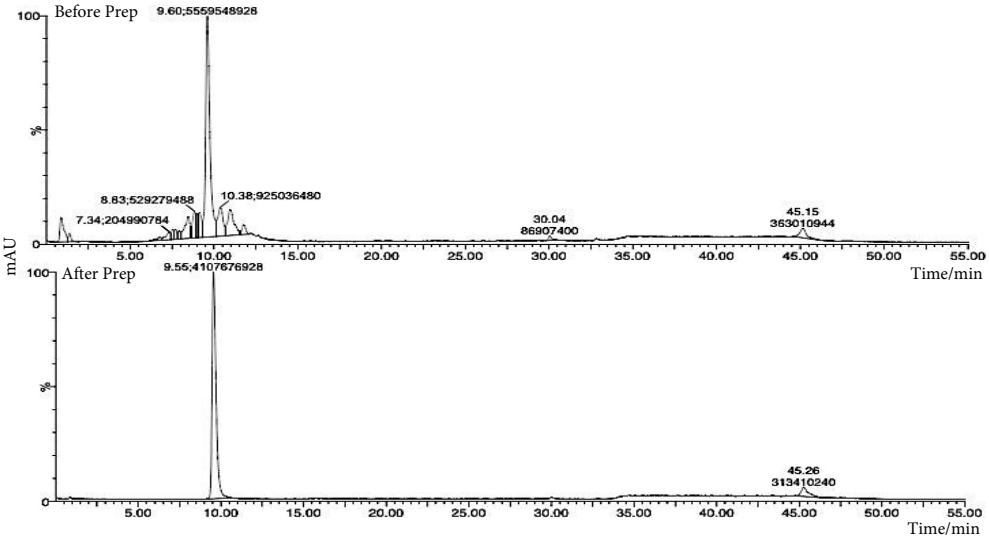
(i) 8HBD-mod8



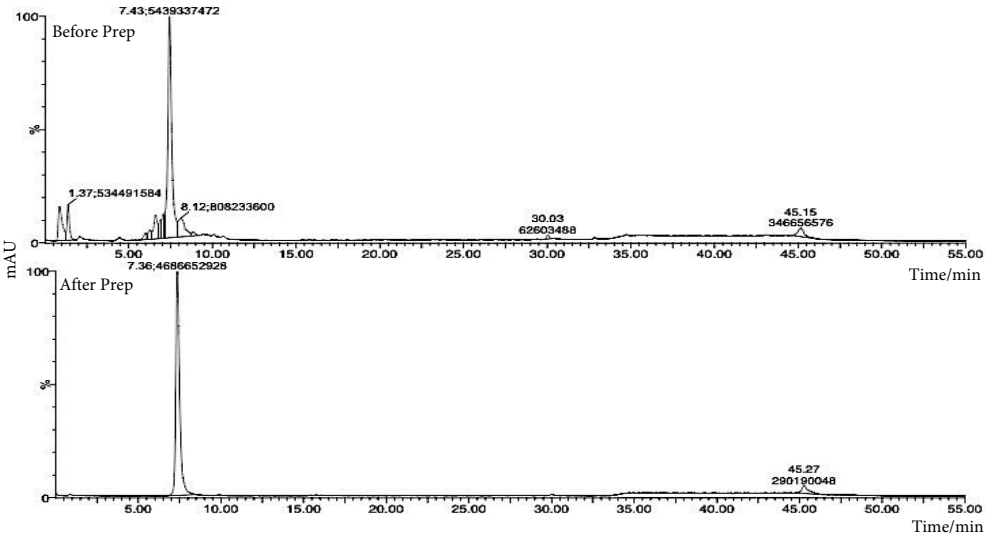
(j) 9HBD-mod8



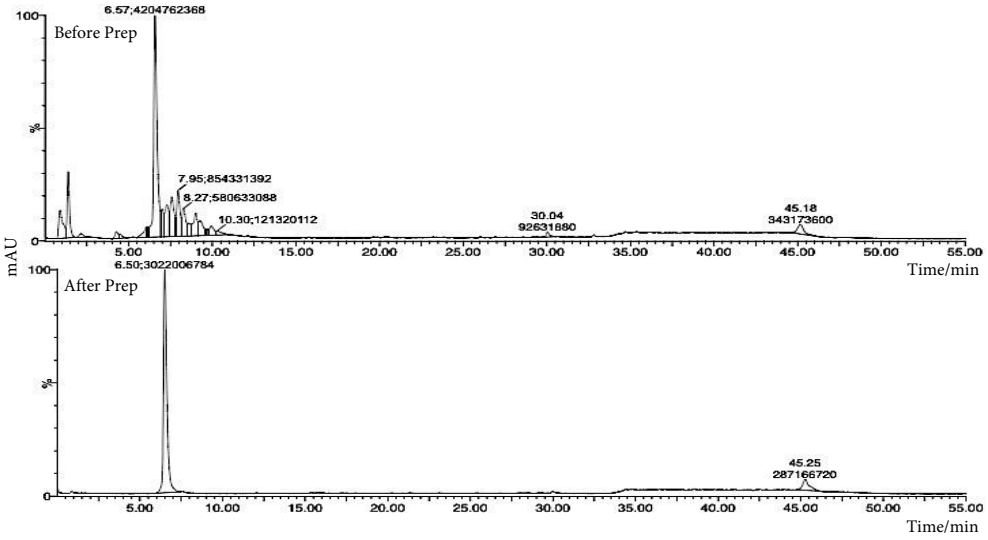
(k) 10HBD-mod8



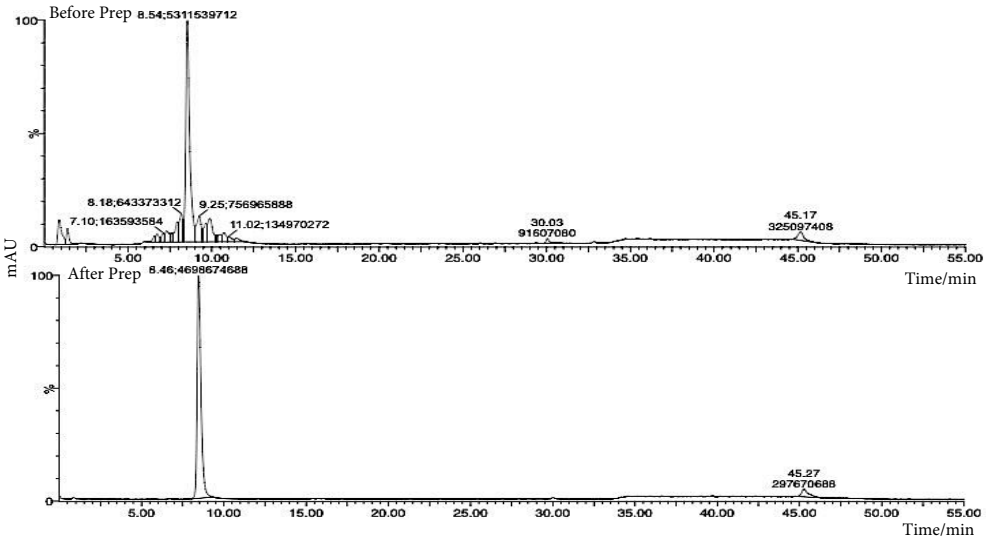
(l) 11HBD-mod8



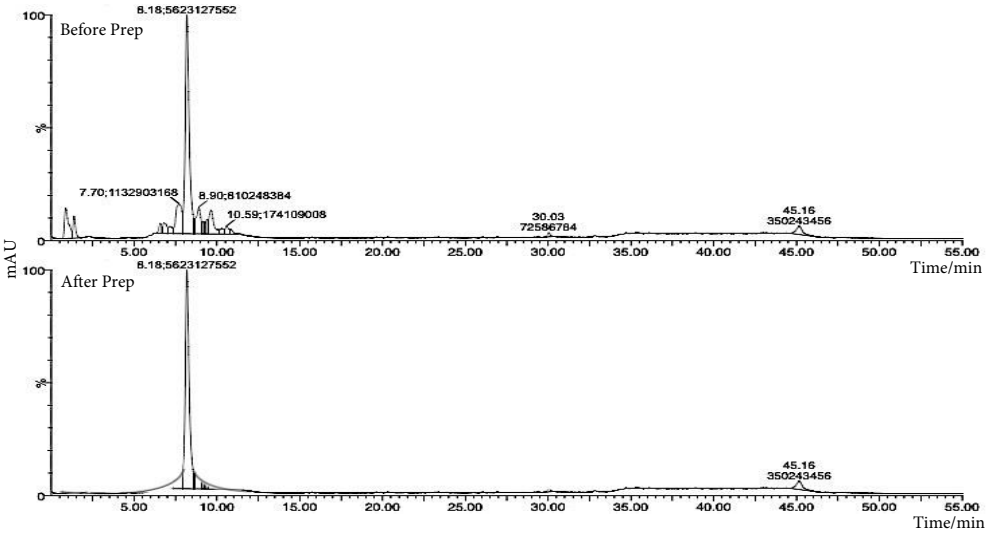
(m) 12HBD-mod8



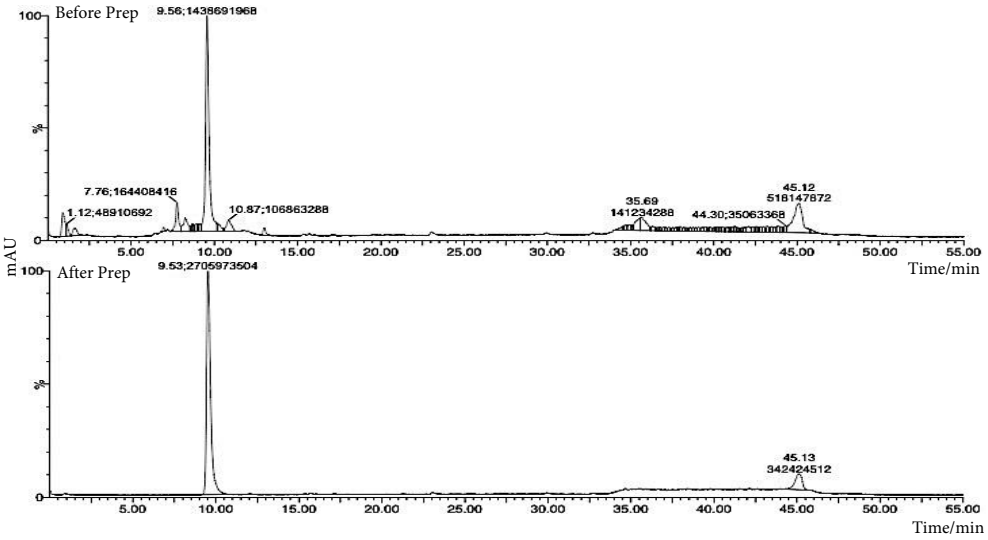
(n) 13HBD-mod8



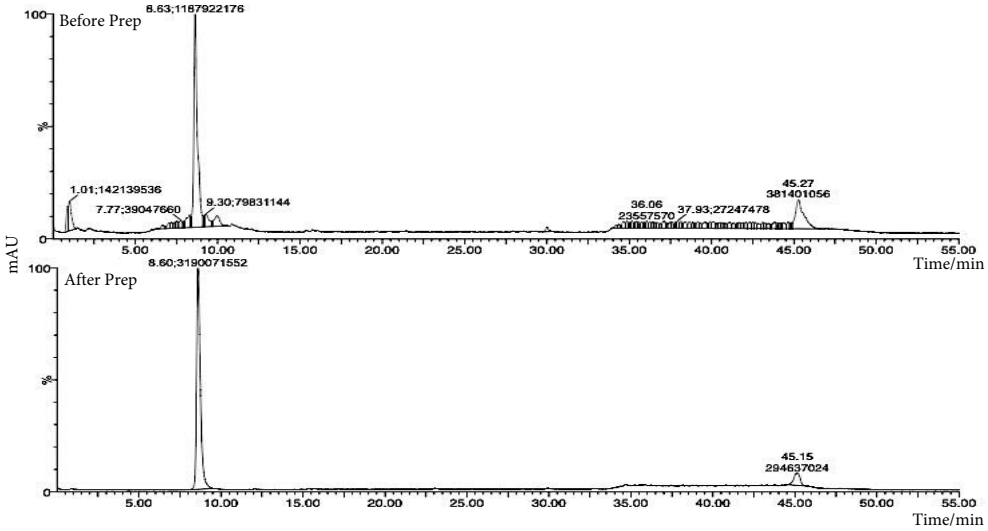
(o) 14HBD-mod8



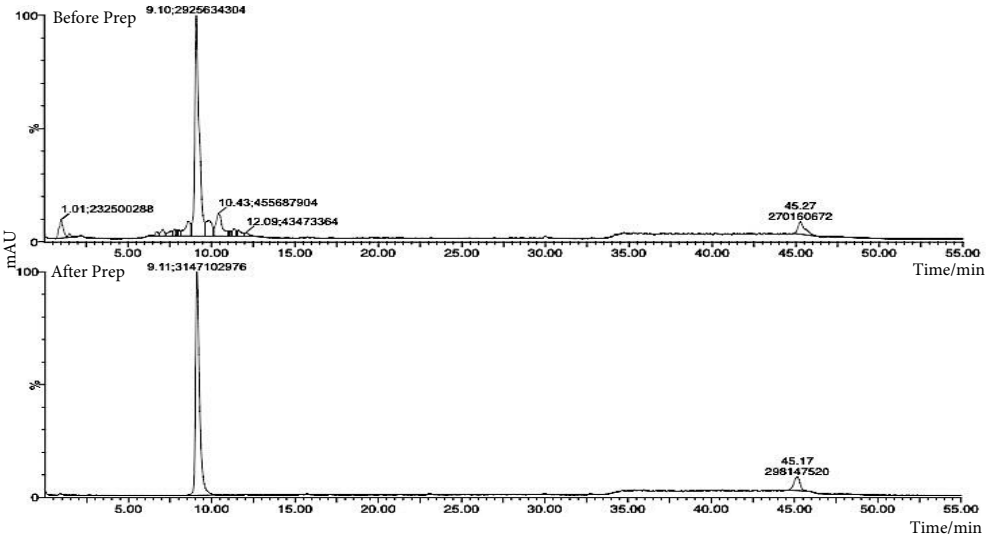
(p) 15HBD-mod8



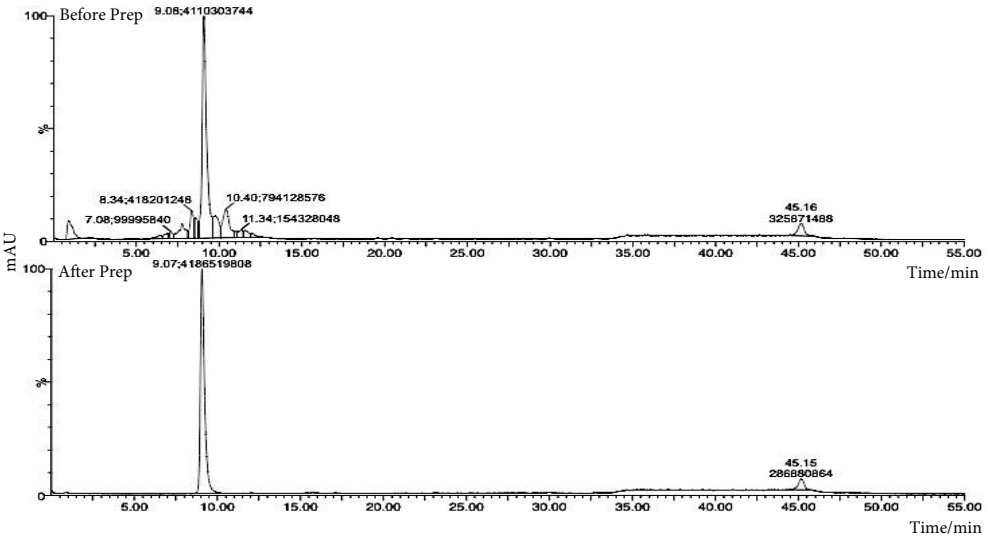
(q) 16HBD-mod8



(r) 17HBD-mod8



(s) 18HBD-mod8



(t) 19HBD-mod8

Figure 4.3: Comparison between the purity of the peptides based the alanine scanning of HBD-mod8 peptides before and after purification step on LC-MS.

Chapter Five

Secondary Structure

5.0.1 Introduction

To determine the structural conformation for each peptide and find the correlation between the structural details and the antimicrobial activity, the peptides were subjected to different environments to find the change in their structure. Each condition was carefully selected to stimulate a certain effect on the peptide structure to mimic the environment of bacteria and normal cells.

PBS was chosen to represent the free form peptide and SDS was chosen as the anionic environment that was shown to force an alpha helical structure on the peptide. The first series of peptides were only analysed in these buffers.

Each peptide series was analysed in percentage of secondary structure and three different graph types were produced. The bar graphs show the overall percentage of secondary structure split between three types of helical, strand, and unordered to provide an overall picture of the effect that different buffers had on the peptide structure. The pie charts which represent a more detailed structural results showing the helix in more detail with helix 1(i.e ordered) and helix 2 (i.e non ordered), strand in strand 1 (i.e ordered) and strand 2 (i.e unordered) and turn and unordered in different categories. The third graph types that are presented in appendix section two (B) show the raw data from the absorbance that was produced by the CD software.

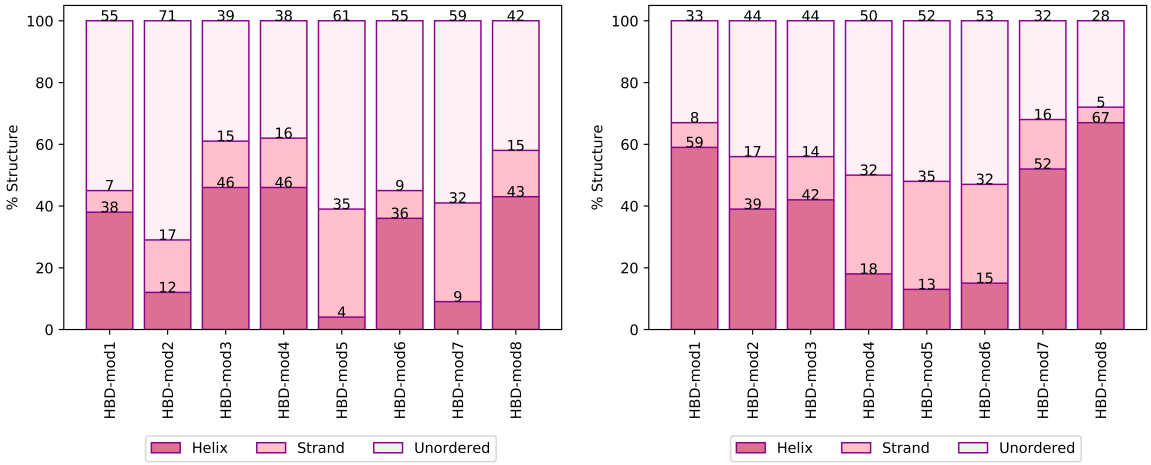
5.1 Peptides based on hBD1

5.1.1 Results

There is a clear divide between the structure of peptides based on hBD1 when dissolved in PBS compared to when they are suspended in SDS. Figure 5.1 shows the changes

between these two where Figure 5.1a shows the series of peptide in PBS and Figure 5.1b shows the series of peptide in SDS. Through this figure it can be seen that each peptide changes its secondary structure in favour of a helix structure when in SDS. The percentage of strand structure stays relatively unchanged in HBD-mod1, -mod2 and -mod3, and for HBD-mod4 and -mod6 the percentage of strand structure increases by approximately 2-folds where their kl;,./helix structure were reduced unlike the other peptides in the series. HBD-mod5 on the other hand, preserves its strand structure in SDS and it shows a relatively similar structure in both conditions. It is notable that HBD-mod4, -mod5 and -mod6 all share a similar structural profile when in an anionic environment.

The largest difference between the change in the peptide structure can be seen in HBD-mod7 where the % helical has changed drastically by 8-folds between the two different conditions. It is also evident that the % of unordered structure for all the peptide in this series were shown to be similar with values ranging from 28-50% with the lowest in HBD-mod8 at only 28% where the majority was found to form a helix at 67% marking the highest percentage of helix formation in the series.



(a) The percentage of secondary structure in PBS

(b) The percentage of secondary structure in SDS

Figure 5.1: Summarised version of the secondary structure of peptides based on hBD1 including HBD-mod1, HBD-mod2, HBD-mod3, HBD-mod4, HBD-mod5, HBD-mod6, HBD-mod7 and HBD-mod8 in PBS and SDS. The summarised version shows only the percentage of helix, strand and unordered in the structure of each peptide where helix is a combination of helix1 and 2, strand is a combination of strand 1 and 2 and unordered is a combination of turn and unordered. All the datapoints displayed in Figure B.2 represents a culmination of 3 measurements taken from the same peptide in each condition. The measured values are θ which is the machine unit used by the CD instrument.

The percentage of unordered secondary structure is highly prevalent in all peptides in PBS but this percentage is reduced in SDS for HBD-mod1, HBD-mod2 , HBD-mod7 and HBD-mod8, where the percentage of helix has increased considerably in these peptides by approximately, 1.5-, 3-, 6- and 1.5-folds respectively.

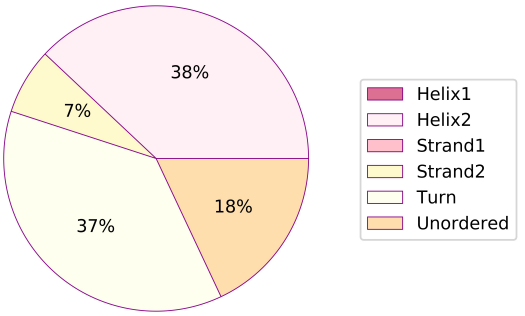
To be able to express the secondary structure in more detail, Figure 5.2 was produced and through these sub-figures it can be seen that the percentage of helix 1 structure throughout the peptide series based on hBD1 increases in SDS. It is also evident that HBD-mod4 in Figure 5.2h, -mod5 in Figure 5.2j and -mod6 in Figure 5.2l have a very close percentage in their helix content similar to the results shown in Figure 5.1. In fact it is more clear that the structure of these peptides in this environment is indistinguishable from one another.

Similar observation can be seen in the structure of HBD-mod2 in Figure 5.2d and -mod3 in Figure 5.2f in SDS. The highest helix 1 content is presented in Figure 5.2p at 44%. This is important since the helix 1 structure was not observed in this peptide in PBS shown in Figure 5.2o, and only helix 2 can be seen at 43%, but when in SDS this peptide changes conformation to a helix 1 and helix 2 and presents an overall highest helical conformation in this series.

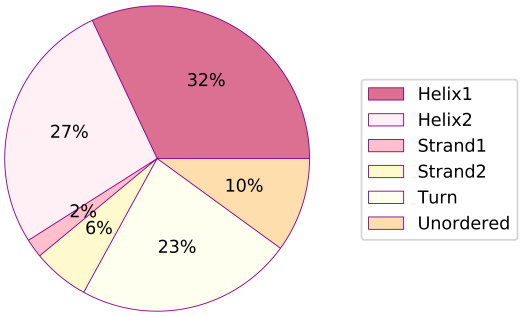
All the data presented here can be found in appendix section (B) in its raw format which was used to determine the percentage of different structural components. The raw data for peptides based on hBD1 can be found in Figure B.2.

5.1.2 Discussion

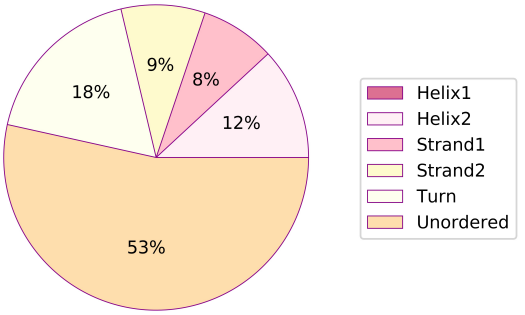
As it was shown with the results from the peptides based on hBD1 the structure of HBD-mod4, -mod5 and -mod6 resembles one another closely. This could be attributed to their close relationship shown in the family tree in Figure 3.2 in Chapter 3. HBD-mod7 and -mod8 also resemble each other due to their close relationship according to the phylogenic tree. Since HBD-mod2 and -mod3 also share similarities between their sequences shown by their close relationship on the phylogenic tree in Figure 3.2, they showed a similar secondary structure profile as seen with the other peptides in this series.



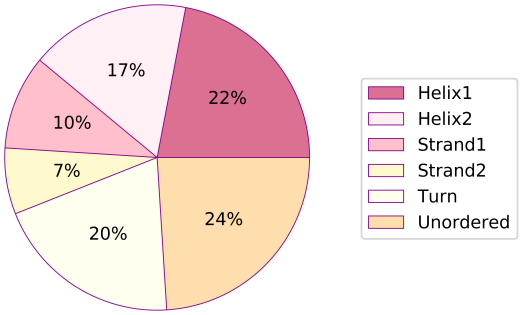
(a) HBD-mod1 in PBS



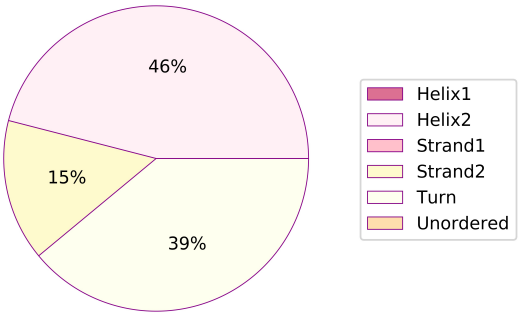
(b) HBD-mod1 in SDS



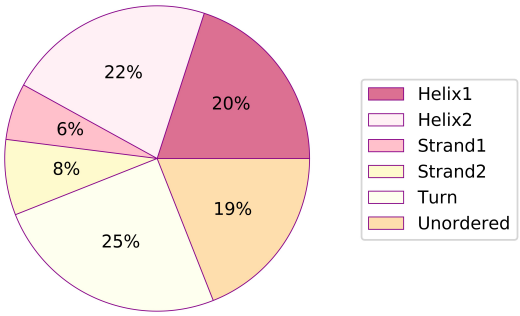
(c) HBD-mod2 in PBS



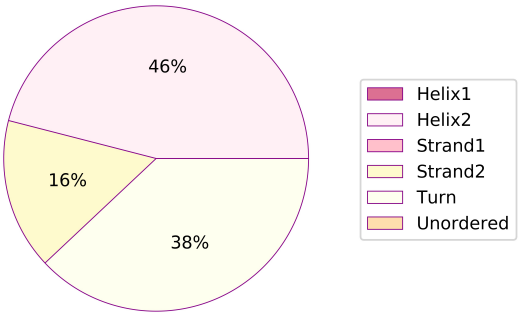
(d) HBD-mod2 in SDS



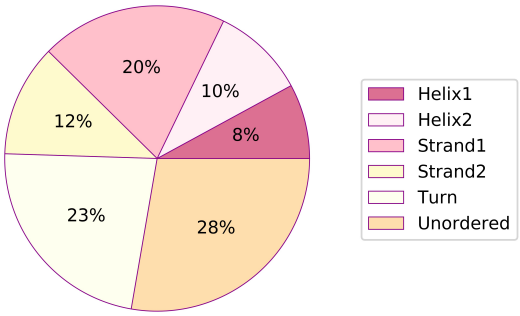
(e) HBD-mod3 in PBS



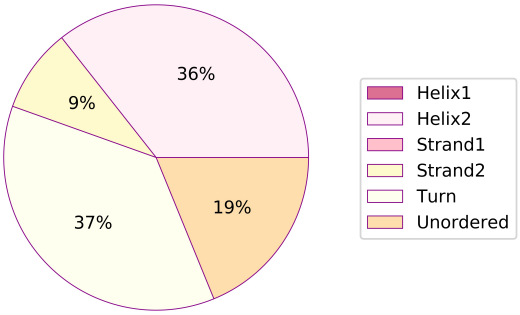
(f) HBD-mod3 in SDS



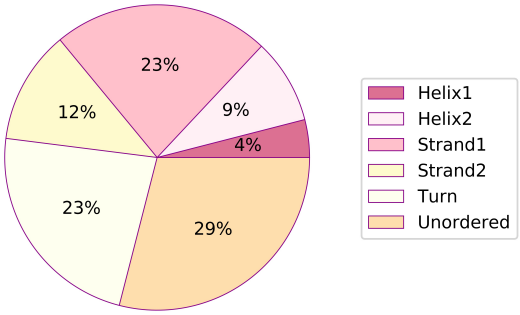
(g) HBD-mod4 in PBS



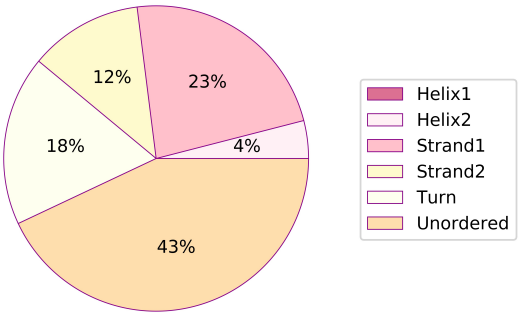
(h) HBD-mod4 in SDS



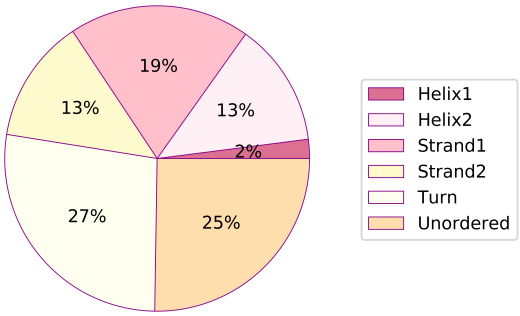
(i) HBD-mod5 in PBS



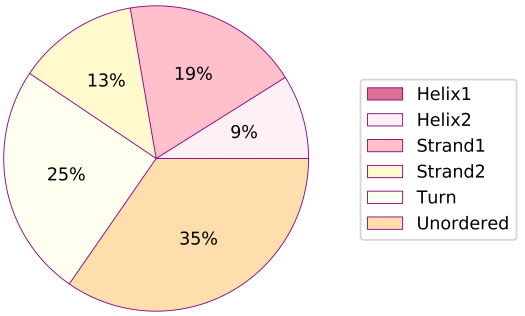
(j) HBD-mod5 in SDS



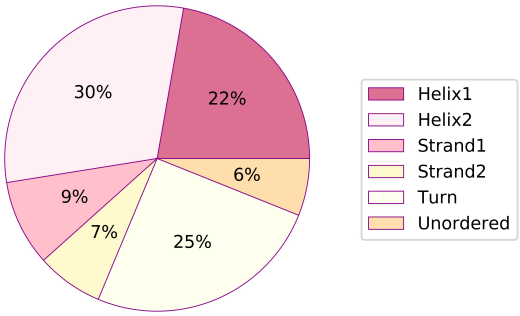
(k) HBD-mod6 in PBS



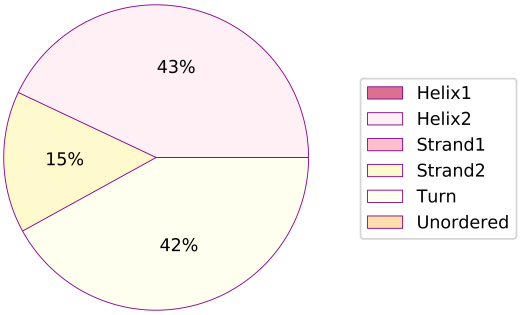
(l) HBD-mod6 in SDS



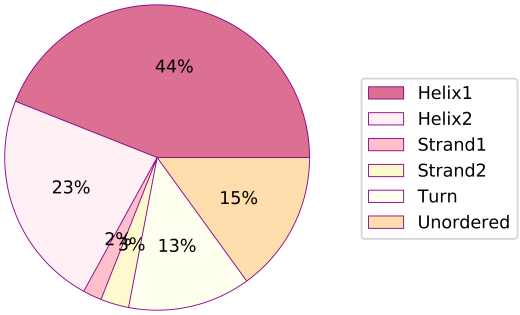
(m) HBD-mod7 in PBS



(n) HBD-mod7 in SDS



(o) HBD-mod8 in PBS



(p) HBD-mod8 in SDS

Figure 5.2: Expanded version of the secondary structure percentages of peptides based on hBD1 that shows the helix 1, helix 2, strand 1, strand 2, turn and unordered portion of each peptide in two different condition on PBS and SDS shown side by side for better comparison. The highest percentage of secondary structure in most peptides in this series can mostly be attributed to turn and unordered in PBS with the exception of HBD-mod8 where the percentage of helix and unordered were similar before the addition of SDS.

These figures were produced by the measurement of polarised light that has a specific finger print that can be attributed to different structure types. The analysis was performed through Dichroweb.

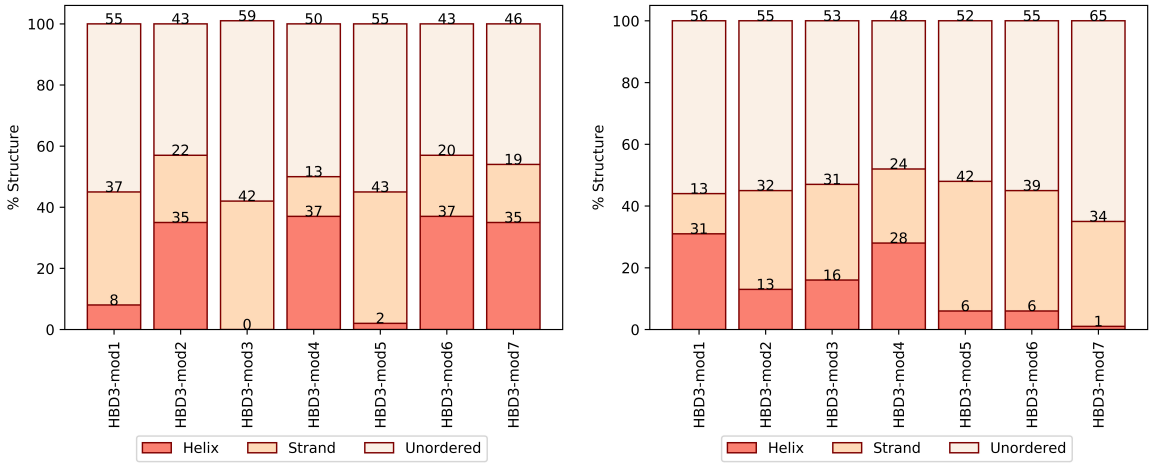
5.2 Peptides based on hBD3

5.2.1 Results

Even though the structure of peptides usually undergoes a forced alpha helical conformation under SDS, as shown in Figure 5.3a this does not apply to this specific peptide series. As presented in Figure 5.3 the percentage of helix in these peptides is negligible but the percentage of strand is prominent in both buffers. As expected the percentage of unordered is the highest across the series of peptides in both buffers and it stays consistent regardless of the buffer type throughout each peptide structure ranging from 43-58% in PBS and 48-65% in SDS.

There is one peptide of note in this series since it shows a percentage helical structure of 0%. HBD3-mod3 shows an approximately equal secondary structure between strand and unordered in PBS but when in SDS this peptide undergoes a change in conformation and it shows 16% helix conformation while the percentage of both unordered and strand decreases. Other notable peptides include HBD3-mod2, -mod4, -mod6 and -mod7 showing a helix conformation in PBS however this conformation showed a reduction in SDS where there was an increase in the percentage of strand structure.

HBD3-mod1 and -mod5 follow the same pattern as expected from peptides in SDS where their helix conformation increase in this buffer when compared to the PBS. The most notable conformational change belongs to HBD3-mod1 where the percentage of helix structure increases dramatically in the presence of SDS consistent with its predicated structure in Figure 3.7a.



(a) The percentage of secondary structure in PBS

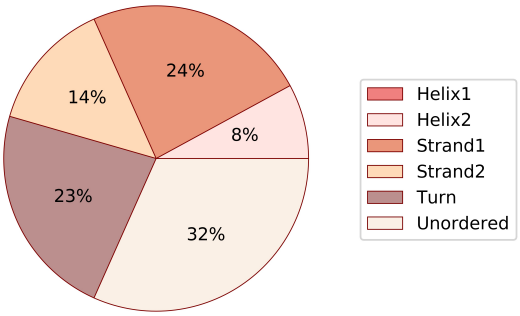
(b) The percentage of secondary structure in SDS

Figure 5.3: Summarised version of the secondary structure of peptides based on hBD3 including HBD3-mod1, HBD3-mod2, HBD3-mod3, HBD3-mod4, HBD3-mod5, HBD3-mod6, HBD3-mod7 and in PBS and SDS. The summarised version shows only the percentage of helix, strand and unordered in the structure of each peptide where helix is a combination of helix1 and 2, strand is a combination of strand 1 and 2 and unordered is a combination of turn and unordered. All the data points displayed in Figure B.3 represents a culmination of 3 measurements taken from the same peptide in each condition. The measured values are θ which is the machine unit used by the CD instrument.

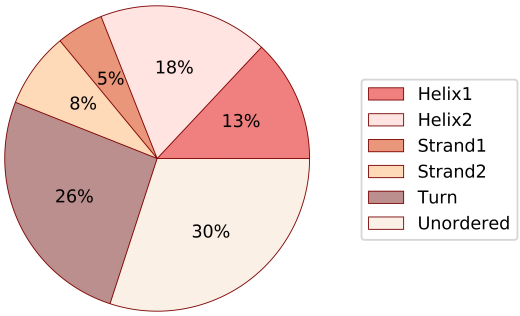
The percentage of unordered secondary structure is highly prevalent in all peptides in both PBS and SDS and that the buffer that the peptide resides in does not effect its structure drastically.

A more in depth look at the structure of these peptides in both conditions, shown in Figure 5.4, highlights the breakdown of each structure into their individual components. The increase in helix conformation of HBD3-mod1 shown in Figure 5.4b showed approximately equal increase in both helix1 and 2. This trend was also observed

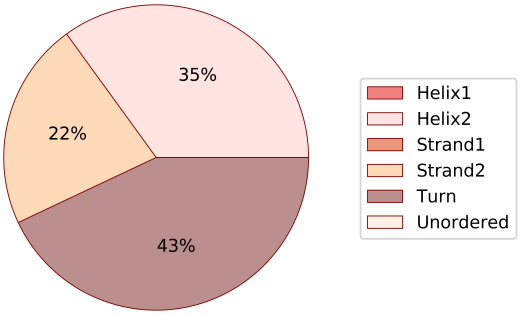
in HBD3-mod2, -mod4 and -mod5. Other notable similarities between the structures in SDS buffer was the equality between the turn and unordered for all peptides except HBD3-mod7 where the structure is fully changed from turn to unordered in PBS to SDS respectively. HBD3-mod3 showed a majority unordered structure that belongs in the same category but this was reduced when in the anionic buffer and replaced by a higher turn and strand structure with the addition of both helix structures.



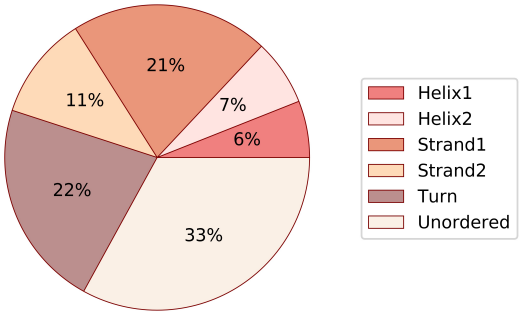
(a) HBD3-mod1 in PBS



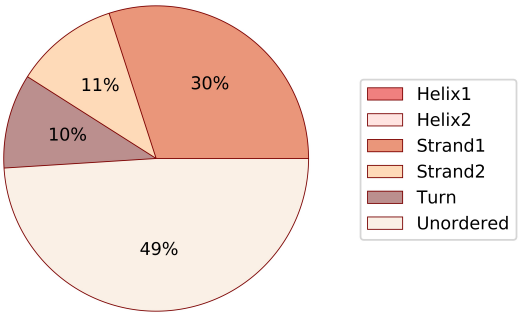
(b) HBD3-mod1 in SDS



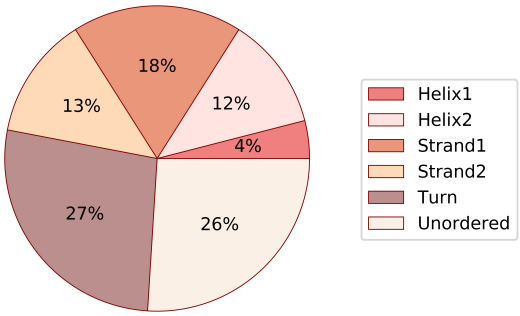
(c) HBD3-mod2 in PBS



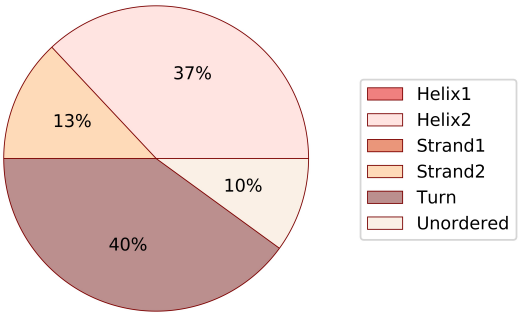
(d) HBD3-mod2 in SDS



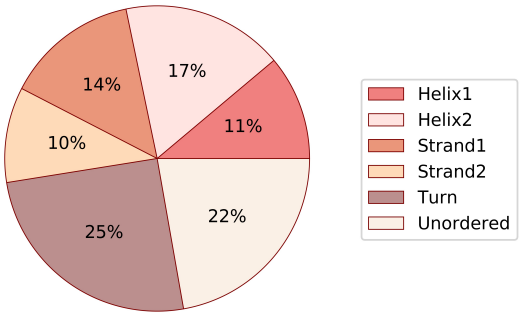
(e) HBD3-mod3 in PBS



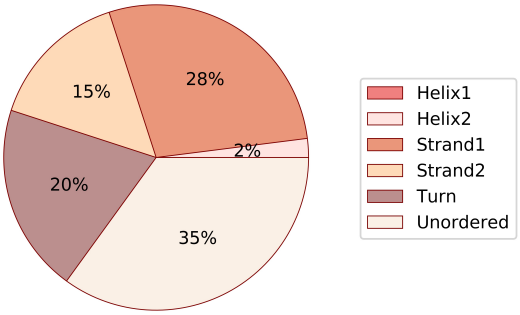
(f) HBD3-mod3 in SDS



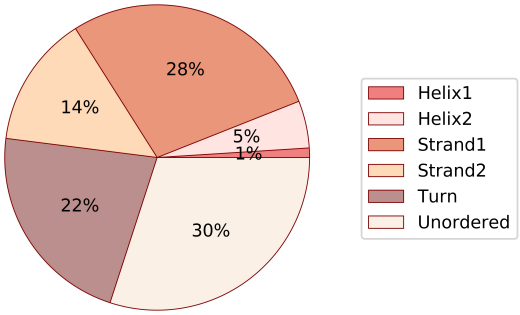
(g) HBD3-mod4 in PBS



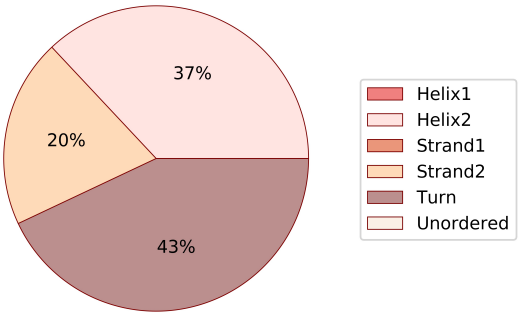
(h) HBD3-mod4 in SDS



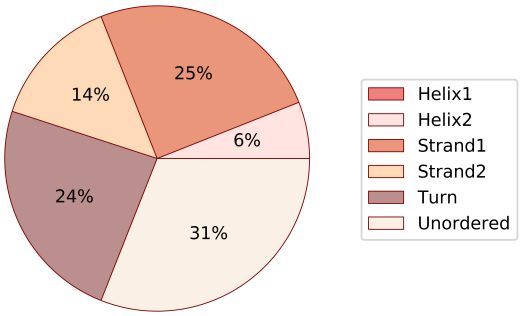
(i) HBD3-mod5 in PBS



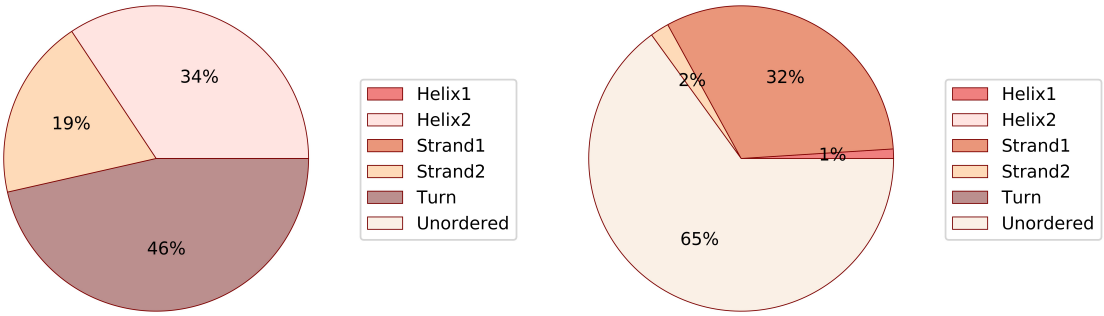
(j) HBD3-mod5 in SDS



(k) HBD3-mod6 in PBS



(l) HBD3-mod6 in SDS



(m) HBD3-mod7 in PBS

(n) HBD3-mod7 in SDS

Figure 5.4: Expanded version of the secondary structure percentages of peptides based on hBD3 that shows the helix 1, helix 2, strand 1, strand 2, turn and unordered portion of each peptide in two different condition on PBS and SDS shown side by side for better comparison. There is no clear pattern between different peptides and their corresponding structures but the turn and unordered structures seem to be the most prominent in comparison to the rest of the structures. Although the percentage of unordered structure spikes in SDS.

5.2.2 Discussion

The peptides based on hBD3 did not follow the same trend observed with the previous series and the percentage of unordered was shown to increase in the presence of SDS. The peptides showing a decrease in helix conformation from PBS to SDS work in the opposite direction to the literature where it states the presence of detergent like anionic buffer forces a helical conformation on the peptide structure.[178] This is of note since it could indicate the activity level of the peptide and that when in an anionic environment this peptide changes conformation to a less favourable structure type for the purpose of this experimental design since the goal was to design an alpha helical structure.

5.3 Alanine substitution of peptide HBD-mod8 and the impact on structural conformation

5.3.1 Introduction

In this section the changes in the conformational structure of HBD-mod8 and its alanine substitutes were evaluated. The structures have been shown in 5 different buffer types to show varying membrane mimicking environments. These buffers include the two original buffers used previously, PBS, SDS and the new buffers DPC which shows an effect close to that of SDS. LPS and LTA that were also chosen to mimic the bacterium membranes and were representative of Gram-negative and Gram-positive bacteria respectively. For simplicity the results were condensed into Figures shown in this section that are based on Figures shown in appendix section (B) split between Figures B.4, B.5, B.6 and B.7 displaying the full range of buffers on each peptides per page.

5.3.2 Results

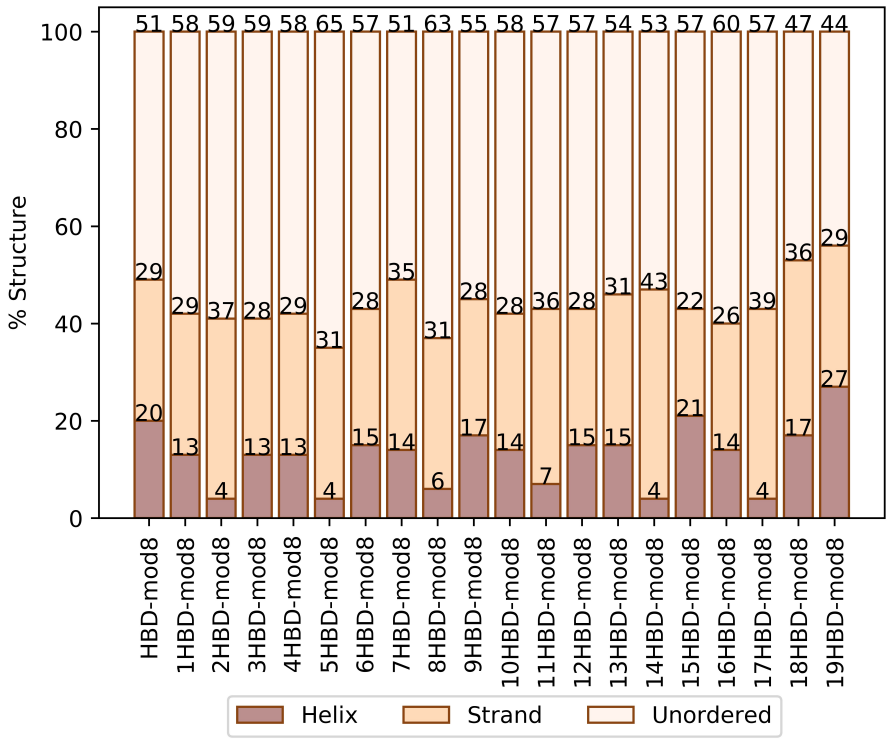
The Peptides across the whole alanine substitution range showed the lowest structural conformation in helix in PBS buffer shown in Figure 5.5a. The highest level of conformation in this buffer belonged to unordered ranging from 44-63%. The strand structure was consistent throughout these peptides with values ranging from 22-43%. The structures were all forced into a helical conformation in SDS in Figure 5.5b and DPC in Figure 5.5e ranging from 43-67% in SDS which showed the lowest helical structure that belonged to 13HBD-mod8 and the highest to 14HBD-mod8 and 31-65% in DPC showing the lowest helical components in 13HBD-mod8 and the highest in 19HBD-mod8.

In membrane mimics of LPS and LTA shown in Figures 5.5c and 5.5d HBD-mod8 shows a mid level range in helical structure with 49% when the highest percentage belonged to 19HBD-mod8 at 59%. 1HBD-mod8 shows the lowest level of helical structure in this buffer at 9%. In LTA however HBD-mod8 shows a lower level of helical component with 19HBD-mod8 showing the highest level at 59% similar to LPS. 2HBD- and 13HBD-mod8 also show a low level of helical conformation showing 4 and 8%, respectively.

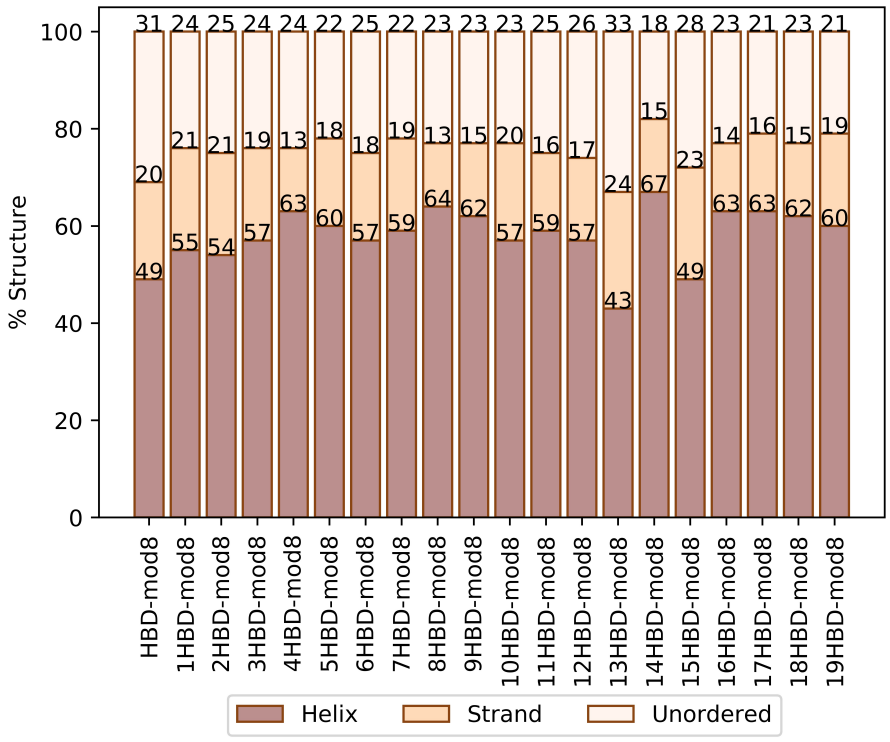
5.3.3 Discussion

It has been reported that the simple change of an alanine residue in place of another amino acid would not have detrimental effect on the conformation of the resulting peptides [207]. Though the antimicrobial effect of these peptides remains to be seen in later chapters. From the reported results it is expected that 19HBD-mod8 would show the most consistent antimicrobial activity across the different bacteria types since it has shown the most conformationally favourable change in LPS and LTA. Across the whole of the peptide series, they all show consistent increase in alpha helical conformation in SDS and DPC when compared to PBS.

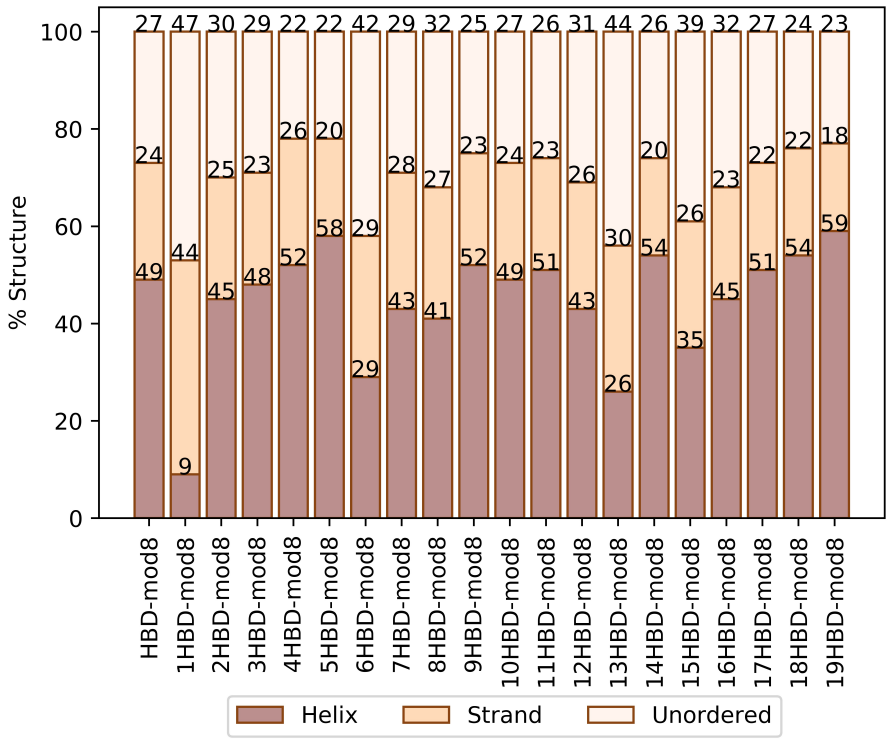
However this does not apply to LPS and especially not to LTA with 4HBD-, 5HBD-, 8HBD-, 14HBD-, 16HBD-, 17HBD-, 18HBD- and 19HBD-mod8 showing an increase in alpha helical content whilst 7, 10, 12, 13HBD-mod8 all showed an increase in beta sheet content in LTA when compared to PBS. HBD-mod8 itself showed a mid range conformational change toward a favourable structure when compared to the peptides in the series with 1HBD-mod8 showing the lowest conformational change towards a helical structure in both the two LTA and LPS buffers.


% Structure
0
20
40
60
80
100
HBD-mod8
1HBD-mod8
2HBD-mod8
3HBD-mod8
4HBD-mod8
5HBD-mod8
6HBD-mod8
7HBD-mod8
8HBD-mod8
9HBD-mod8
10HBD-mod8
11HBD-mod8
12HBD-mod8
13HBD-mod8
14HBD-mod8
15HBD-mod8
16HBD-mod8
17HBD-mod8
18HBD-mod8
19HBD-mod8
Helix
Strand
Unordered

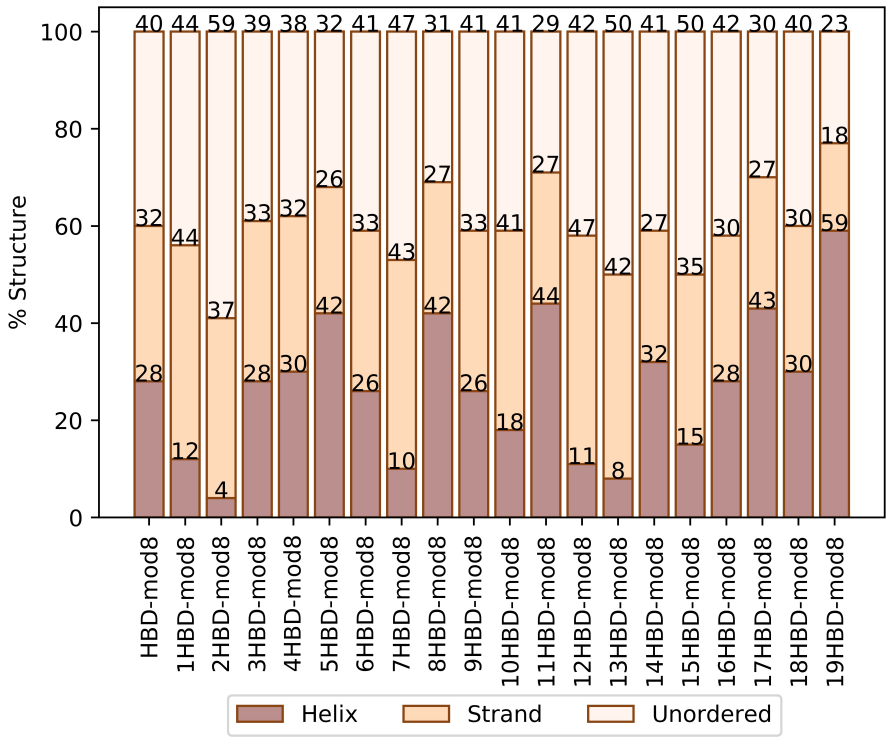
(a) PBS


% Structure
0
20
40
60
80
100
HBD-mod8
1HBD-mod8
2HBD-mod8
3HBD-mod8
4HBD-mod8
5HBD-mod8
6HBD-mod8
7HBD-mod8
8HBD-mod8
9HBD-mod8
10HBD-mod8
11HBD-mod8
12HBD-mod8
13HBD-mod8
14HBD-mod8
15HBD-mod8
16HBD-mod8
17HBD-mod8
18HBD-mod8
19HBD-mod8
Helix
Strand
Unordered

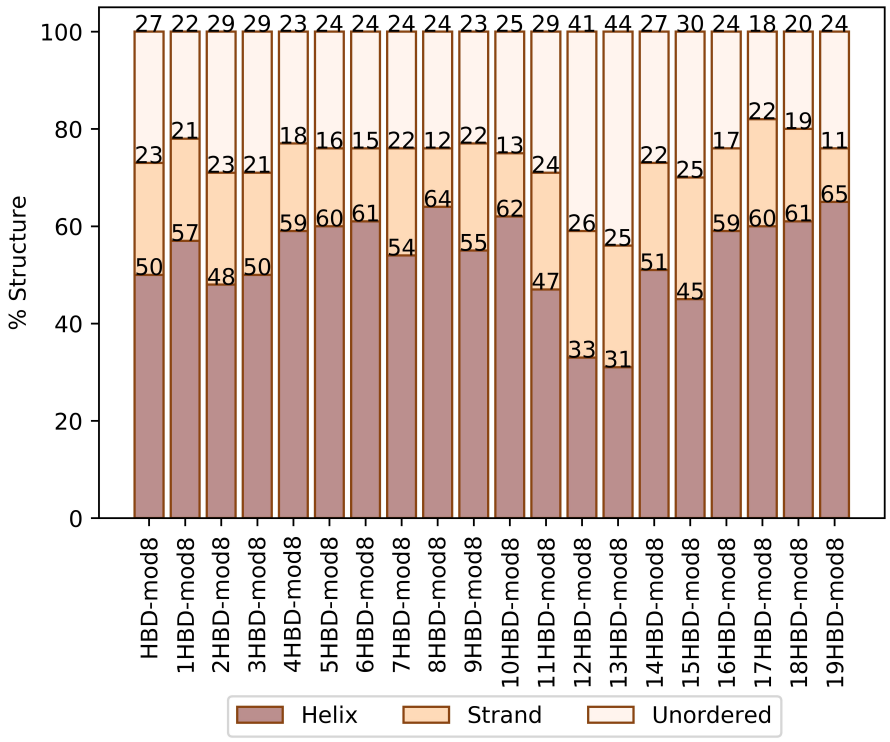
(b) SDS


% Structure
0
20
40
60
80
100
HBD-mod8
1HBD-mod8
2HBD-mod8
3HBD-mod8
4HBD-mod8
5HBD-mod8
6HBD-mod8
7HBD-mod8
8HBD-mod8
9HBD-mod8
10HBD-mod8
11HBD-mod8
12HBD-mod8
13HBD-mod8
14HBD-mod8
15HBD-mod8
16HBD-mod8
17HBD-mod8
18HBD-mod8
19HBD-mod8
Helix
Strand
Unordered

(c) LPS


% Structure
0
20
40
60
80
100
HBD-mod8
1HBD-mod8
2HBD-mod8
3HBD-mod8
4HBD-mod8
5HBD-mod8
6HBD-mod8
7HBD-mod8
8HBD-mod8
9HBD-mod8
10HBD-mod8
11HBD-mod8
12HBD-mod8
13HBD-mod8
14HBD-mod8
15HBD-mod8
16HBD-mod8
17HBD-mod8
18HBD-mod8
19HBD-mod8
Helix
Strand
Unordered

(d) LTA



(e) DPC

Figure 5.5: Secondary structure of HBD-mod8 alongside its alanine substitutes expressed in the percentage of helix, strand and unordered that were calculated by combining helix 1 and 2, strand 1 and 2 and turn and unordered respectively. These peptides were all tested in 5 different conditions in PBS, SDS, DPC, LPS and LTA. Showing a clear change in the strctureu from PBS to SDS and with LPS and LTA showing very similar results just as with SDS and DPC.

5.4 Molecular dynamic simulation of HBD-mod8 in POPC and DMPG/DMPC

5.4.1 Introduction

To be able to present more information regarding the conformational changes of HBD-mod8, this peptide was used to simulate the interaction between the membrane bilayer and the peptide. This was performed using the two different bilayers that were representative of mammalian and bacterial membranes to understand the effect of different membrane structure on the conformation of the peptide under constant pressure and temperature. The result for the Molecular Dynamic Simulation (MD) was reported in terms of its mass density. Mass density refers to the distribution of the atoms along the membrane. Electron density and mass density profiles are similar in typical MD simulations therefore reporting of one entity can be interpreted to reflect the other. The centre of mass of the membrane was calculated in the first step of the MD simulation, so that the coordinates of each atom was considered with respect to the centre.

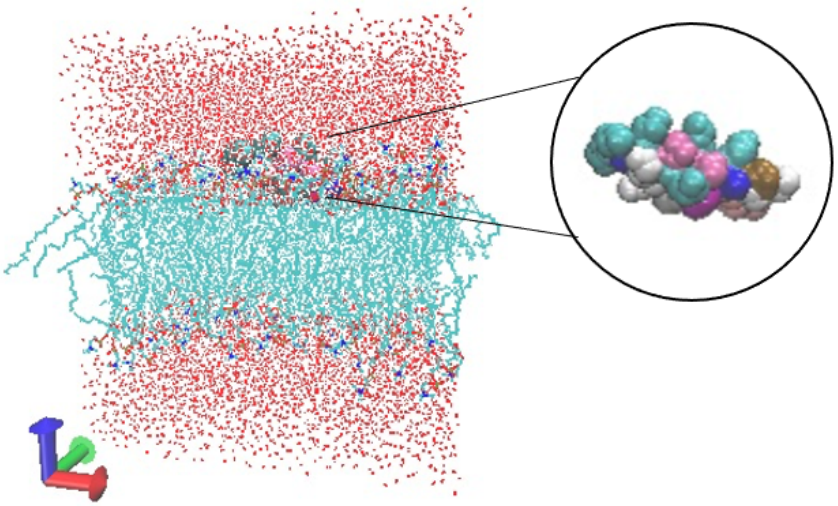
5.4.2 Results

As seen from Figures 5.6 and 5.7 the peptide took a flat conformation on top of POPC in Figure 5.6a however this peptide was shown to have a more angular downward trajectory when in DMPG/DMPC shown in Figure 5.7a. This was also reflected in the NVT/NPT density referring to the acronym for three components of the MD ensemble where N stands for number of particles, V/P stand for volume and T stands for temperature of the peptides showing the lipid tail and the placement of the peptide. The interaction of the peptide with the lipid headgroups and the acyl chain shown in Figures 5.6b and 5.7b shows a complete different insertion pattern. In Figure 5.7b that

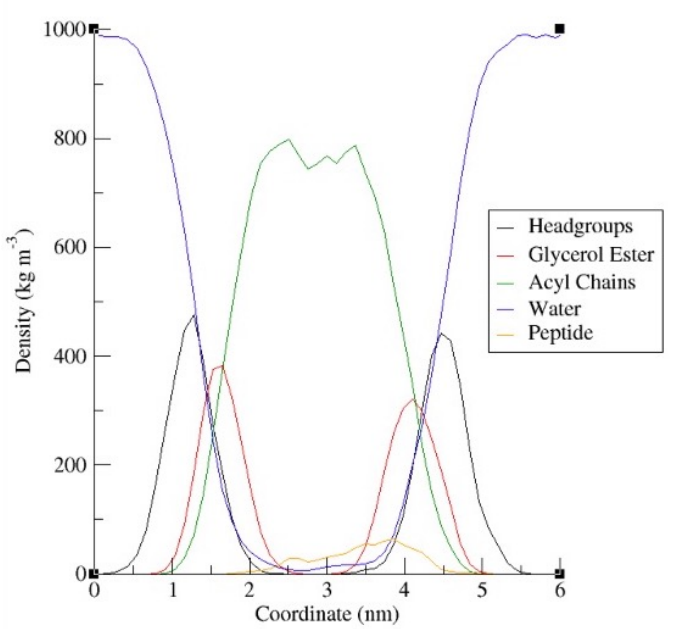
represents bacterial membrane it can be seen that the peptide is completely inserted within the membrane acyl chain whereas in Figure 5.6b the peptide is only inserted on top of the lipid headgroup and it is still suspended within the water molecules.

5.4.3 Discussion

The insertion of the peptide within the acyl chain of the membrane mimicking bacterial environment indicates that this peptide should show clear activity against bacteria. According to [99], [208] the determination of the MD simulations is extremely crucial in finding a suitable antimicrobial peptide designed through either de-novo approaches or through already existing antimicrobial peptides and their modifications. MD simulation can be a useful tool to assess the insertion pattern of each peptides in different membrane bilayers representing different environments and will save time and resources to test more hypothesis.



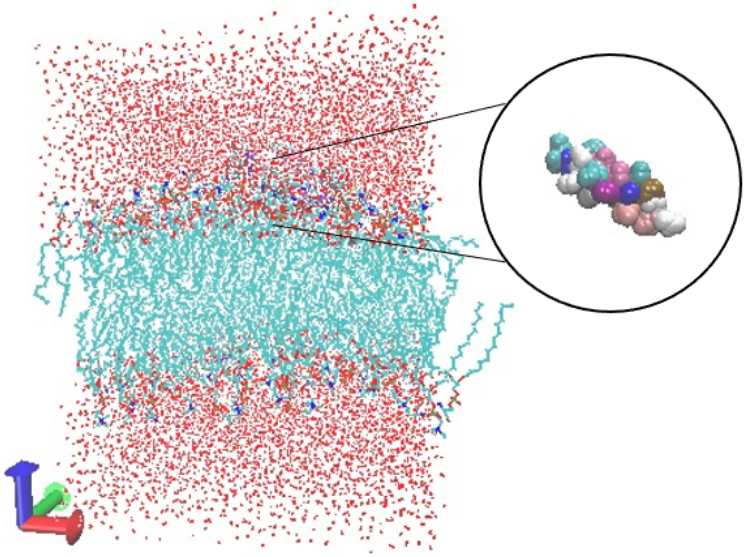
(a) POPC



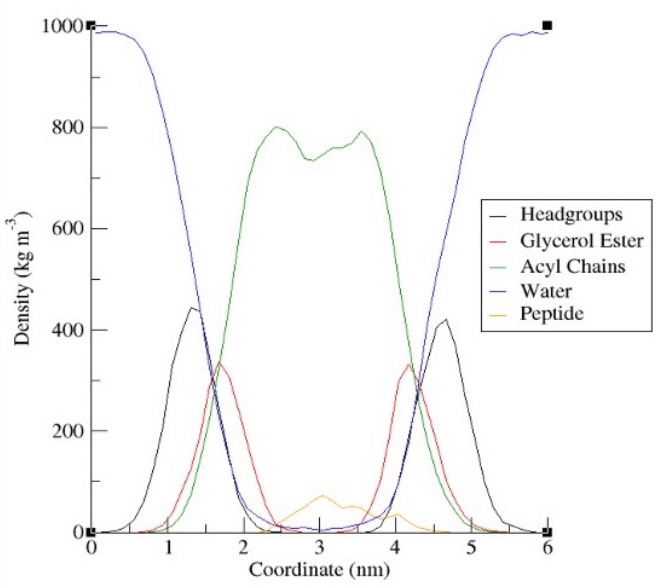
(b) Mass density of the peptide calculated using the information collected during NVT step

Figure 5.6: Molecular dynamic simulation showing the difference in the conformation of HBD-mod8 in 1-palmitoyl-2-oleoyl-sn-glycero-3-phosphocholine (POPC). Produced using a combination of Charmm-gui membrane builder and Gromacs through 10ns of equilibration. The NVT mass distribution was also calculated through Gromacs NVT which shows the distribution of the peptide within the bilayer through mass density consideration and constant temperature and pressure.

The molecules in Water, Lipid tail and the peptide is shown in the black circle to the side of (a).



(a) DMPG/DMPC



(b) Mass density of the peptide calculated using the information collected during NVT step

Figure 5.7: Molecular dynamic simulation showing the difference in the conformation of HBD-mod8 in Dimyristoylphosphatidylglycerol/Dimyristoylphosphatidylcholine (DMPG/DMPC). Produced using a combination of Charmm-gui membrane builder and Gromacs through 10ns of equilibration. The NVT mass distribution was also calculated through Gromacs NVT which shows the distribution of the peptide within the bilayer through mass density consideration and constant temperature and pressure. The molecules in Water, Lipid tail and the peptide is shown in the black circle to the side of (a).

Chapter Six

Biological characterisation

6.1 Microbiology

In this section the peptide activity against *S. aureus* and *P. aeruginosa* is presented and discussed. These two bacteria were chosen to represent a common Gram-positive and a common Gram-negative pathogen. These bacteria were also shown to be prevalent at the site of implant incisions and on implant surfaces. Once the peptide or peptides with an activity comparable to its corresponding antibiotic were identified through the use of Minimum Inhibitory Concentration (MIC), they were investigated further through alanine scanning to find the most effective moieties of the peptide responsible for the antimicrobial activity against *S. aureus*, *P. aeruginosa* and *E. coli* which was also included in this study as an added representation for Gram-negative bacteria. The bacterial mechanism of resistance against the most effective peptide was also studied for *S. aureus*, *P. aeruginosa* and *E. coli*.

6.1.1 Bacterial viability for hBD1 analogous

Introduction

In order to study the effect of the designed peptides based on hBD1 on bacterial viability, six different concentrations were used to establish an active concentration compared to the control.

The initial concentration used in this experiment was $500\mu M$ and through 2-fold dilutions the final peptide concentration was $16\mu M$. Each dose response graph in Figures 6.1 and 6.2 represents the percentage of bacterial growth after 24hrs incubation at six different log concentrations for all 8 peptides and their control for each bacteria included in the legend. The control used for each bacteria is vancomycin for *S. aureus* and polymixin B for *P. aeruginosa*. The percentage of bacterial growth at each concentration against each peptide was calculated by subtracting the Optical Density (OD) of

the peptides from the overall OD of the bacteria on the same plate and normalising to 100% viability. If a bacteria had negative growth value it was an indication of a larger growth than 100% viability. The effect of the peptides on the percentage of bacterial growth shows a variety of different results depending on the peptide. In order to find the difference between each peptide and its concentration as a whole a One Factor ANOVA test was used with Dunnett's and Tukey HSD as a follow up. The antibiotic variations used for the ANOVA test were the result of different tests on different days and the concentration was kept at a consistence MIC. Through this analysis where the p-value was above 0.05 and the mean value of the peptide is close or above the mean percentage of bacterial growth of the antibiotic, the peptide was considered to show non-inferior activity compared to the control antibiotic. Where the p-value of the peptide was below 0.05 with the mean mean percentage of bacterial growth value above the antibiotic this result is significant and shows antimicrobial activity better than that of the antibiotic.

Results

Though it can be seen that HBD-mod8 shows high activity levels against *S. aureus* and *P. aeruginosa* across all concentrations, this observation can be better interpreted using statistical analysis and the results are as followed. Figure 6.1 shows the activity of the peptides and their different concentration on the percentage of bacterial growth in comparison to antibiotic vancomycin. It can be seen from this figure, that HBD-mod8 and HBD-mod7 show high activity against *S. aureus* at their highest concentration ($500\mu M$). Although HBD-mod8 maintains this activity at $250\mu M$ concentration, HBD-mod7 does not. These observations are accompanied by their corresponding p-values of 0.13 and 0.97 respectively, showing that the the overall activity of HBD-mod7 and HBD-mod8 are not significantly different than that of vancomycin, with their mean values similar to the antibiotic whilst the activity of the other peptides

show unfavourable significant difference with p-values lower than 0.05 and mean values lower than the mean values of the antibiotic.

It can also be seen from this figure that the activity of HBD-mod8 against the bacteria diminishes at concentrations below $250\mu M$ and that the other peptides in the series based on hBD1 do not show similar activity against the bacteria to that of a the antibiotic at any concentration. Since the overall activity of HBD-mod8 and antibiotic were similar as shown previously, the activity at $250\mu M$ concentration was compared showing the mean value higher than vancomycin at 76 and 68((± 25) respectively. With p-value of 9.9×10^{-5} this concentration shows a significant difference between their activities. The statistical analysis between the activity of HBD-mod7 at $500\mu M$ concentration and control also showed this to be the concentration that shows comparable activity to vancomycin against *S. aureus* with mean value of 53 and 68 with a p-vale of 0.57 showing similar activity to the antibiotic with no signifiant difference.

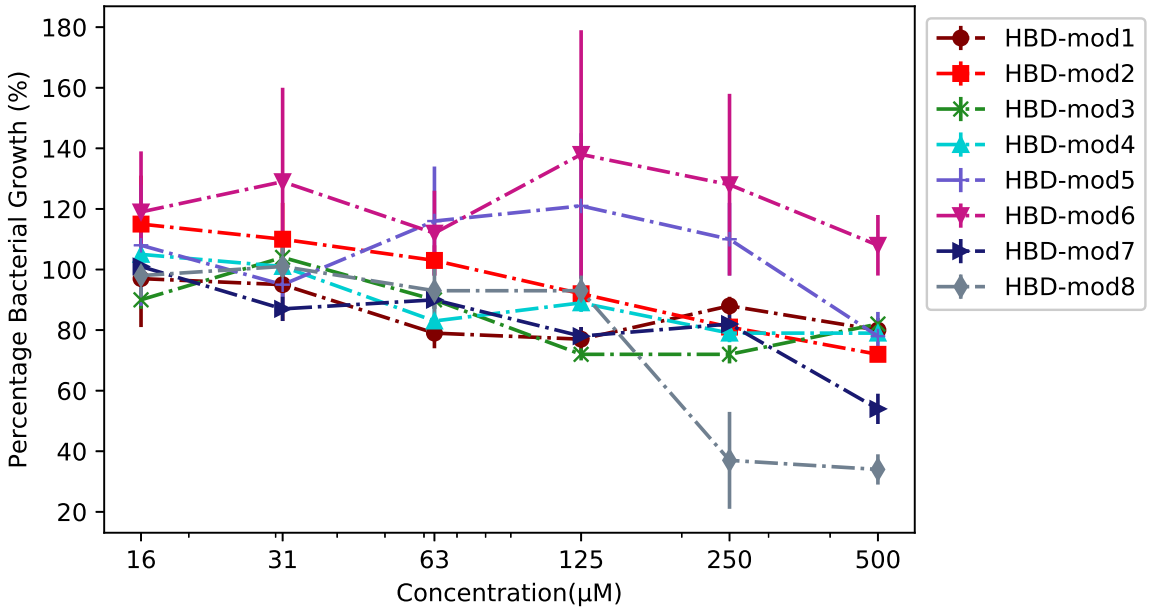


Figure 6.1: The effect of peptides as well as their differing concentrations on *S. aureus* survival with its corresponding antibiotics (Vancomycin) as control. (a)-(f) shows the 2-fold dilutions of peptides based on hBD1. The overall mean percentage of bacterial growth values for each peptide was used to calculate the p-values are 68(±25), 86, 96, 15, 85, 105, 122, 82 and 76 for antibiotic and HBD-mod1 to HBD-mod8, respectively. The p-value between HBD-mod1, HBD-mod2, HBD-mod3, HBD-mod4, HBD-mod5, HBD-mod6, HBD-mod7, HBD-mod8 and the control is 0.008, 0.000, 0.017, 0.000, 0.000, 0.000, 0.13* and 0.97* respectively.

* shows favourable non significant difference

Figure 6.2 reports the activity of different concentration of designed peptides based on hBD1 against *P. aeruginosa* compared to the antibiotic Polymixin B. Similar to the activity of HBD-mod8 against *S. aureus*, this peptide shows no significant overall difference with the p-value of 1.0 when compared to the antibiotic and an overall mean mean percentage of bacterial growth value of 69 and 68($\pm$9) respectively for HBD-mod8 and antibiotic. To find the the lowest concentration for this peptide that showed comparable activity to the antibiotic the lowest concentration was considered and for this bacteria at 250μM concentration the peptide showed comparable activity to the antibiotic with p-value of 1.0 and mean value of 68, showing no significant difference. Although this peptide shows better activity at concentration 500μM with p-value of 7.5×10^{-5} and mean percentage of bacterial growth value of 35 showing a significant different activity when compared to Polymixin B against *P. aeruginosa*, it was not used as the final testing concentration for *P. aeruginosa*. Instead, 250μM which showed similar activity to the antibiotic was used as the final testing concentration. Similarly, HBD-mod7 showed comparable activity with p-value of 0.15 and mean value of 55% showing no significant difference between its activity and the activity of the antibiotic. This peptide was not considered in the end due to its poor activity levels overall across all concentrations. The rest of the peptides showed poor activity with their p-values below 0.05 and mean percentage of bacterial growth values below the antibiotic.

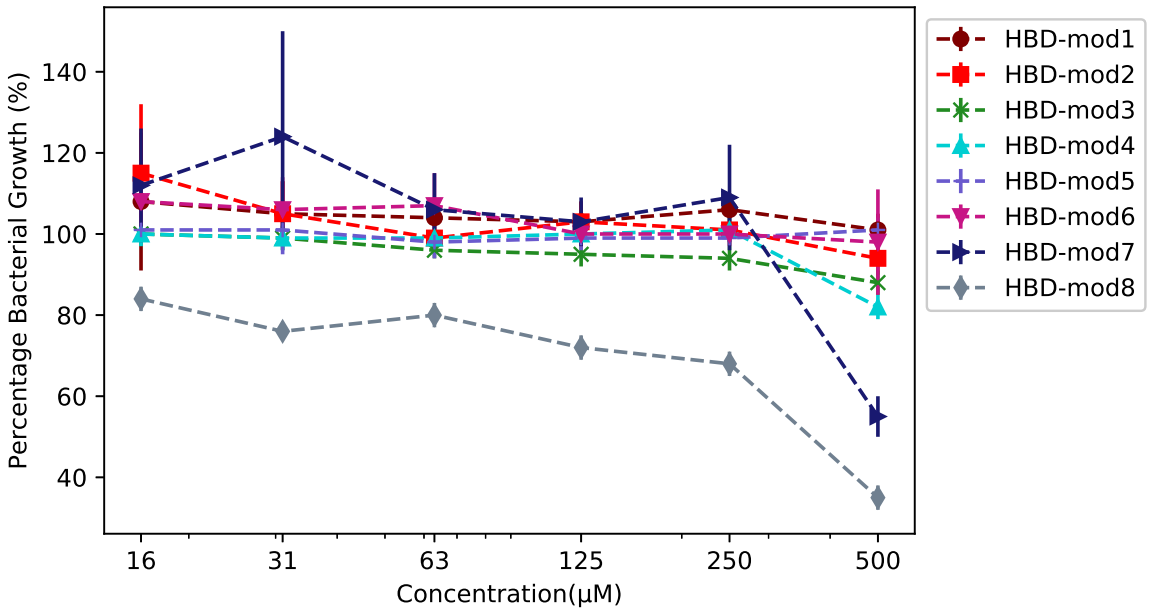


Figure 6.2: The mean values for each peptide used to calculate are 68(±9), 105, 103, 95, 97, 100, 103, 102 and 69 for Antibiotic and HBD-mod1 until HBD-mod8, respectively. The p-value between HBD-mod1, HBD-mod2, HBD-mod3, HBD-mod4, HBD-mod5, HBD-mod6, HBD-mod7 and the control was 1.0×10^{-13} and between HBD-mod8 and the control was 1.0*. At $500\mu M$, HBD-mo8 with p-value 7.5×10^{-5} ** and it shows a better activity than antibiotic it also shows similar activity to the antibiotic with p-value of 1.0* at concentration of $250\mu M$.

* shows favourable non significant difference / ** shows favourable significant difference

Discussion

The results from the peptides based on hBD1 show that HBD-mod8 showed comparable activity to their control, Vancomycin and Polymixin B, respectively against *S. aureus* and *P. aeruginosa* with no significant difference in the overall activity in comparison to the antibiotics. Taking into consideration the concentrations, HBD-mod8 showed a significant different activity against *S. aureus* at $250\mu M$ and at the same concentration it showed comparable activity to the antibiotic against *P. aeruginosa*. Therefore this peptide was chosen as the peptide with activity against both bacteria at a concentration of $250\mu M$.

Though HBD-mod7 also showed comparable overall activity to the antibiotic vancomycin against *S. aureus*, its activity against *P. aeruginosa* was not comparable to Polymixin B, hence this peptide is not a good candidate in terms of its antimicrobial activity when taking into consideration both bacteria.

Although the initial comparison between the peptide and antibiotic activity was made using their overall activity levels without taking into consideration the concentration for ease of comparison, the concentration was later taken into consideration when choosing the value in which the inhibition of bacterial growth was comparable to the control. If the activity of the peptide including the concentration was taken into consideration initially, most if not all peptides would have passed the antimicrobial activity test since they all showed comparable levels of activity to the control at their highest concentration. In order to avoid having to choose the highest concentration since in most instances higher concentrations of peptides are costly [158] and they usually lead to cell toxicity [209], the method used was designed so the concentration did not effect the selection process initially and it was only used to find the comparable value to the control in the most effective peptide after the selection process.

Since HBD-mod8 showed the most activity compared to the other peptides,

this can be attributed to its ideal alpha helical structure and the investigation into its alanine scan will reveal its most active moieties for its activity against both bacteria. Since this peptide is a combination of active residues at each position in the antimicrobial peptide databases and hBD1 where each position was changed to achieve an alpha helical structure, it is understandable that it showed the most antimicrobial activity.

It is also important to note that this peptide shows better activity level against *S. aureus*, which is against the literature with most positively charged antimicrobial peptides showing better activity levels against Gram-negative bacteria due to the electrostatic attraction [89], [210]. This could be attributed to the 33% hydrophobicity of HBD-mod8, which has been proven to be an important factor in the activity of antimicrobial peptides against Gram-negative bacteria [56]. Other reasons, could be attributed to the activity of this peptide which is not solely based on membrane attraction and structure. This peptide could be neutralising the bacteria toxins such as exotoxin A of *P. aeruginosa* [91] and *S. aureus* exotoxins, seen in the literature, especially with defensins that generally show their activity through different mechanisms [55].

6.1.2 Bacterial viability for hBD3 analogous

Introduction

Similar to the peptides based on hBD1, Figures 6.3 and 6.4 show the activity of the peptides based on hBD3 against *S. aureus* and *P. aeruginosa* at six concentrations to find the most effective peptide that shows comparable activity to the control, vancomycin and Polymixin B, respectively.

The percentage of bacterial growth values were also calculated similar to the last experiment mentioned above by taking into consideration the OD of the bacteria for each experiment on each day to insure that data collected on different days are comparable to one another. The starting concentration of the peptides used was $500\mu M$ and using 2-fold dilution the final concentration was $16\mu M$. The p-values were calculated through One Factor ANOVA test with the follow up of Dunnett's and Tukey HSD to find the significance of the activity of each peptide in comparison to the antibiotic as a whole with and without the consideration of the concentration. Through this analysis where the p-value was above 0.05 and the mean value of the peptide is close or above the mean percentage of bacterial growth of the antibiotic, the peptide was considered to show non-inferior activity compared to the control antibiotic. Where the p-value of the peptide was below 0.05 with the mean mean percentage of bacterial growth value above the antibiotic this result is significant and shows antimicrobial activity better than that of the antibiotic.

Results

Figure 6.3 shows the activity of the peptides based on hBD3 against *S. aureus* with the antibiotic vancomycin as the control. Each peptide activity was compared to the activity of the antibiotic and the statistical analysis shows no significant difference

between the overall activity of HBD3-mod1 and the activity of vancomycin with a p-value of 0.06 and the mean value greater than the mean value of vancomycin at 30 and 41($\pm$9)%, respectively. This peptide shows a high level of activity across all concentrations but the lowest concentration that shows comparable activity to the control was shown to be $31\mu M$ with a p-value of 0.9 showing no significant difference with the mean percentage of bacterial growth of 36%. This peptide does not retain its activity levels at $16\mu M$ concentration with a p-value of 2×10^{-14}.

The remaining peptides show activity of significant difference compared to the activity of vancomycin with mean percentage of bacterial growth, lower than the antibiotic. This Figure also shows the different concentrations starting from $500\mu M$ and ending with the concentration of $16\mu M$. It can be seen that all the peptides show similar activity to the vancomycin against the bacteria at the highest concentration of $500\mu M$.

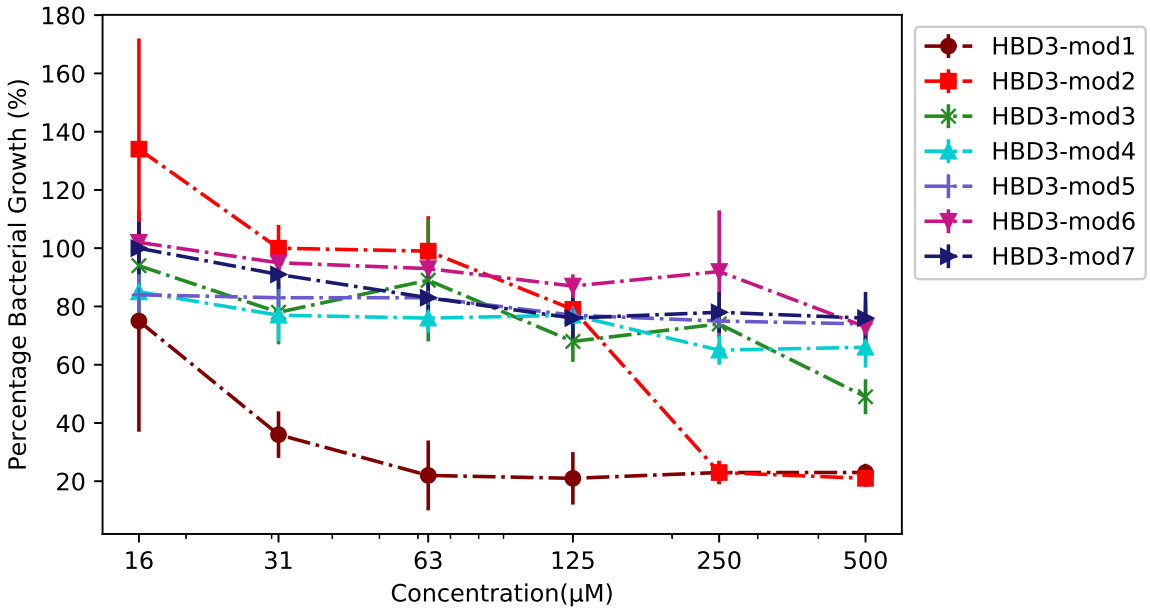


Figure 6.3: The effect of peptides based on hBD3 as well as their differing concentrations on *S. aureus* survival with its corresponding antibiotics (Vancomycin). The overall mean percentage of bacterial growth values for each peptide used to calculate the p-values are 41(±9), 30, 76, 75, 74, 79, 97 and 87 for Antibiotic and HBD3-mod1 until HBD3-mod7, respectively. The p-value between HBD3-mod1 and the control was 0.06*, between HBD3-mod2, HBD3-mod3, HBD3-mod4, HBD3-mod5, HBD3-mod6, HBD3-mod7 and the control was, 1.2×10^{-13}. HBD3-mod1 no significant difference with p-value of 0.9* at $31\mu M$

* shows favourable no significant difference

Figure 6.4 shows the activity of the peptides based on hBD3 against *P. aeruginosa* and its control, Polymixin B. From this figure and the statistical analysis it can be seen that all peptides show significantly different overall activity in comparison to the activity of Polymixin B against the bacteria. With all the mean values smaller than the mean value of the Polymixin B this significant difference is notable. This figure shows the comparison between the activity of peptides in different concentrations against the bacteria starting from $500\mu M$ and ending with the concentration of $16\mu M$.

Although the activity of the peptides against the bacteria does not follow the same trend as that of *S. aureus*, it is notable to mention that HBD3-mod1 shows high activity levels against the bacteria at the majority of the concentrations and to compare the activity of the peptide in a specific concentration, it shows comparable activity to the antibiotic with a p-value of 0.06 at $31\mu M$ concentration. Similarly, HBD3-mod2 also shows comparable activity to the antibiotic at $125\mu M$ concentration with p-value of 0.9 where its mean percentage of bacterial growth value, similar to the antibiotic. These two concentrations could both be considered as they showed comparable activity to the control against *P. aeruginosa*.

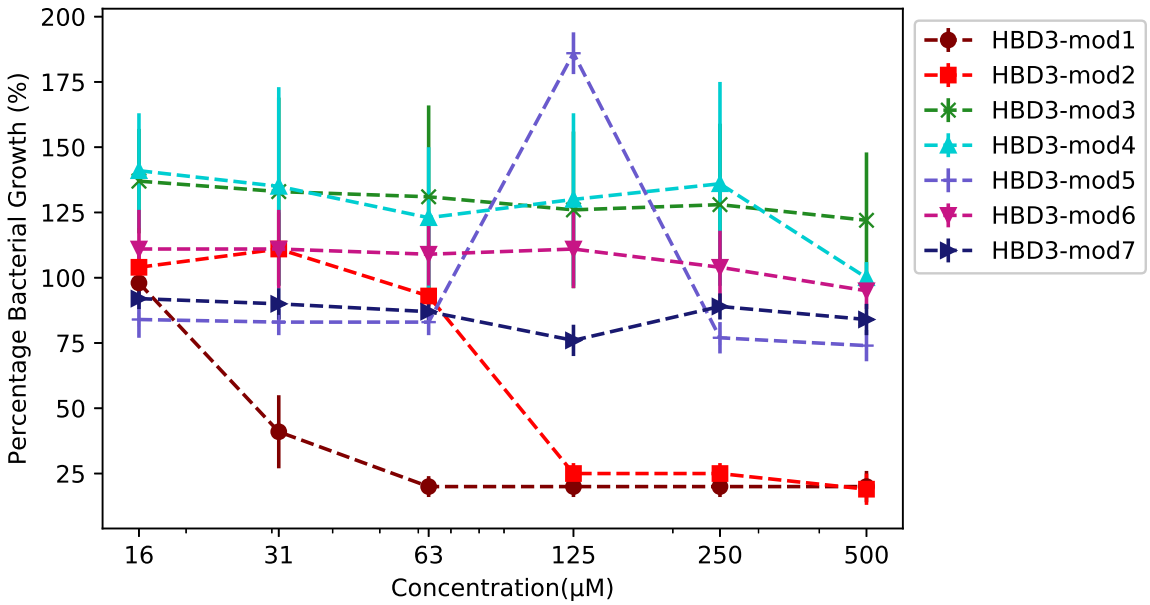


Figure 6.4: The effect of peptides as well as their concentrations on *P. aeruginosa* survival with its corresponding antibiotics (Polymixin B) as control showing the 2-fold dilutions of peptides based on hBD3. The mean values for each peptide used to calculate the p-value are 24($\pm$5), 37, 62, 129, 127, 79, -106, 88 for Antibiotic and HBD3-mod1 until HBD3-mod7, respectively. The p-value between HBD3-mod1 and the control is 0.02 and 1.2×10^{-13} between HBD3-mod2, HBD3-mod3, HBD3-mod4, HBD3-mod5, HBD3-mod6, HBD3-mod7 and the control. All values show a significant difference between their activity against *P. aeruginosa* and the peptides meaning none of the peptides show an overall activity similar to the antibiotic tested with HBD3-mod1* and HBD3-mod2* showing favourable significance Although the antibiotic is included in every graph it was only tested at its critical MIC found in the literature and was not tested at different concentration.

* shows favourable no significant difference

Discussion

The statistical analysis on the activity of peptides based against hBD3 against the two bacteria, *P. aeruginosa* and *S. aureus* shows that HBD3-mod1 shows comparable activity to the antibiotic against both strains active concentration of $31\mu M$. Although this peptide does not show an overall activity comparable to the activity of Polymixin B against *P. aeruginosa* the activity at each concentration is comparable to the activity of Polymixin B. HBD3-mod2 also shows high activity against *P. aeruginosa* with MIC of $125\mu M$ and against *S. aureus* with active concentration of $250\mu M$. The remaining peptides based on hBD3 all show a significant difference when compared to the antibiotic against both bacteria with mean values all below the antibiotic's.

The high level of activity of HBD3-mod1 can be attributed to its alpha helical structure and the placement of its hydrophobic residues equally situated on both sides of the helical structure in clusters of three 3.7a, which is shown in the literature to be the optimal antimicrobial structure [211]. The lack of activity for the remaining peptides can also be attributed to the loss of hydrophobicity in the sequence of the peptide coupled with its loss of equally positioned hydrophobic residues on both sides of the helical structure.

This peptide also shows equal activity against both bacteria showing that the sequence shows the most promise to be an effective antimicrobial peptide.

6.1.3 The effect of alanine substitution on the activity of HBD-mod8 against Gram-positive and Gram-negative bacteria

Introduction

To find the most important residues conferring activity in HBD-mod8 an alanine substitution test was carried out. This substitution was performed for different concentrations of the peptides from $500\mu M$ to $16\mu M$ shown in log form. Each peptide was numbered after each substitution and when an Ala residue already resided in the sequence, the sequence was not modified and was kept as its original HBD-mod8 format. The results are also shown in bar chart format in appendix section three(C).

Additionally, each result section was split into two different comparisons, one between the original peptide HBD-mod8 and the substituted peptides and one between the antibiotics and the substituted peptides. The p-values reported in the legend of each figure draw the comparison between the activity of each peptide and the activity of the antibiotic.

Similar to the previous sections, a One Factor ANOVA test was performed along with the Dunnett's test and the Tukey HSD test as a follow-up to find the significant difference between the activity of that of the antibiotic and the alanines substitution of the HBD-mod8. This test was also done to find the significant difference of the substitutions on the activity of the HBD-mod8.

In this section however, in addition to the two bacteria *P. aeruginosa* and *S. aureus*, *E. coli* was also used due to its frequency as a pathogen of the gut and urogenital tract. Although this bacterium is not common in the site of incisions or the implant surface it is an important bacterium that is frequently studied in the literature as a representation of Gram-negative model organism [86], [212]. Additionally, this bacteria is one of the most resistant strains similar to the other two bacterium and to find a

peptide that may bypass this resistance is valuable [1], [213].

Results

The effect of alanine substitution on the activity of HBD-mod8 against *S. aureus*

Figure 6.5 shows the effect of alanine substitution on the activity of HBD-mod8 (7.1) against *S. aureus*. As seen in this figure 3HBD-mod8, 10HBD-mod8, 13-15HBD-mod8 all show similar activity in comparison to HBD-mod8 against *S. aureus*. The p-values are 0.9, 0.08, 1, 0.9 and 1, respectively showing no significant difference between their activity. The remaining peptides all show a significant different activity when compared to the activity of HBD-mod8 with p-values lower than 0.05 and mean values lower than the mean percentage of bacterial growth for HBD-mod8 therefore their activity is less desirable than HBD-mod8.

The effect of alanine substitutions in comparison to Vancomycin against *S. aureus*

The comparison between the activity of the alanine substituted peptides and the antibiotic shows a significant difference between 3HBD-mod8 and 13-15HBD-mod8 with p-values below 0.05 and mean percentage of bacterial growth higher than antibiotic. Although, 10HBD-mod8 maintains its activity pattern when compared to the antibiotic and it shows no significant different activity against the bacteria. In addition to 10HBD-mod8, 11HBD-mod8 also shows no significant difference when compared to the activity of antibiotic with mean values close to the antibiotic. As shown previously in section 6.1.1, HBD-mod8 displays strong activity against *S. aureus* with the mean value of 44 percentage of bacterial growth when compared to the activity of the an-

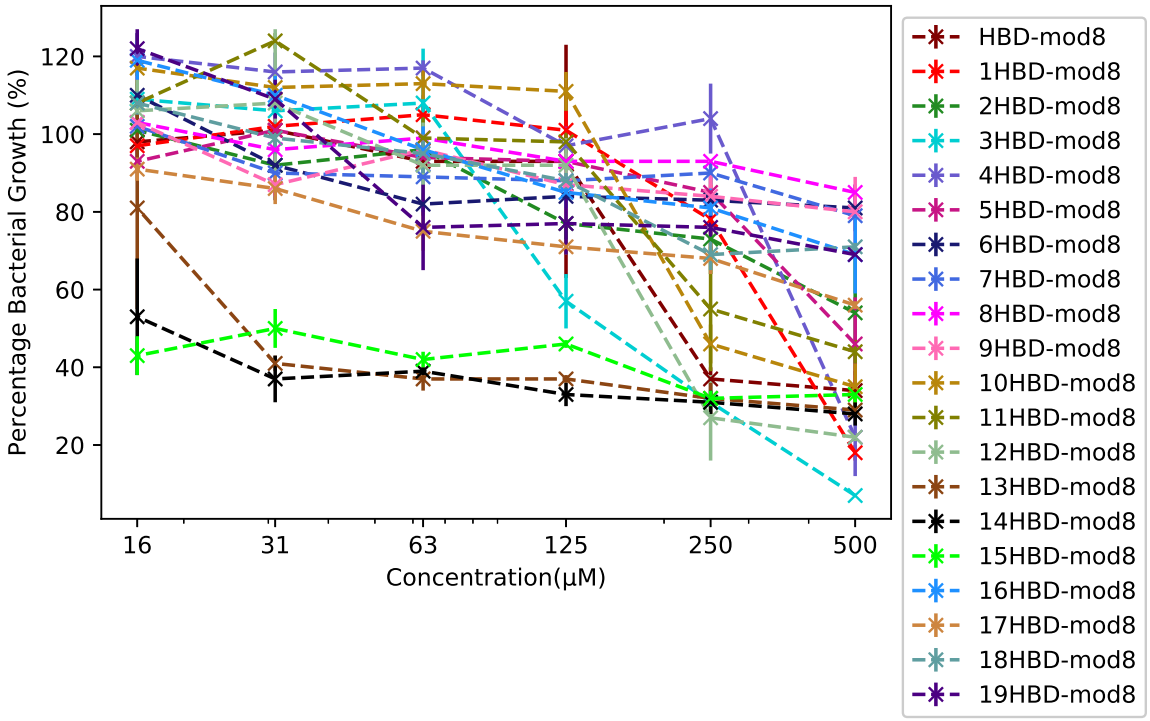


Figure 6.5: The effect of alanine substitution on antimicrobial activity of HBD-mod8 against *S. aureus*.

According to the statistical analysis HBD-mod8, shows significant difference when compared to the activity of vancomycin with a p-value of 0.002. Similarly, 3HBD-mod8, 13HBD-mod8, 14HBD-mod and 15HBD-mod8 also show a significant difference when compared to the activity of vancomycin with the p-values of 5.2×10^{-5}, 0.001, 3.9×10^{-5} and 6.8×10^{-5}. On the other hand 10HBD-mod8 and 11HBD-mod8 show an activity comparable to that of the antibiotic with mean value of 49($\pm$14) and p-values of 1 and 0.9 respectively.

tibiotic with the mean percentage of bacterial growth of 49($\pm$14)%, showing significant different activity with a p-value of 0.002.

The effect of alanine substitution on the activity of HBD-mod8 against *P. aeruginosa*

Figure 6.6 shows the effect of the alanine substitution on the activity of the HBD-mod8 against *P. aeruginosa*. With p-value of 0.08, 1HBD-mod8 shows similar activity to that of the HBD-mod8 with mean percentage of bacterial growth value of 14% when compared to to that of 35% for HBD-mod8. 4HBD-mod8, on the other hand shows significantly different activity with higher mean percentage of bacterial growth at 9% and a p-value of 0.001. The remaining peptides either show weaker activity with p-values indicative of unfavourable significance with mean values below that of HBD-mod8.

The effect of alanine substitutions in comparison to Polymixin B against *P. aeruginosa*

The p-values reported in the legend of figure 6.6 reflect the comparison of the activity between the antibiotic and the peptides showing no significant difference between the activity of HBD-mod8 as shown previously in section 6.1.1. This trend continues with 1HBD-mod8 where the p-value of 0.2 indicates no significant difference between the two activities. Similarly the activity of 4HBD-mod8 is significantly different in favour of the peptide with a mean value higher than the antibiotic. The remaining peptides all show significantly different activity and lower mean value than the activity of the antibiotic with 33($\pm$8)% mean percentage of bacterial growth.

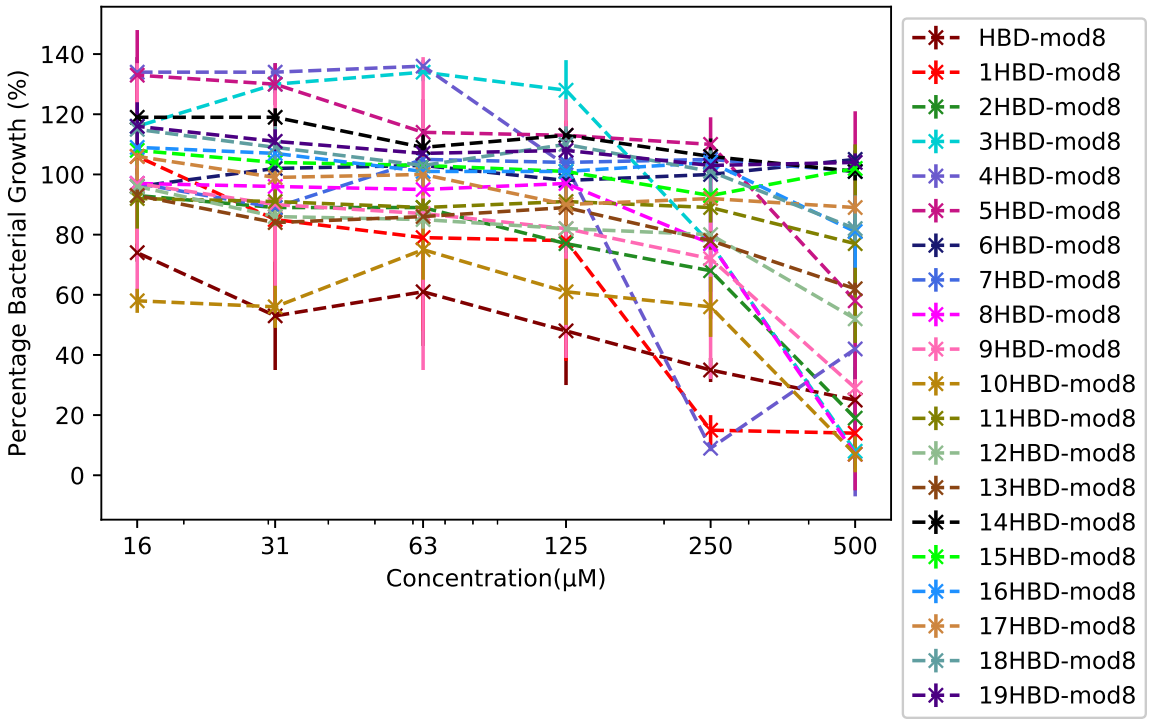


Figure 6.6: The activity of alanine substitution on the activity of HBD-mod8 against *P. aeruginosa*.

According to the statistical analysis HBD-mod8, shows no significant difference with the activity of the antibiotic as previously shown with a p-value of 1 against *P. aeruginosa*. 1HBD-mod8 also shows comparable activity to that of Polymixin B with the p-value of 0.2. On the other hand 4HBD-mod8 shows a better activity than the antibiotic with a p-value of 0.005 and the mean value of 9% which is also larger than the mean value of the antibiotic at 33(±8)%. The other peptides all show a significantly different activity when compared to the activity of the antibiotic with mean values smaller than the mean value of the antibiotic.

The effect of alanine substitution on the activity of HBD-mod8 against *E. coli*

The activity of the substituted peptides against *E. coli* is shown in Figure 6.7. The activity comparison between the alanine substituted peptides and HBD-mod8 shows similar activity against *E. coli*, in the majority of the peptides with the exception of 1-2HBD-mod8, 6HBD-mod8, 8-9HBD-mod8,12-13HBD-mod8, and 15HBD-mod8 showing significant difference with p-values below 0.05 and mean values below that of HBD-mod8. The remaining peptides (HBD-mod8, 3-5HBD-mod8, 7HBD-mod8, 10-11HBD-mod8, 14HBD-mod8, 16-19HBD-mod8 all show similar activity to HBD-mod8 with a p-values of 1 showing no significant difference between their activity and mean values either higher or similar to that of HBD-mod8 showing, 9% mean percentage of bacterial growth.

The effect of alanine substitutions in comparison to Ciprofloxacin against *E. coli*

The activity of the substituted peptides compared to the antibiotic mimics the similarity between the result of the comparison between the peptides and their original sequence, HBD-mod8 where, 1-2HBD-mod8, 6HBD-mod8, 8-9HBD-mod8,12-13HBD-mod8, and 15HBD-mod8 show significantly different activity and 3-5HBD-mod8, 7HBD-mod8, 10-11HBD-mod8, 14HBD-mod8, 16-19HBD-mod8 show no significant difference when compared to the antibiotic.

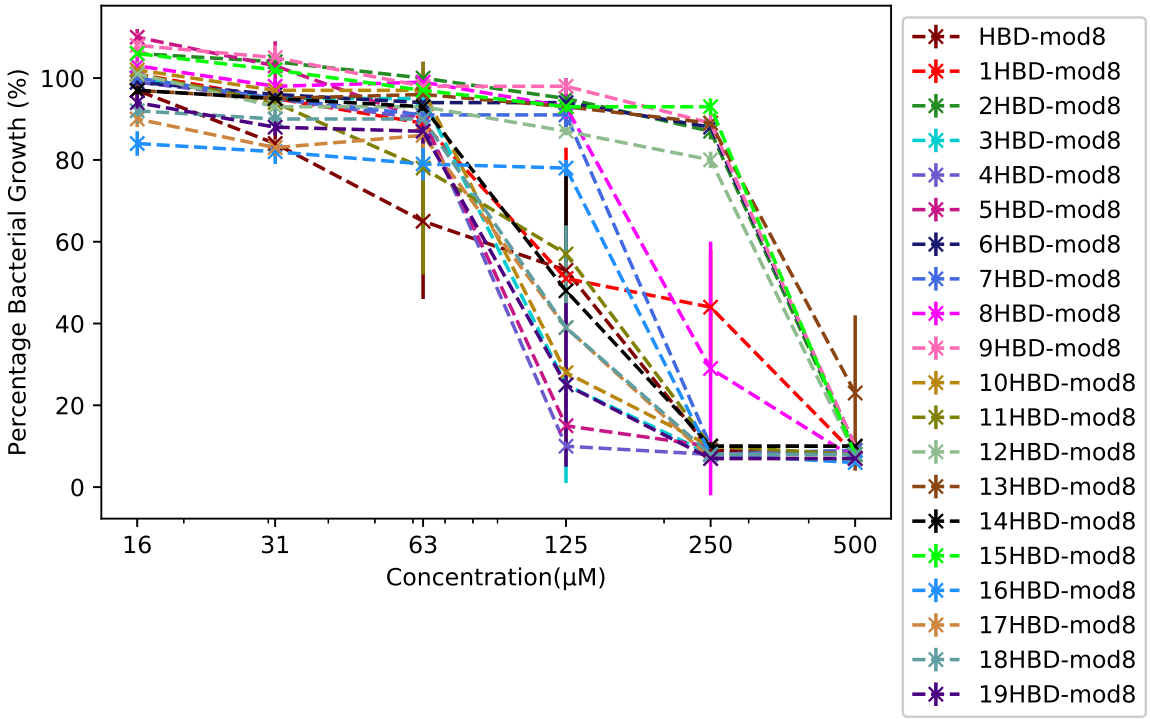


Figure 6.7: The activity of alanine substitution on the activity of HBD-mod8 against *E. coli*.

According to the statistical analysis the majority of the peptides show no significant difference when compared to the activity of the antibiotic at 14(±6)%. 1-2HBD-mod8, 6-9HBD-mod8, 12-13HBD-mod8 and 15HBD-mod8 all show a significant difference when compared to the activity of the antibiotic ciprofloxacin with mean values below that of the antibiotics.

Discussion

According to the data presented, peptide 3HBD-mod8 with the sequence GLAP-KLAKIFTLTKWKTYRGKAK and 14HBD-mod8 GLGPKLAKIFTLTAWKTYRGKAK with hydrophobicity of 61% show similar activity to that of the original HBD-mod8 with the sequence GLGPKLAKIFTLTKWKTYRGKAK against *S. aureus* and *E. coli* which suggests the insignificance of Glycine (Gly - G) in the 3rd and Lysine (Lys - K) in the 14th position of the peptide when considering their activity against the mentioned bacteria.

10HBD-mod8 with the sequence of GLGPKLAKIFALAKWKTYRGKAK with hydrophobicity of 43% is the only peptide that shows comparable activity to that of HBD-mod8 although its activity against *P. aeruginosa* does show significantly different results, the p-value is close to 0.05 with a mean value close to that of HBD-mod8, hence this peptide is also taken into consideration in this comparison due to its good activity levels against the two other bacteria. This activity could be attributed to its high level of hydrophobicity.

Of note is 4HBD-mod8 with the sequence of GLGAKLAKIFTLTKWKTYRGKAK that shows notably high activity against both Gram-negative bacteria whilst showing a very poor activity against the Gram-positive bacteria. This could be attributed to the presence of Proline (Pro - P) which may help fold the structure in favour of the Gram-negative bacteria. It is also notable that most of the peptides that did not show an activity against the other two bacteria showed a very high activity against *E. coli*. Which could be explained by the targeted activity of these positively charged peptides against the least challenging Gram-negative bacteria.

Figure 6.8 shows the heatmap highlighting the most effective peptides with the alanine substitutes that can be used to determine the most active motifs within the peptide responsible for the activity of HBD-mod8 against each bacteria. This

heatmap also includes information regarding the least favourable amino acid residues that either do not have an effect on the activity of the peptide or reduce its activity against the bacteria. Peptides 6HBD-, 8HBD- and 9HBD-mod8 as well as 12HBD-mod8 show the weakest activity across all the species of bacteria. The importance of the motif LAKIFTL can be highlighted since it shows to be detrimental to the activity of HBD-mod8. The last RGKAK motif is also important since the activity of the peptide is compromised in *S. aureus* and *P. aeruginosa* but it is retained in *E. coli*. The importance of the mentioned motif can be due to the penetrative ability of the peptide towards the membrane. The motif with AKI is also shown to be present in an antimicrobial peptide that is active against Gram-positive, Gram-negaive and fungi with the sequence of FLPKLFAKITKKNMAHIR.

It is important to note the discrepancy between the effect of the peptides against *P. aeruginosa* and *E. coli*, even though both peptides are of Gram-negative origin, most if not all peptides except for 2HBD-, 6HBD-, 9HBD-, 12HBD-, 13HBD- and 15HBD-mod8 show low level of activity against *E. coli*. The same statemnt cannot be concluded from the activity of the peptides against *P. aeruginosa*, with 5HBD-, 6HBD-, 7HBD-, 11HBD-, 12HBD-, 14-19HBD-mod8 all showing low level of activity and the only peptides shared between the two showing lower activity levels are 6HBD- and 12HBD-mod8. The reason for this discrepancy can be attributed to the overall better activity of antimicrobial peptides against *E. coli*. This was also observed with *Klebsiella pneumoniae (K.pneumoniae)* and *P. aeruginosa* where the discrepancy was explained by the increased stability of the AMPs against *P. aeruginosa* [214]. Although it is of note that the *E. coli* strain also showed high level of growth inhibition against the antibiotic so the activity level of the peptides could also be due to the freshness of the bacterial species which may have not built as much resistance due to higher passage number.

	S-aur	P.aer	E.coli
Antiobitic	0.05	0.05	0.05
HBD-mod8	0.002	1	1
1HBD-mod8	3.4417E-14	0.08476728	3.5083E-14
2HBD-mod8	3.4306E-14	2.6927E-06	3.4417E-14
3HBD-mod8	0.99999882	5.7239E-10	1
4HBD-mod8	3.4417E-14	0.00154114	1
5HBD-mod8	3.4417E-14	3.4417E-14	1
6HBD-mod8	3.4417E-14	3.4528E-14	3.4417E-14
7HBD-mod8	3.4417E-14	3.4417E-14	1
8HBD-mod8	3.4417E-14	3.6473E-10	2.534E-05
9HBD-mod8	3.4417E-14	3.7185E-08	3.4417E-14
10HBD-mod8	0.08215066	0.02085051	1
11HBD-mod8	2.62E-07	3.5194E-14	1
12HBD-mod8	3.4528E-14	1.2219E-11	3.4417E-14
13HBD-mod8	1	1.9358E-10	3.4417E-14
14HBD-mod8	0.99999614	3.4417E-14	1
15HBD-mod8	0.99999964	3.5083E-14	3.4417E-14
16HBD-mod8	3.4417E-14	3.4306E-14	1
17HBD-mod8	3.475E-14	3.475E-14	1
18HBD-mod8	3.5083E-14	3.4306E-14	1
19HBD-mod8	3.4306E-14	3.4528E-14	1

(a) p-values

	S-aur	P.aer	E.coli
Antiobitic	49	33	14
HBD-mod8	34	35	9
1HBD-mod8	78	15	44
2HBD-mod8	73	68	87
3HBD-mod8	31	77	8
4HBD-mod8	104	9	8
5HBD-mod8	85	110	10
6HBD-mod8	83	100	88
7HBD-mod8	90	105	10
8HBD-mod8	93	77	29
9HBD-mod8	84	72	89
10HBD-mod8	46	56	10
11HBD-mod8	55	89	10
12HBD-mod8	73	80	80
13HBD-mod8	32	78	89
14HBD-mod8	31	106	10
15HBD-mod8	32	93	93
16HBD-mod8	81	104	8
17HBD-mod8	68	92	7
18HBD-mod8	69	101	8
19HBD-mod8	76	103	7

Unfavourable-significant difference
Favourable/unfavourable-significant difference
No favourable-significant difference

(b) Mean percentage of bacterial growth

Figure 6.8: The heatmap of the effectiveness of each peptide based on their p-value as well as the mean percentage of bacterial growth Each colour is representative of the effectiveness of the peptide against each bacteria. The colour Green is indicative of an effective peptide with either a larger mean value in comparison to HBD-mod8 or a mean value similar to that of the HBD-mod8. Colour Yellow is indicative of significant different values that could be caused by a larger mean value which called favourable significant different or lower mean value called unfavourable significant difference. Colour Red is indicative of unfavourable significant difference. The two heatmaps should be considered together for the result interpretation.

6.1.4 Development of bacterial resistance against HBD-mod8

Introduction

To study the emergence of resistance against HBD-mod8, a series of cultures were designed using the mixture of bacteria and the peptide at sub-MIC concentration as the inoculum instead of the standard bacteria only inoculum. Each inoculum was then diluted to an optical density of 0.1 OD and the experiments were conducted similar to the methodology mentioned in section 2.4 of the microbial studies. This study was performed to determine how fast resistance against the peptide might arise. The cycles were continued until all three wells showed a mean percentage of bacterial growth of below 50%.

Results

Figure 6.9 shows the resistance cycle of *S. aureus* against HBD-mod8. As it can be seen in this figure, the bacteria show resistance towards the peptide in second cycle. The experiments were continued to find whether the resistance was due to the growth phase of the bacteria. For this bacteria cycle 15 was the last cycle in which the experiments were stopped due to the cut off point of 90% growth of bacteria at the highest concentration. Figure 6.10 shows the resistance cycle of *P. aeruginosa* against HBD-mod8. As it can be seen in this figure, the bacteria show resistance towards the peptide in third cycle and it specifically only showed favourable activity at its highest concentration of $500\mu M$ in the first cycle whilst other concentrations showed subpar activity. The experiments were continued to find whether the resistance was due to the growth phase of the bacteria. For this bacteria cycle 19 was the last cycle in which the experiments were stopped due to the cut off point of 90% growth of bacteria at the highest concentration.

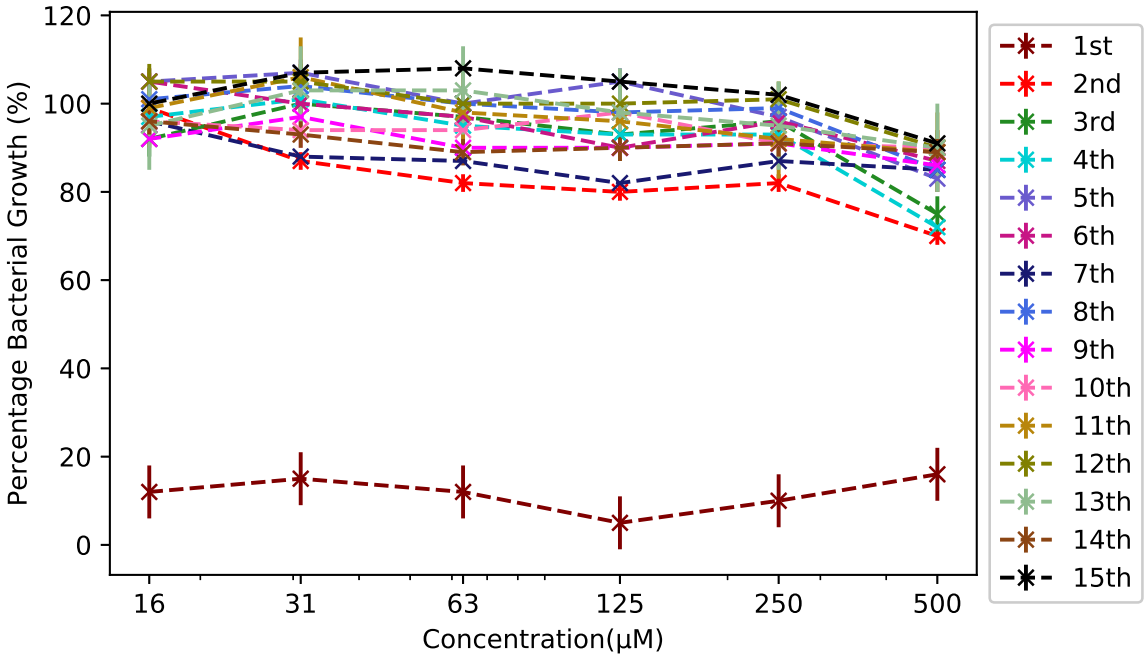


Figure 6.9: Resistance cycles of HBD-mod8 against *S. aureus*. The cycles were repeated until a percentage of bacterial growth had reached 90% is reached. It can be seen that *S. aureus* continues its growth pattern for 15 cycles against HBD-mod8 before becoming full resistance.

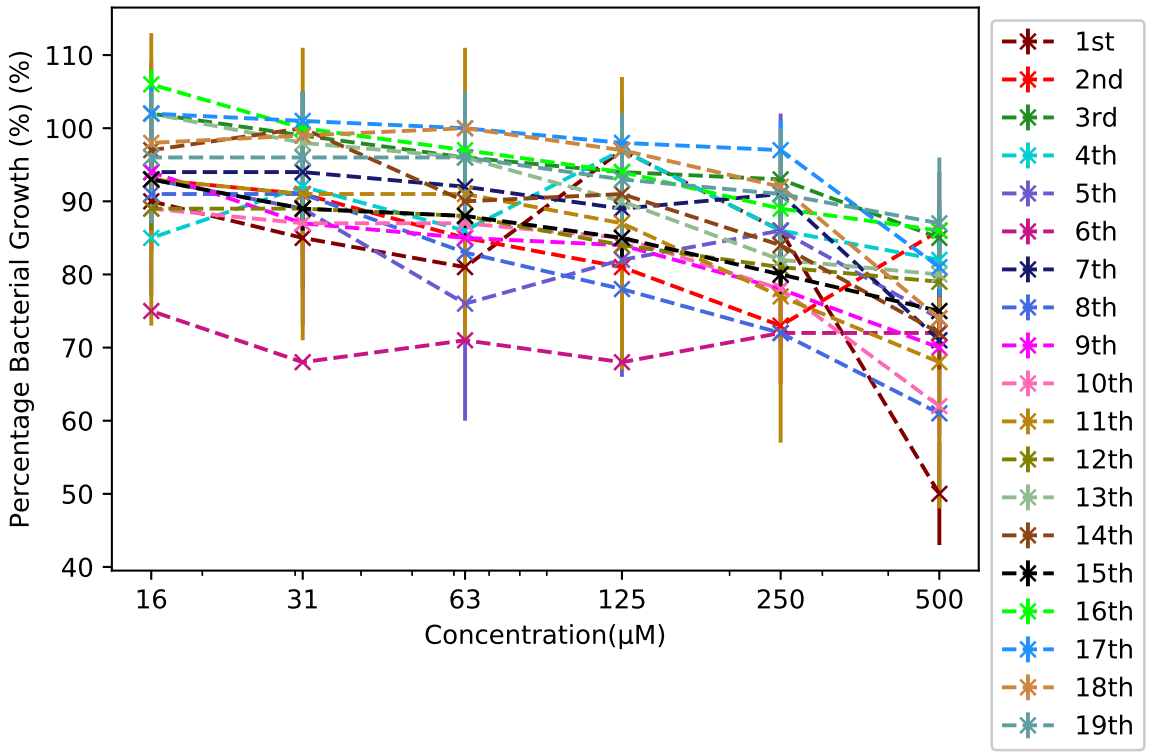


Figure 6.10: Resistance cycles of HBD-mod8 against *P. aeruginosa*. The cycles were repeated until a percentage of bacterial growth had reached 90% is reached. It can be seen that *P. aeruginosa* continues its growth pattern for 16 cycles against HBD-mod8 before becoming full resistance.

Figure 6.11 shows the resistance cycle of *E. coli* against HBD-mod8. The experiments were continued until 19th cycle and when the percentage of bacterial growth reached above 90% in all three wells the experiments and the cycles continually followed the downward trend of activity of the peptide they were no longer continued. Due to the fluctuations in the growth of the bacteria the experiments were continued since it would not show consistent stunted growth. Once a consistent stunted growth above 90% was reached the cycles were stopped. Overall, the bacteria shows non resistance with a cut off of 50% at the 7th cycle with the 16th cycle as an outlier showing high activity levels at the highest concentration.

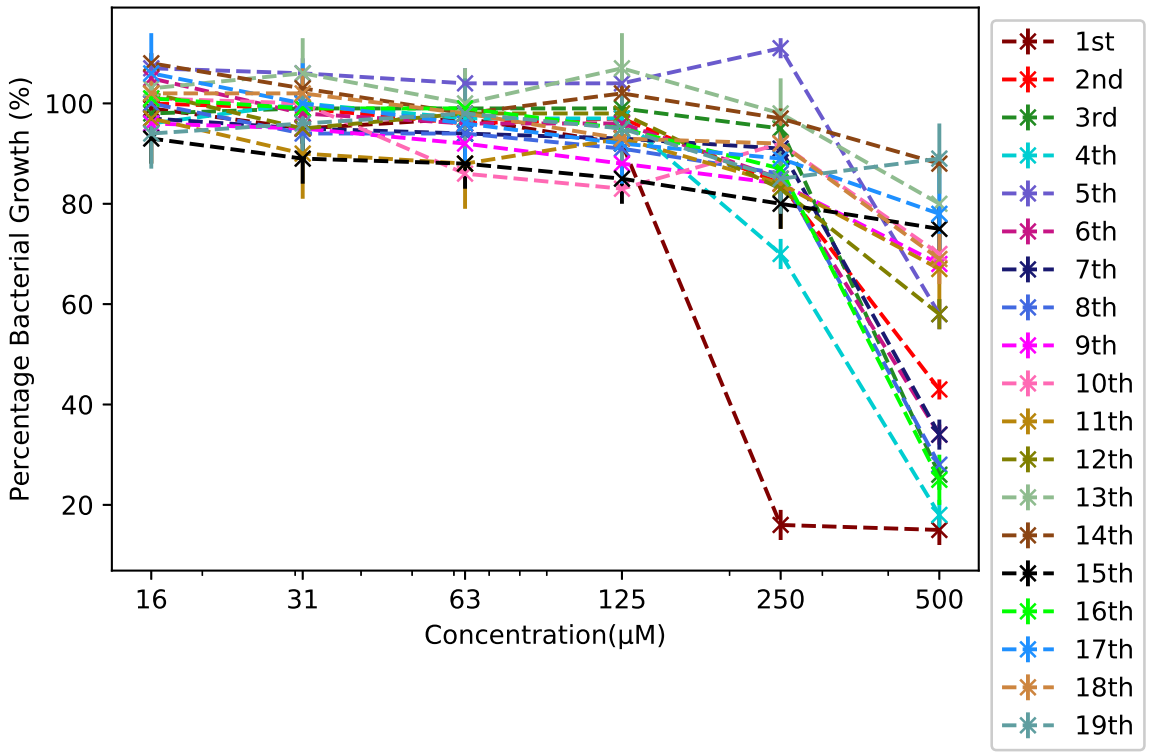


Figure 6.11: Resistance cycles of HBD-mod8 against *E. coli*. The cycles were repeated until a percentage of bacterial growth had reached 90% is reached. It can be seen that *E. coli* continues its growth pattern for 19 cycles against HBD-mod8 before becoming full resistance.

Discussion

It can be seen from these results that the peptide did not combat bacterial resistance and only until the second cycle for both *S. aureus* and *P. aeruginosa* it showed an activity. Unlike these bacteria *E. coli* showed a mix of resistance in different cycles so it is difficult to draw a cohesive conclusion from these results. Each bacteria showed a noticeable resistance in between each cycle, but the peptide was able to overcome this resistance against *E. coli*. Since *S. aureus* showed the fastest resistance development which is consistent with the literature as *S. aureus* is one of the most difficult bacteria to overcome in terms of its resistance mechanisms against antimicrobial agents. It

could also be explained by the bacterium growth stage from which the inoculum was taken, which could have varied greatly between each cycle. Bacteria have three stages of growth, first is the Lag phase second is a long phase third is the stationary phase which is followed by bacterial death. The presence of bacteria in the stationary phase in the cycles which showed the most least percentage bacterial growth could explain the mixed trend observed in the cycles especially in *E. coli* [215].

6.2 The effect of HBD-mod8 and its alanine substitutes on the viability of HeLa cells.

Introduction

Since it was established that HBD-mod8 is a strong contender as an antimicrobial agent, this peptide was tested against human HeLa cells. The cells were chosen as a model epithelial cells to mimic the cells that normally produce antimicrobial peptides. Hence they would be the best model to study the affect of these peptides on viability of the cells [191]. In addition to testing the activity of HBD-mod8 at all 6 concentrations against HeLa cells the activity of the alanine substitutes of this peptide were also tested to find a pattern between the sequence and the cytotoxicity of this peptide. The resulting OD was measured after the addition of MTT assay determining mitochondrial dehydrogenase activity in the living cells [190]. During this reaction the MTT molecules interact with the dehydrogenase (3-[4,5- dimethylthiazol-2-yl]-2,5-diphenyl tetrazolium bromide) and through reduction produce formazan crystals that will lead to the formation of a dark blue colour helping, the colorimetric measurement of cell viability [77]. Due to the overgrowth of cells which was observed to be higher than 100% viability the results were all normalised to show a maximum of 100%.

Results

As shown in figure 6.12, HBD-mod8 shows a slight cytotoxic activity towards HeLa cells at its highest concentration of $500\mu M$ with 20% of cell death observed. However due to the normalisation of the results this value is increased to 30% on the graph and the cell viability shows 60%. to Due to the normalisation used to treat the results the viability of cells are lower than the actual results at this concentration. Although HBD-mod8 shows the best activity towards cells when compared to other peptides in the alanien substitution series. This pattern was also observed in all peptides with the alanine substitutions except in 2-5HBD-mod8 where they display a toxic effect roughly through the highest 3 concentrations. It can also be seen that the remaining peptides except for 1HBD-mod8, 6HBD-mod8 and 9HBD-mod8, all show complete cell death at $500\mu M$. At concentrations below $31\mu M$ it can be seen that all the peptides induce no cytotoxicity in the cells and they promote growth of the cells that is combated by the normalisation of the data. Figure C.11 in appendix C, shows the bar chart data for these peptide series without normalisation.

Discussion

These results highlight the effect of HBD-mod8 as its original form showing the highest activity against the bacterial species tested and it is also the least toxic at its lowest concentration that invoked activity against all bacteria tested. It can also be seen that 1HBD-mod8 shows similar pattern to HBD-mod8 against HeLa cells meaning that the Gly at the start of the sequence does not have a cytotoxic effect. Similarly, 6HBD-mod8 with the sequence GLGPKAAKIFTKWKTYRGKAK where the first Leucine (Leu - L) was substituted with Ala, is also not as toxic towards these cells. 5HBD-mod8 with the sequence GLGPALAKIFTKWKTYRGKAK is one of the worst performing

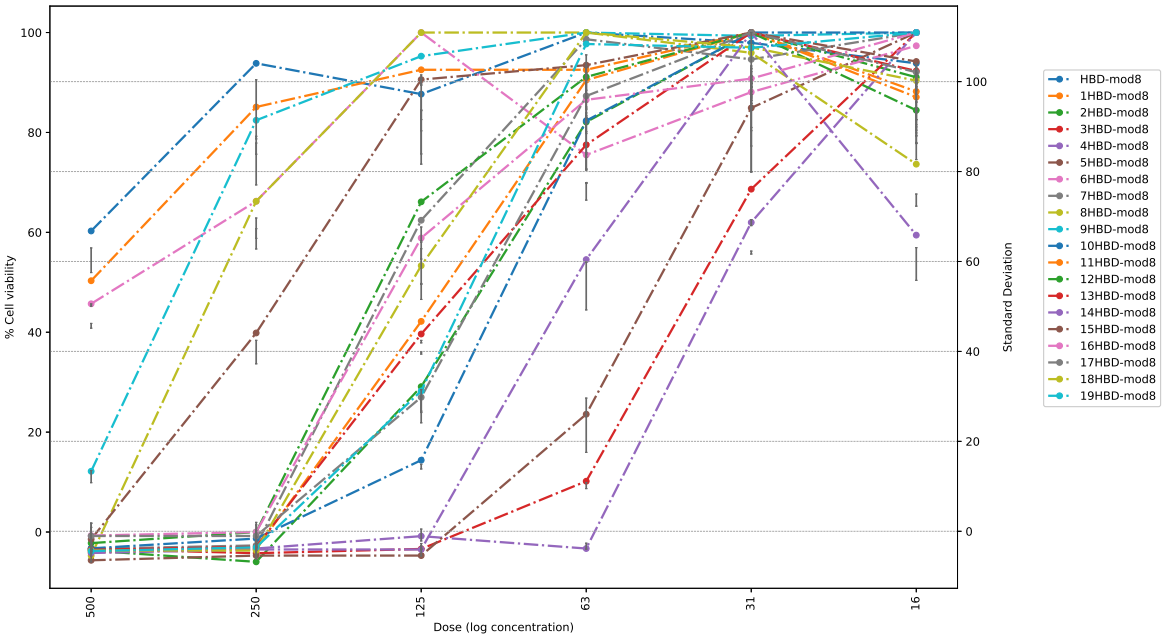


Figure 6.12: The effect of HBD-mod8 and its alanine substitutes on HeLa cells. This figure was produced using three repeats of each peptide in three different wells on three different plates and the combination of the results produced the standard deviation lines shown in black after 24 hour incubation of cells with the peptides and the results were shown for MTT assay after 4 hour incubation. The data was normalised to show a 100% cell viability as the maximum amount so other values were reduced.

peptides when compared to the rest of the peptides in this series. This highlights the importance of the Lysine (Lys - K) in the sequence considering its activity poor activity against the bacteria but it's strong activity against the cells that leads to cell death in concentrations concentrations higher than $31\mu M$.

In general the first motif of LGPK seems to be detrimental to the low cytotoxicity of HBD-mod8 against the HeLa cells. It can also be concluded that the motif after 9HBD-mod8, TKWKTYRGKAK also plays an important role on the toxicity of the peptides at the higher concentrations with 14HBD-mod8, displaying similar activity to that of 5HBD-mod8 with slight improvement on the activity against the cells at 63uM concentrations.

According to [216] the replacement of Leucine (Leu, L) and IsoLeucine (Ile, I) in the substituted peptides increases the toxicity level of the overall peptide. In the present study this hypothesis has partly applied, and the only peptide that negates this hypothesis is 6HBD-mod8 that shows similar cytotoxicity profile as HBD-mod8.

Additionally, the activity of 4HBD-mod8 that shows high level of activity against both Gram-negative bacteria is also amongst one of the most cytotoxic peptides in the series highlighting the importance of Proline (Pro, P) in the Gram-positive activity and the non cytotoxic affect of these peptides.

Chapter Seven

Human Serum Analysis

7.1 Serum Analysis

7.1.1 Introduction

The peptide that showed the most antimicrobial activity was subjected to the stability analysis to find whether its activity on the biological membrane is due to its sequence as a whole or the activity is due to the fractions of peptides that are formed in a biological environment. Additionally, this peptide along with its alanine substitutes were also analysed to find a pattern of degradation and to find which motifs in the sequence of these peptides show the most stability in a biological environment. To do so, a combination of results were taken into consideration from different methodologies. The combination of the chromatogram and spectrum from the LC-MS were first produced and the mass spectrum of the most likely peak in the serum sample of the peptide was then generated to find which fractions existed in the sample with the serum when compared to the original peptide sample in normal media. This sample was then placed on MALDI-TOF and analysed further to find more information about their overall mass spectrum finger print. Serum control can be found in appendix A in figure A.4.

7.1.2 Results

Table 7.1 shows the alanine substitution sequences based on HBD-mod8 which according to chapter 6 was shown to produce the most consistent antimicrobial activity against all pathogens considered for this study while maintaining its non cytotoxic activity against normal human cell lines. This table also shows the molecular weight of the peptides which was used to analyse the serum stability of each peptide according to the mass spectrometry data shown in figure 7.1 recorded through the use of LC-MS. The alanine substituted residues are indicated by a red colour in the table for ease of tracking.

Table 7.1: Alanine(Ala, A) substitution of HBD-mod8 shown alongside the molecular weight of the sequences. A key for amino acid figure A.1 one letter word and their structure can be found in appendix A

Name	Sequence	Molecular Weight(MW)(g/mol)
HBD-mod8	GLGPKLAKIFTKWKTYRGKAK	2391
1HBD-mod8	ALGPKLAKIFTKWKTYRGKAK	2405
2HBD-mod8	GAGPKLAKIFTKWKTYRGKAK	2350
3HBD-mod8	GLAPKLAKIFTKWKTYRGKAK	2406
4HBD-mod8	GLGAKLAKIFTKWKTYRGKAK	2334
5HBD-mod8	GLGPALAKIFTKWKTYRGKAK	2334
6HBD-mod8	GLGPKAAKIFTKWKTYRGKAK	2349
7HBD-mod8	GLGPKLAAIFTKWKTYRGKAK	2334
8HBD-mod8	GLGPKLAKAFTKWKTYRGKAK	2349
9HBD-mod8	GLGPKLAKIATKWKTYRGKAK	2316
10HBD-mod8	GLGPKLAKIFAKWKTYRGKAK	2362
11HBD-mod8	GLGPKLAKIFTAWKTYRGKAK	2335
12HBD-mod8	GLGPKLAKIFTKAKTYRGKAK	2278
13HBD-mod8	GLGPKLAKIFTKWATYRGKAK	2335
14HBD-mod8	GLGPKLAKIFTKWKAYRGKAK	2362
15HBD-mod8	GLGPKLAKIFTKWKTARGKAK	2230
16HBD-mod8	GLGPKLAKIFTKWKTYAGKAK	2307
17HBD-mod8	GLGPKLAKIFTKWKTYRAKAK	2406
18HBD-mod8	GLGPKLAKIFTKWKTYRGAAK	2335
19HBD-mod8	GLGPKLAKIFTKWKTYRGKAA	2335

HBD-mod8 in figure 7.1i shows the presence of motif IFTK which has a mass of 507 present in this figure at 2.475 minute followed by motif PKLAKIFTKTWKTYR with mass of 1881 which is shown by the highest peak in this figure at 627(m/z). This motif shows a digestion site for Glycine (Gly - G) since it begins after a Gly residue and is ended before one. 1HBD-mod8 in figure 7.1b shows the motif LGPKLAKIFTK with the molecular weight of 1225 which is shown by 404(m/z) and 608(m/z) on the mass spectrum at 2.886. This spectrum also shows the 1205 mass which could indicate this motif as +10 charges are added. Motif AKLAKIFTKWK with the mass to charge ratio of 672 and molecular weight of 1333 is shown in figure 7.1e along with KLAKIFT with the mass of 820 for peptide 4HBD-mod8 at 2.372. There is also the peak at 1024 which could be indicative of motif AKLAKIFTK. Figure 7.1g shows the motif KWKTYRGKAK formed from 6HBD-mod8 with the mass of 1265 at 2.44. Motif PKAAKIFTKWKTYR is also found in this figure under 1738 mass to charge peak. Motif PKAAKIFTKWKTYRGKAK is also present at 707 mass to charge ratio. AAKIFTKWKTYRGK is shown by 842 with the loss of NH_2. Figure 7.1h and 7.1i show the fragment FTKWTYRGKAK with the mass to charge ratio of 693 which is the highest peak in their corresponding spectrum both eluting at 2.406 minute. Figure 7.1j shows the fragments PKLAKIATKWKTYRGKAK and KIATKWKTYRGKAK shown on peaks 698 and 561, respectively.

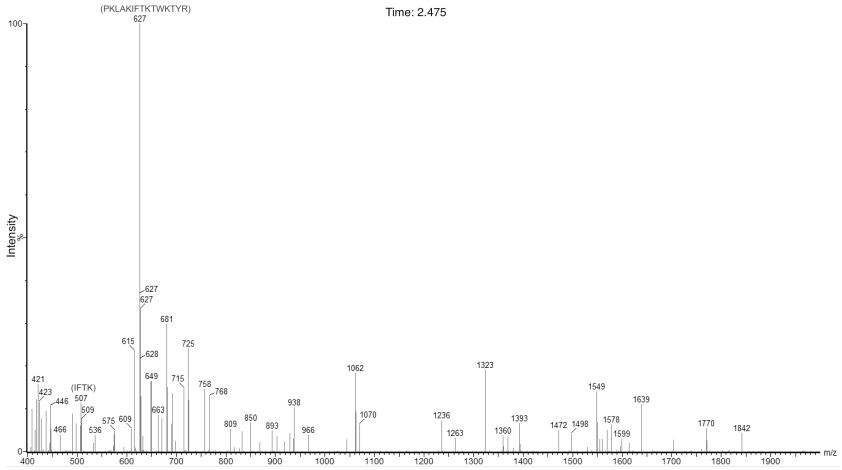
Figures 7.1k and 7.1l show the fragment of LAKIFTAWKTYRGKAK at 2.475 and 2.44 minutes, respectively with mass to charge ratio of 627. 11HBD-mod8 also shows a peak at 1251 that belongs to the fraction FTAWKTYRGK. 12HBD-mod8 in figure 7.1m shows the fragment of FTKAKTYRGKAK with the mass to charge ratio of 698. 13HBD-mod8 makes similar fragments to that of 11HBD-mod8 since the change is between two Lysine (Lys - K) residues on either side of the Tryptophan (Try - W). Hence the fragmented motif is LAKIFTKWATYRGKAK at 2.476 minute shown in figure 7.1n as well as fragment FTKWATYRGK at 1252 which was also present in 11HBD-mod8 due to the Lysine (Lys - K) replacement in both instances. However, this

peptide is also fragmented at GLGPKLAKIFTKWAT with the mass to charge ratio of 544 at 2.783 minutes shown in figure 7.1o. YRGKAK is the fragment from 14HBD-mod8 shown in figure 7.1p with the mass of 726 at 2.44 minutes. AKIFTKWK is also formed from this peptide represented by 1023 mass to charge ratio. 15HBD-mod8 showed the fragment AKIFTKWKTARG at 2.475 minutes with mass to charge ratio of 698 and the fragment LAKIFTKWKTA at 1312 mass to charge ratio corresponding to the peaks in figure 7.1q.

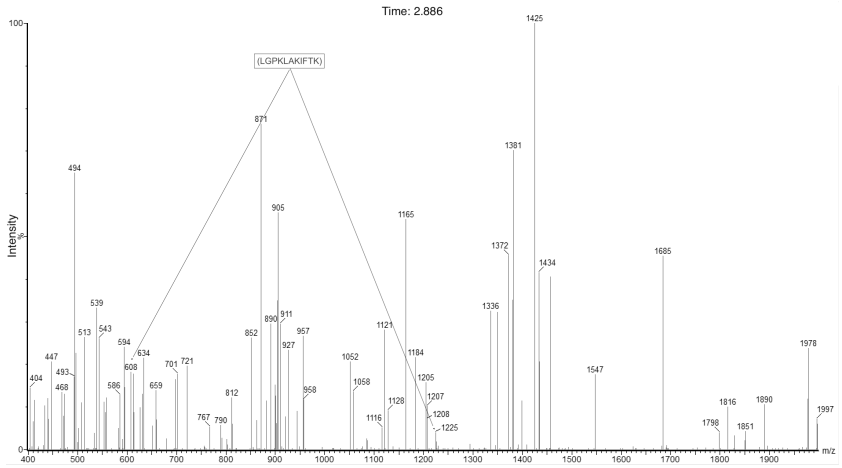
16HBD-mod8 at 2.475 corresponds to the motif PKLAKIFTKWKTYAGK with the mass to charge ratio of 626 with 3+ charges shown in figure 7.1r. Figure 7.1s represents the motif LAKIFTKWKTY with mass to charge ratio of 698 with 2+ charges at 2.406. 17HBD-mod8 showed the motif WKTY with the mass of 596 as well as AIFTKWKTYRAKA with the mass to charge ratio of 793 shown in figure 7.1t. In this figure AKIF is also fragmented from the full sequence shown through the mass of 477. Similar to 16HBD-mod8, both 18HBD-mod8 and 19HBD-mod8, fragment at PKLAKIFTKWKTYAGK shown in figure 7.1v and 7.1x respectively at 2.475 minutes and LAKIFTKWKTY fragment at 2.405 minutes respectively shown in figure 7.1u and 7.1w respectively. 18HBD-mod8 also shows the fragment of TKWKTYRG at 1031 shown in figure 7.1u.

Figure 7.1c and 7.1k show 2HBD-mod8 and 10HBD-mod8 which remain intact in serum with m/z ratio of 585 charge of +4 at 2.04 minute and 787 at 2.475 with the charge of +3. This peptide however also fragments into either KTYRG or TYRGK with the mass of 624.

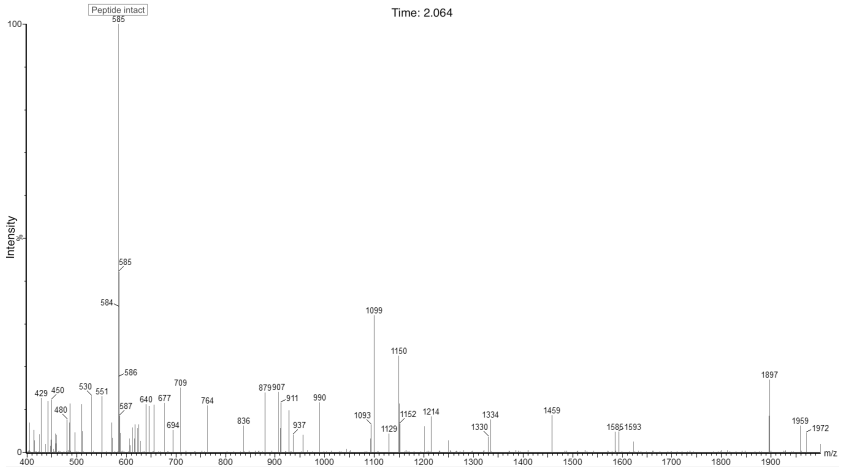
3HBD-mod8 in figure 7.1d and 5HBD-mod8 in figure 7.1f show the mass to charge ratio spectrum for which does not show any clear pattern that would suggest the formation of a specific motif.



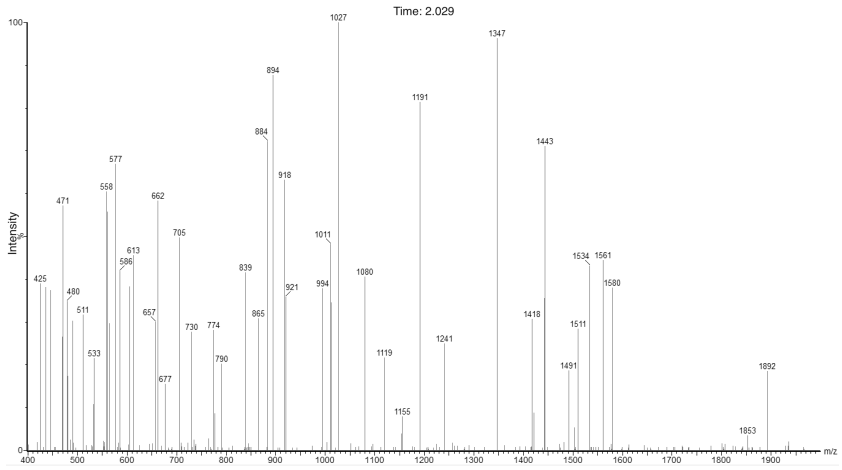
(a) Mass spectrum of the highest chromatographic peak of HBD-mod8 in Serum



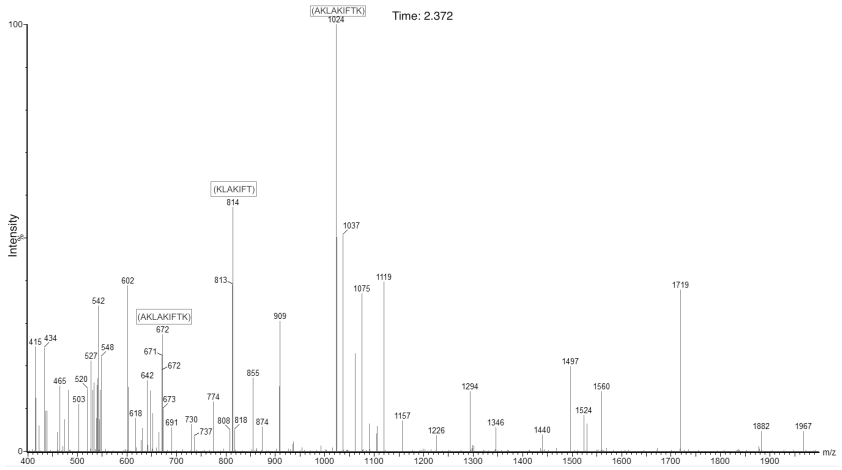
(b) Mass spectrum of the highest chromatographic peak of 1HBD-mod8 in Serum



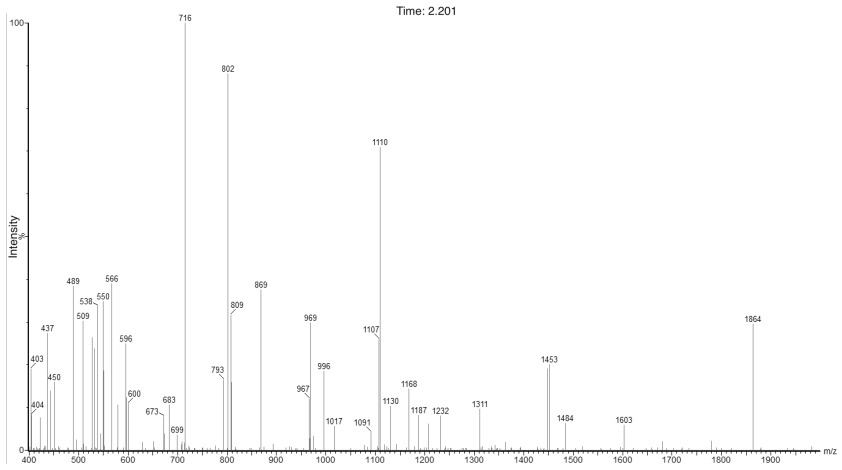
(c) Mass spectrum of the highest chromatographic peak of 2HBD-mod8 in Serum



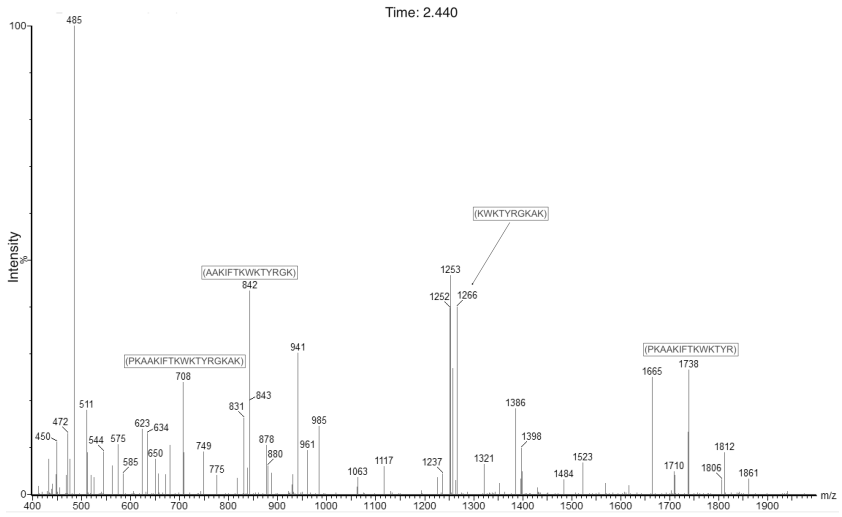
(d) Mass spectrum of the chromatographic peak of 3HBD-mod8 in Serum



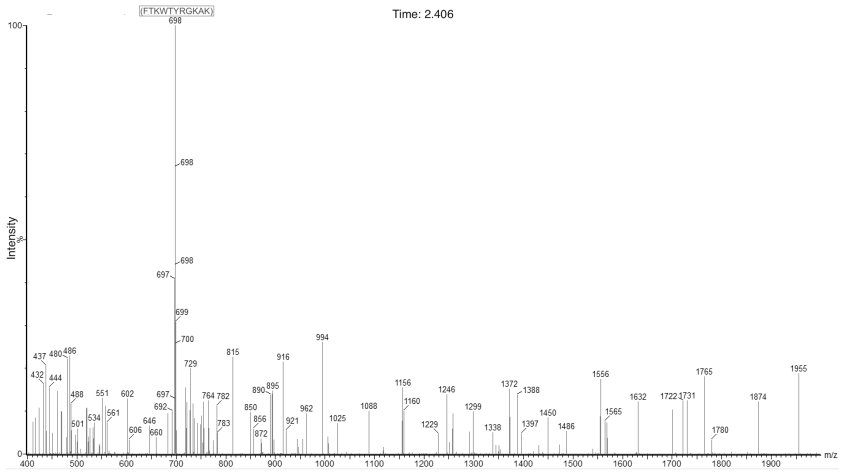
(e) Mass spectrum of the chromatographic peak of 4HBD-mod8 in Serum



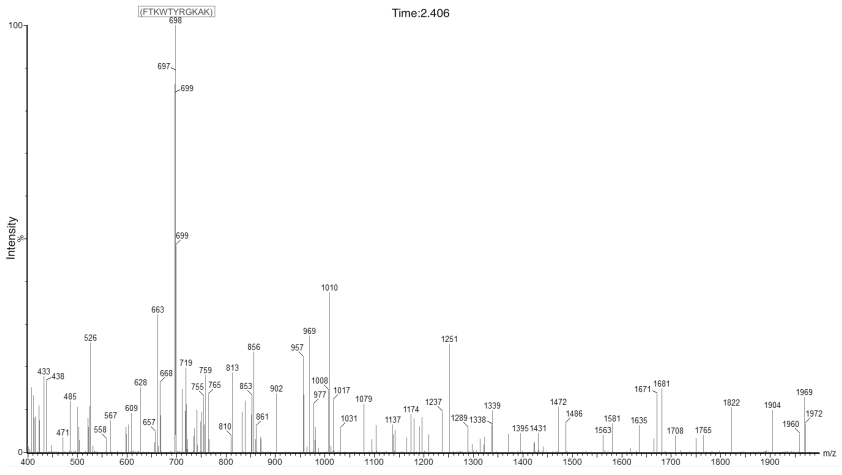
(f) Mass spectrum of the chromatographic peak of 5HBD-mod8 in Serum



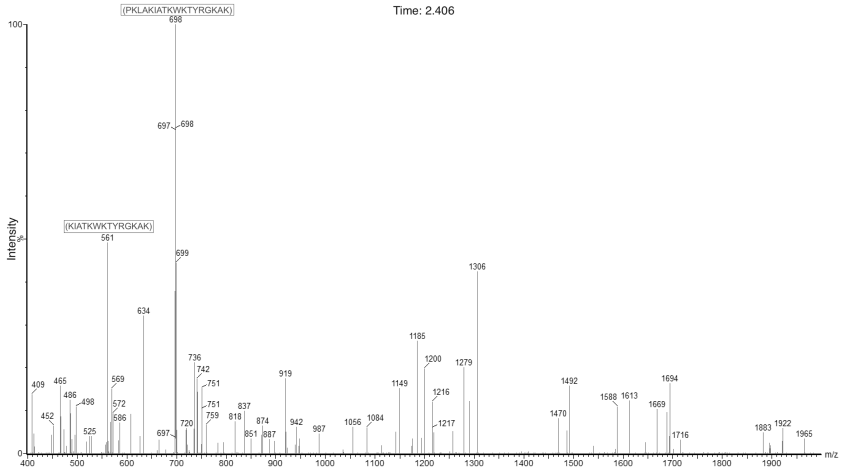
(g) Mass spectrum of the chromatographic peak of 6HBD-mod8 in Serum



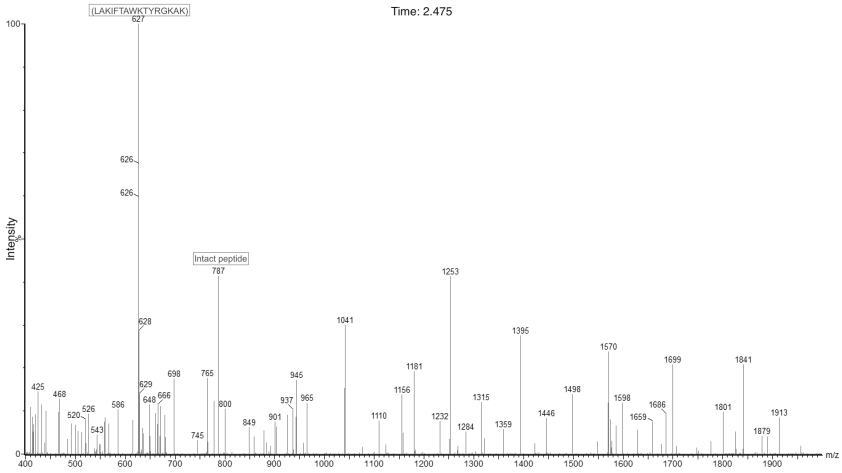
(h) Mass spectrum of the chromatographic peak of 7HBD-mod8 in Serum



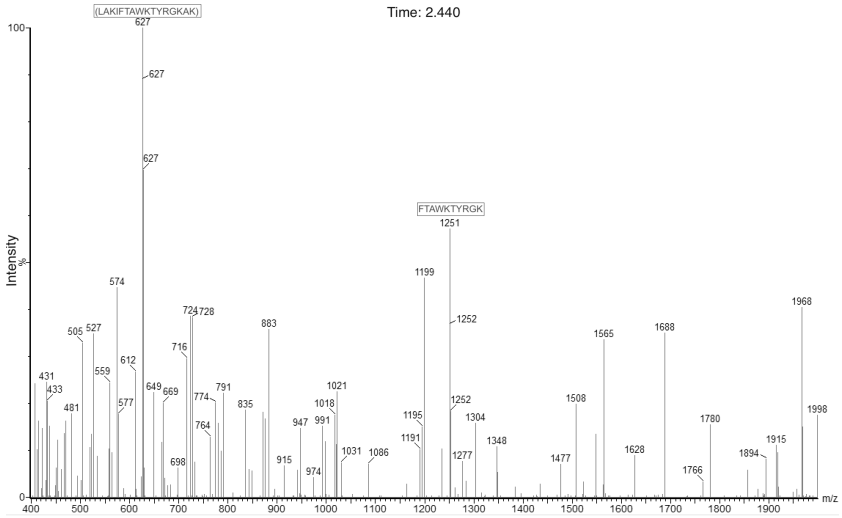
(i) Mass spectrum of the chromatographic peak of 8HBD-mod8 in Serum



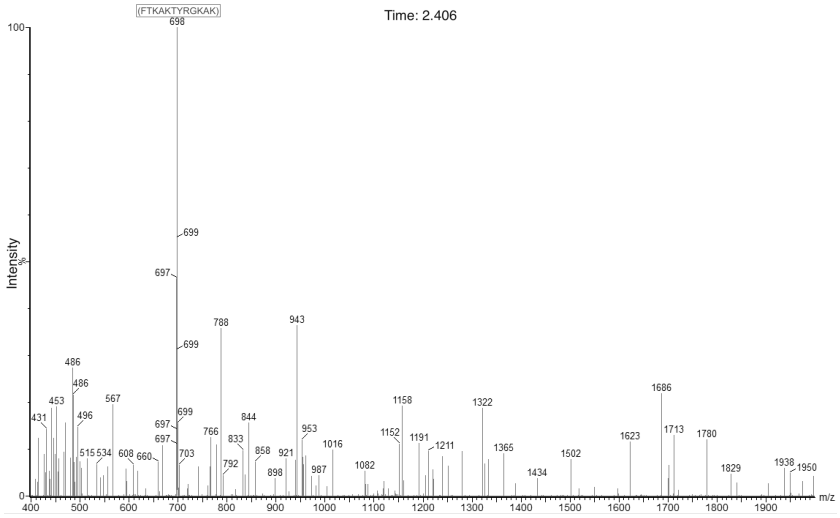
(j) Mass spectrum of the chromatographic peak of 9HBD-mod8 in Serum



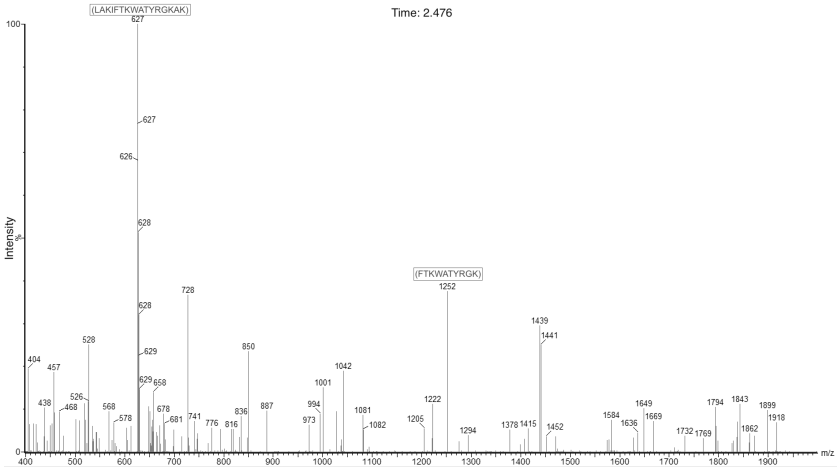
(k) Mass spectrum of the chromatographic peak of 10HBD-mod8 in Serum



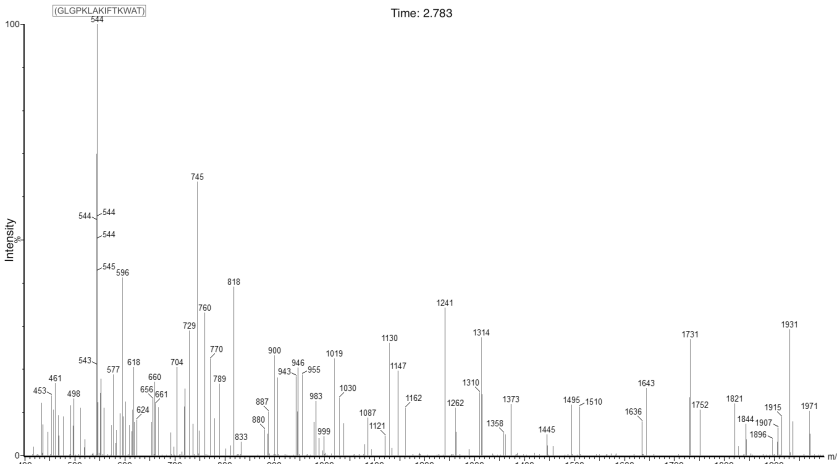
(l) Mass spectrum of the chromatographic peak of 11HBD-mod8 in Serum



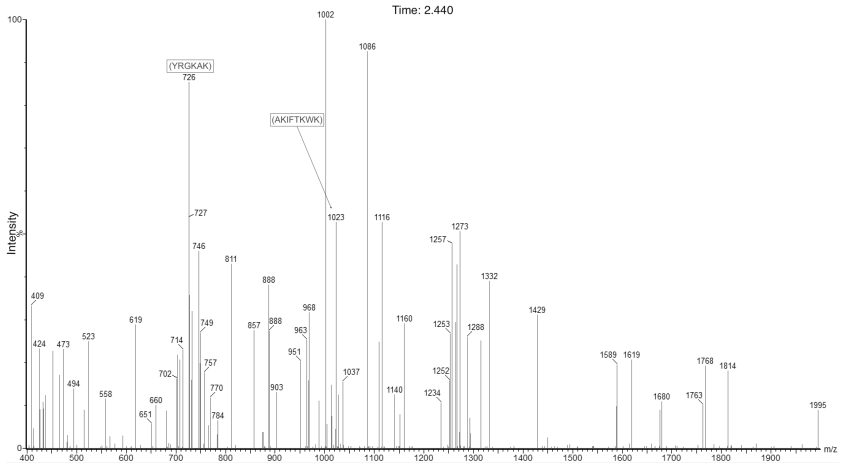
(m) Mass spectrum of the chromatographic peak of 12HBD-mod8 in Serum



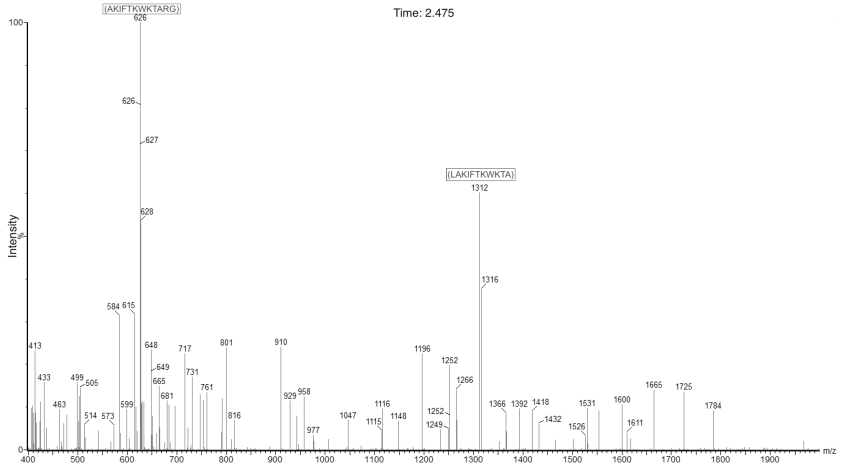
(n) Mass spectrum of the 1st chromatographic peak of 13HBD-mod8 in Serum



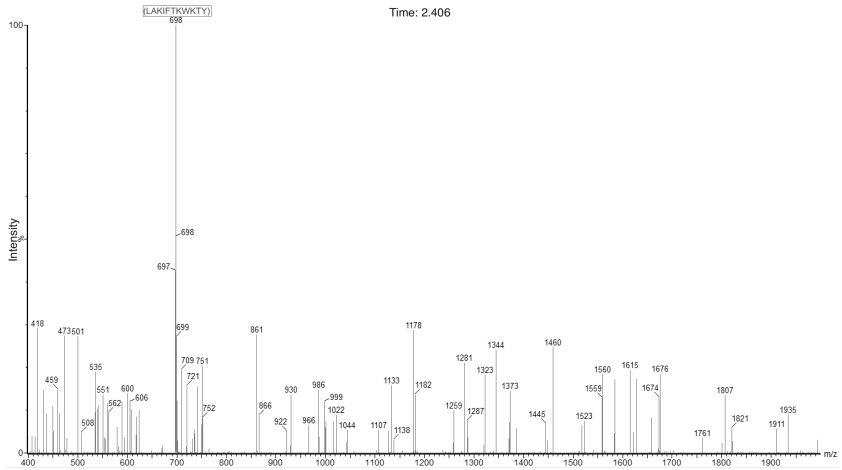
(o) Mass spectrum of the 2nd chromatographic peak of 13HBD-mod8 in Serum



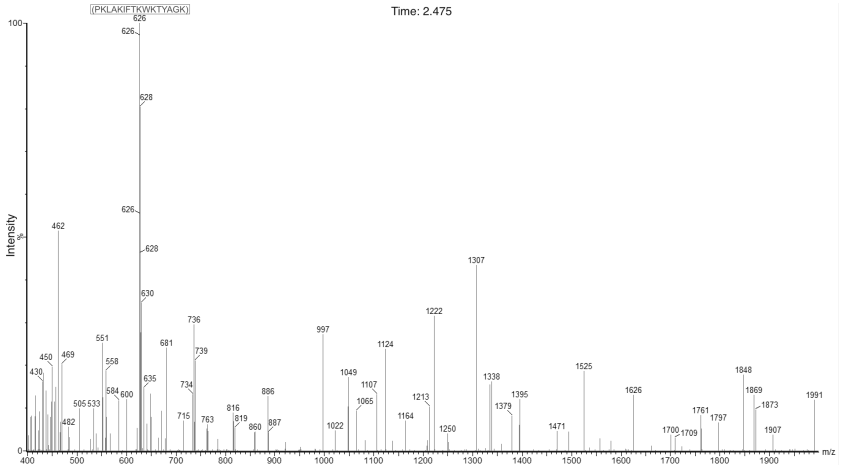
(p) Mass spectrum of the chromatographic peak of 14HBD-mod8 in Serum



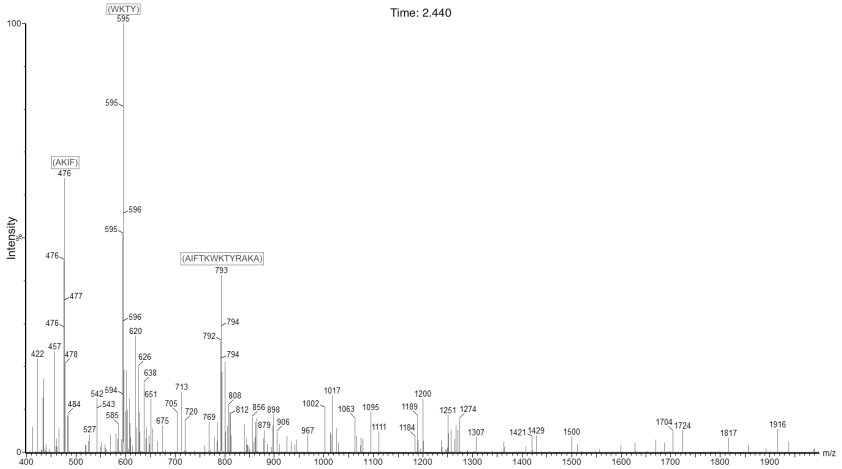
(q) Mass spectrum of the chromatographic peak of 15HBD-mod8 in Serum



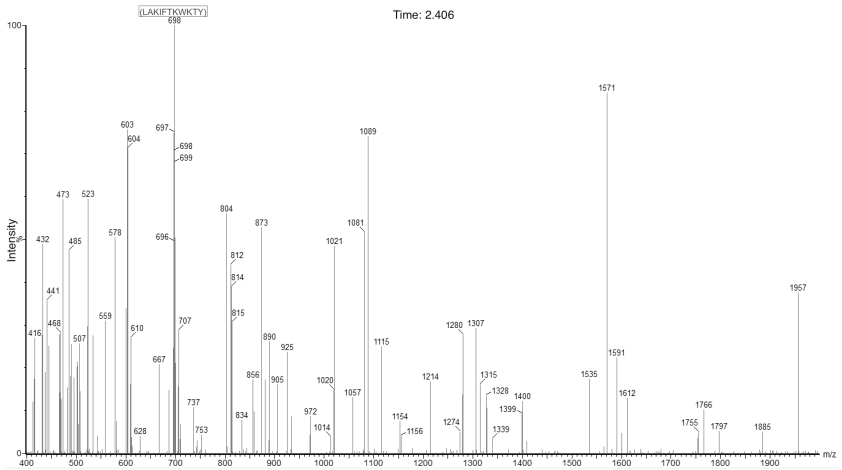
(r) Mass spectrum of the 1st chromatographic peak of 16HBD-mod8 in Serum



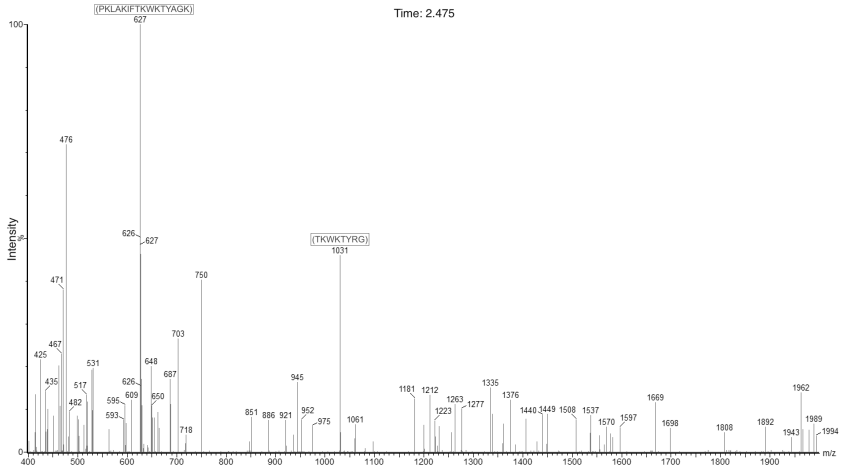
(s) Mass spectrum of the 2nd chromatographic peak of 16HBD-mod8 in Serum



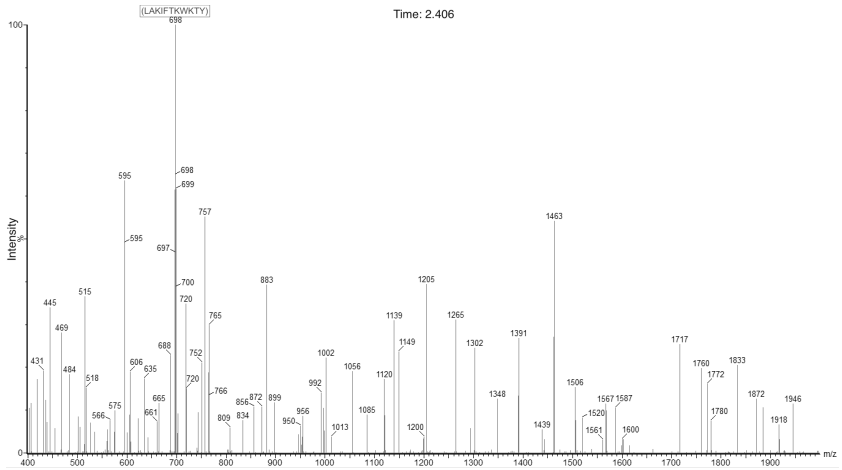
(t) Mass spectrum of the chromatographic peak of 17HBD-mod8 in Serum



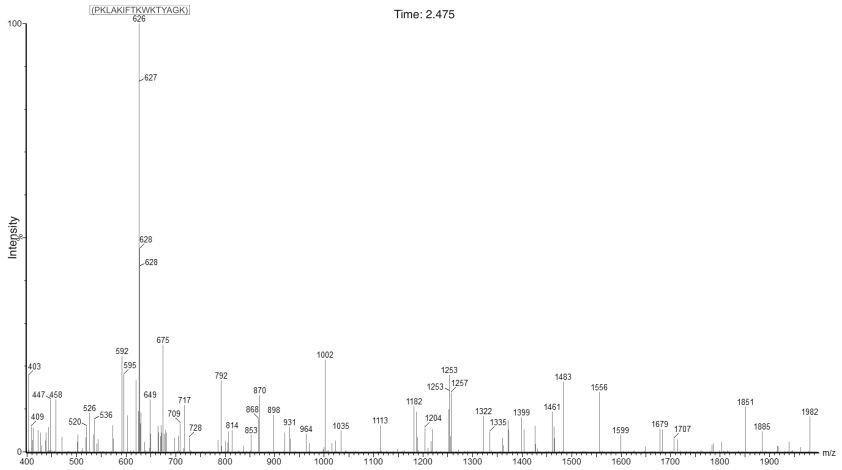
(u) Mass spectrum of the 1st chromatographic peak of 18HBD-mod8 in Serum



(v) Mass spectrum of the 2nd chromatographic peak of 18HBD-mod8 in Serum



(w) Mass spectrum of the 1st chromatographic peak of 19HBD-mod8 in Serum



(x) Mass spectrum of the 2nd chromatographic peak of 19HBD-mod8 in Serum

Figure 7.1: LC-MS data showing the degradation of the peptides with alanine substitutions based on HBD-mod8 in the most prominent peak found through chromatography. Using this methodology the most active motif of the peptide after degradation can be found through combination of this results and microbiology analysis of the activity of each peptide.
These figures were produced using the MassLynx, and the peaks were identified manually.

The fragmentation pattern discussed have also been shown in table 7.2 for HBD-mod8 and its alanine substitutes. This table shows the mass to charge ratio and the charge of each fragment which can then be multiplied to calculate the actual mass of the peptide. For those with 1+ charge the mass is identical to the mass to charge ratio of the fragments.

Table 7.2: Fragmentation pattern of alanine substituted HBD-mod8 peptides against human serum.

Name	Fragments	Mass to charge ratio(m/z)	Charge
HBD-mod8	PKLAKIFTKTWKTYR	627	3+
HBD-mod8	IFTK	507	1+
1HBD-mod8	LGPKLAKIFTK	608	2+
2HBD-mod8	GLAPKLAKIFTKWKTYRGKAK	585	4+
4HBD-mod8	AKLAKIFTKWK	672	2+
4HBD-mod8	KLAKIFT	820	1+
4HBD-mod8	AKLAKIFTK	1024	1+
6HBD-mod8	KWKTYRGKAK	1265	1+
6HBD-mod8	PKAAKIFTKWKTYR	1738	1+
6HBD-mod8	PKAAKIFTKWKTYRGKAK	707	4+
6HBD-mod8	AAKIFTKWKTYRGK	842	2+
7 and 8HBD-mod8	FTKWTYRGKAK	693	2+
9HBD-mod8	PKLAKIATKWKTYRGKAK	698	3+
9HBD-mod8	KLAKIATKWKTYRGKAK	663	3+
11 and 13HBD-mod8	LAKIFTAWKTYRGKAK	627	3+
12HBD-mod8	FTKAKTYRGKAK	698	2+
13HBD-mod8	GLGPKLAKIFTKWAT	544	3+
14HBD-mod8	YRGKAK	721	1+
14HBD-mod8	AKIFTKWK	1023	1+
15HBD-mod8	AKIFTKWKTARG	698	2+
15HBD-mod8	LAKIFTKWKTA	1312	1+
16, 18 and 19HBD-mod8	PKLAKIFTKWKTYAGK	627	3+
16, 18 and 19HBD-mod8	LAKIFTKWKTY	698	2+
17HBD-mod8	WKTY	596	1+
17HBD-mod8	AIFTKWKTYRAKA	793	2+
17HBD-mod8	AIF	477	1+
18HBD-mod8	TKWKTYRG	1031	1+

7.1.3 Discussion

3HBD-mod8 and 5HBD-mod8 showed no fragmentation pattern and unlike 2HBD-mod8 these peptides did not remain intact. They did not show a conclusive peak in which the pattern was able to be recognised, as opposed to 2HBD-mod8 which showed the fragment as is and without any breakdown in its original peptide sequence.

The activity of HBD-mod8 could be attributed to the "PKLAKIFTKWKTYR" fragment motif which is not found in any other peptide fragmentation pattern. Although that fragment site beside the third Glycine (Gly - G) appears in 6HBD-, 9HBD- and 16HBD-mod8 the outcome of the fragment is not the same since the end fragmentation pattern does not follow the same trend and the Alanine substitute is present in this motif within those peptides. 7HBD-mod8 does not show the fragment "IFT" due to the presence of Alanine (Ala - A) next to the Isolucine (Ile - I) which could effect its binding to the neighbouring amino acids namely, Phenylalanine (Phe - F). This is observed in 8HBD-mod8 where the Ala replaces Ile fragments that neighbours Phe residue similar to 7HBD-mod8, this peptide does not show this motif, but unlike 7HBD-mod8 the reason for the lack of this fragment is the replacement of Ile for Ala in 8HBD-mod8. It can be seen that with 9HBD-mod8 this fragment is restored and is no longer cleaved at the Ala site and it mostly resembles the patterns observed with the remaining alanine substituted peptides.

Other fragments of note, are "PKLAKIFTKWKTYAGK" and "LAKIFTKWKTA", observed in all the fragmentation pattern regardless of the presence of the alanine substitute suggests the importance of this motif especially the "IFTK" motif in the stability of the peptides. This motif is of note since it is also present in the parent hBD1. A study focusing on the change of the amino acids from L- to D- enantiomers of the hBD1 peptides showed that the Ile in this fraction is extremely crucial in the activity of the peptides and it does not play a role whether it is in its L- or D- form. This study was included the change of Arg residues so the activity of the peptide cannot only be contributed to the Ile residue. however the peptides shown in this research were of a different sequence, this research highlights the importance of this motif. This study also evaluated the activity of the peptides with the substitution of the D-amino acids which enhanced the activity of the peptides even in their reduced form [73].

The effect of of Ala residue can also be highlighted with regards to the cell

binding ability of peptides when substituted instead of a Pro residue reducing its binding ability in the process [217], which highlights the importance of this residue in this peptide shown through the "PKLAKIFTKWKTYAGK" motif.

Chapter Eight

Discussion

The data from the molecular dynamic simulation HBD-mod8 shows a different trajectory when in contact with different membranes. It was observed in the literature that the MDS is a useful tool to assess the effectiveness of the designed peptides [159], [218]. In this instance the data shows a clear divide between the different lipid bilayers where the peptide penetrates the membrane mimicking the bacteria but does not do so when in contact with the zwitterionic membrane. This is also proven by the results from both the microbiology analysis shown in figure C.1b/C.2b and the cell culture data shown in figure 6.12, where the peptide showed high levels of activity against all bacteria but allowed the growth of the HeLa cells.

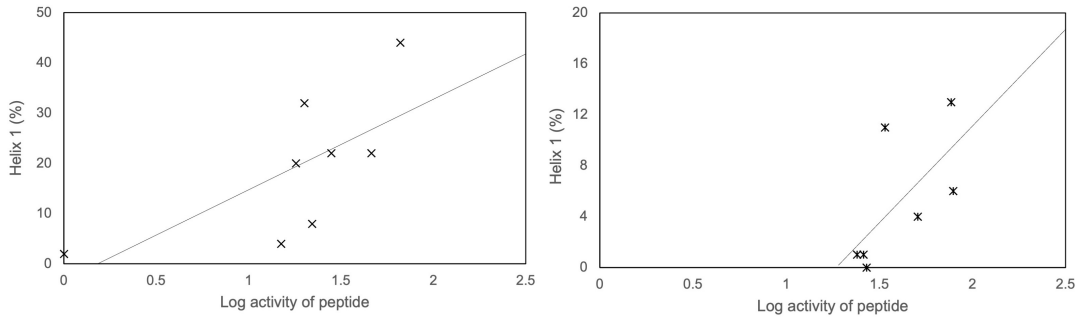
In terms of the peptides based on hBD3 they mostly show a different structural integrity in the experimental version than they do in the predicted version of the analysis. HBD3-mod1 according to the predicted data shows the most alpha helix content when compared to the rest of the peptides in its series, however this content is not reflected in the CD data presented. Similarly, HBD3-mod3 and -mod5 also show an alpha helix portion and when considering the CD data the percentage of the alpha helix portion was at 0% in PBS. The rest of this family of peptides however show a similar structural information. So comparing both predicted and experimental data, out of 15 peptides designed and tested, only 4 peptides showed discrepancies between the results, and only 73% of the predicted data was shown to reflect the laboratory data collected while, 27% were predicted incorrectly.

It is important to note that for the peptides based on hBD1 the activity of the peptides correlates between the CD data and its similarity to the predicated structure. Meaning wherever the predicted data showed a similar structural content to that of the CD data the peptide showed better activity against both bacteria. This however, is not the case with peptides based on hBD3. Although this discrepancy could be explained by structural changes that peptides undergo depending on the buffer chosen. For example HBD3-mod1 shows exceptional activity against both *S. aureus* and *P.*

aeruginosa which does correlate with its structural change from PBS to SDS where its alpha helix portion increases by 4-folds and the rest of the peptides show poor helix content when in SDS. It is interesting to note that HBD3-mod2 also shows exceptional activity against *S. aureus* and at its highest concentration towards *P. aeruginosa* which is different to that of HBD3-mod1. This could be explained by its structural content in PBS instead of SDS where the percentage of helix content is higher in this peptide.

There is also the percentage of helix1 when considering the breakdown of the CD data in more detail. This was shown to be the key for the activity of the peptide. Where in HBD-mod6 it shows the lowest percentage at 2% this peptide shows the worst activity even at its highest concentration against both bacteria tested. This is also shown in the presence of 44% of this type of helical structure in HBD-mod8 which showed the highest percentage of helix1 in all the peptides in this series. The same principle applies to HBD3-mod1 showing the highest percentage of helix1 in the series and equally showing the best activity against both bacteria when compared to the rest of the peptides in its series.

A general rule can be concluded from these results which states that the higher the structural change between the two buffers the higher the level of activity against both bacteria observed. This was the case with both HBD-mod7, -mod8 of hBD1 series and HBD3-mod1 and -mod2 of hBD3 series where they undergo the most structural change in the two chosen buffers. The correlation between the Helix 1 and the activity of the peptide against the bacteria is shown in figure 8.1



(a) Peptides based on hBD1 (b) Peptides based on hBD3

Figure 8.1: Correlation between the log activity of the peptides based on beta defensins and the percentage of helix 1.
It shows an upward trend where with the increase of helix 1 content of the peptide structure, the activity of the peptide also increases. The line of best fit is also shown to have a negative intercept in both instances. It can be seen that the percentage of helix 1 content of peptides based on hBD3 is much lower than hBD1.

It is difficult to find previous research on the topic of CD data and its analysis since the data have mostly been shown qualitatively, that is included in this research in the appendix section [96]. Most research only considers those graphs and does not provide a more detailed breakdown on the peptide structure. Therefore it is difficult to pinpoint whether these results have been found elsewhere in literature or if they are a novel discovery shown here. It should also be noted that the breakdown of the peptide structures is only as good as the series of databases that they have been matched to and the percentages are only representative of how well the peptides fit into the database chosen. The presence of many different databases as well as algorithms that can be used for producing these data, provides a challenge in the comparability of the data produced using these methodologies. Therefore there is a need for a gold standard methodology to ensure reproducibility of data and allow the comparison between peptides designed

by different groups.

16, 17, 18, 19HBD-mod8 all showed an increase in the alpha helical content from PBS to SDS This is consistent with their fragmentation pattern observed in chapter 7.1. All peptides showed an increase alpha helical content in LPS when compared to PBS except for 1HBD-mod8. According to the CD results most if not all the peptides based on hBD1 and their predicted structures were similar to that of their experimental counterparts. For example, HBD-mod8 and -mod7 showed highly similar structures to the experimental results in PBS, this statement is also true for HBD-mod1, -mod2, -mod4, -mod5 and -mod6 which show similar structural percentage to the predicted results. For HBD-mod3, however, an alpha helix structure is not reflected in the predicted CD data.

Since 4HBD-mod8 showed activity in only Gram-negative bacteria and a very toxic effect on the HeLa cells and it showed moderate alpha helical structure in LPS and its extreme strcutureal change form PBS to any other buffer used, it can be concluded that this type of strcutural change is not ideal in the overall activity of the peptide. On the other hand 1HBD-mod8 that shows moderate structural change and moderate activity against all bacteria alike with the lowest activity in *S. aureus* showed comparable results to the original sequence. In fact, peptides 2HBD-, 3HBD-, 4HBD-, 5HBD-, 15HBD-, 16HBD- and 17HBD-mod8 all show strong structural change in buffers other than PBS and this was shown to increase the cytotoxicity of the peptides.

Name	Sequence	Antimicrobial Activity at 250uM			Cell Viability %	Degree of Helix change		
		S.aureus	*P.aeroginosa*	*E.coli*		LPS	LTA	Total
{HBD-mod8}	GLGPKLAKIFTKWKTYRGKAK	34	35	9	100	29	8	19
{1HBD-mod8}	ALGPKLAKIFTKWKTYRGKAK	78	15	44	100	-4	-1	-3
{2HBD-mod8}	GAGPKLAKIFTKWKTYRGKAK	73	68	87	40	41	0	21
{3HBD-mod8}	GLAPKLAKIFTKWKTYRGKAK	31	77	8	10	35	15	25
{4HBD-mod8}	GLGAKLAKIFTKWKTYRGKAK	104	9	8	0	39	17	28
{5HBD-mod8}	GLGPALAKIFTKWKTYRGKAK	85	110	10	0	54	38	46
{6HBD-mod8}	GLGPKAAKIFTKWKTYRGKAK	83	100	88	100	14	11	13
{7HBD-mod8}	GLGPKLAAIFTKWKTYRGKAK	90	105	10	0	29	-4	13
{8HBD-mod8}	GLGPKLAKAFTKWKTYRGKAK	93	77	29	100	35	36	36
{9HBD-mod8}	GLGPKLAKIATKWKTYRGKAK	84	72	89	100	35	9	22
{10HBD-mod8}	GLGPKLAKIFAKWKTYRGKAK	46	56	10	0	35	4	20
{11HBD-mod8}	GLGPKLAKIFTAWKTYRGKAK	55	89	10	0	44	37	41
{12HBD-mod8}	GLGPKLAKIFTKAKTYRGKAK	73	80	80	0	31	-4	14
{13HBD-mod8}	GLGPKLAKIFTKWATYRGKAK	32	78	89	0	11	-7	2
{14HBD-mod8}	GLGPKLAKIFTKWKAYRGKAK	31	106	10	0	50	28	39
{15HBD-mod8}	GLGPKLAKIFTKWKTARGKAK	32	93	93	60	14	-6	4
{16HBD-mod8}	GLGPKLAKIFTKWKTYAGKAK	81	104	8	0	31	14	23
{17HBD-mod8}	GLGPKLAKIFTKWKTYRAKAK	68	92	7	0	47	39	43
{18HBD-mod8}	GLGPKLAKIFTKWKTYRGAAK	69	101	8	0	37	13	25
{19HBD-mod8}	GLGPKLAKIFTKWKTYRGKAA	76	103	7	0	32	32	32

Figure 8.2: Heatmap of culmination of the data showing the importance of a large structural change in the overall cytotoxicity of the peptides.

From that observation, it is clear that the more helix structure each peptide shows the better their activity will be. To find the validity of this hypothesis in the alanine scanned HBD-mod8 peptide as the most consistently active peptide of its series the peptides alongside HBD-mod8 where all tested using the same methodology as previously discussed, with the addition of new buffers LPS, LTA and DPC. From these data and the combination of both cell viability and bactericidal activity it can be seen that 19HBD-mod8 which was shown to have the most consistent alpha helix structure does not show a good activity level against the bacteria, and additionally shows poor cell viability at the two highest concentrations. Since the peptides in this experiment were also tested against *E. coli* it is easier to compare the helix results with activity of each peptide since they mostly all showed high levels of activity against this particular bacteria. All peptides except 2HBD-, 6HBD-, 9HBD-, 12HBD-, 13HBD- and 15HBD-mod8 all showed high levels of activity against this bacteria. It is important to note that the last two peptides mentioned showed high levels of activity against the Gram-positve bacteria and showed poor levels against the two Gram-negative bacteria. So that could be attributed to change in their sequence due to the alanine substitution. It

was shown that 2HBD-mod8 and 6HBD-mod8 have poor level of helix structure in at least one of the two condition of LPS and LTA. 13HBD-mod8 was also showing poor helix formation when in LTA but relatively good formation of helix in LPS which does not explain its activity level against *S. aureus* since LTA was meant to represent and mimic *S. aureus*. This has also been observed in 1HBD-mod8 showing the lowest level of helix formation in both LPS and LTA but it shows relatively good activity against all bacteria types with lower levels against *S. aureus*. Since none of the alanine scanned peptides follow a logical pattern and correlation between their helix content and the level of activity against the bacteria, it could be concluded that the activity of these peptides is irrespective of their helix content and it depends entirely on their stability in the presence of bacteria.

To assess whether there is a correlation between the serum stability of these peptides and their antimicrobial activity, their degradation in human serum was studied. According to [219] these fragmentation patterns can examine the activity of the peptides and produce better peptides in the future. The prominence of the 'PKLAKIFTK-WKTYR' fragment in the peptides that show better activity than those which do not have this fragmentation pattern could explain the inactivity of those peptides and suggests the importance of this motif in the activity of the HBD-mod8. Those peptides that share this motif however with a slight difference in the sequence due to the substitution of alanine such as 6HBD-, 9HBD- and 16HBD-mod8 did not retain the broad activity of HBD-mod8. These peptides are among the poorest in terms of activity against all three bacteria and they show relatively lower levels of toxicity when compared to the other substituted peptides. The importance of this motif and its exact sequence is further enhanced by the presence of alanine in the sequence of 6HBD-mod8 that falls inside this fragment's sequence replacing a Leucine (Leu - L) for the alanine residue. Therefore, the presence of a Leu residue is crucial for any activity rendered on behalf of the peptide. This effect has been shown in the anti-tubercular peptides and the importance of Leu residue in their sequences [220].

Another important residue for the activity of the peptide is 'IFT', which resides inside the bigger motif mentioned above. Each peptide that does not show this motif in its fragmentation pattern either due to substitution or removal by proximity to the substituted alanine residue which ultimately results in a different fragmentation site, was also shown to have poor activity against the tested bacteria and showed higher level of cytotoxicity compared to the peptides in the series.

The poor cytotoxicity results from 2HBD-, 3HBD-, 5HBD-mod8 could be attributed to the lack of fragmentation. Although 2HBD-mod8 was intact and did not show any fragmentation, it falls under the same category as 3HBD- and 5HBD-mod8 in that it has no clear fragmentation pattern. These peptides however showed a mix activity level against the tested bacteria. With both 3HBD- and 5 HBD-mod8 showing higher levels of activity against *E. coli* than 2HBD-mod8.

From these results it could be argued that the reason for the activity of HBD-mod8 is PKLAKIFTKWKTYR therefore, more studies into the activity of this motif could reveal that the rest of the similar activity levels to its parent, HBD-mod8. This conclusion does have a basis in that, most amino acids featured in this sequence, are known for their importance in antimicrobial activity of peptides such as Arg, Thr, Leu, Ile [47], [108], [151].

Chapter Nine

Conclusions and future works

The goal of this thesis was to find an antimicrobial peptide that shows non-inferior activity to that of the most currently used antibiotic for each bacterium used with minimal to no cytotoxic activity at its active concentration. HBD-mod8, was the only candidate peptide that showed this activity and fulfilled the criteria of an active peptide having comparable activity to the antibiotics tested for each bacteria. It is important to note, due to limited laboratory availability and shortage of biological facility none of the original peptides based on hBD1 and hBD3 were tested against human cells to assess their cytotoxicity. This is not important for the peptides based on hBD1 since they all showed poor levels of activity against at least one of the tested bacterium. However, since HBD3-mod1 and HBD3-mod2 both showed high level of activity against both *S. aureus* and *P. aeruginosa* they fall under the category of peptides that should have been tested against human cells to find their cytotoxicity. These results were not produced due to the short timeframe in which access to cell culture labs were gained and these peptides would have had to been synthesised and cleaned again for the purpose of performing these analysis. Therefore to assess their biological feasibility these peptides should be tested in the future to find whether they produce a toxic effect on human cells.

Additionally, these peptides were also not tested any further since HBD-mod8 was found to show high level of activity therefore this peptide and its alanine scanned analogs were the only peptides tested in serum degradation studies. Going forward it would be beneficial to perform the degradation studies on all peptides even the ones that did not show any activity towards the bacteria. Although this was shown in the alanine scanned results for HBD-mod8, it is not representative of a wider array of sequences which may have resulted in major difference in fragmentation patterns.

It is also important to note the addition of *E. coli* in the experiments on the substituted peptides since most of the peptides in the substitution series showed high level of activity agaisn this bacteria but did not necessarily follow the same trend

with *P. aeruginosa*. This bacterium was not available at the earliest stage of the antimicrobial experiments therefore the presence of both Gram-positve and Gram-neagtive bacteria was sufficient in that stage. However, once this bacterium was made available its addition added a level of complexity to the results since most of the peptides showed high levels of activity against this bacteria. This could be explained by the activity of HBD-mod8 against *E. coli* which may be retained through alanine scans of this peptide. To find the activity levels of the rest of the designed peptides they should all be tested against the same bacteria to produce cohesive results that can be compared more adequately.

The structural analysis, early experiments were performed using CD in temperature and the preliminary data for a different peptide that was not designed by myself showed large differences between the structural data at $37°C$ and at room temperature. Therefore it would be beneficial to perform the same analysis on the designed peptides and find the differences the application of heat will make to the structure of the peptide.

Although Molecular dynamic simulations were performed on HBD-mod8 it should also be noted that there was no laboratory experiments performed to provide information regarding the mode of action for this peptide or to prove the results from the simulation. More experiments such as membrane mimicking vesicles as well as confocal microscopy should be performed to better understand the reason behind the performance of each peptide against each bacteria. The MD simulations were performed to ensure the effectiveness of HBD-mod8 prior to the collection of laboratory data on any biological analysis. However this research could benefit from additional production of MD simulations on different peptides and not only those that show antimicrobial activity to be used as negative control. This was not achievable in the timescale of this project due to lack of computer power which was the limiting factor in the performance of these simulations for longer timeframes as well as on the peptides that did not show

similar activity to that of HBD-mod8.

In conclusion, HBD-mod8 showed high levels of activity and low cytotoxicity and its comparison to its alanine substitutes showed that this peptide in its original sequence was the most effective in terms of activity and cytotoxicity levels.

References

[1] N. R. Naylor, K. B. Pouwels, R. Hope, *et al.*, "The health and cost burden of antibiotic resistant and susceptible Escherichia coli bacteraemia in the English hospital setting: A national retrospective cohort study," *PLoS ONE*, vol. 14, no. 9, S. Leekha, Ed., e0221944, 2019. DOI: 10.1371/journal.pone.0221944.

[2] Jim O'Neill, "Securing New Drugs for Future Generations: The Pipeline Of Antibiotics," *PLOS ONE*, vol. 14, no. 9, S. Leekha, Ed., e0221944, 2019.

[3] WHO, *Antimicrobial resistance*.

[4] C. L. Ventola, "The antibiotic resistance crisis: part 1: causes and threats.," *P T : a peer-reviewed journal for formulary management*, vol. 40, no. 4, pp. 277–83, 2015.

[5] The Pew Charitable Trusts, *Antibiotics Currently in Clinical Development*, 2014.

[6] O. V. Makhlynets and G. A. Caputo, "Characteristics and therapeutic applications of antimicrobial peptides," *Biophysics Reviews*, vol. 2, no. 1, p. 011 301, 2021. DOI: 10.1063/5.0035731.

[7] A. T. Yeung, S. L. Gellatly, and R. E. Hancock, "Multifunctional cationic host defence peptides and their clinical applications," *Cellular and Molecular Life Sciences*, vol. 68, no. 13, pp. 2161–2176, 2011. DOI: 10.1007/s00018-011-0710-x.

[8] A. Bahar and D. Ren, "Antimicrobial Peptides," *Pharmaceuticals*, vol. 6, no. 12, pp. 1543–1575, 2013. DOI: 10.3390/ph6121543.

[9] R. E. Hancock, "Cationic antimicrobial peptides: towards clinical applications," *Expert Opinion on Investigational Drugs*, vol. 9, no. 8, pp. 1723–1729, 2005. DOI: 10.1517/13543784.9.8.1723.

[10] F. Schweizer, "Cationic amphiphilic peptides with cancer-selective toxicity," *European Journal of Pharmacology*, vol. 625, no. 1-3, pp. 190–194, 2009. DOI: 10.1016/j.ejphar.2009.08.043.

[11] J. N. Cole and V. Nizet, "Bacterial Evasion of Host Antimicrobial Peptide Defenses," in *Virulence Mechanisms of Bacterial Pathogens, Fifth Edition*, 1, vol. 4, NIH Public Access, 2016, pp. 413–443. DOI: 10.1128/microbiolspec.vmbf-0006-2015.

[12] K. L. Brown and R. E. Hancock, "Cationic host defense (antimicrobial) peptides," *Current Opinion in Immunology*, vol. 18, no. 1, pp. 24–30, 2006. DOI: 10.1016/j.coi.2005.11.004.

[13] E. Gazit, I. R. Miller, P. C. Biggin, M. S. P. Sansom, and Y. Shai, "Structure and Orientation of the Mammalian Antibacterial Peptide Cecropin P1 within Phospholipid Membranes," *Journal of Molecular Biology*, vol. 258, no. 5, pp. 860–870, 1996. DOI: 10.1006/jmbi.1996.0293.

[14] R. J. Dubos, "Studies On A Bactericidal Agent Extracted From A Soil Bacillus," *Journal of Experimental Medicine*, vol. 70, no. 1, pp. 1–10, 1939. DOI: 10.1084/jem.70.1.1.

[15] H. L. Van Epps, "René Dubos: unearthing antibiotics.," *The Journal of experimental medicine*, vol. 203, no. 2, p. 259, 2006. DOI: 10.1084/jem.2032fta.

[16] A Fleming and B. A. lexander F leming, "On a remarkable bacteriolytic element found in tissues and secretions," *Proceedings of the Royal Society of London. Series B, Containing Papers of a Biological Character*, vol. 93, no. 653, pp. 306–317, 1922. DOI: 10.1098/rspb.1922.0023.

[17] D. J. Vocadlo, G. J. Davies, R. Laine, and S. G. Withers, "Catalysis by hen egg-white lysozyme proceeds via a covalent intermediate," *Nature*, vol. 412, no. 6849, pp. 835–838, 2001. DOI: 10.1038/35090602.

[18] R Fernandez De Caleya, B. Gonzalez-Pascual, F Garcia-Olmedo, and P. Carbonero, "Susceptibility of Phytopathogenic Bacteria to Wheat Purothionins In Vitro," *APPLIED MICROBIOLOGY*, vol. 23, no. 5, pp. 998–1000, 1972.

[19] M. Simmaco, G. Kreil, and D. Barra, *Bombinins, antimicrobial peptides from Bombina species*, 2009. DOI: 10.1016/j.bbamem.2009.01.004.

[20] M. L. Groves, R. F. Peterson, and C. A. Kiddy, "Polymorphism in the red protein isolated from milk of individual cows," *Nature*, vol. 207, no. 5000, pp. 1007–1008, 1965. DOI: 10.1038/2071007a0.

[21] D. Lau, H. Mollnau, J. P. Eiserich, *et al.*, "Myeloperoxidase mediates neutrophil activation by association with CD11b/CD18 integrins," *Proceedings of the National Academy of Sciences*, vol. 102, no. 2, pp. 431–436, 2005. DOI: 10.1073/pnas.0405193102.

[22] A. Egesten, J. Breton-Gorius, J. Guichard, U. Gullberg, and I. Olsson, "The heterogeneity of azurophil granules in neutrophil promyelocytes: immunogold localization of myeloperoxidase, cathepsin G, elastase, proteinase 3, and bactericidal/permeability increasing protein," *Blood*, vol. 83, no. 10, pp. 2985–2994, 1994. DOI: 10.1182/blood.V83.10.2985.2985.

[23] H. I. Zeya and J. K. Spitznagel, "Antibacterial and enzymic basic proteins from leukocyte lysosomes: Separation and identification," *Science*, vol. 142, no. 3595, pp. 1085–1087, 1963. DOI: 10.1126/science.142.3595.1085.

[24] H. I. Zeya and J. K. Spitznagel, "Cationic proteins of polymorphonuclear leukocyte lysosomes. II. Composition, properties, and mechanism of antibacterial action.," *Journal of bacteriology*, vol. 91, no. 2, pp. 755–762, 1966. DOI: 10.1128/jb.91.2.755-762.1966.

[25] J. K. Spitznagel and A. Iio1g-Ytjk' Chi, "Cationic Proteins And Antibacterial Properties Of Infected Tissues And Leukocytes,"

[26] D. Angelakos, "Book reviews - Topics in intersystem electromagnetic compatibility," *IEEE Antennas and Propagation Group Newsletter*, vol. 14, no. 4, pp. 14–14, 1972. DOI: 10.1109/MAP.1972.27137.

[27] D. Roos, R. Van Bruggen, and C. Meischl, "Oxidative killing of microbes by neutrophils," *Microbes and Infection*, vol. 5, no. 14, pp. 1307–1315, 2003. DOI: 10.1016/j.micinf.2003.09.009.

[28] H. Kuwata, T.-T. Yip, C. L. Yip, M. Tomita, and T. Hutchens, "Bactericidal Domain of Lactoferrin: Detection, Quantitation, and Characterization of Lactoferricin in Serum by SELDI Affinity Mass Spectrometry," *Biochemical and Biophysical Research Communications*, vol. 245, no. 3, pp. 764–773, 1998. DOI: 10.1006/bbrc.1998.8466.

[29] T. Ganz, M. E. Selsted, D. Szklarek, *et al.*, "Defensins. Natural Peptide Antibiotics of Human Neutrophils," *Journal of Clinical Investigation*, DOI: 10.1172/JCI112120.

[30] M. E. Selsted, D. Szklarek, R. I. Lehrer, *et al.*, "Purification and Antibacterial Activity of Antimicrobial Peptides of Rabbit Granulocytest Six antimicrobial peptides, corresponding to the family of "Ilysosomal cationic proteins" described previously," vol. 45, no. 1, pp. 150–154, 1984.

[31] J. Patterson-Delafield, R. J. Martinez,' And, and R. I. Lehrer2, "Microbicidal Cationic Proteins in Rabbit Alveolar Macrophages: a Potential Host Defense Mechanismt," vol. 30, no. 1, pp. 180–192, 1980.

[32] R. I. Lehrer and T. Ganz, "Defensins of vertebrate animals," *Current Opinion in Immunology*, vol. 14, no. 1, pp. 96–102, 2002. DOI: 10.1016/S0952-7915(01)00303-X.

[33] M. Zanetti, R. Gennaro, and D. Romeo, *Cathelicidins: a novel protein family with a common proregion and a variable C-terminal antimicrobial domain*, 1995. DOI: 10.1016/0014-5793(95)01050-O.

[34] M. Zanetti, "Cathelicidins, multifunctional peptides of the innate immunity," *Journal of Leukocyte Biology*, vol. 75, no. 1, pp. 39–48, 2004. DOI: 10.1189/jlb.0403147.

[35] O. Levy, "Antimicrobial proteins and peptides: anti-infective molecules of mammalian leukocytes," *Journal of Leukocyte Biology*, vol. 76, no. 5, pp. 909–925, 2004. DOI: 10.1189/jlb.0604320.

[36] C. Chan, L. L. Burrows, and C. M. Deber, "Helix induction in antimicrobial peptides by alginate in biofilms.," *The Journal of biological chemistry*, vol. 279, no. 37, pp. 38 749–54, 2004. DOI: 10.1074/jbc.M406044200.

[37] R. E. Hancock and H. G. Sahl, *Antimicrobial and host-defense peptides as new anti-infective therapeutic strategies*, 2006. DOI: 10.1038/nbt1267.

[38] K. A. Brogden, "Antimicrobial peptides: pore formers or metabolic inhibitors in bacteria?" *Nature Reviews Microbiology*, vol. 3, no. 3, pp. 238–250, 2005. DOI: 10.1038/nrmicro1098. arXiv: NIHMS150003.

[39] A. Peschel and H. G. Sahl, *The co-evolution of host cationic antimicrobial peptides and microbial resistance*, 2006. DOI: 10.1038/nrmicro1441.

[40] B.-C. Zhao, H.-C. Lin, D. Yang, X. Ye, and Z.-G. Li, "Disulfide Bridges in Defensins," *Current Topics in Medicinal Chemistry*, vol. 16, no. 2, pp. 206–219, 2015. DOI: 10.2174/1568026615666150701115911.

[41] R. Hare, "The Scientific Activities Of Alexander Fleming, Other Than The Discovery Of Penicillin," vol. 27, pp. 347–372, 1983.

[42] M. E. Selstedls, D. M. Browny, R. J. Delanged, and R. I. Lehrerl, "Primary structures of MCP-1 and MCP-2, natural peptide antibiotics of rabbit lung macrophages.," vol. 258, no. 23, pp. 14 485–14 489, 1983. DOI: 10.1016/S0021-9258(17)43888-9.

[43] T. Ganz and R. I. Lehrer, "Antimicrobial peptides of leukocytes," *Current Opinion in Hematology*, vol. 4, no. 1, pp. 53–58, 1997. DOI: 10.1097/00062752-199704010-00009.

[44] D. E. Jones$#, C. L. Bevinsstll, D. Jones, and C. Bevins, "Paneth cells of the human small intestine express an antimicrobial peptide gene," *Journal of Biological Chemistry*, vol. 267, no. 32, pp. 23 216–23 225, 1992. DOI: 10.1016/S0021-9258(18)50079-X.

[45] A. J. Quayle, E. Porter, A. A. Nussbaum, *et al.*, "Gene Expression, Immunolocalization, and Secretion of Human Defensin-5 in Human Female Reproductive Tract," vol. 152, no. 5, 1998.

[46] Y. Z. Lin, X. H. Ke, and J. P. Tam, "Synthesis and structure-activity study of myxoma virus growth factor," *Biochemistry*, vol. 30, no. 13, pp. 3310–3314, 1991. DOI: 10.1021/bi00227a020.

[47] S. Das, N. Nikolaidis, H. Goto, *et al.*, "Comparative Genomics and Evolution of the Alpha-Defensin Multigene Family in Primates," *Molecular Biology and Evolution*, vol. 27, no. 10, pp. 2333–2343, 2010. DOI: 10.1093/molbev/msq118.

[48] S. Solomon, "Corticostatins," *Trends in Endocrinology & Metabolism*, vol. 4, no. 8, pp. 260–264, 1993. DOI: 10.1016/1043-2760(93)90096-W.

[49] R. I. Lehrer and W. Lu, "alpha-Defensins in human innate immunity," *Immunological Reviews*, vol. 245, no. 1, pp. 84–112, 2012. DOI: 10.1111/j.1600-065X.2011.01082.x.

[50] A. Maemoto, X. Qu, K. J. Rosengren, *et al.*, "Functional analysis of the alpha-defensin disulfide array in mouse cryptdin-4," *Journal of Biological Chemistry*, vol. 279, no. 42, pp. 44 188–44 196, 2004. DOI: 10.1074/jbc.M406154200.

[51] A. Szyk, W. Lu, Z. Wu, J. Lubkowski, K. Tucker, and D. Yang, "Crystal structures of human alpha-defensins HNP4, HD5, and HD6," *Protein Science*, vol. 15, no. 12, pp. 2749–2760, 2006. DOI: 10.1110/ps.062336606.

[52] D. M. Bowdish, D. J. Davidson, and R. E. Hancock, "Immunomodulatory properties of defensins and cathelicidins," *Current Topics in Microbiology and Immunology*, vol. 306, pp. 27–66, 2006. DOI: 10.1007/3-540-29916-5_2.

[53] C. Xie, A. Prahl, B. Ericksen, *et al.*, "Reconstruction of the conserved beta-bulge in mammalian defensins using D-amino acids," *Journal of Biological Chemistry*, vol. 280, no. 38, pp. 32 921–32 929, 2005. DOI: 10.1074/jbc.M503084200.

[54] M. E. Selsted and A. J. Ouellette, *Mammalian defensins in the antimicrobial immune response*, 2005. DOI: 10.1038/ni1206.

[55] M. Rajabi, B. Ericksen, X. Wu, *et al.*, "Functional determinants of human enteric α-defensin HD5: Crucial role for hydrophobicity at dimer interface," *Journal of Biological Chemistry*, vol. 287, no. 26, pp. 21 615–21 627, 2012. DOI: 10.1074/jbc.M112.367995.

[56] M. Pazgier, G. Wei, B. Ericksen, *et al.*, "Sometimes It Takes Two to Tango," 2012. DOI: 10.1074/jbc.M111.332205.

[57] K. W. Bensch, M. Raida, H. J. Mägert, P. Schulz-Knappe, and W. G. Forssmann, "hBD-1: a novel beta-defensin from human plasma," *FEBS Letters*, vol. 368, no. 2, pp. 331–335, 1995. DOI: 10.1016/0014-5793(95)00687-5.

[58] Y. Yamaguchi, T. Nagase, R. Makita, *et al.*, "Identification of Multiple Novel Epididymis-Specific beta-Defensin Isoforms in Humans and Mice," *The Journal of Immunology*, vol. 169, no. 5, pp. 2516–2523, 2002. DOI: 10.4049/jimmunol.169.5.2516.

[59] M. Pazgier, D. M. Hoover, D. Yang, W. Lu, and J. Lubkowski, *Human beta-defensins*, 2006. DOI: 10.1007/s00018-005-5540-2.

[60] L. Liu, C. Zhao, H. H. Heng, and T. Ganz, "The Human beta-Defensin-1 and α-Defensins Are Encoded by Adjacent Genes: Two Peptide Families with Differing Disulfide Topology Share a Common Ancestry," *Genomics*, vol. 43, no. 3, pp. 316–320, 1997. DOI: 10.1006/geno.1997.4801.

[61] D. L. Diamond, J. R. Kimball, S. Krisanaprakornkit, T. Ganz, and B. A. Dale, "Detection of beta-defensins secreted by human oral epithelial cells," *Journal of Immunological Methods*, vol. 256, no. 1-2, pp. 65–76, 2001. DOI: 10.1016/S0022-1759(01)00442-2.

[62] E. Prado-Montes de Oca, "Human beta-defensin 1: A restless warrior against allergies, infections and cancer," *The International Journal of Biochemistry & Cell Biology*, vol. 42, no. 6, pp. 800–804, 2010. DOI: 10.1016/j.biocel.2010.01.021.

[63] J.-R. García, F. Jaumann, S. Schulz, *et al.*, "Identification of a novel, multifunctional beta-defensin (human beta-defensin 3) with specific antimicrobial activity," *Cell and Tissue Research*, vol. 306, no. 2, pp. 257–264, 2001. DOI: 10.1007/s004410100433.

[64] C. A. Semple, P. Gautier, K. Taylor, and J. R. Dorin, "The changing of the guard: Molecular diversity and rapid evolution of beta-defensins," *Molecular Diversity*, vol. 10, no. 4, pp. 575–584, 2006. DOI: 10.1007/s11030-006-9031-7.

[65] E. V. Valore, C. H. Park, A. J. Quayle, K. R. Wiles, P. B. McCray, and T. Ganz, "Human beta-defensin-1: an antimicrobial peptide of urogenital tissues.," *Journal of Clinical Investigation*, vol. 101, no. 8, pp. 1633–1642, 1998. DOI: 10.1172/JCI1861.

[66] P. B. McCray and L. Bentley, "Human Airway Epithelia Express a beta-defensin," *American Journal of Respiratory Cell and Molecular Biology*, vol. 16, no. 3, pp. 343–349, 1997. DOI: 10.1165/ajrcmb.16.3.9070620.

[67] B. O. Schroeder, Z. Wu, S. Nuding, *et al.*, "Reduction of disulphide bonds unmasks potent antimicrobial activity of human beta-defensin 1," *Nature*, vol. 469, no. 7330, pp. 419–423, 2011. DOI: 10.1038/nature09674.

[68] P. K. Singh, H. P. Jia, K. Wiles, *et al.*, "Production of beta-defensins by human airway epithelia," *Proceedings of the National Academy of Sciences*, vol. 95, no. 25, pp. 14 961–14 966, 1998. DOI: 10.1073/pnas.95.25.14961.

[69] A. Dunsche, Y. Açil, H. Dommisch, R. Siebert, J.-M. Schröder, and S. Jepsen, "The novel human beta-defensin-3 is widely expressed in oral tissues," *European Journal of Oral Sciences*, vol. 110, no. 2, pp. 121–124, 2002. DOI: 10.1034/j.1600-0722.2002.11186.x.

[70] X. Chen, F. Niyonsoba, H. Ushio, *et al.*, "Antimicrobial peptides human beta-defensin (hBD)-3 and hBD-4 activate mast cells and increase skin vascular permeability," *European Journal of Immunology*, vol. 37, no. 2, pp. 434–444, 2007. DOI: 10.1002/eji.200636379.

[71] J. Harder, J. Bartels, E. Christophers, and J.-M. Schröder, "Isolation and Characterization of Human mu-Defensin-3, a Novel Human Inducible Peptide Antibiotic," *Journal of Biological Chemistry*, vol. 276, no. 8, pp. 5707–5713, 2001. DOI: 10.1074/jbc.M008557200.

[72] Z. Wu, D. M. Hoover, D. Yang, *et al.*, "Engineering disulfide bridges to dissect antimicrobial and chemotactic activities of human $\beta$$-defensin3," *Proceedings of the National Academy of Sciences*, vol. 100, no. 15, pp. 8880–8885, 2003. DOI: 10.1073/pnas.1533186100.

[73] S. Olli, N. Rangaraj, and R. Nagaraj, "Effect of Selectively Introducing Arginine and D-Amino Acids on the Antimicrobial Activity and Salt Sensitivity in Analogs of Human Beta-Defensins," *PLoS ONE*, vol. 8, no. 9, D. Chakravortty, Ed., e77031, 2013. DOI: 10.1371/journal.pone.0077031.

[74] T. X. Nguyen, A. M. Cole, and R. I. Lehrer, "Evolution of primate theta-defensins: a serpentine path to a sweet tooth," *Peptides*, vol. 24, no. 11, pp. 1647–1654, 2003. DOI: 10.1016/j.peptides.2003.07.023.

[75] S. A. Gallo, W. Wang, S. S. Rawat, *et al.*, "theta-Defensins Prevent HIV-1 Env-mediated Fusion by Binding gp41 and Blocking 6-Helix Bundle Formation," *Journal of Biological Chemistry*, vol. 281, no. 27, pp. 18 787–18 792, 2006. DOI: 10.1074/jbc.M602422200.

[76] D. Tran, P. Tran, K. Roberts, *et al.*, "Microbicidal Properties and Cytocidal Selectivity of Rhesus Macaque Theta Defensins," *Antimicrobial Agents and Chemotherapy*, vol. 52, no. 3, pp. 944–953, 2008. DOI: 10.1128/AAC.01090-07.

[77] A. M. Cole, T. Hong, L. M. Boo, *et al.*, "Retrocyclin: A primate peptide that protects cells from infection by T- and M-tropic strains of HIV-1," *Proceedings of the National Academy of Sciences*, vol. 99, no. 4, pp. 1813–1818, 2002. DOI: 10.1073/pnas.052706399.

[78] E. Arnett, R. I. Lehrer, P. Pratikhya, W. Lu, and S. Seveau, "Defensins enable macrophages to inhibit the intracellular proliferation of Listeria monocytogenes," *Cellular Microbiology*, vol. 13, no. 4, pp. 635–651, 2011. DOI: 10.1111/j.1462-5822.2010.01563.x.

[79] M. Magana, M. Pushpanathan, A. L. Santos, *et al.*, "The value of antimicrobial peptides in the age of resistance," *The Lancet Infectious Diseases*, vol. 20, no. 9, e216–e230, 2020. DOI: 10.1016/S1473-3099(20)30327-3.

[80] H. Gong, J. Zhang, X. Hu, *et al.*, "Hydrophobic Control of the Bioactivity and Cytotoxicity of de Novo-Designed Antimicrobial Peptides," *ACS Applied Materials and Interfaces*, vol. 11, no. 38, pp. 34 609–34 620, 2019. DOI: 10.1021/acsami.9b10028.

[81] G. Wei, E. de Leeuw, M. Pazgier, *et al.*, "Through the Looking Glass, Mechanistic Insights from Enantiomeric Human Defensins," *Journal of Biological Chemistry*, vol. 284, no. 42, pp. 29 180–29 192, 2009. DOI: 10.1074/jbc.M109.018085.

[82] D Rapaport and Y Shai, "Interaction of fluorescently labeled pardaxin and its analogues with lipid bilayers.," *The Journal of biological chemistry*, vol. 266, no. 35, pp. 23 769–75, 1991.

[83] S. J. Ludtke, K. He, W. T. Heller, T. A. Harroun, L. Yang, and H. W. Huang, "Membrane Pores Induced by Magainin," *Biochemistry*, vol. 35, no. 43, pp. 13 723–13 728, 1996. DOI: 10.1021/bi9620621.

[84] D. Allende, S. A. Simon, and T. J. McIntosh, "Melittin-induced bilayer leakage depends on lipid material properties: Evidence for toroidal pores," *Biophysical Journal*, vol. 88, no. 3, pp. 1828–1837, 2005. DOI: 10.1529/biophysj.104.049817.

[85] D. I. Fernandez, A. P. Le Brun, T. C. Whitwell, M.-A. Sani, M. James, and F. Separovic, "The antimicrobial peptide aurein 1.2 disrupts model membranes via the carpet mechanism," *Physical Chemistry Chemical Physics*, vol. 14, no. 45, p. 15 739, 2012. DOI: 10.1039/c2cp43099a.

[86] M. Wu, E. Maier, R. Benz, and R. E. W. Hancock, "Mechanism of Interaction of Different Classes of Cationic Antimicrobial Peptides with Planar Bilayers and with the Cytoplasmic Membrane of Escherichia coli," *Biochemistry*, vol. 38, no. 22, pp. 7235–7242, 1999. DOI: 10.1021/bi9826299.

[87] M. C. Territo, T. Ganz, M. E. Selsted, and R. Lehrer, "Monocyte-chemotactic activity of defensins from human neutrophils.," *Journal of Clinical Investigation*, vol. 84, no. 6, pp. 2017–2020, 1989. DOI: 10.1172/JCI114394.

[88] Y. V Chaly, E. M Paleolog, T. S Kolesnikova, I. I Tikhonov, E. V Petratchenko, and N. N Voitenok, "Neutrophil alpha-defensin human neutrophil peptide modulates cytokine production in human monocytes and adhesion molecule expres-

sion in endothelial cells.," *European cytokine network*, vol. 11, no. 2, pp. 257–66, 2000.

[89] R. E. Hancock and A. Rozek, "Role of membranes in the activities of antimicrobial cationic peptides," *FEMS Microbiology Letters*, vol. 206, no. 2, pp. 143–149, 2002. DOI: 10.1111/j.1574-6968.2002.tb11000.x.

[90] A. M. Van Der Does, S. J. Bogaards, B. Ravensbergen, H. Beekhuizen, J. T. Van Dissel, and P. H. Nibbering, "Antimicrobial peptide hLF1-11 directs granulocyte-macrophage colony-stimulating factor-driven monocyte differentiation toward macrophages with enhanced recognition and clearance of pathogens," *Antimicrobial Agents and Chemotherapy*, vol. 54, no. 2, pp. 811–816, 2010. DOI: 10.1128/AAC.00652-09.

[91] R. I. Lehrer, G. Jung, P. Ruchala, *et al.*, "Human alpha-Defensins Inhibit Hemolysis Mediated by Cholesterol-Dependent Cytolysins," *Infection and Immunity*, vol. 77, no. 9, pp. 4028–4040, 2009. DOI: 10.1128/IAI.00232-09.

[92] K. Miles, D. J. Clarke, W. Lu, *et al.*, "Dying and Necrotic Neutrophils Are Anti-Inflammatory Secondary to the Release of alpha-Defensins," *The Journal of Immunology*, vol. 183, no. 3, pp. 2122–2132, 2009. DOI: 10.4049/jimmunol.0804187.

[93] E. de Leeuw, C. Li, P. Zeng, *et al.*, "Functional interaction of human neutrophil peptide-1 with the cell wall precursor lipid II," *FEBS Letters*, vol. 584, no. 8, pp. 1543–1548, 2010. DOI: 10.1016/j.febslet.2010.03.004.

[94] J. J. Oppenheim, "The 2005 Dolph Adams awards and the state of the Journal of Leukocyte Biology," *Journal of Leukocyte Biology*, vol. 79, no. 1, pp. 1–3, 2006. DOI: 10.1189/jlb.0805480.

[95] J. W. Lillard, P. N. Boyaka, O. Chertov, J. J. Oppenheim, and J. R. McGhee, "Mechanisms for induction of acquired host immunity by neutrophil peptide

defensins," *Proceedings of the National Academy of Sciences*, vol. 96, no. 2, pp. 651–656, 1999. DOI: 10.1073/pnas.96.2.651.

[96] D. Wade, A. Bomant, B. Wxhlint, *et al.*, "All-D amino acid-containing channel-forming antibiotic peptides," vol. 87, pp. 4761–4765, 1990.

[97] D. Yang, Z.-h. Liu, P. Tewary, Q. Chen, G. de la Rosa, and J. Oppenheim, "Defensin Participation in Innate and Adaptive Immunity," *Current Pharmaceutical Design*, vol. 13, no. 30, pp. 3131–3139, 2007. DOI: 10.2174/138161207782110453.

[98] L. J. Zhang and R. L. Gallo, *Antimicrobial peptides*, 2016. DOI: 10.1016/j.cub.2015.11.017.

[99] F. H. Waghu, S. Joseph, S. Ghawali, *et al.*, "Designing antibacterial peptides with enhanced killing kinetics," *Frontiers in Microbiology*, vol. 9, no. FEB, p. 325, 2018. DOI: 10.3389/fmicb.2018.00325.

[100] M. R. Yeaman and N. Y. Yount, "Mechanisms of Antimicrobial Peptide Action and Resistance," *Pharmacological reviews*, vol. 55, no. 1, pp. 27–55, 2003. DOI: 10.1124/pr.55.1.2.27.

[101] N. Funderburg, M. M. Lederman, Z. Feng, *et al.*, "Human beta-defensin-3 activates professional antigen-presenting cells via Toll-like receptors 1 and 2," *Proceedings of the National Academy of Sciences*, vol. 104, no. 47, pp. 18 631–18 635, 2007. DOI: 10.1073/pnas.0702130104.

[102] D. Yang, O. Chertov, S. N. Bykovskaia, *et al.*, "beta-Defensins: Linking Innate and Adaptive Immunity Through Dendritic and T Cell CCR6," *Science*, vol. 286, no. 5439, pp. 525–528, 1999. DOI: 10.1126/science.286.5439.525.

[103] O. E. Sørensen, J. B. Cowland, K. Theilgaard-Mönch, L. Liu, T. Ganz, and N. Borregaard, "Wound Healing and Expression of Antimicrobial Peptides/Polypeptides in Human Keratinocytes, a Consequence of Common Growth Factors," *The Journal of Immunology*, vol. 170, no. 11, pp. 5583–5589, 2003. DOI: 10.4049/jimmunol.170.11.5583.

[104] F. G. Avci, B. S. Akbulut, and E. Ozkirimli, "Membrane Active Peptides and Their Biophysical Characterization," *Biomolecules*, vol. 8, no. 3, p. 77, 2018. DOI: 10.3390/biom8030077.

[105] H. E. Hasper, N. E. Kramer, J. L. Smith, *et al.*, "An Alternative Bactericidal Mechanism of Action for Lantibiotic Peptides That Target Lipid II," *Science*, vol. 313, no. 5793, pp. 1636–1637, 2006. DOI: 10.1126/science.1129818.

[106] V. R. Tenge, A. P. Gounder, M. E. Wiens, W. Lu, and J. G. Smith, "Delineation of Interfaces on Human Alpha-Defensins Critical for Human Adenovirus and Human Papillomavirus Inhibition," *PLoS Pathogens*, vol. 10, no. 9, E. S. Robertson, Ed., e1004360, 2014. DOI: 10.1371/journal.ppat.1004360.

[107] A. P. Gounder, M. E. Wiens, S. S. Wilson, W. Lu, and J. G. Smith, "Critical Determinants of Human alpha-Defensin 5 Activity against Non-enveloped Viruses," *Journal of Biological Chemistry*, vol. 287, no. 29, pp. 24 554–24 562, 2012. DOI: 10.1074/jbc.M112.354068.

[108] G. Wei, M. Pazgier, E. de Leeuw, *et al.*, "Trp-26 Imparts Functional Versatility to Human alpha-Defensin HNP1," *Journal of Biological Chemistry*, vol. 285, no. 21, pp. 16 275–16 285, 2010. DOI: 10.1074/jbc.M110.102749.

[109] Y. Zhang, W. Lu, and M. Hong, "The Membrane-Bound Structure and Topology of a Human alpha-Defensin Indicate a Dimer Pore Mechanism for Membrane Disruption," *Biochemistry*, vol. 49, no. 45, pp. 9770–9782, 2010. DOI: 10.1021/bi101512j.

[110] X. Ran, J. Chen, L. Chen, Y. Li, and M. Wu, "Beta-defensin gene (DEFB1) polymorphisms are associated with the susceptibility to chronic respiratory diseases," *Genes and Genomics*, vol. 38, no. 7, pp. 645–658, 2016. DOI: 10.1007/S13258-016-0388-4/TABLES/4.

[111] M. Pazgier, A. Prahl, D. M. Hoover, and J. Lubkowski, "Studies of the biological properties of human beta-defensin 1," *Journal of Biological Chemistry*, vol. 282, no. 3, pp. 1819–1829, 2007. DOI: 10.1074/jbc.M607210200.

[112] K. M. Varney, A. M. Bonvin, M. Pazgier, *et al.*, "Turning Defense into Offense: Defensin Mimetics as Novel Antibiotics Targeting Lipid II," *PLoS Pathogens*, vol. 9, no. 11, M. Zasloff, Ed., e1003732, 2013. DOI: 10.1371/journal.ppat.1003732.

[113] E. de Leeuw, S. R. Burks, X. Li, J. P. Kao, and W. Lu, "Structure-dependent functional properties of human defensin 5," *FEBS Letters*, vol. 581, no. 3, pp. 515–520, 2007. DOI: 10.1016/j.febslet.2006.12.036.

[114] E. Klüver, S. Schulz-Maronde, S. Scheid, B. Meyer, W.-G. Forssmann, and K. Adermann, "Structure-Activity Relation of Human beta-Defensin 3: Influence of Disulfide Bonds and Cysteine Substitution on Antimicrobial Activity and Cytotoxicity," *Biochemistry*, vol. 44, no. 28, pp. 9804–9816, 2005. DOI: 10.1021/bi050272k.

[115] T. K. Phan, F. T. Lay, and M. D. Hulett, "Importance of phosphoinositide binding by human beta-defensin 3 for Akt-dependent cytokine induction," *Immunology and Cell Biology*, vol. 96, no. 1, pp. 54–67, 2018. DOI: 10.1111/imcb.1017.

[116] S. Chen, R. Gopalakrishnan, T. Schaer, *et al.*, "Dithiol amino acids can structurally shape and enhance the ligand-binding properties of polypeptides," *Nature chemistry*, vol. 6, no. 11, pp. 1009–1016, 2014. DOI: 10.1038/nchem.2043.

[117] G. Musumeci, M. L. Carnazza, C. C. Loreto, R. Leonardi, and C. C. Loreto, "beta-Defensin-4 (HBD-4) is expressed in chondrocytes derived from normal and osteoarthritic cartilage encapsulated in PEGDA scaffold," *Acta Histochemica*, vol. 114, no. 8, pp. 805–812, 2012. DOI: 10.1016/j.acthis.2012.02.001.

[118] W. T. Penberthy, S. Chari, A. L. Cole, and A. M. Cole, *Retrocyclins and their activity against HIV-1*, 2011. DOI: 10.1007/s00018-011-0715-5.

[119] L. Chen, L. Jia, Q. Zhang, *et al.*, "A novel antimicrobial peptide against dental-caries-associated bacteria," *Anaerobe*, vol. 47, pp. 165–172, 2017. DOI: 10.1016/j.anaerobe.2017.05.016.

[120] R. I. Lehrer, A. Barton, K. A. Daher, S. S. Harwig, T. Ganz, and M. E. Selsted, "Interaction of human defensins with Escherichia coli. Mechanism of bactericidal activity," *Journal of Clinical Investigation*, vol. 84, no. 2, pp. 553–561, 1989. DOI: 10.1172/JCI114198.

[121] Y. Huan, Q. Kong, H. Mou, and H. Yi, "Antimicrobial Peptides: Classification, Design, Application and Research Progress in Multiple Fields," *Frontiers in Microbiology*, vol. 11, no. October, pp. 1–21, 2020. DOI: 10.3389/fmicb.2020.582779.

[122] Y. Cho, J. S. Turner, N. N. Dinh, and R. I. Lehrer, "Activity of Protegrins against yeast-phase Candida albicans," *Infection and Immunity*, vol. 66, no. 6, pp. 2486–2493, 1998. DOI: 10.1128/iai.66.6.2486-2493.1998.

[123] D. A. Steinberg, M. A. Hurst, C. A. Fujii, *et al.*, "Protegrin-1: A broad-spectrum, rapidly microbicidal peptide with in vivo activity," *Antimicrobial Agents and Chemotherapy*, vol. 41, no. 8, pp. 1738–1742, 1997. DOI: 10.1128/aac.41.8.1738.

[124] K. T. Miyasaki, R. Iofel, A. Oren, T. Huynh, and R. I. Lehrer, "Killing of Fusobacterium nucleatum, Porphyromonas gingivalis and Prevotella intermedia by protegrins," *Journal of Periodontal Research*, vol. 33, no. 2, pp. 91–98, 1998. DOI: 10.1111/j.1600-0765.1998.tb02297.x.

[125] S. B. Willingham, J.-P. Volkmer, A. J. Gentles, *et al.*, "The CD47-signal regulatory protein alpha (SIRPa) interaction is a therapeutic target for human solid tumors," *Proceedings of the National Academy of Sciences*, vol. 109, no. 17, pp. 6662–6667, 2012. DOI: 10.1073/pnas.1121623109.

[126] T. D. Madigan, Michael T; Martinko, John M; Brock, *Biology of Microorganisms*, 11th ed. 2006, pp. 12 345 678–12 345 678.

[127] R. E. Hancock and D. S. Chapple, *Peptide antibiotics*, 1999. DOI: 10.1128/aac.43.6.1317.

[128] R. I. Lehrer, G. Jung, P. Ruchala, S. Andre, H. J. Gabius, and W. Lu, "Multivalent Binding of Carbohydrates by the Human alpha-Defensin, HD5," *The Journal of Immunology*, vol. 183, no. 1, pp. 480–490, 2009. DOI: 10.4049/jimmunol.0900244.

[129] R. I. Lehrer, "Primate defensins," *Nature Reviews Microbiology*, vol. 2, no. 9, pp. 727–738, 2004. DOI: 10.1038/nrmicro976.

[130] S. L and M. C, "The Role of Antimicrobial Peptides in Lung Cancer Therapy," *Journal of Antimicrobial Agents*, vol. 03, no. 01, pp. 1–6, 2017. DOI: 10.4172/2472-1212.1000134.

[131] M. A. Lemmon, "Membrane recognition by phospholipid-binding domains," *Nature Reviews Molecular Cell Biology*, vol. 9, no. 2, pp. 99–111, 2008. DOI: 10.1038/nrm2328.

[132] B. Sharma and S. S. Kanwar, "Phosphatidylserine: A cancer cell targeting biomarker," *Seminars in Cancer Biology*, vol. 52, no. August 2017, pp. 17–25, 2018. DOI: 10.1016/j.semcancer.2017.08.012.

[133] X. Qi, Z. Chu, Y. Y. Mahller, K. F. Stringer, D. P. Witte, and T. P. Cripe, "Cancer-Selective Targeting and Cytotoxicity by Liposomal-Coupled Lysosomal Saposin C Protein," *Clinical Cancer Research*, vol. 15, no. 18, pp. 5840–5851, 2009. DOI: 10.1158/1078-0432.CCR-08-3285.

[134] R. S. Bullard, W. Gibson, S. Bose, *et al.*, "Functional Analysis of the Host Defense Peptide Human Beta Defensin-1: New Insight into Its Potential Role in Cancer," vol. 45, no. 3, pp. 839–848, 2008.

[135] C. Q. Sun, R. Arnold, C. Fernandez-Golarz, *et al.*, "Human beta-Defensin-1, a Potential Chromosome 8p Tumor Suppressor: Control of Transcription and

Induction of Apoptosis in Renal Cell Carcinoma," *Cancer Research*, vol. 66, no. 17, pp. 8542–8549, 2006. DOI: 10.1158/0008-5472.CAN-06-0294.

[136] A. Semlali, A. Al Amri, A. Azzi, *et al.*, "Expression and New Exon Mutations of the Human Beta Defensins and Their Association on Colon Cancer Development," *PLOS ONE*, vol. 10, no. 6, I. A. Chemin, Ed., e0126868, 2015. DOI: 10.1371/journal.pone.0126868.

[137] A. Persidis, "Cancer multidrug resistance," *Nature Biotechnology 1999 17:1*, vol. 17, no. 1, pp. 94–95, 1999. DOI: 10.1038/5289.

[138] J. R. Henriksen, T. Etzerodt, T. Gjetting, and T. L. Andresen, "Side Chain Hydrophobicity Modulates Therapeutic Activity and Membrane Selectivity of Antimicrobial Peptide Mastoparan-X," *PLOS ONE*, vol. 9, no. 3, e91007, 2014. DOI: 10.1371/JOURNAL.PONE.0091007.

[139] J. Thundimadathil, "Cancer Treatment Using Peptides: Current Therapies and Future Prospects," *Journal of Amino Acids*, vol. 2012, pp. 1–13, 2012. DOI: 10.1155/2012/967347.

[140] Y. Lai and R. L. Gallo, *AMPed up immunity: how antimicrobial peptides have multiple roles in immune defense*, 2009. DOI: 10.1016/j.it.2008.12.003.

[141] M. Stigter, J. Bezemer, K. De Groot, and P. Layrolle, "Incorporation of different antibiotics into carbonated hydroxyapatite coatings on titanium implants, release and antibiotic efficacy," *Journal of Controlled Release*, vol. 99, no. 1, pp. 127–137, 2004. DOI: 10.1016/j.jconrel.2004.06.011.

[142] S. Galdiero, A. Falanga, R. Berisio, P. Grieco, G. Morelli, and M. Galdiero, "Antimicrobial Peptides as an Opportunity Against Bacterial Diseases," *Current Medicinal Chemistry*, vol. 22, no. 14, pp. 1665–1677, 2015. DOI: 10.2174/092986732266615031114563 2.

[143] K. C. L. Mulder, L. A. Lima, V. J. Miranda, S. C. Dias, and O. L. Franco, "Current scenario of peptide-based drugs: the key roles of cationic antitumor and antiviral peptides," *Frontiers in Microbiology*, vol. 4, no. October, pp. 1–23, 2013. DOI: 10.3389/fmicb.2013.00321.

[144] M. De, S. Ghosh, T. Sen, *et al.*, "A Novel Therapeutic Strategy for Cancer Using Phosphatidylserine Targeting Stearylamine-Bearing Cationic Liposomes," *Molecular Therapy - Nucleic Acids*, vol. 10, no. March, pp. 9–27, 2018. DOI: 10.1016/j.omtn.2017.10.019.

[145] J. Despanie, J. P. Dhandhukia, S. F. Hamm-Alvarez, and J. A. MacKay, "Elastin-like polypeptides: Therapeutic applications for an emerging class of nanomedicines," *Journal of Controlled Release*, vol. 240, pp. 93–108, 2016. DOI: 10.1016/j.jconrel.2015.11.010.

[146] M. T. Weinstock, J. N. Francis, J. S. Redman, and M. S. Kay, *Protease-resistant peptide design-empowering nature's fragile warriors against HIV*. 2012. DOI: 10.1002/bip.22073.

[147] M. E. Selsted, M. J. Novotny, W. L. Morris, Y. Q. Tang, W. Smith, and J. S. Cullor, "Indolicidin, a novel bactericidal tridecapeptide amide from neutrophils," *Journal of Biological Chemistry*, vol. 267, no. 7, pp. 4292–4295, 1992.

[148] E. F. Haney and R. E. W. Hancock, "Peptide design for antimicrobial and immunomodulatory applications," *Biopolymers*, vol. 100, no. 6, pp. 572–583, 2013. DOI: 10.1002/bip.22250.

[149] W. F., O. N., and O. L., "Prediction and Rational Design of Antimicrobial Peptides," in *Protein Structure*, InTech, 2012. DOI: 10.5772/38023.

[150] J. B. O. Mitchell, "Machine learning methods in chemoinformatics," *WIREs Computational Molecular Science*, vol. 4, no. 5, pp. 468–481, 2014. DOI: 10.1002/wcms.1183.

[151] V. Kumar, P. Agrawal, R. Kumar, *et al.*, "Prediction of Cell-Penetrating Potential of Modified Peptides Containing Natural and Chemically Modified Residues," *Frontiers in Microbiology*, vol. 9, no. APR, pp. 1–10, 2018. DOI: 10.3389/fmicb.2018.00725.

[152] F. Plisson, O. Ramírez-Sánchez, and C. Martínez-Hernández, "Machine learning-guided discovery and design of non-hemolytic peptides," *Scientific Reports*, vol. 10, no. 1, pp. 1–19, 2020. DOI: 10.1038/s41598-020-73644-6.

[153] S. Lata, B. K. B. Sharma, and G. P. Raghava, "Analysis and prediction of antibacterial peptides," *BMC Bioinformatics*, vol. 8, no. 1, pp. 1–10, 2007. DOI: 10.1186/1471-2105-8-263.

[154] R. Saravanan, X. Li, K. Lim, *et al.*, "Design of short membrane selective antimicrobial peptides containing tryptophan and arginine residues for improved activity, salt-resistance, and biocompatibility," *Biotechnology and Bioengineering*, vol. 111, no. 1, pp. 37–49, 2014. DOI: 10.1002/bit.25003.

[155] G. Wang, X. Li, and Z. Wang, "APD3: the antimicrobial peptide database as a tool for research and education," *Nucleic Acids Research*, vol. 44, no. D1, pp. D1087–D1093, 2016. DOI: 10.1093/NAR/GKV1278.

[156] G. Shi, X. Kang, F. Dong, *et al.*, "DRAMP 3.0: an enhanced comprehensive data repository of antimicrobial peptides," *Nucleic Acids Research*, vol. 50, no. D1, pp. D488–D496, 2022. DOI: 10.1093/NAR/GKAB651.

[157] F. H. Waghu, R. S. Barai, P. Gurung, and S. Idicula-Thomas, "CAMPR3: a database on sequences, structures and signatures of antimicrobial peptides," *Nucleic Acids Research*, vol. 44, no. Database issue, p. D1094, 2016. DOI: 10.1093/NAR/GKV1051.

[158] M. Pirtskhalava, A. A. Amstrong, M. Grigolava, *et al.*, "DBAASP v3: database of antimicrobial/cytotoxic activity and structure of peptides as a resource for

development of new therapeutics," *Nucleic Acids Research*, vol. 49, no. D1, p. D288, 2021. DOI: 10.1093/NAR/GKAA991.

[159] M. D. Torres, S. Sothiselvam, T. K. Lu, and C. de la Fuente-Nunez, "Peptide Design Principles for Antimicrobial Applications," *Journal of Molecular Biology*, vol. 431, no. 18, pp. 3547–3567, 2019. DOI: 10.1016/j.jmb.2018.12.015.

[160] D. Kim, J. P. Barraza, R. A. Arthur, *et al.*, "Spatial mapping of polymicrobial communities reveals a precise biogeography associated with human dental caries," *Proceedings of the National Academy of Sciences of the United States of America*, vol. 117, no. 22, pp. 1–12, 2020. DOI: 10.1073/pnas.1919099117.

[161] K. Bazaka, M. V. Jacob, W. Chrzanowski, and K. Ostrikov, "Anti-bacterial surfaces: natural agents, mechanisms of action, and plasma surface modification," *RSC Advances*, vol. 5, no. 60, pp. 48 739–48 759, 2015. DOI: 10.1039/C4RA17244B.

[162] B. ter Horst, G. Chouhan, N. S. Moiemen, and L. M. Grover, *Advances in keratinocyte delivery in burn wound care*, 2018. DOI: 10.1016/j.addr.2017.06.012.

[163] D. K. Rai and S. Qian, "Interaction of the Antimicrobial Peptide Aurein 1.2 and Charged Lipid Bilayer," *Scientific Reports*, vol. 7, no. 1, p. 3719, 2017. DOI: 10.1038/s41598-017-03795-6.

[164] R. Tesse, F. Cardinale, T. Santostasi, *et al.*, "Association of beta-defensin-1 gene polymorphisms with Pseudomonas aeruginosa airway colonization in cystic fibrosis," *Genes and Immunity*, vol. 9, no. 1, pp. 57–60, 2008. DOI: 10.1038/sj.gene.6364440.

[165] K. Xiong, X. Chen, H. Hu, H. Hou, P. Gao, and L. Zou, "Antimicrobial Effect of a Peptide Containing Novel Oral Spray on Streptococcus mutans," *BioMed Research International*, vol. 2020, pp. 1–13, 2020. DOI: 10.1155/2020/6853652.

[166] K.-H. Grellmann Waltham, D. F. Elliott, G. P. Lewis, *et al.*, "Solid Phase Peptide Synthesis. II. The Synthesis of Bradykinin," vol. 6, no. 3, p. 5, 1961.

[167] O. F. Luna, J. Gomez, C. Cárdenas, F. Albericio, S. H. Marshall, and F. Guzmán, "Deprotection reagents in Fmoc solid phase peptide synthesis: Moving away from piperidine?" *Molecules*, vol. 21, no. 11, p. 1542, 2016. DOI: 10.3390/molecules21111542.

[168] M. SCHNölzer, P. ALEWOOD, A. JONES, D. ALEWOOD, and S. B. KENT, "In situ neutralization in Boc-chemistry solid phase peptide synthesis," *International Journal of Peptide and Protein Research*, vol. 40, no. 3-4, pp. 180–193, 2010. DOI: 10.1111/j.1399-3011.1992.tb00291.x.

[169] B. Information, "Overview of Solid-Phase Peptide Synthesis (SPPS) and Secondary Structure Determination by FTIR Introduction," 1960.

[170] R. Subir-Funosas, R. R. Prohens, R. Barbas, *et al.*, "Oxyma: An Efficient Additive for Peptide Synthesis to Replace the Benzotriazole-Based HOBt and HOAt with a Lower Risk of Explosion," *Chemistry - A European Journal*, vol. 15, no. 37, pp. 9394–9403, 2009. DOI: 10.1002/chem.200900614.

[171] S. R. Manne, A. Sharma, A. Sazonovas, A. El-Faham, B. G. de la Torre, and F. Albericio, "Understanding OxymaPure as a Peptide Coupling Additive: A Guide to New Oxyma Derivatives," *ACS Omega*, vol. 7, no. 7, pp. 6007–6023, 2022. DOI: 10.1021/acsomega.1c06342.

[172] M. Erny, M. Lundqvist, J. H. Rasmussen, O. Ludemann-Hombourger, F. Bihel, and J. Pawlas, "Minimizing HCN in DIC/Oxyma-Mediated Amide Bond-Forming Reactions," *Organic Process Research and Development*, vol. 24, no. 7, pp. 1341–1349, 2020. DOI: 10.1021/acs.oprd.0c00227.

[173] A. El-Faham and F. Albericio, "Peptide Coupling Reagents, More than a Letter Soup," *Chemical Reviews*, vol. 111, no. 11, pp. 6557–6602, 2011. DOI: 10.1021/cr100048w.

[174] D. A. T. Pires, M. P. Bemquerer, and C. J. do Nascimento, "Some Mechanistic Aspects on Fmoc Solid Phase Peptide Synthesis," *International Journal of Peptide Research and Therapeutics*, vol. 20, no. 1, pp. 53–69, 2014. DOI: 10.1007/s10989-013-9366-8.

[175] Protein technologies Inc, "Introduction to Fmoc Solid Phase Peptide Synthesis," pp. 1–6, 2006.

[176] V. Vergote, C. Burvenich, C. Van de Wiele, and B. De Spiegeleer, "Quality specifications for peptide drugs: a regulatory-pharmaceutical approach," *Journal of Peptide Science*, vol. 15, no. 11, pp. 697–710, 2009. DOI: 10.1002/psc.1167.

[177] M. W. Duncan, D. Nedelkov, R. Walsh, and S. J. Hattan, *Applications of MALDI mass spectrometry in clinical chemistry*, 2016. DOI: 10.1373/clinchem.2015.239491.

[178] A. J. Miles and B. A. Wallace, *Circular dichroism spectroscopy of membrane proteins*, 2016. DOI: 10.1039/c5cs00084j.

[179] A. Rodger, "Circular Dichroism Spectroscopy: Units," in *Encyclopedia of Biophysics*, 2013, pp. 316–317. DOI: 10.1007/978-3-642-16712-6_647.

[180] A. Rodger and D. Marshall, "Beginners guide to circular dichroism," *The Biochemist*, vol. 43, no. 2, pp. 58–64, 2021. DOI: 10.1042/bio_2020_105.

[181] L. Whitmore and B. A. Wallace, "Protein secondary structure analyses from circular dichroism spectroscopy: Methods and reference databases," *Biopolymers*, vol. 89, no. 5, pp. 392–400, 2008. DOI: 10.1002/bip.20853.

[182] L. Otvos, *Peptide-Based Drug Design: Preface*. 2008, vol. 494.

[183] L. Bush, *Escherichia coli Infections - Infections - MSD Manual Consumer Version*, 2020.

[184] Larry M. Bush, *Staphylococcus aureus Infections - Infections - MSD Manual Consumer Version*, 2019.

[185] N. Valdez, C. Hughes, S. O. Palmer, *et al.*, "Rational Design of an Antimicrobial Peptide Based on Structural Insight into the Interaction of Pseudomonas aeruginosa Initiation Factor 1 with Its Cognate 30S Ribosomal Subunit," *ACS Infectious Diseases*, vol. 7, no. 12, pp. 3161–3167, 2021. DOI: 10.1021/acsinfecdis.1c00256.

[186] P. J. Baudry-Simner, A. Singh, J. A. Karlowsky, D. J. Hoban, G. G. Zhanel, and Canadian Antimicrobial Resistance Alliance, "Mechanisms of Reduced Susceptibility to Ciprofloxacin in Escherichia coli Isolates from Canadian Hospitals," *Canadian Journal of Infectious Diseases and Medical Microbiology*, vol. 23, no. 3, e60–e64, 2012. DOI: 10.1155/2012/569093.

[187] Y. W. Lin, M. L. Han, J. Zhao, *et al.*, "Synergistic combination of polymyxin B and enrofloxacin induced metabolic perturbations in extensive drug-resistant pseudomonas aeruginosa," *Frontiers in Pharmacology*, vol. 10, p. 1146, 2019. DOI: 10.3389/fphar.2019.01146.

[188] V. K. Moses, V. Kandi, and S. K. D. Rao, "Minimum Inhibitory Concentrations of Vancomycin and Daptomycin Against Methicillin-resistant Staphylococcus Aureus Isolated from Various Clinical Specimens: A Study from South India," *Cureus*, vol. 12, no. 1, 2020. DOI: 10.7759/cureus.6749.

[189] D. Terrone, S. L. W. Sang, L. Roudaia, and J. R. Silvius, "Penetratin and Related Cell-Penetrating Cationic Peptides Can Translocate Across Lipid Bilayers in the Presence of a Transbilayer Potential," *Biochemistry*, vol. 42, no. 47, pp. 13 787–13 799, 2003. DOI: 10.1021/bi035293y.

[190] D. GmbH, "Measuring Cell Viability / Cytotoxicity," *Dojindo Molecular Technologies Inc.*, pp. 1–12, 2012.

[191] I. Greco, N. Molchanova, E. Holmedal, *et al.*, "Correlation between hemolytic activity, cytotoxicity and systemic in vivo toxicity of synthetic antimicrobial

peptides," *Scientific Reports*, vol. 10, no. 1, pp. 1–13, 2020. DOI: 10.1038/s41598-020-69995-9.

[192] Y Zhang, *I-TASSER server for protein structure and function prediction*, 2008.

[193] J. Lee, D. S. Patel, J. Ståhle, *et al.*, "CHARMM-GUI Membrane Builder for Complex Biological Membrane Simulations with Glycolipids and Lipoglycans," *Journal of Chemical Theory and Computation*, vol. 15, no. 1, pp. 775–786, 2019. DOI: 10.1021/acs.jctc.8b01066.

[194] C. Gromacs, "Gromacs Gromacs," pp. 1–85,

[195] A. Tsutsumi, N. Javkhlantugs, A. Kira, *et al.*, "Structure and Orientation of Bovine Lactoferrampin in the Mimetic Bacterial Membrane as Revealed by Solid-State NMR and Molecular Dynamics Simulation," *Biophysical Journal*, vol. 103, no. 8, pp. 1735–1743, 2012. DOI: 10.1016/j.bpj.2012.09.010.

[196] A. Benedetto, R. J. Bingham, and P. Ballone, "Structure and dynamics of POPC bilayers in water solutions of room temperature ionic liquids," *The Journal of Chemical Physics*, vol. 142, no. 12, p. 124 706, 2015. DOI: 10.1063/1.4915918.

[197] Antimicrobial Peptide database, *ADP3*.

[198] D. Of antimicrobial activity, S. of peptides, D. Antimicrobial activity, *et al.*, *DBAASP*, 2021.

[199] Collection of Anti-Microbial Peptides, *CAMPr3*, 2015.

[200] X. Feng, S. Jin, M. Wang, *et al.*, "The Critical Role of Tryptophan in the Antimicrobial Activity and Cell Toxicity of the Duck Antimicrobial Peptide DCATH," *Frontiers in Microbiology*, vol. 11, p. 1146, 2020. DOI: 10.3389/fmicb.2020.01146.

[201] EMBL-EBL, *Clustal Omega*.

[202] S. logo Generator and S. logo Generator, *Seq2Logo*.

[203] Zhanglab, "I-TASSER,"

[204] W. Humphrey, A. Dalke, and K. Schulten, "VMD: Visual molecular dynamics," *Journal of Molecular Graphics*, vol. 14, no. 1, pp. 33–38, 1996. DOI: 10.1016/0263-7855(96)00018-5.

[205] K. L. Morrison and G. A. Weiss, "Combinatorial alanine-scanning," *Current Opinion in Chemical Biology*, vol. 5, no. 3, pp. 302–307, 2001. DOI: 10.1016/S1367-5931(00)00206-4.

[206] S. Eustache, J. Leprince, and P. Tufféry, "Progress with peptide scanning to study structure-activity relationships: the implications for drug discovery," *Expert Opinion on Drug Discovery*, vol. 11, no. 8, pp. 771–784, 2016. DOI: 10.1080/17460441.2016.1201058.

[207] Guzmán, Wong, Román, *et al.*, "Identification of Antimicrobial Peptides from the Microalgae Tetraselmis suecica (Kylin) Butcher and Bactericidal Activity Improvement," *Marine Drugs*, vol. 17, no. 8, p. 453, 2019. DOI: 10.3390/md17080453.

[208] C. H. Chen, C. G. Starr, E. Troendle, *et al.*, "Simulation-Guided Rational de Novo Design of a Small Pore-Forming Antimicrobial Peptide," *Journal of the American Chemical Society*, vol. 141, no. 12, pp. 4839–4848, 2019. DOI: 10.1021/jacs.8b11939.

[209] C. R. Rathbone, J. D. Cross, K. V. Brown, C. K. Murray, and J. C. Wenke, "Effect of various concentrations of antibiotics on osteogenic cell viability and activity," *Journal of Orthopaedic Research*, vol. 29, no. 7, pp. 1070–1074, 2011. DOI: 10.1002/jor.21343.

[210] D.-M. Hao, Y.-M. Xu, J.-F. Huang, Y.-B. Huang, Y. Chen, and Y. Liu, "Structure-guided de novo design of α-helical antimicrobial peptide with enhanced specificity," *Pure and Applied Chemistry*, vol. 82, no. 1, pp. 243–257, 2010. DOI: 10.1351/pac-con-09-01-12.

[211] M Schiffer and A. B. Edmundson, "Use of Helical Wheels to Represent the Structures of Proteins and to Identify Segments with Helical Potential," *Biophysical Journal*, vol. 7, no. 2, pp. 121–135, 1967. DOI: 10.1016/S0006-3495(67)86579-2.

[212] S Figueredo, J. R. Mastroianni, K. P. Tai, and A. J. Ouellette, *Expression and purification of recombinant alpha-defensins and alpha-defensin precursors in Escherichia coli.* 2010, vol. 618, pp. 47–60. DOI: 10.1007/978-1-60761-594-1_4.

[213] G. Mancuso, A. Midiri, E. Gerace, and C. Biondo, "Bacterial antibiotic resistance: the most critical pathogens," *Pathogens*, vol. 10, no. 10, 2021. DOI: 10.3390/PATHOGENS10101310/S1.

[214] I. D. Ocampo-Ibáñez, Y. Liscano, S. P. Rivera-Sánchez, *et al.*, "A Novel Cecropin D-Derived Short Cationic Antimicrobial Peptide Exhibits Antibacterial Activity Against Wild-Type and Multidrug-Resistant Strains of Klebsiella pneumoniae and Pseudomonas aeruginosa," *Evolutionary Bioinformatics*, vol. 16, p. 117 693 432 093 626, 2020. DOI: 10.1177/1176934320936266.

[215] L. Wang, D. Fan, W. Chen, and E. M. Terentjev, "Bacterial growth, detachment and cell size control on polyethylene terephthalate surfaces," *Scientific Reports*, vol. 5, no. 1, pp. 1–11, 2015. DOI: 10.1038/srep15159.

[216] M. Cantisani, E. Finamore, E. Mignogna, *et al.*, "Structural Insights into and Activity Analysis of the Antimicrobial Peptide Myxinidin," *Antimicrobial Agents and Chemotherapy*, vol. 58, no. 9, pp. 5280–5290, 2014. DOI: 10.1128/AAC.02395-14.

[217] Y. Yamamoto, S. Tamiya, M. Shibuya, I. Nakase, and Y. Yoshioka, "Peptides with the multibasic cleavage site of the hemagglutinin from highly pathogenic influenza viruses act as cell-penetrating via binding to heparan sulfate and neuropilins," *Biochemical and Biophysical Research Communications*, vol. 512, no. 3, pp. 453–459, 2019. DOI: 10.1016/j.bbrc.2019.03.068.

[218] E. Y. Lee, G. C. Wong, and A. L. Ferguson, "Machine learning-enabled discovery and design of membrane-active peptides," *Bioorganic and Medicinal Chemistry*, vol. 26, no. 10, pp. 2708–2718, 2018. DOI: 10.1016/j.bmc.2017.07.012.

[219] J. Wendler, B. O. Schroeder, D. Ehmann, *et al.*, "proteolytic Degradation of reduced Human Beta Defensin 1 generates a Novel Antibiotic octapeptide," DOI: 10.1038/s41598-019-40216-2.

[220] S. S Usmani, S Bhalla, and G. Raghava, "Prediction of antitubercular peptides from sequence information using ensemble classifier and hybrid featurese io," *Frontiers in Pharmacology*, vol. 9, no. AUG, p. 954, 2018. DOI: 10.3389/fphar.2018.00954.

Appendix One

Characterisation

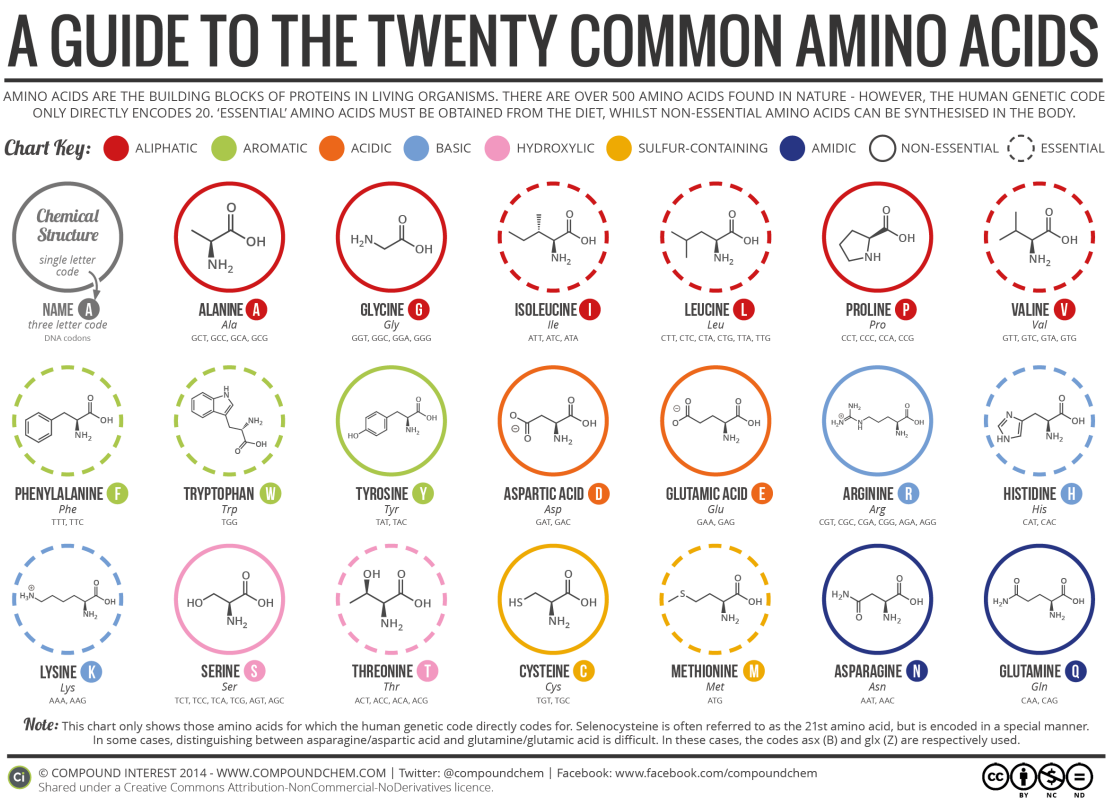


Figure A.1: Amino acids key.
(Web: https://www.compoundchem.com/2014/09/16/aminoacids).

Figures A.2 and A.3 show the blank runs for each LC-MS run made in these experiments. These chromatograms were included for reference purposes and they show the state of the column before the peptide were analysed on them. It also explains the presence of a peak at 45 minutes in all chromatograms which shows this peak was only produced as a result of a dirty column.

Figures 4.1 and 4.2 shows the purity of the peptides based on hBD1 and hBD3 before and after purification. The calculations for the purified peptides used in the experiments in this thesis were done through the use of the numbers generated from performing the LC-MS runs.

Once the peptides were purified these were used for any biological analysis or

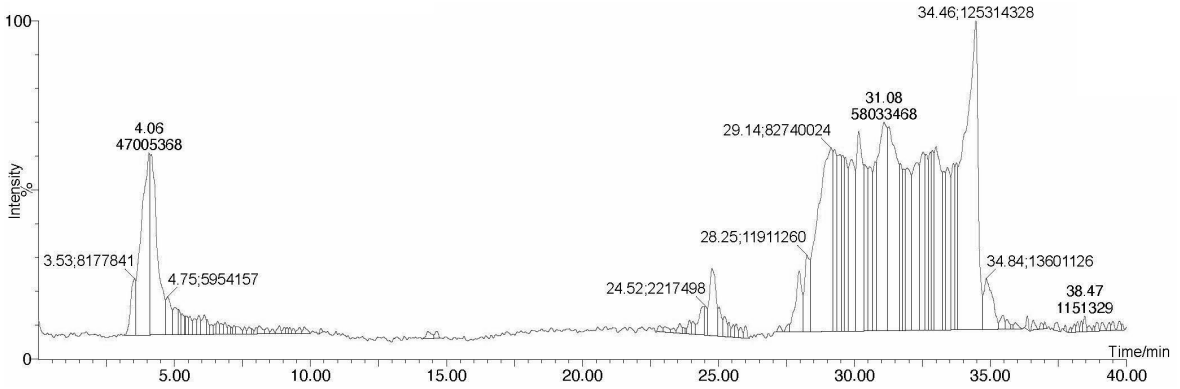


Figure A.2: The blank run for the peptides based on hBD1 and hBD3 on LC-MS.

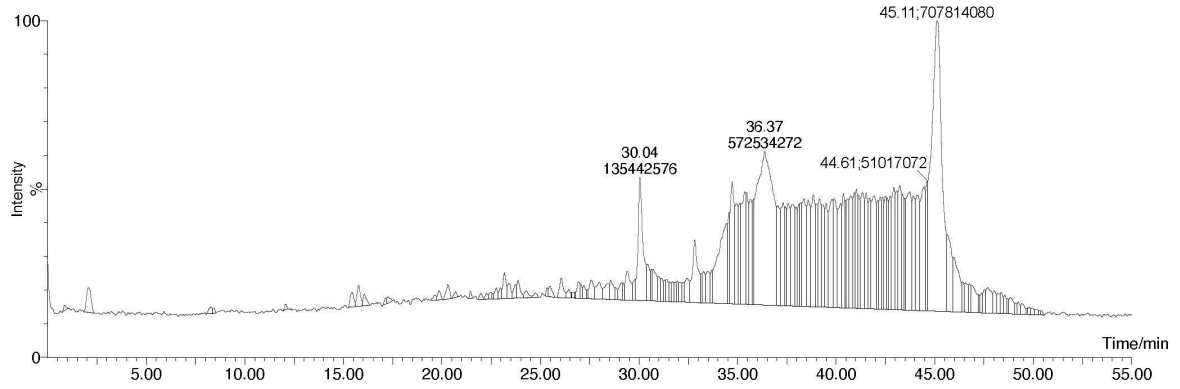


Figure A.3: The blank run for the alanine scan of the peptides based on HBD-mod8 on LC-MS.

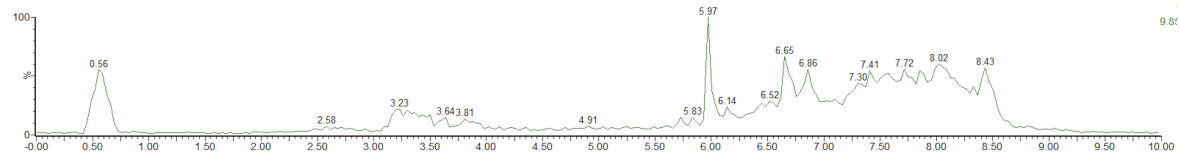
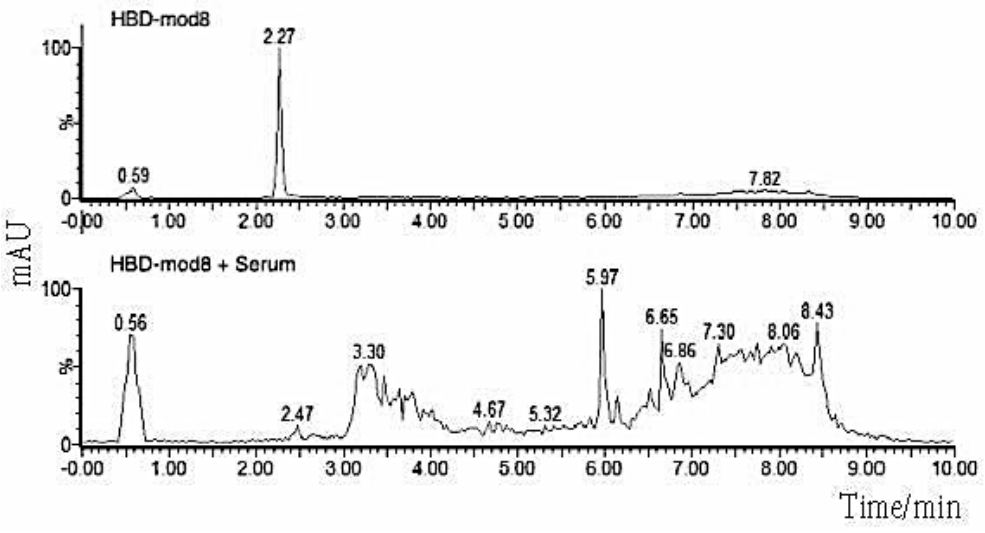


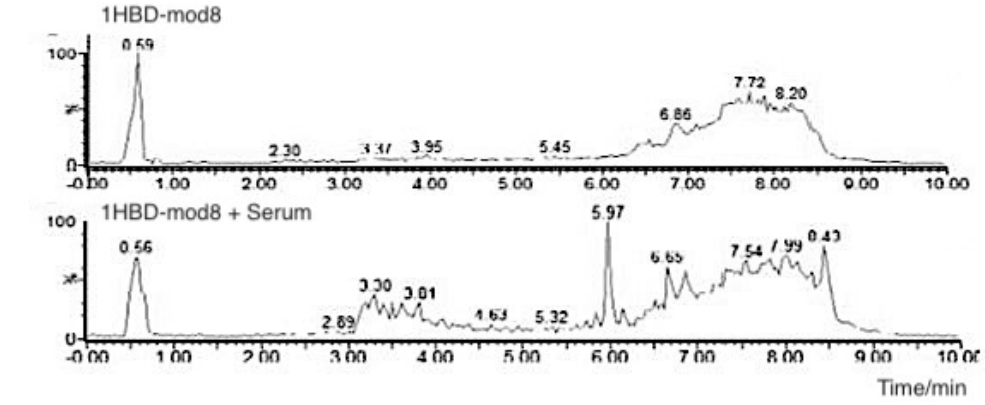
Figure A.4: Serum control

serum and CD analysis. These peptides were then subjected to LC-MS analysis after serum stability studies and the results were confirmed through MALDI-TOF. The results can be found in figure A.6 for MALDI-TOF and with the LC-MS data split between the chromatogams and spectrums shown in figure A.5 and 7.1 respectively

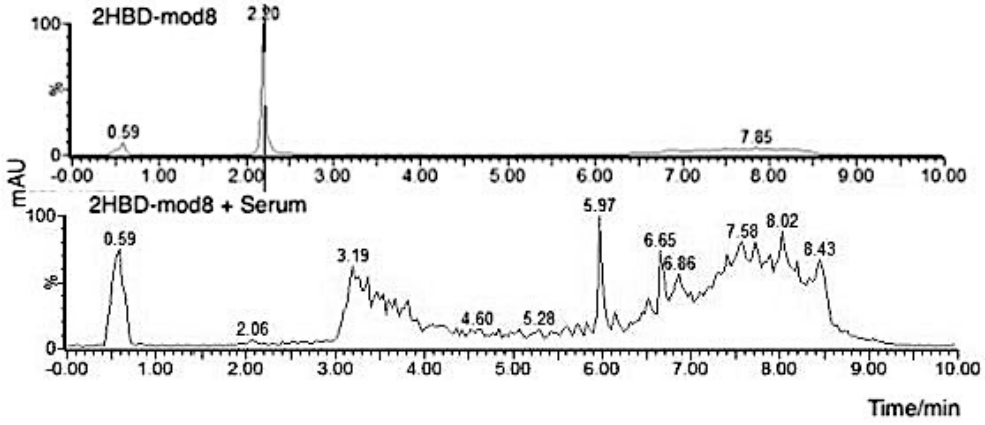
included in section 7.1 due to analysis of fragments done on these spectrum at specific times. The presented mass spectrum in 7.1 is only shown for peaks in the chromatogram that were not present in both peptide before and after serum stability experiments and the time stamp above each spectrum is indicative of the chromatograph peak shown in figure 4.3.



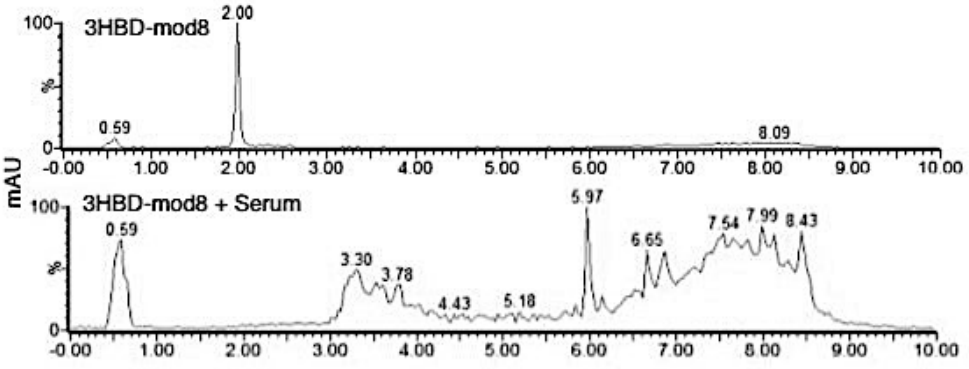
(a) HBD-mod8



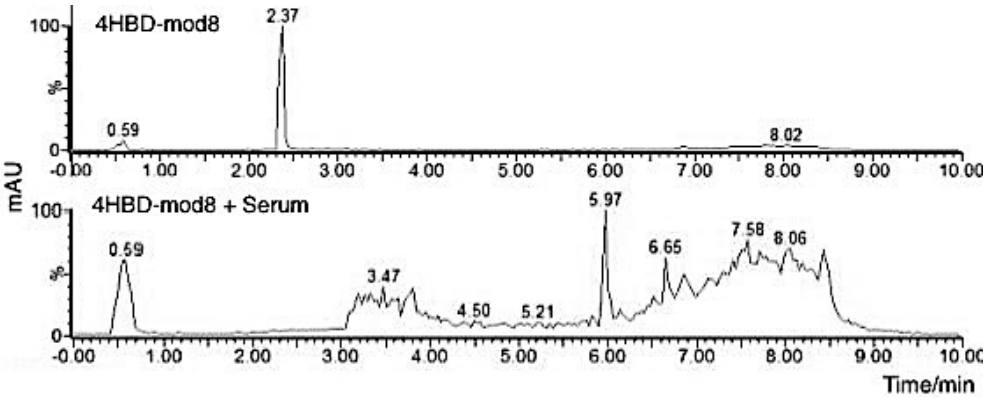
(b) 1HBD-mod8



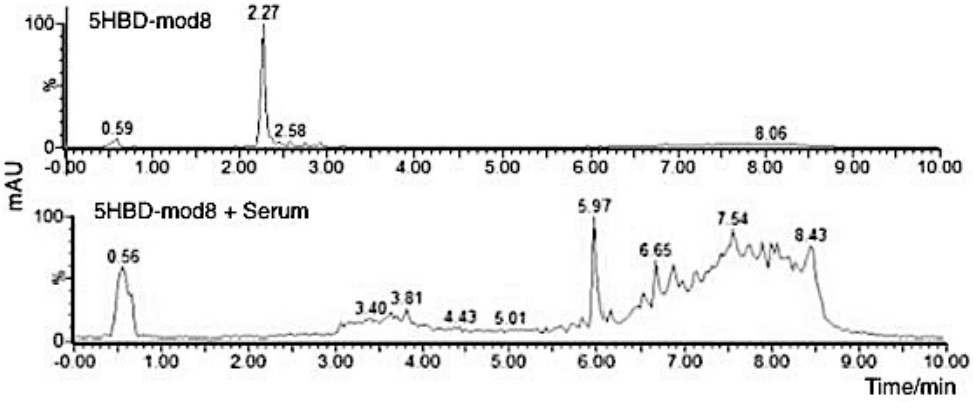
(c) 2HBD-mod8



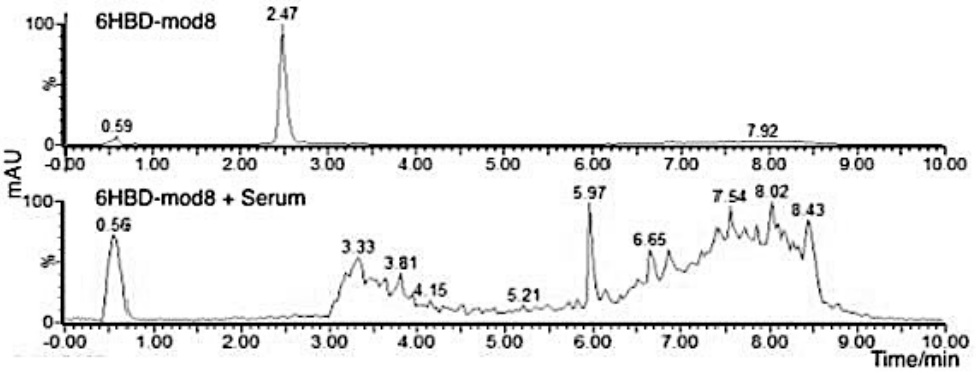
(d) 3HBD-mod8



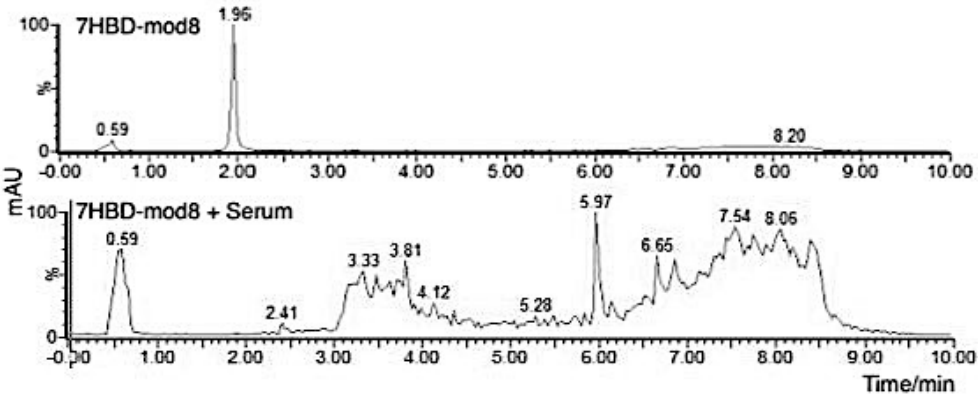
(e) 4HBD-mod8



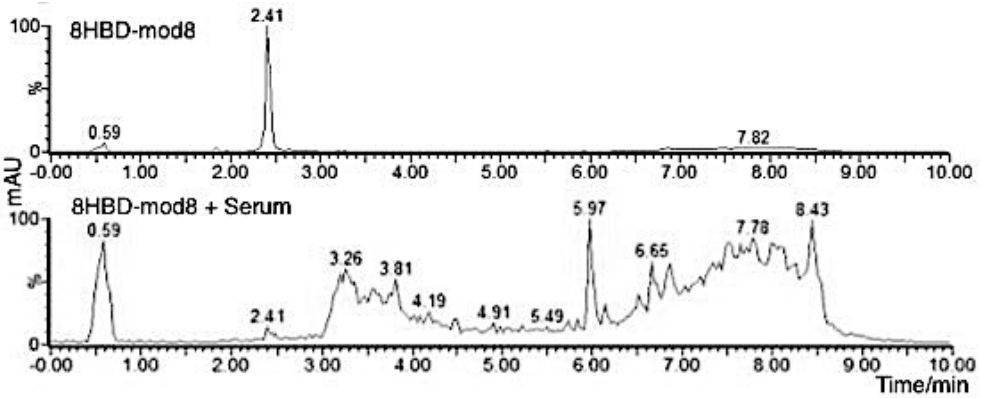
(f) 5HBD-mod8



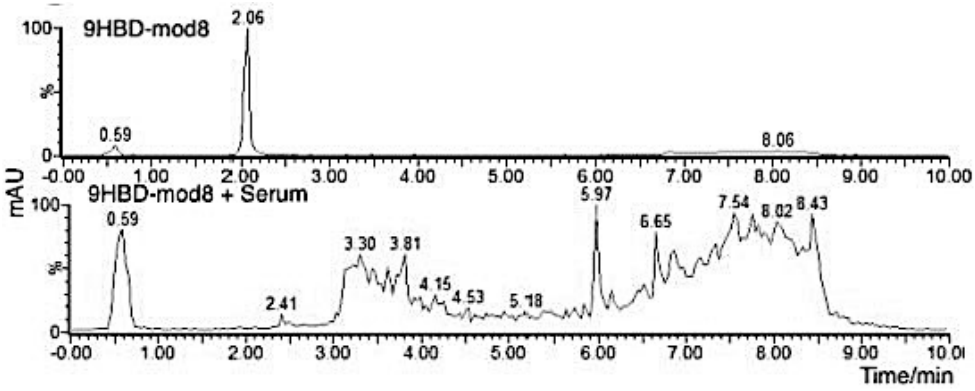
(g) 6HBD-mod8



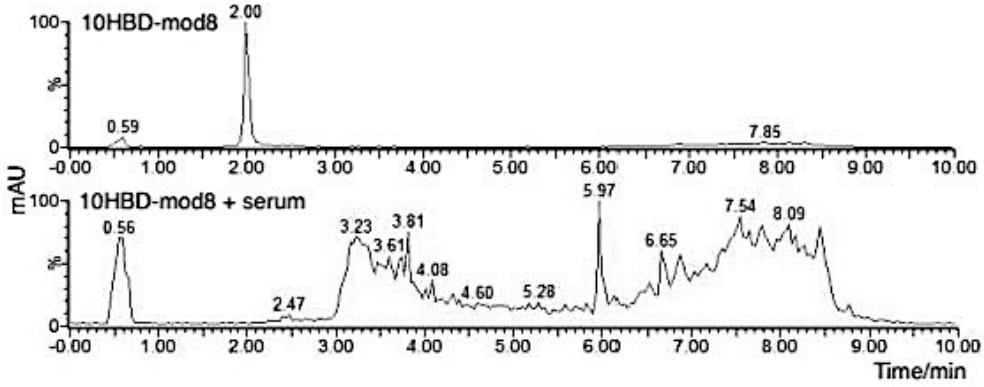
(h) 7HBD-mod8



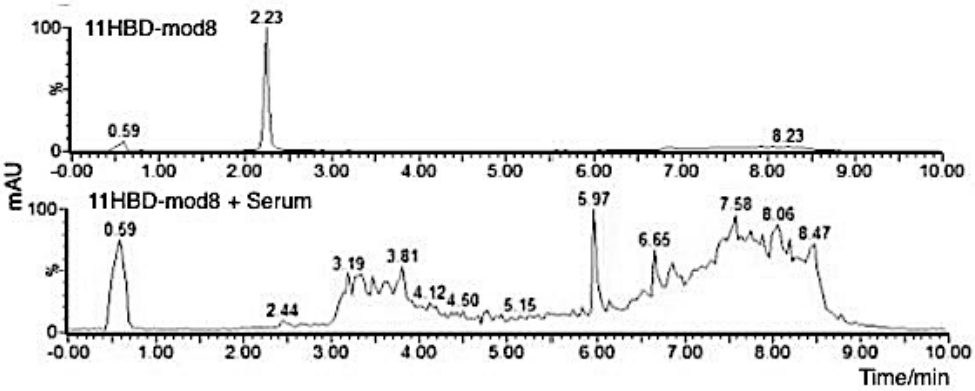
(i) 8HBD-mod8



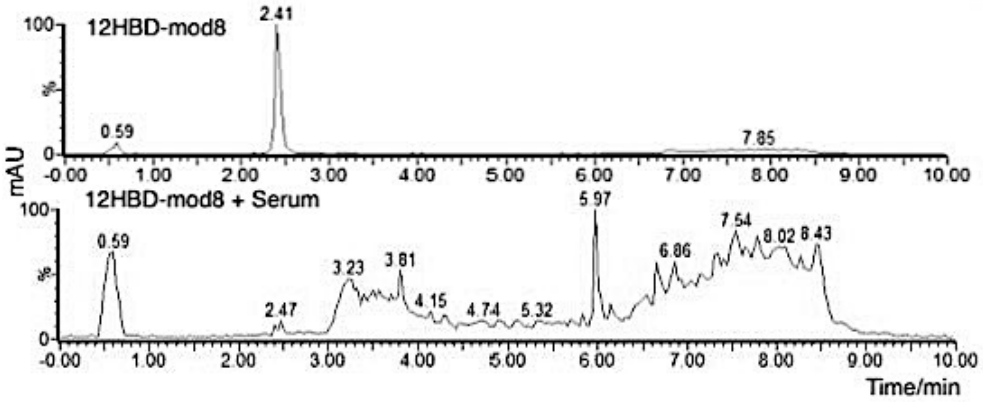
(j) 9HBD-mod8



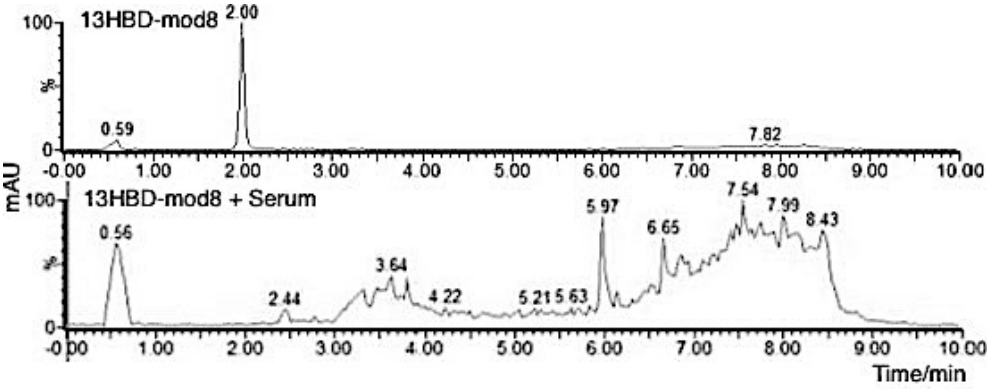
(k) 10HBD-mod8



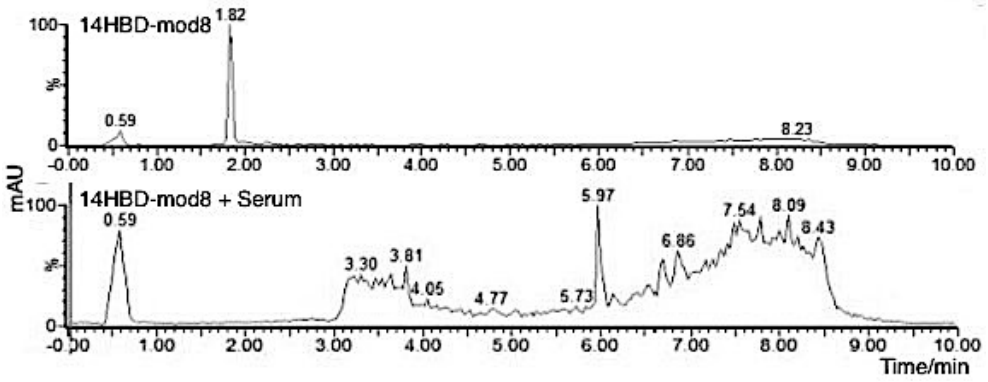
(l) 11HBD-mod8



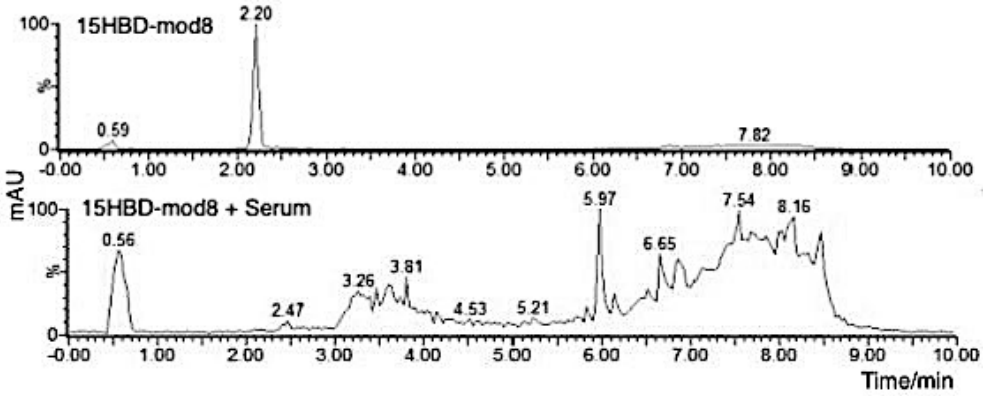
(m) 12HBD-mod8



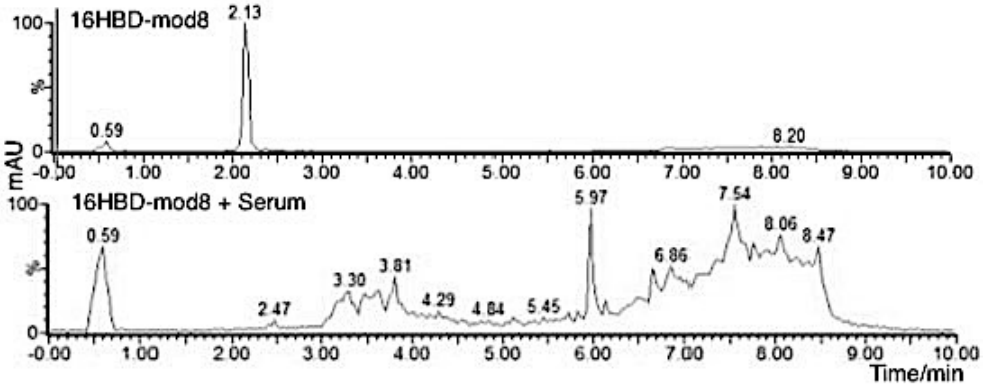
(n) 13HBD-mod8



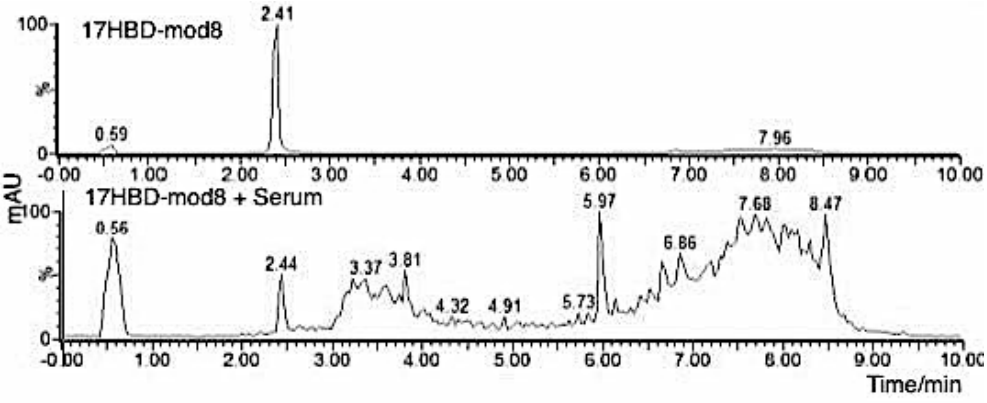
(o) 14HBD-mod8



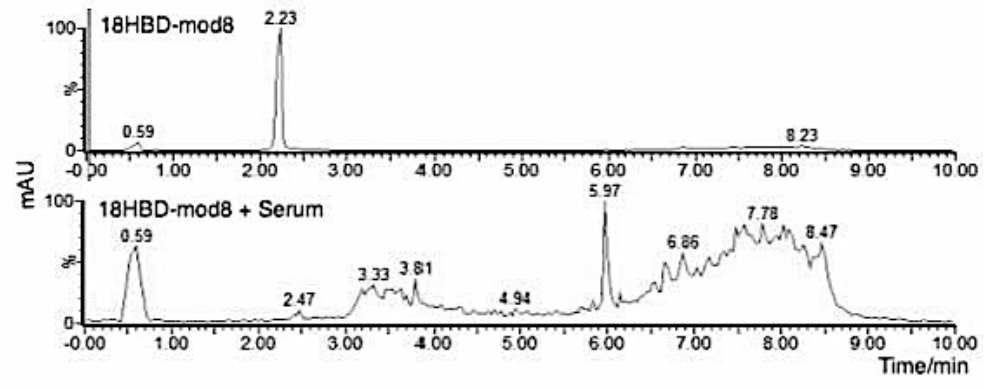
(p) 15HBD-mod8



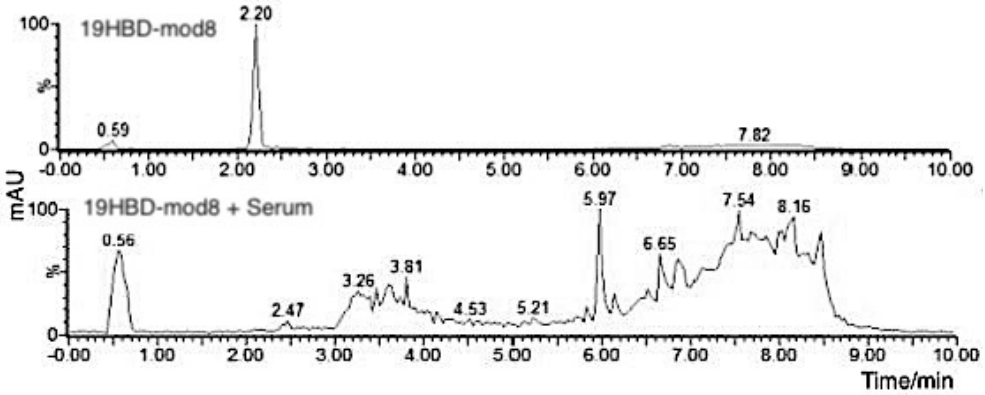
(q) 16HBD-mod8



(r) 17HBD-mod8

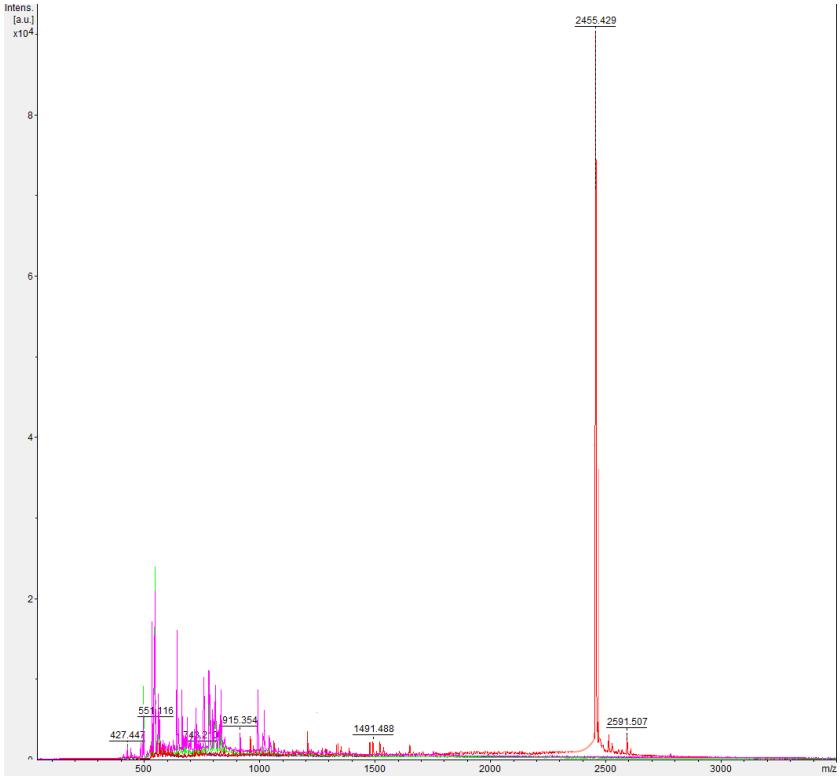


(s) 18HBD-mod8

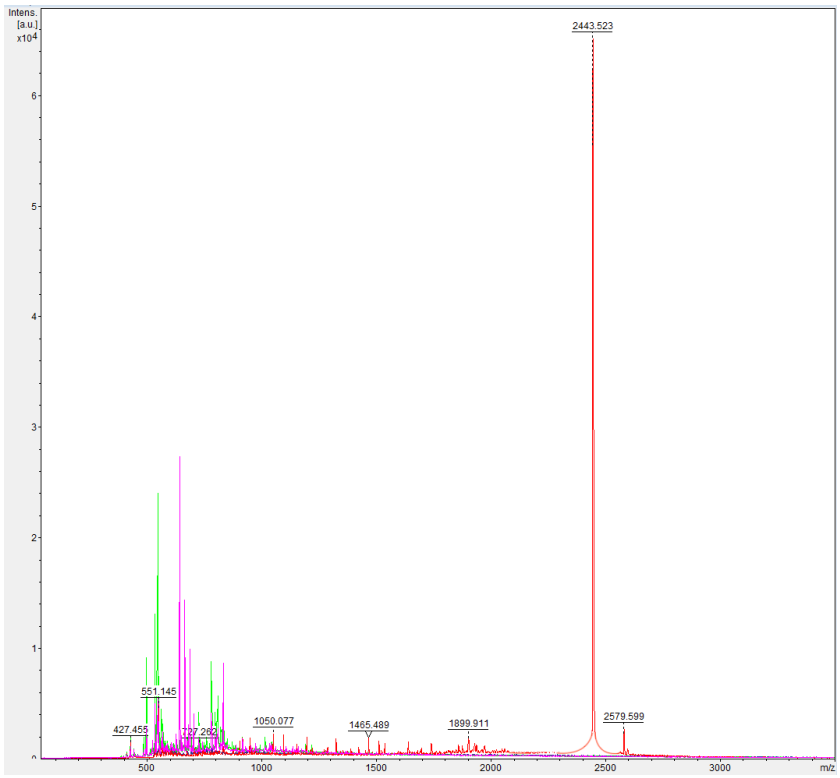


(t) 19HBD-mod8

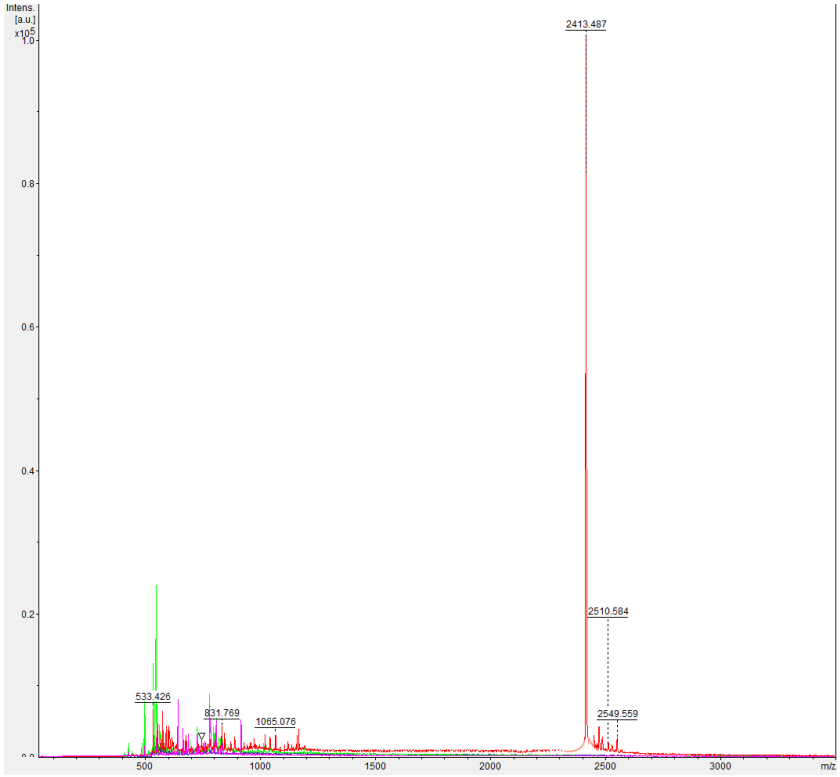
Figure A.5: LC-MS chromatograms of HBD-mod8 and its alanine substituted peptides showing differences between the peptide in serum and peptide in water. it can be seen that some peptides in these series do not show a difference in peak compared to the control but it is clear that for most of these chromatograms the peptide in question is degraded and the spectrum data shown in section7.1 is indicative of these discrepancies.



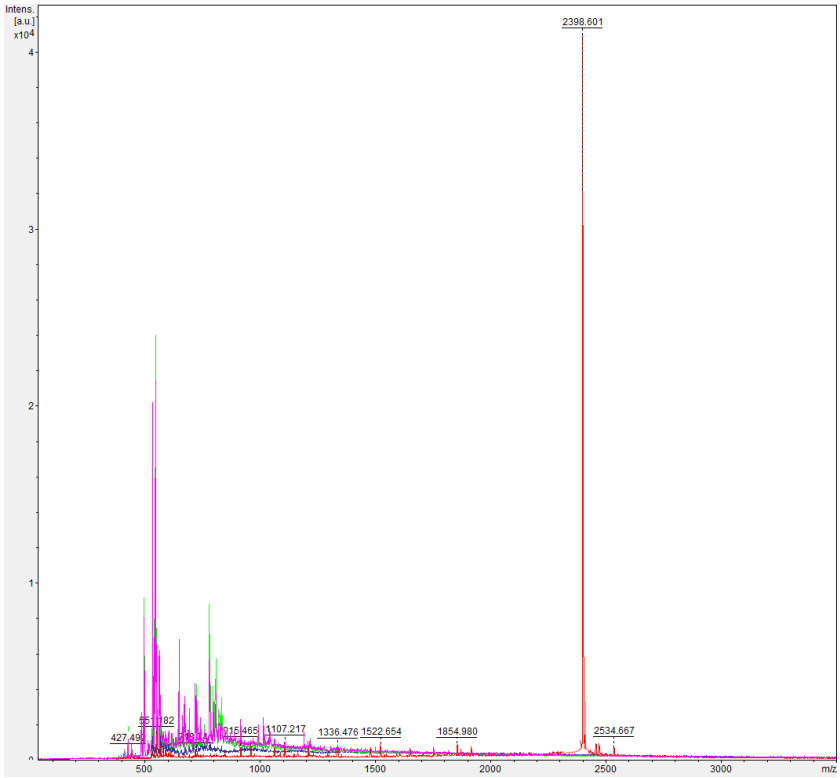
(a) Mass spectrum of the highest chromatographic peak of HBD-mod8 in Serum



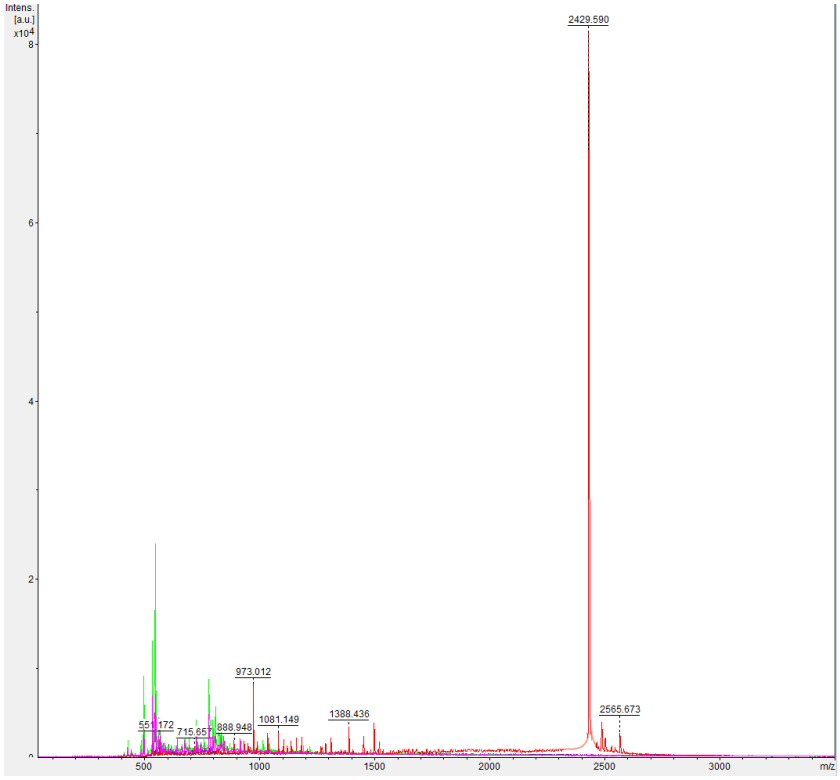
(b) Mass spectrum of the highest chromatographic peak of 1HBD-mod8 in Serum



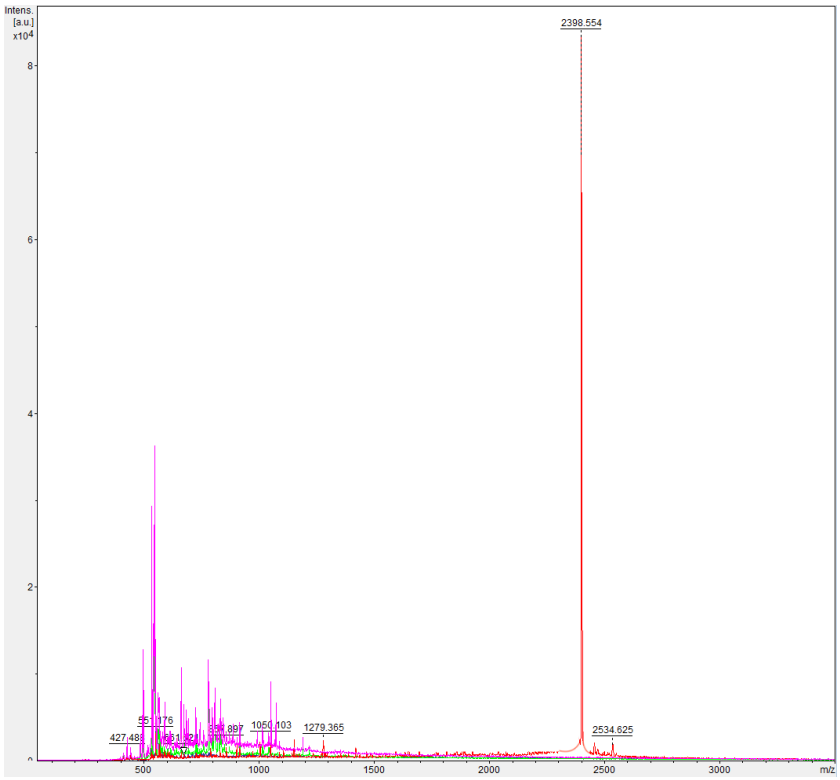
(c) Mass spectrum of the chromatographic peak of 2HBD-mod8 in Serum



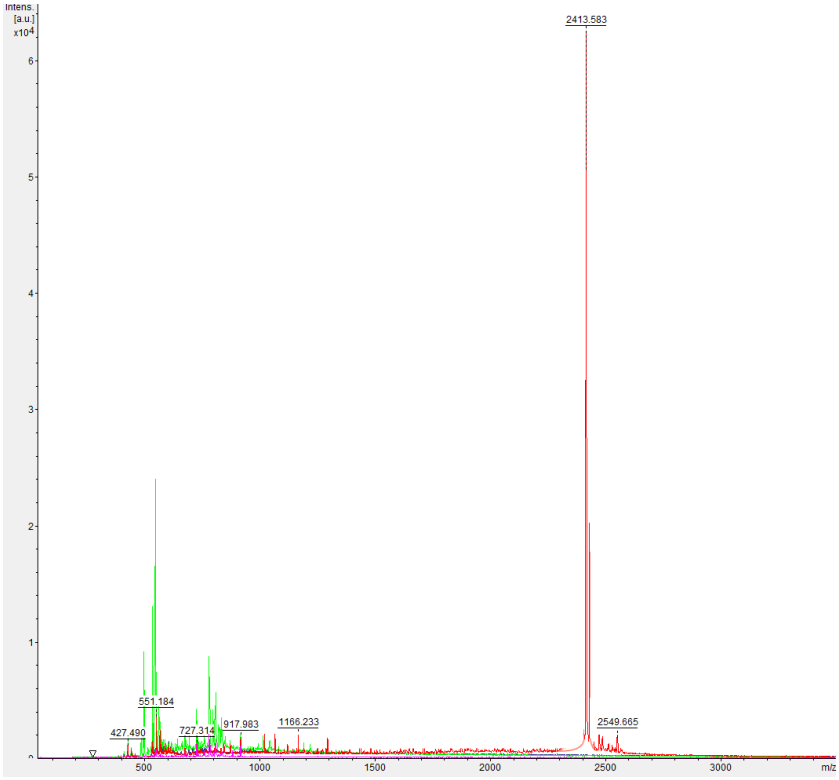
(d) Mass spectrum of the chromatographic peak of 3HBD-mod8 in Serum



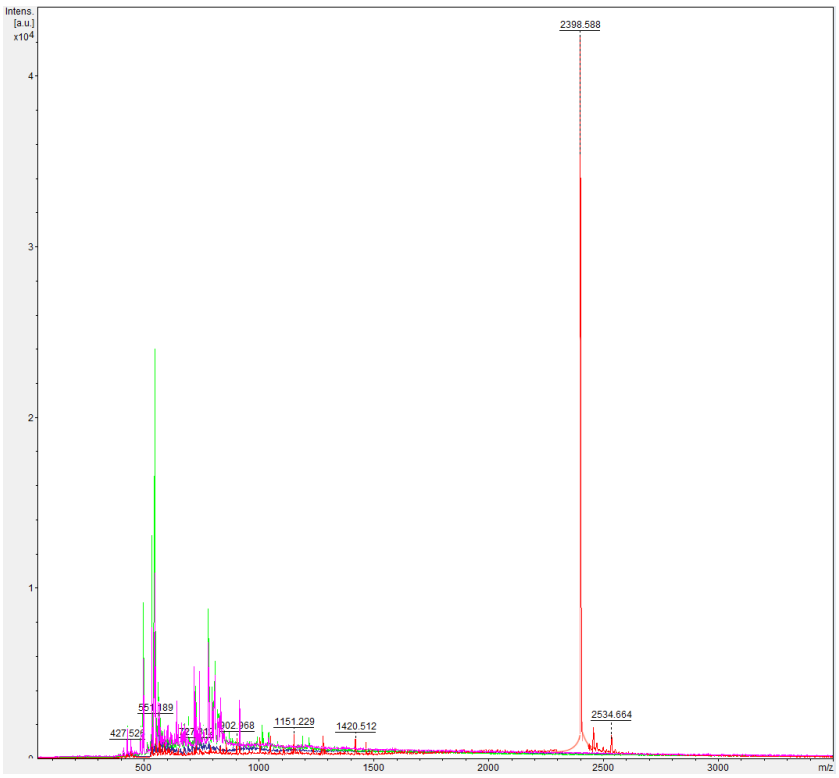
(e) Mass spectrum of the chromatographic peak of 4HBD-mod8 in Serum



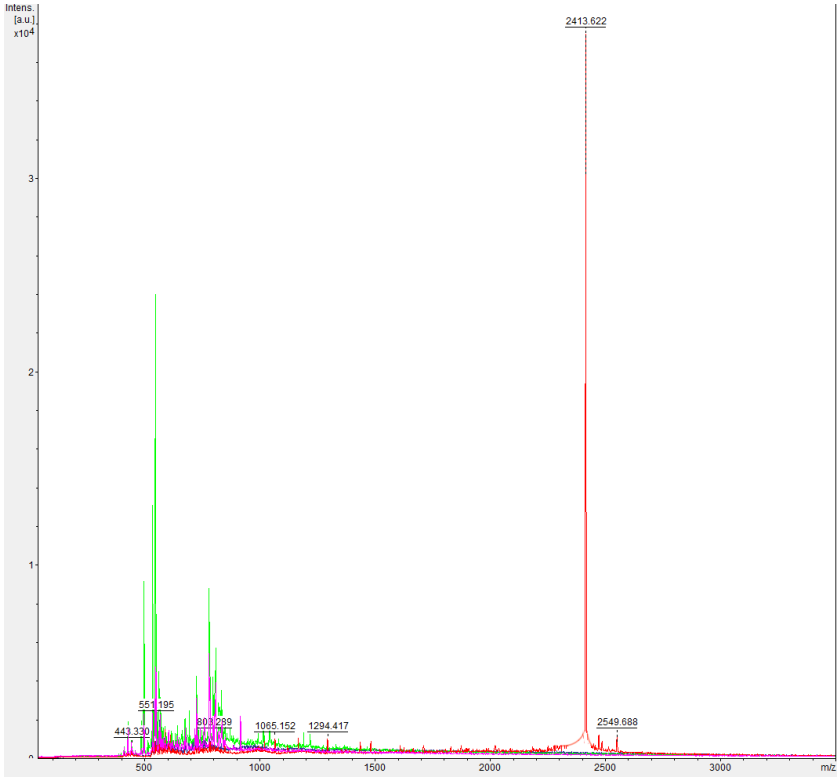
(f) Mass spectrum of the chromatographic peak of 5HBD-mod8 in Serum



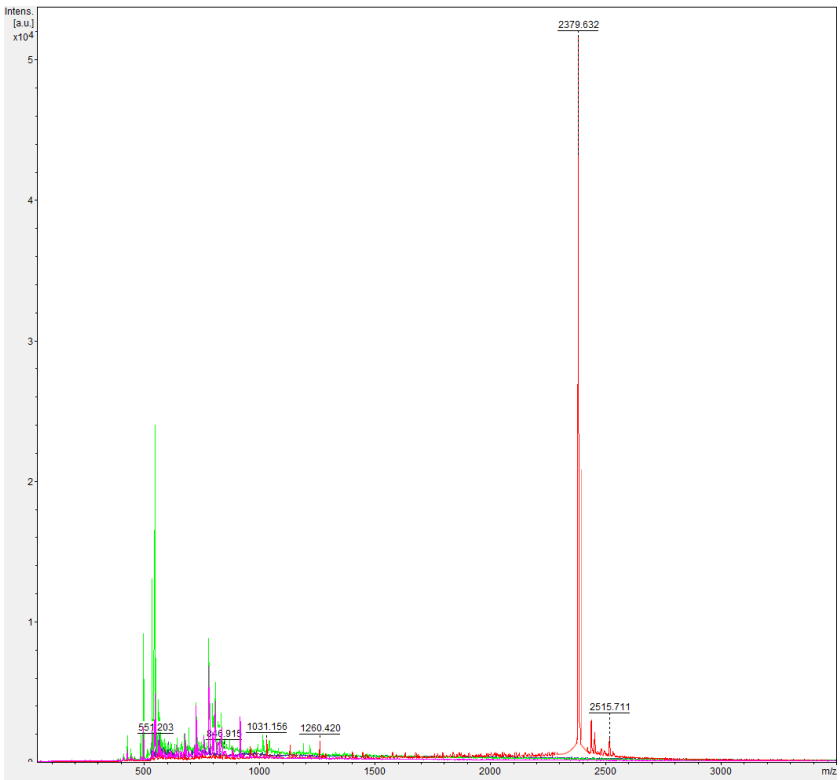
(g) Mass spectrum of the chromatographic peak of 6HBD-mod8 in Serum



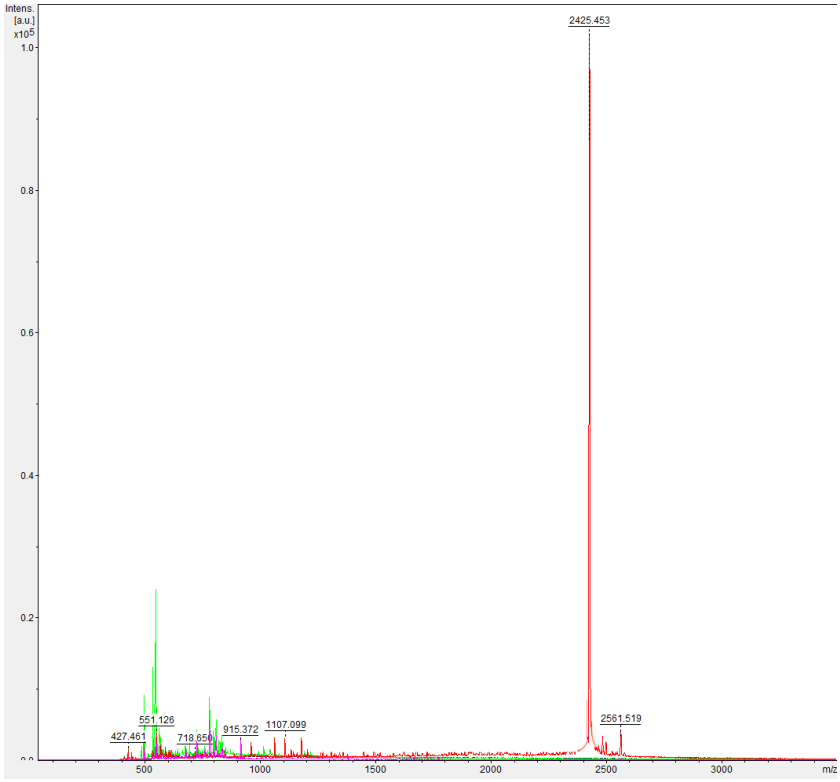
(h) Mass spectrum of the chromatographic peak of 7HBD-mod8 in Serum



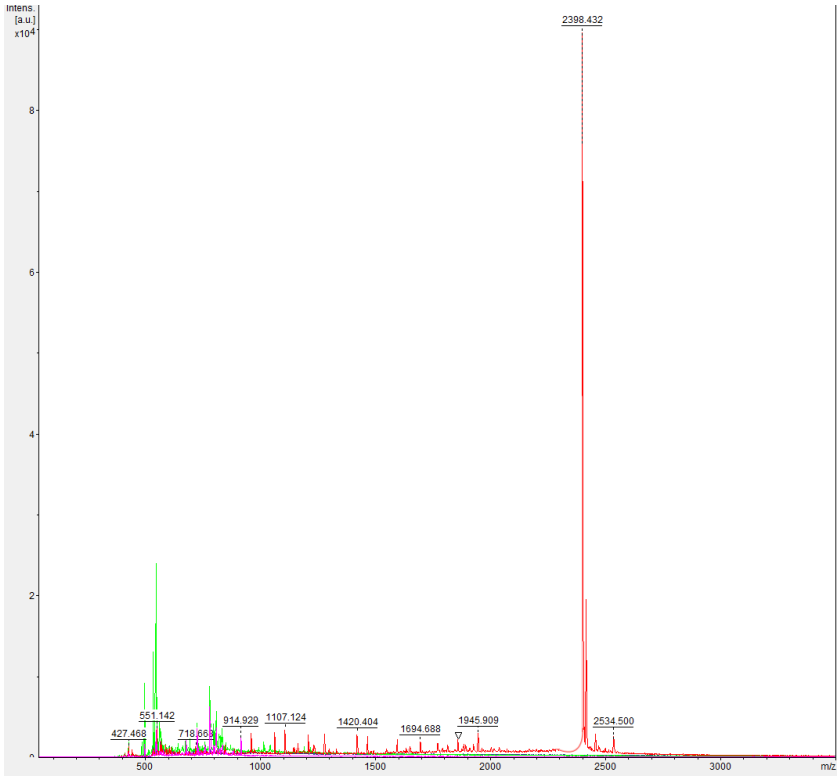
(i) Mass spectrum of the chromatographic peak of 8HBD-mod8 in Serum



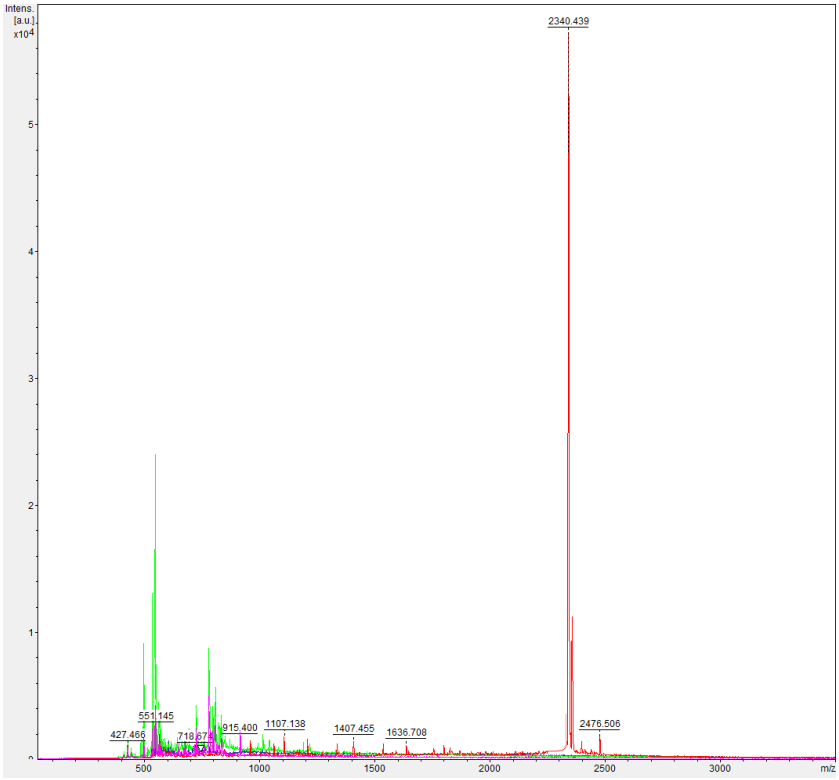
(j) Mass spectrum of the chromatographic peak of 9HBD-mod8 in Serum



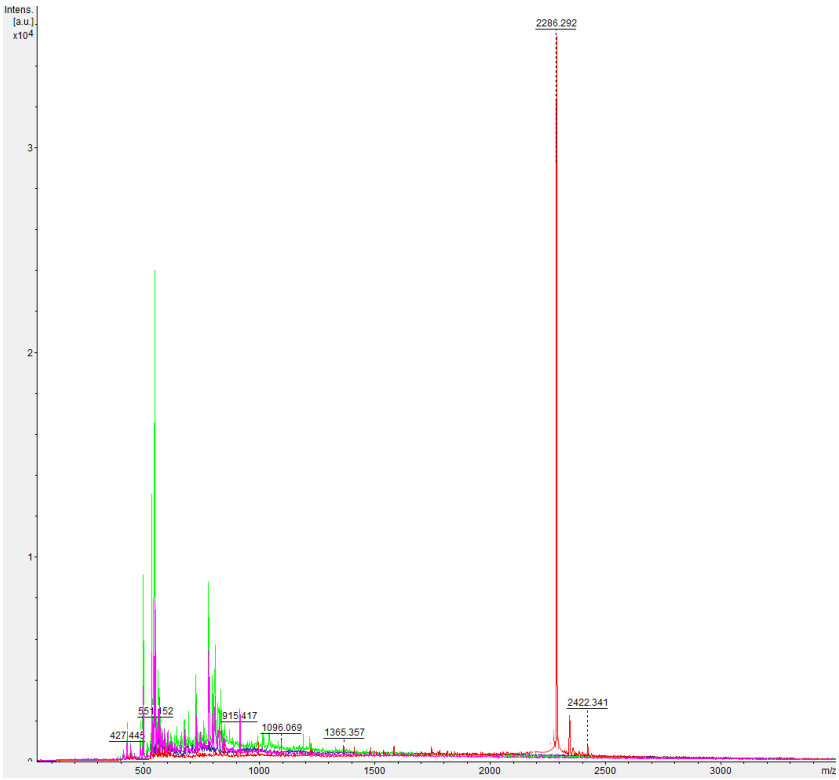
(k) Mass spectrum of the chromatographic peak of 10HBD-mod8 in Serum



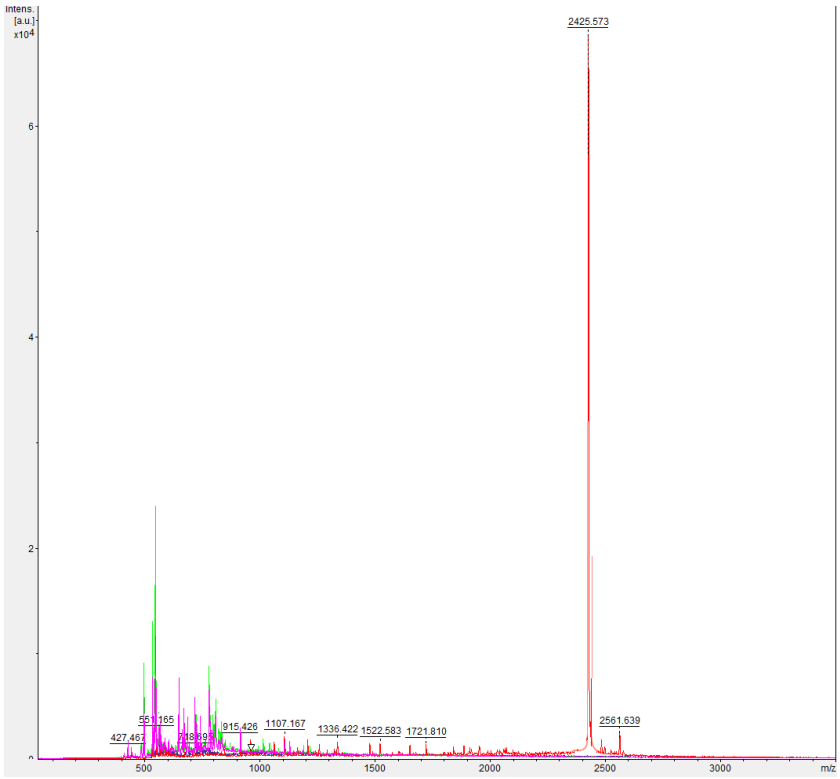
(l) Mass spectrum of the chromatographic peak of 11HBD-mod8 in Serum



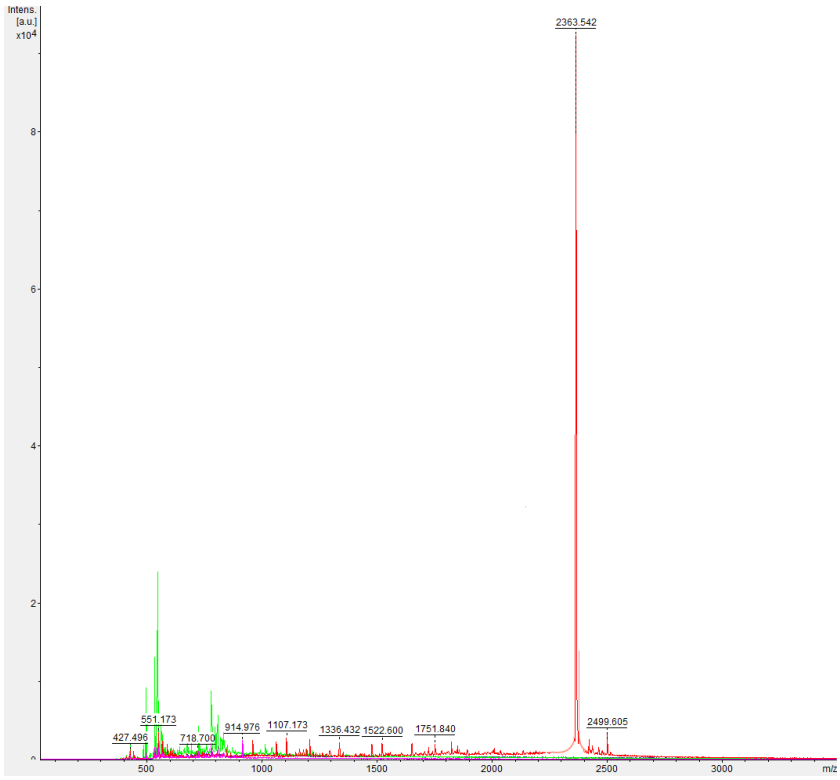
(m) Mass spectrum of the chromatographic peak of 12HBD-mod8 in Serum



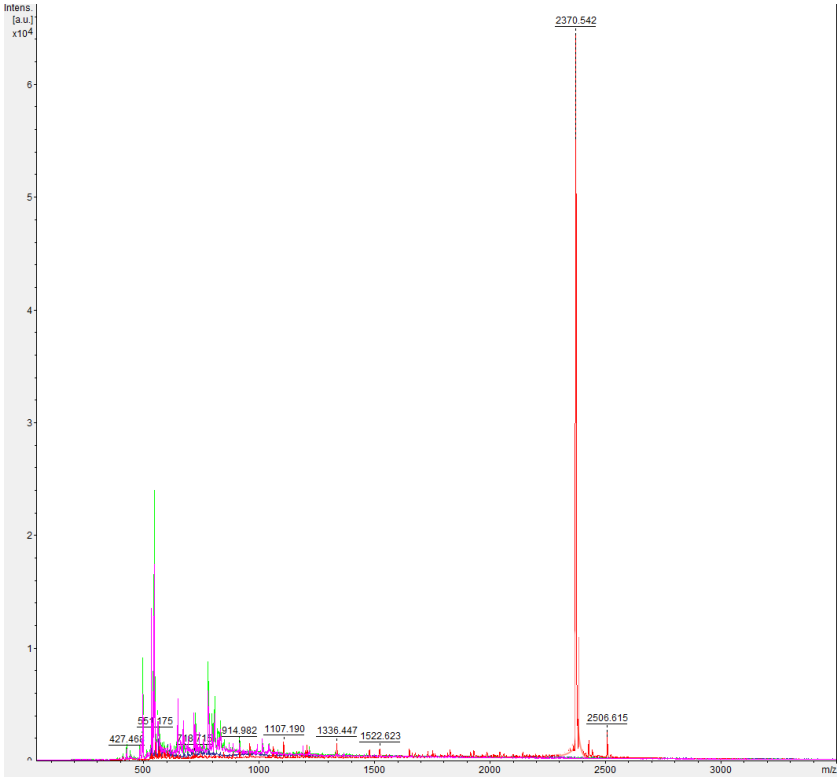
(n) Mass spectrum of the chromatographic peak of 13HBD-mod8 in Serum



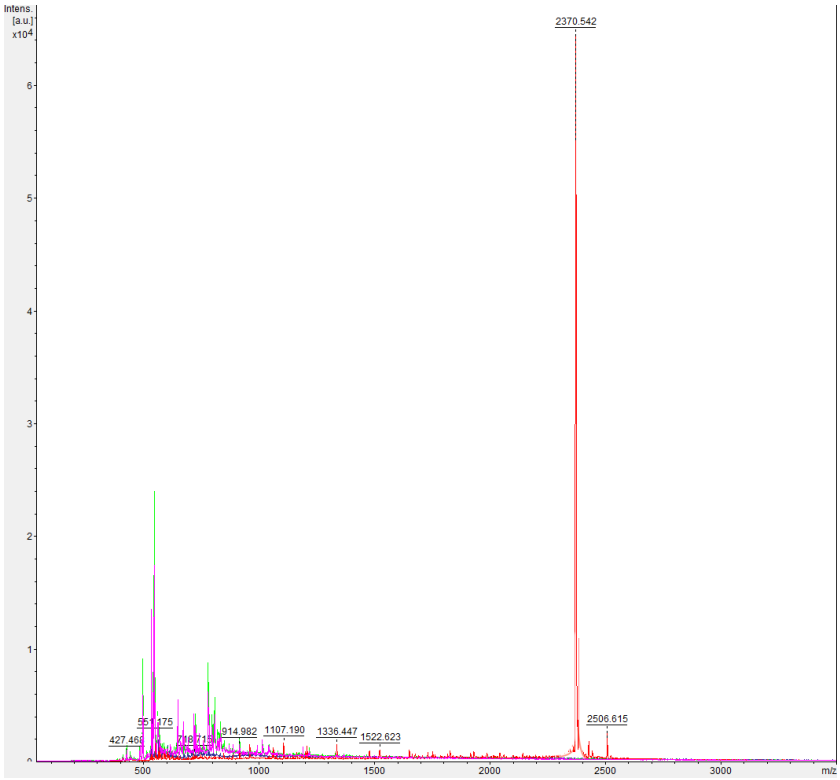
(o) Mass spectrum of the chromatographic peak of 14HBD-mod8 in Serum



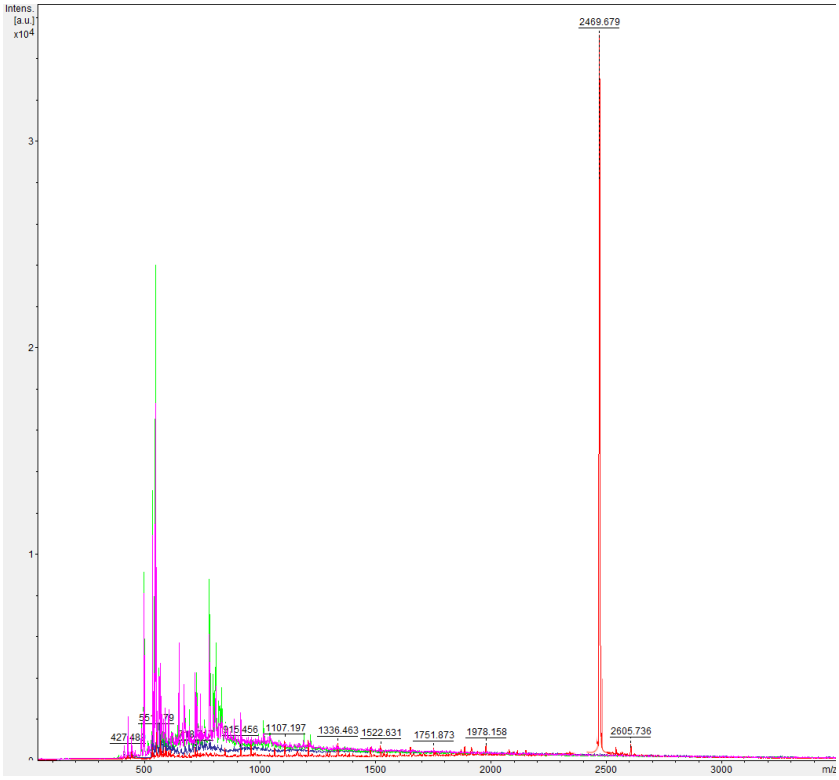
(p) Mass spectrum of the chromatographic peak of 15HBD-mod8 in Serum



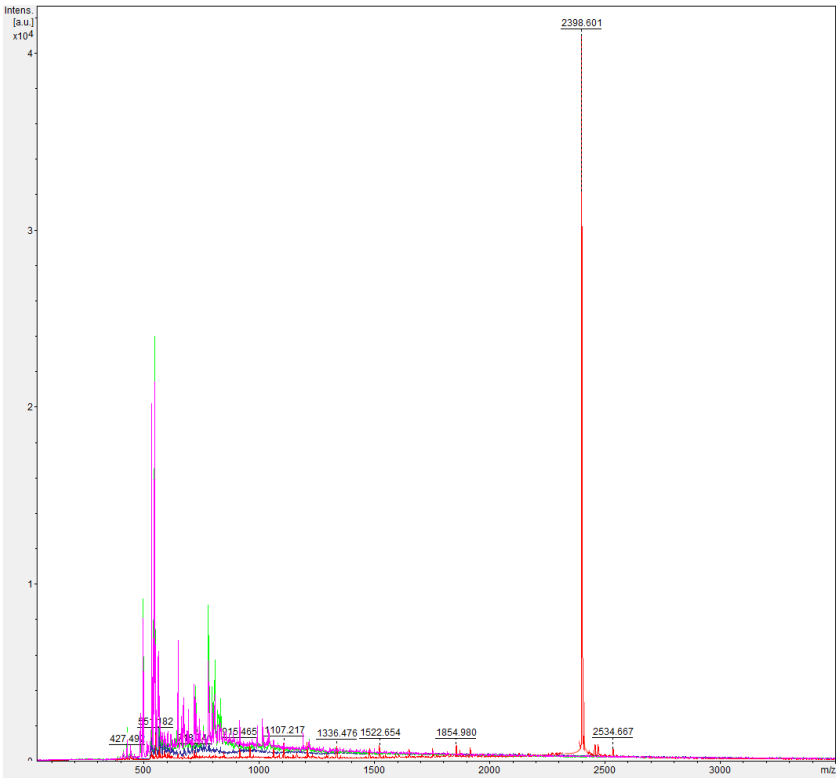
(q) Mass spectrum of the chromatographic peak of 16HBD-mod8 in Serum



(r) Mass spectrum of the chromatographic peak of 17HBD-mod8 in Serum



(s) Mass spectrum of the chromatographic peak of 18HBD-mod8 in Serum



(t) Mass spectrum of the chromatographic peak of 19HBD-mod8 in Serum

Figure A.6: MALDI-TOF data for the fragmentation of HBD-mod8 and its corresponding alanine substitutions.

Appendix Two

Structure

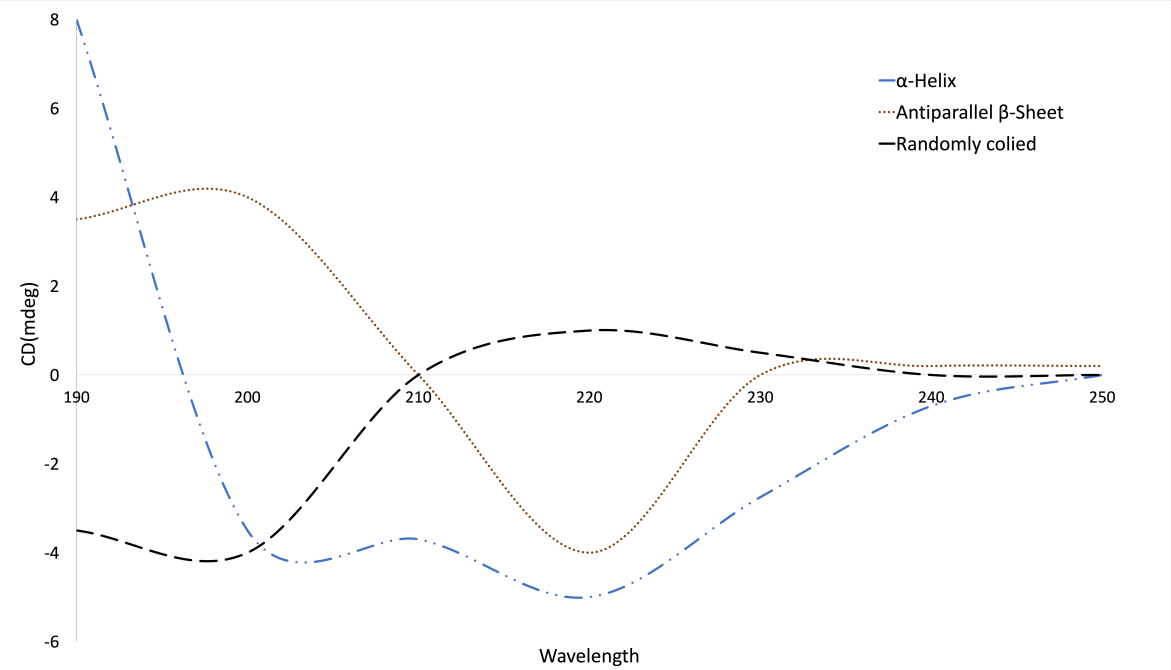
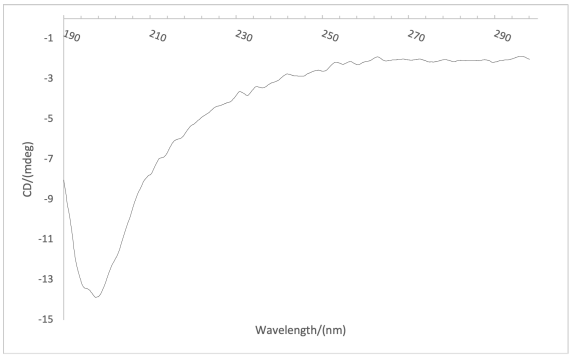
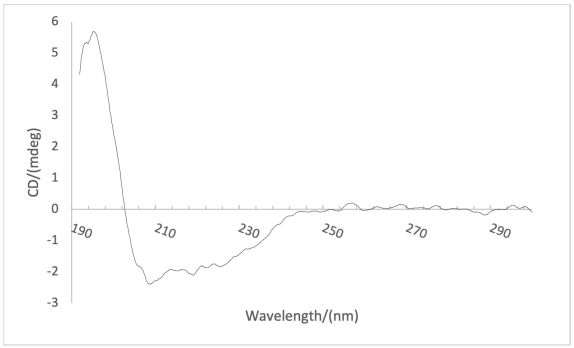


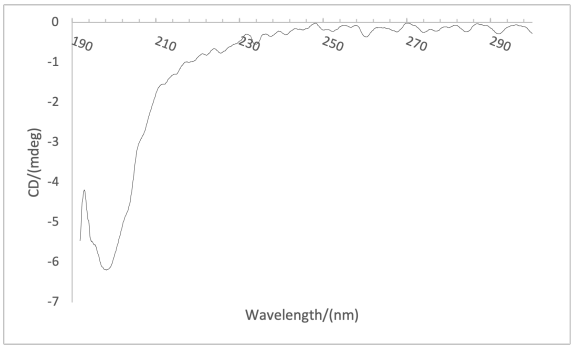
Figure B.1: Showing the varying absorbance patterns in CD qualitatively. This has been used by Dicroweb to produce the percentage results that is presented in section 5



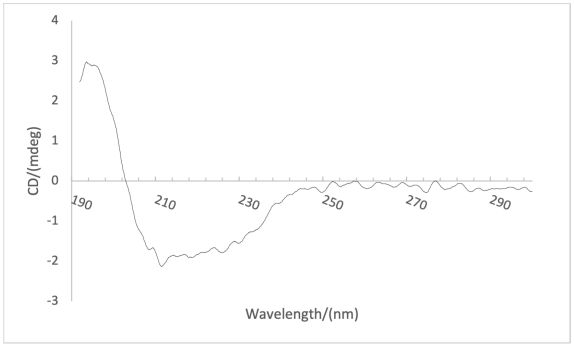
(a) HBD-mod1 in PBS



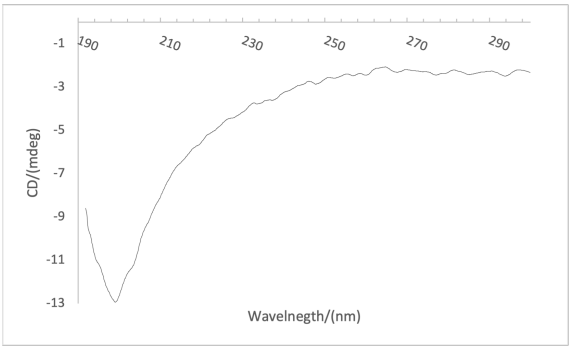
(b) HBD-mod1 in SDS



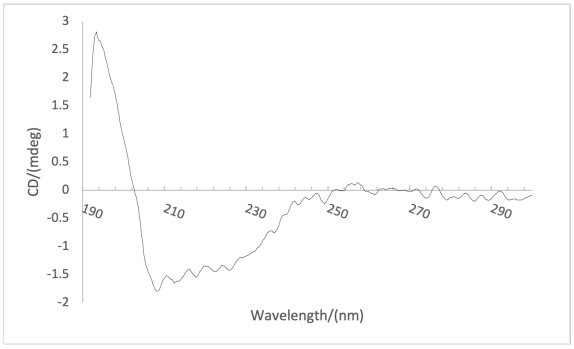
(c) HBD-mod2 in PBS



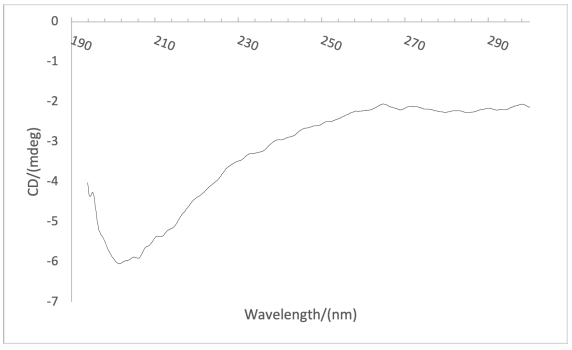
(d) HBD-mod2 in SDS



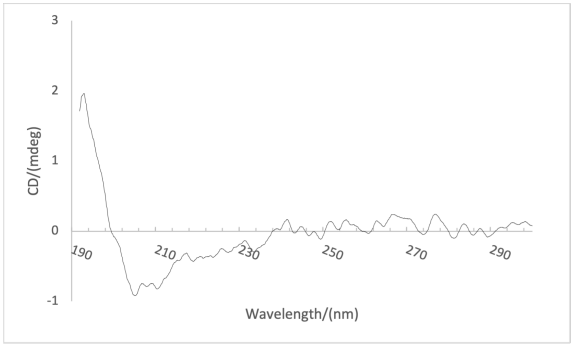
(e) HBD-mod3 in PBS



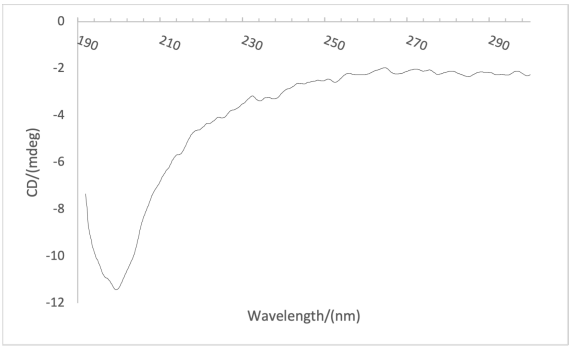
(f) HBD-mod3 in SDS



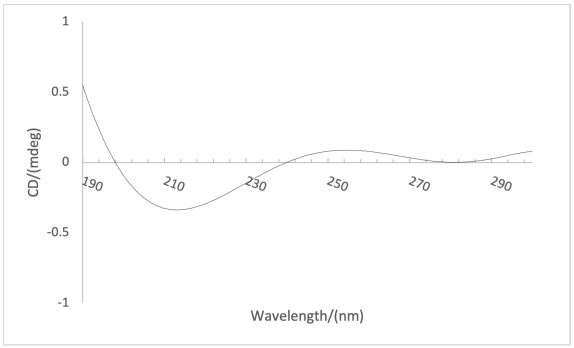
(g) HBD-mod4 in PBS



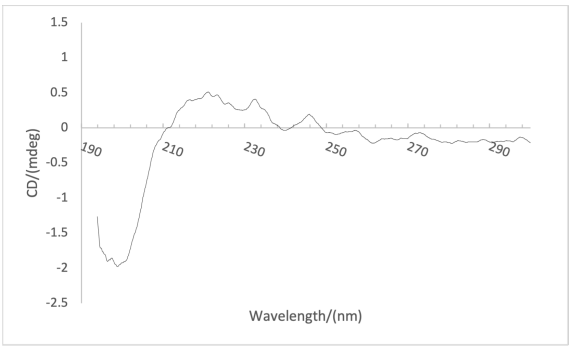
(h) HBD-mod4 in SDS



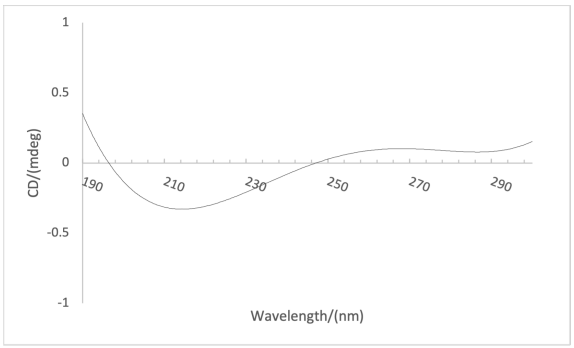
(i) HBD-mod5 in PBS



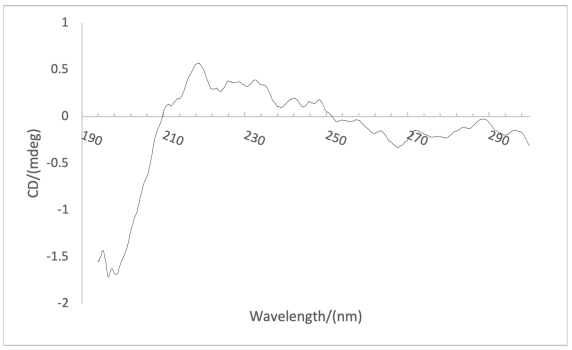
(j) HBD-mod5 in SDS



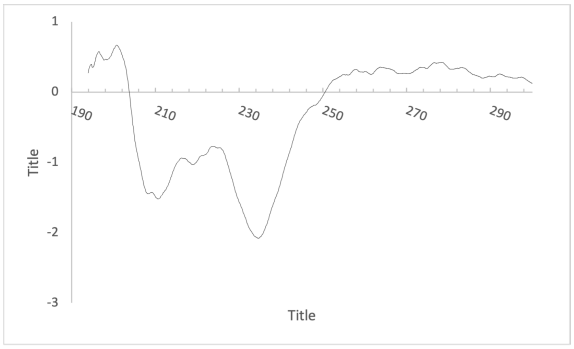
(k) HBD-mod6 in PBS



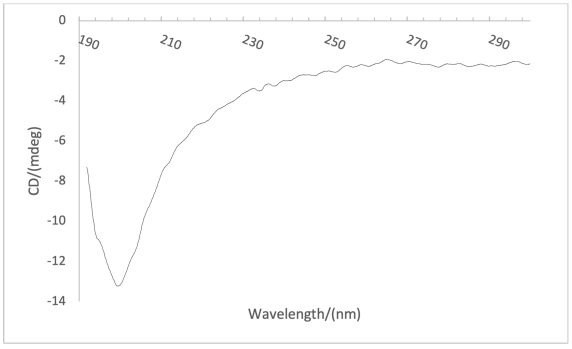
(l) HBD-mod6 in SDS



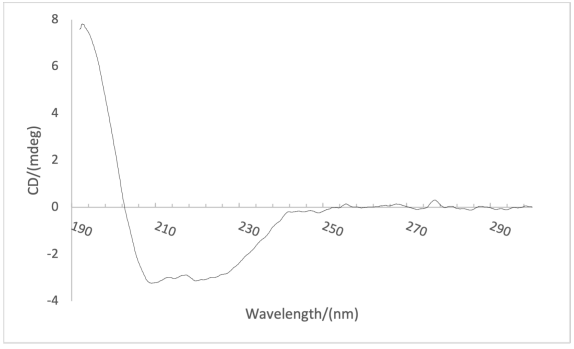
(m) HBD-mod7 in PBS



(n) HBD-mod7 in SDS

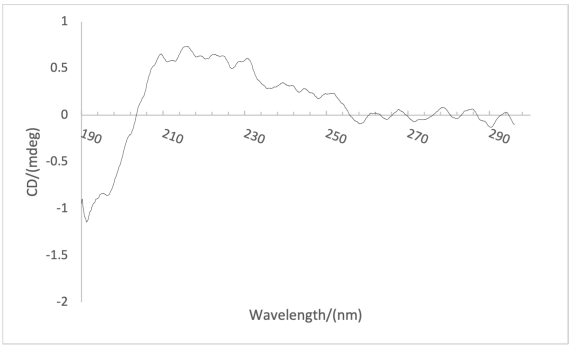


(o) HBD-mod8 in PBS

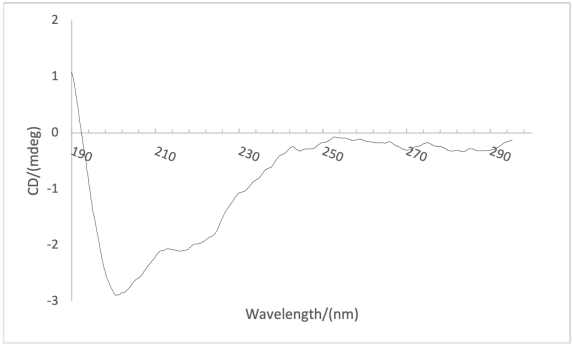


(p) HBD-mod8 in SDS

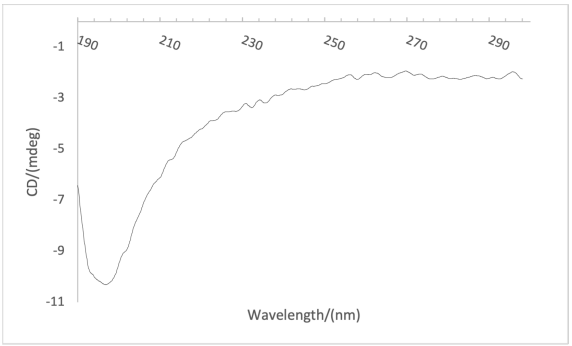
Figure B.2: Showing the secondary structure of peptides based on hBD1 produced from CD in PBS and SDS representing an anionic environments to show the helical conformational change. All graphs were produced from the instrument software by reading the absorbance of the peptide and they are shown in the y-axis and wavelength shown in x-axis.



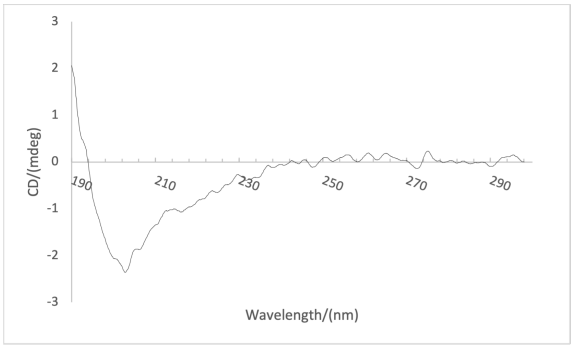
(a) HBD3-mod1 in PBS



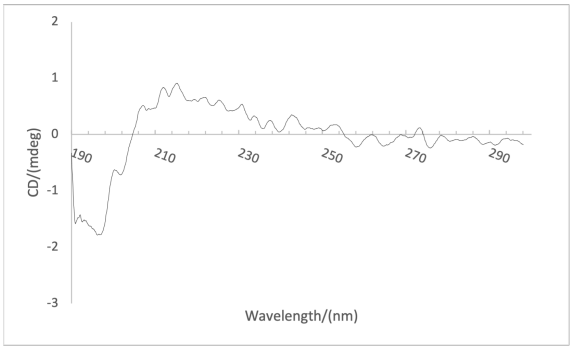
(b) HBD3-mod1 in SDS



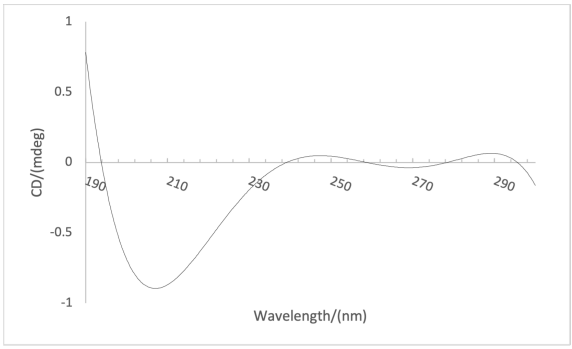
(c) HBD3-mod2 in PBS



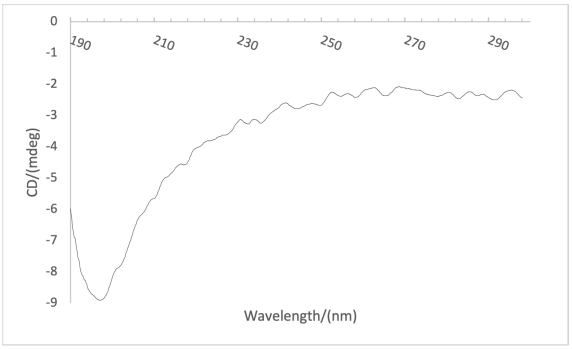
(d) HBD3-mod2 in SDS



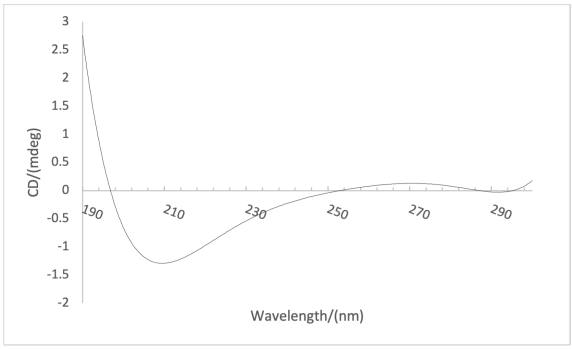
(e) HBD3-mod3 in PBS



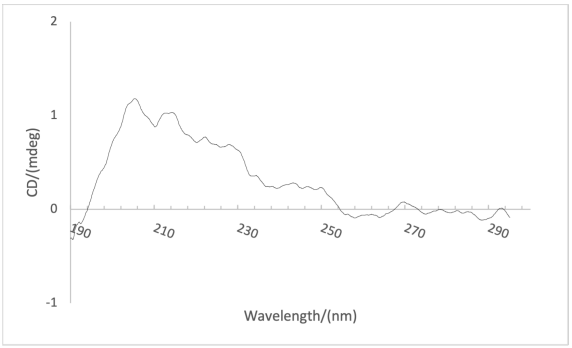
(f) HBD3-mod3 in SDS



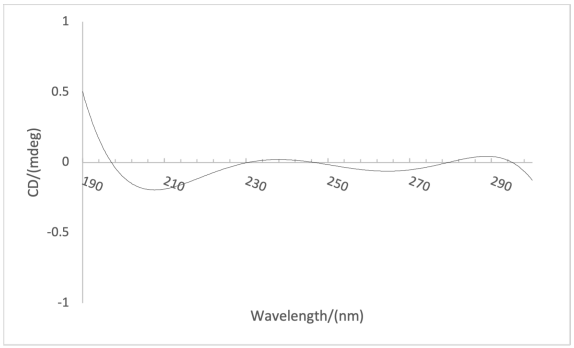
(g) HBD3-mod4 in PBS



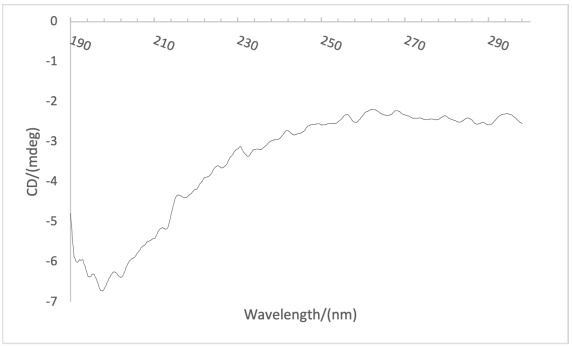
(h) HBD3-mod4 in SDS



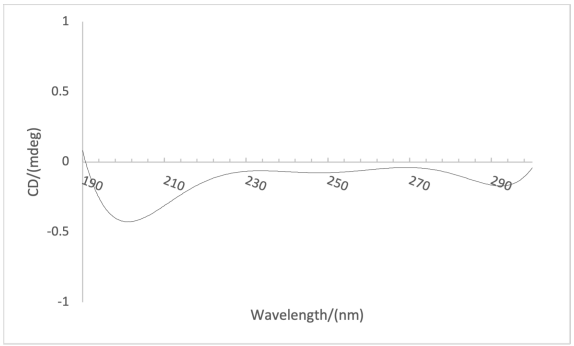
(i) HBD3-mod5 in PBS



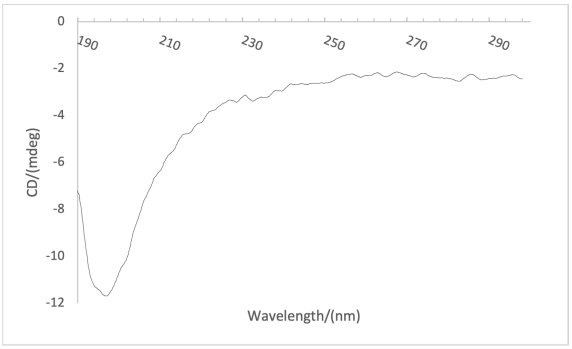
(j) HBD3-mod5 in SDS



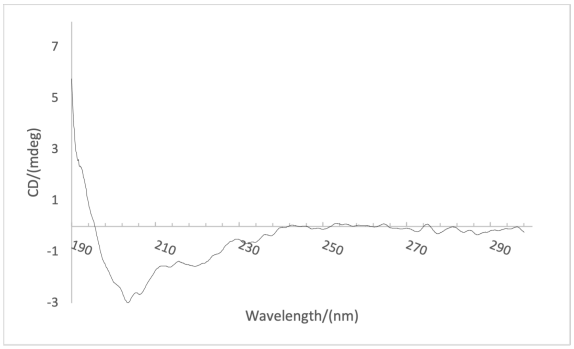
(k) HBD3-mod6 in PBS



(l) HBD3-mod6 in SDS

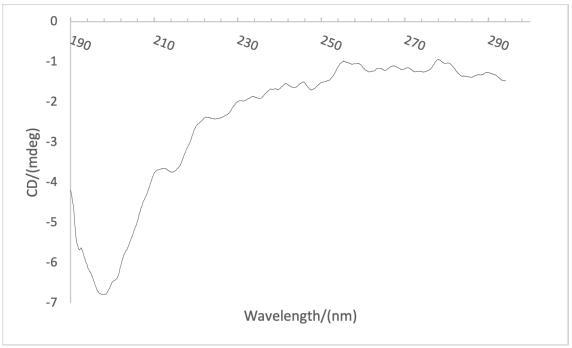


(m) HBD3-mod7 in PBS

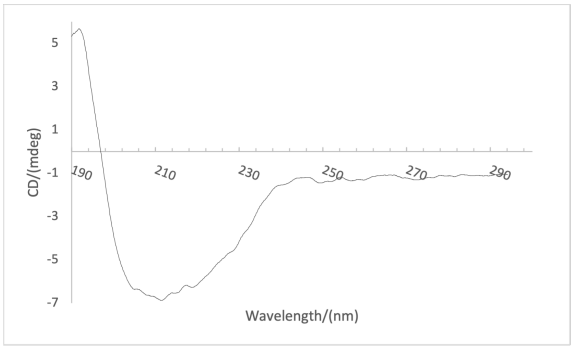


(n) HBD3-mod7 in SDS

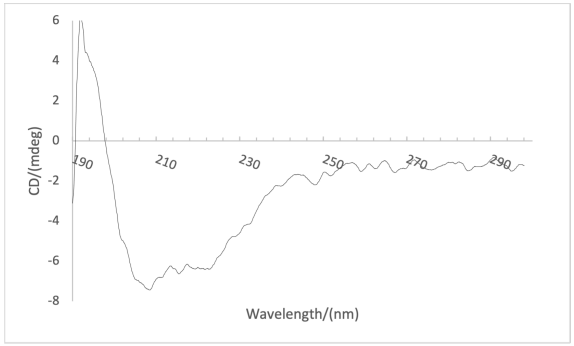
Figure B.3: Showing the secondary structure of peptides based on hBD3 produced from CD in PBS and SDS representing an anionic environments to show the helical conformational change. All graphs were produced from the instrument software by reading the absorbance of the peptide and they are shown in the y-axis and wavelength shown in x-axis.



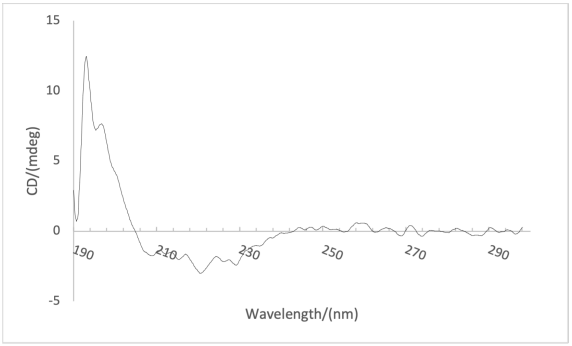
(a) HBD-mod8 in PBS



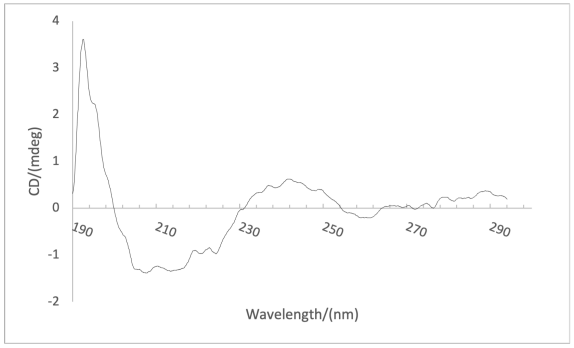
(b) HBD-mod8 in SDS



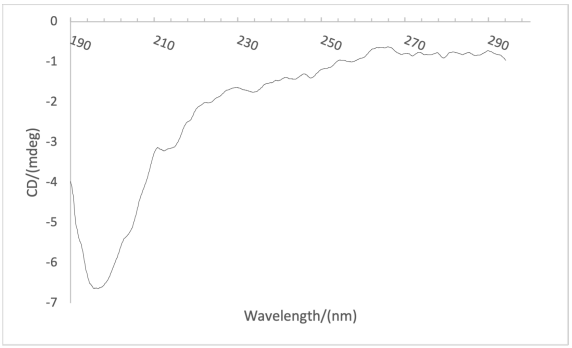
(c) HBD-mod8 in DPC



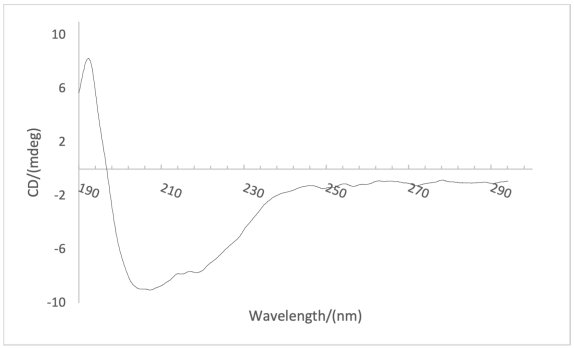
(d) HBD-mod8 in LPS



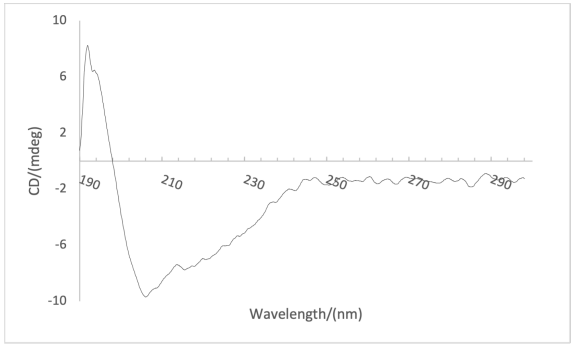
(e) HBD-mod8 in LTA



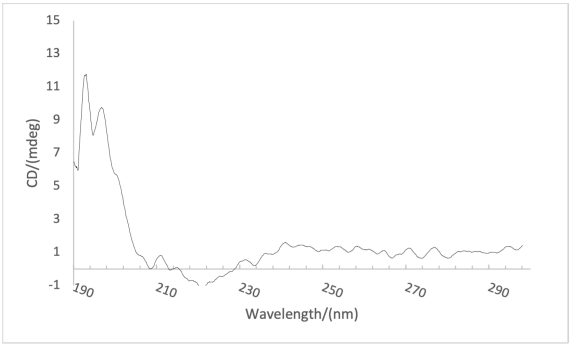
(f) 1HBD-mod8 in PBS



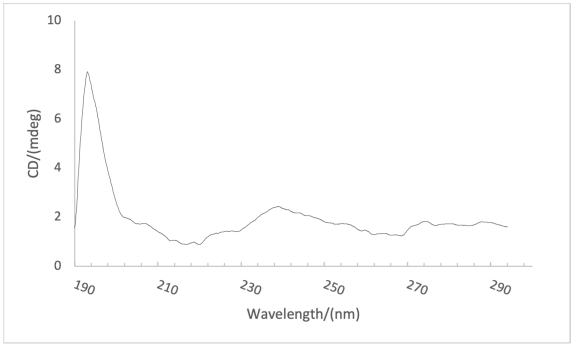
(g) 1HBD-mod8 in SDS



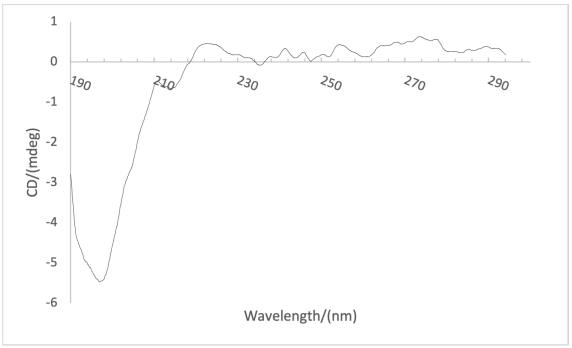
(h) 1HBD-mod8 in DPC



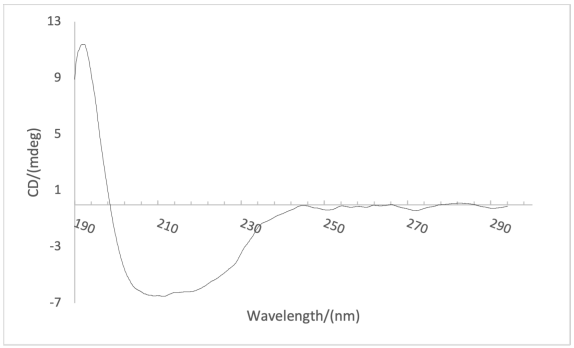
(i) 1HBD-mod8 in LPS



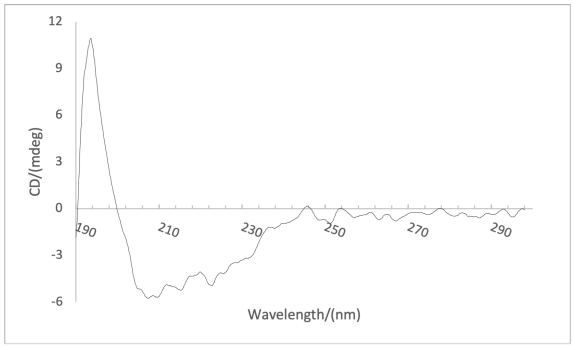
(j) 1HBD-mod8 in LTA



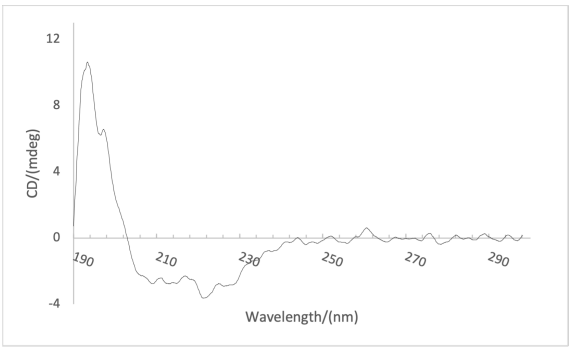
(k) 2HBD-mod8 in PBS



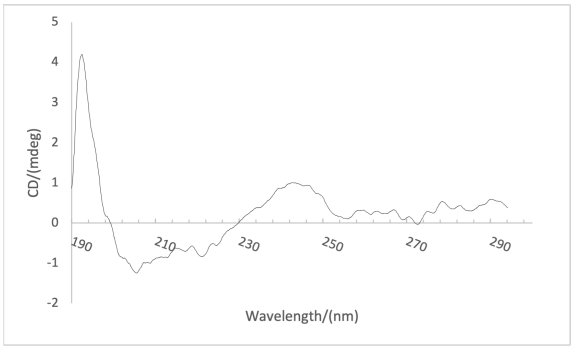
(l) 2HBD-mod8 in SDS



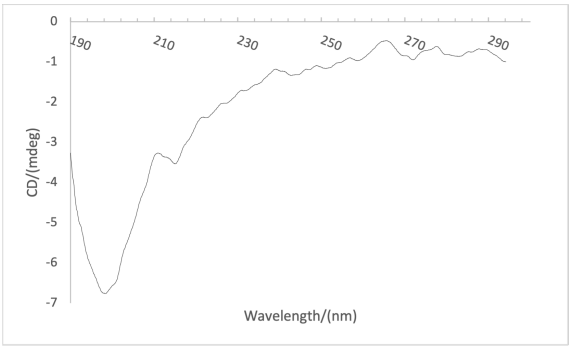
(m) 2HBD-mod8 in DPC



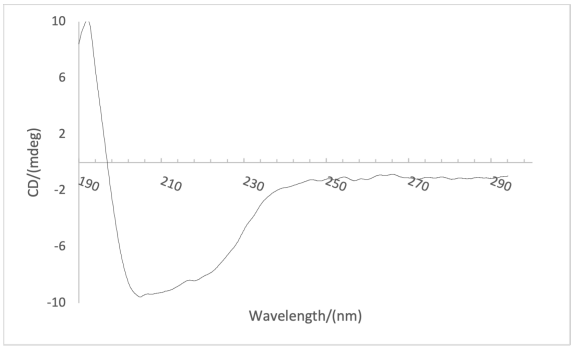
(n) 2HBD-mod8 in LPS



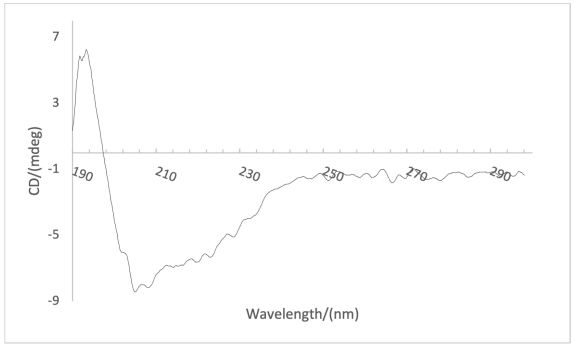
(o) 2HBD-mod8 in LTA



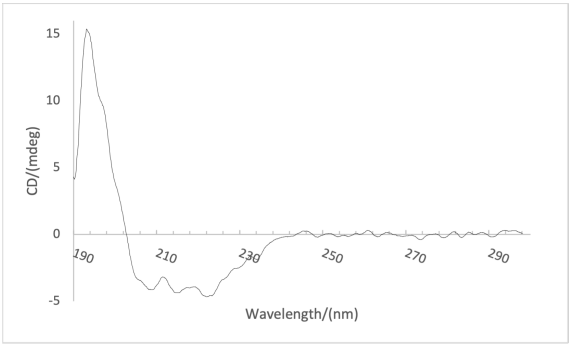
(p) 3HBD-mod8 in PBS



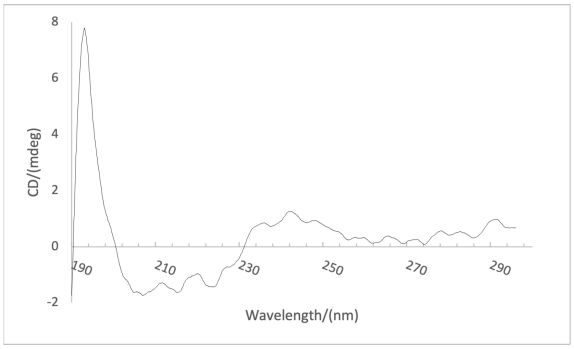
(q) 3HBD-mod8 in SDS



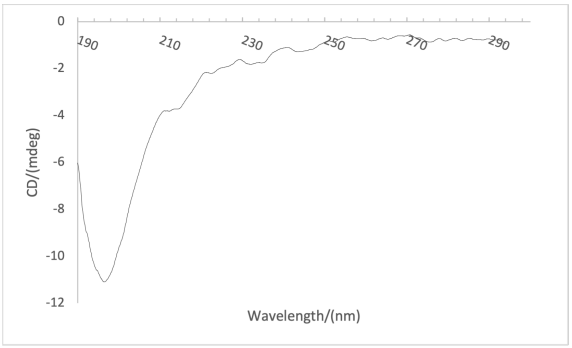
(r) 3HBD-mod8 in DPC



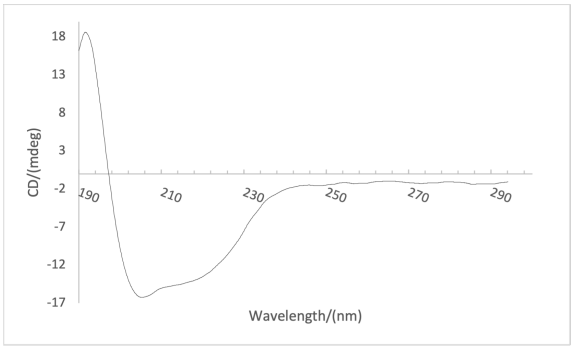
(s) 3HBD-mod8 in LPS



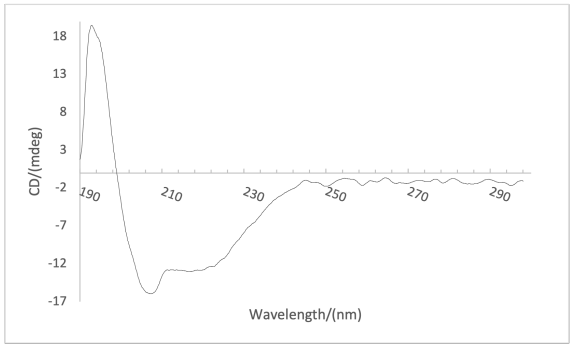
(t) 3HBD-mod8 in LTA



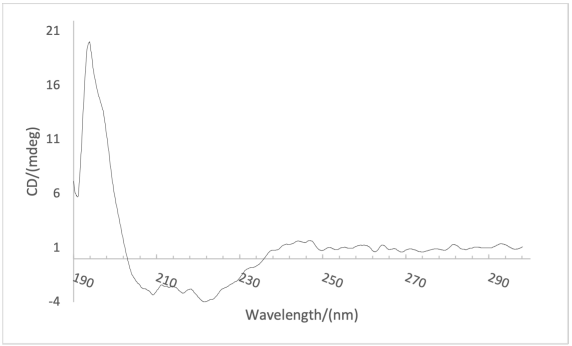
(u) 4HBD-mod8 in PBS



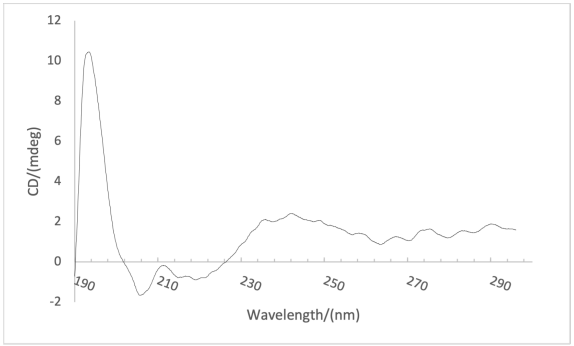
(v) 4HBD-mod8 in SDS



(w) 4HBD-mod8 in DPC

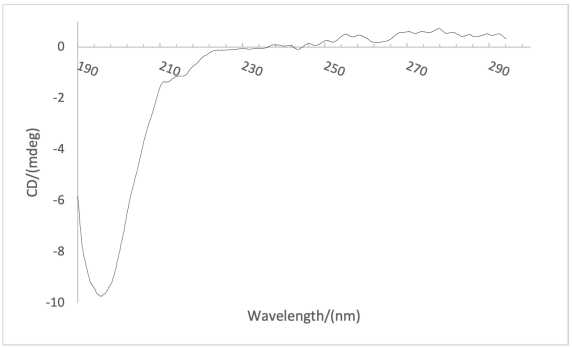


(x) 4HBD-mod8 in LPS

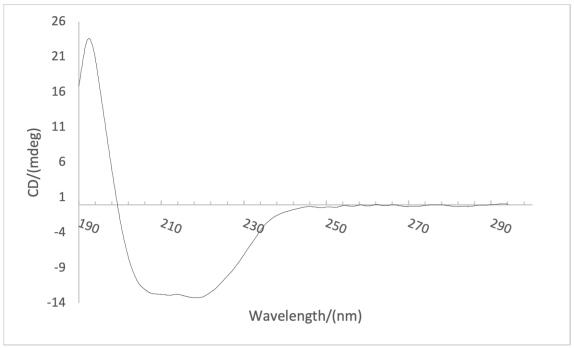


(y) 4HBD-mod8 in LTA

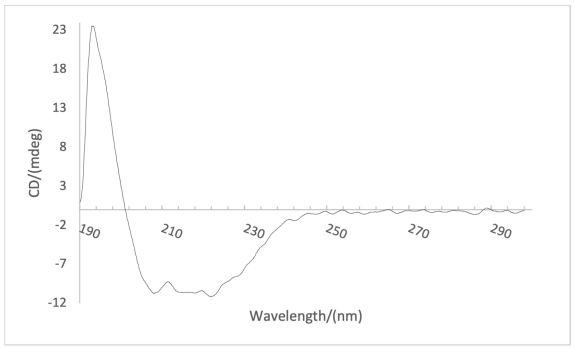
Figure B.4: Showing the secondary structure of peptides based on alanine scan of HBD-mod8 (HBD-mod8-4HBD-mod8) produced from CD in PBS, SDS, LPS, LTA and DPC representing an anionic environments and mimicking bacterial membrane for Gram-negative and -positive bacteria respectively to show the helical conformational change. All graphs were produced from the instrument software by reading the absorbance of the peptide and they are shown in the y-axis and wavelength shown in x-axis.



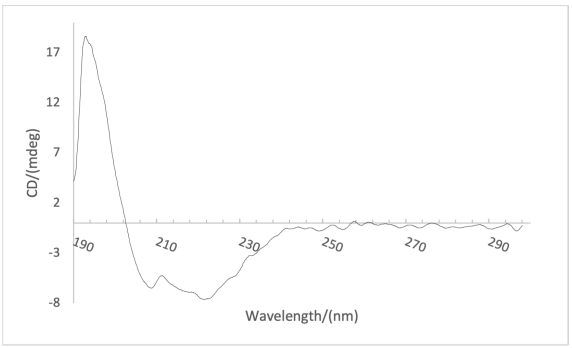
(a) 5HBD-mod8 in PBS



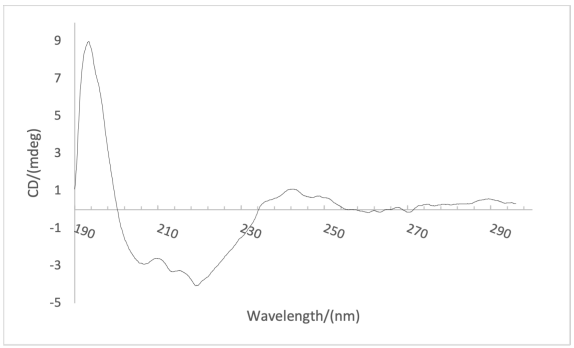
(b) 5HBD-mod8 in SDS



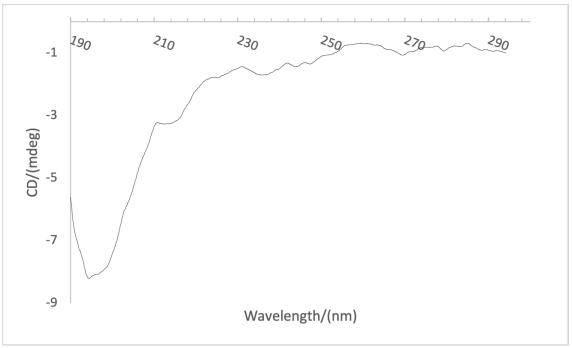
(c) 5HBD-mod8 in DPC



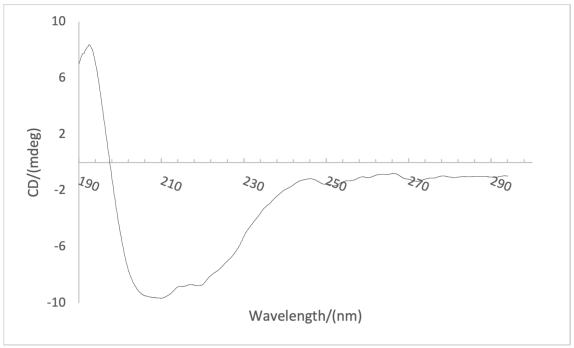
(d) 5HBD-mod8 in LPS



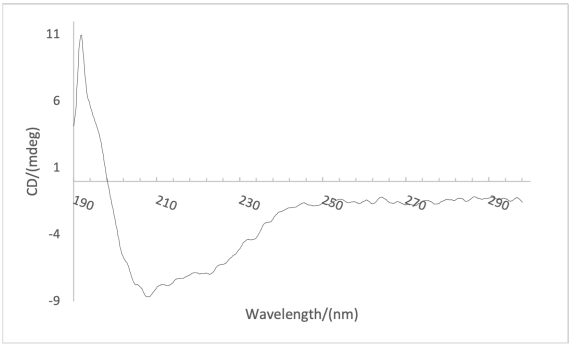
(e) 5HBD-mod8 in LTA



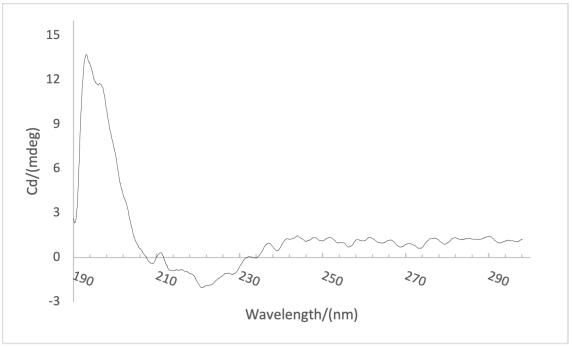
(f) 6HBD-mod8 in PBS



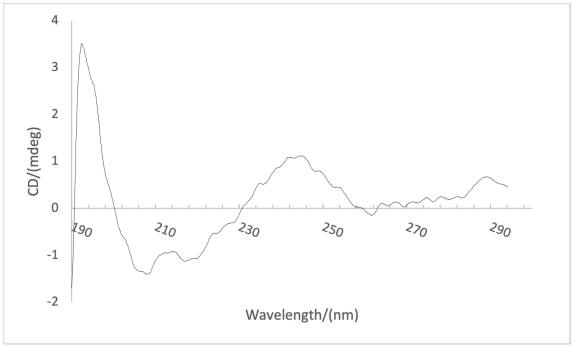
(g) 6HBD-mod8 in SDS



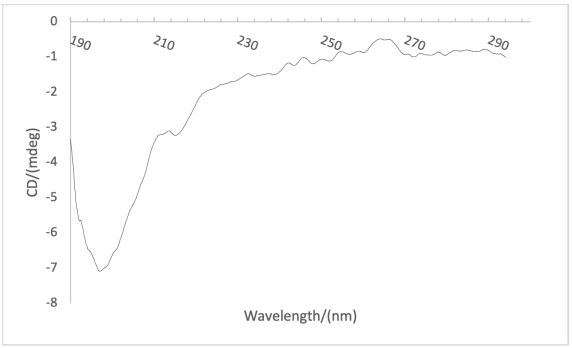
(h) 6HBD-mod8 in DPC



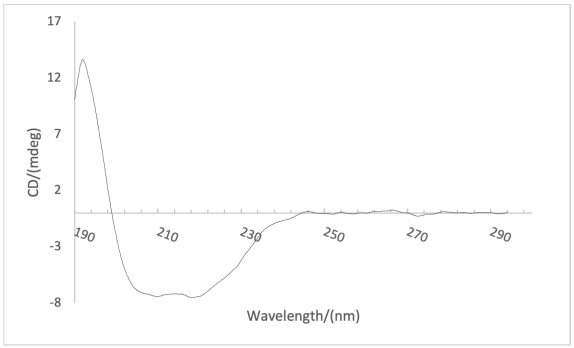
(i) 6HBD-mod8 in LPS



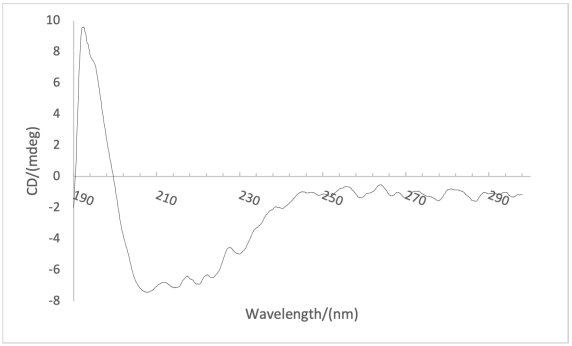
(j) 6HBD-mod8 in LTA



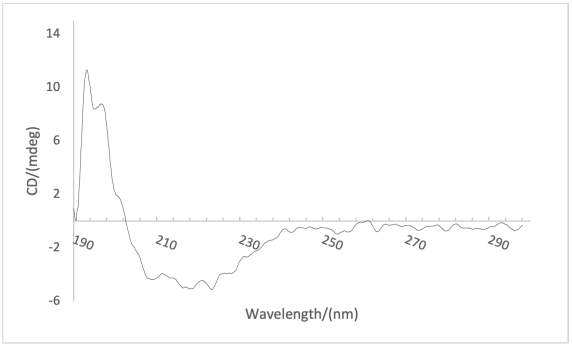
(k) 7HBD-mod8 in PBS



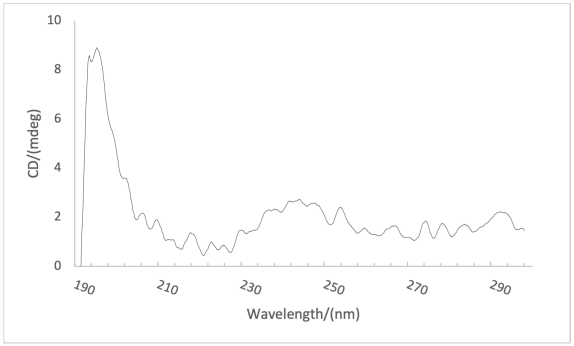
(l) 7HBD-mod8 in SDS



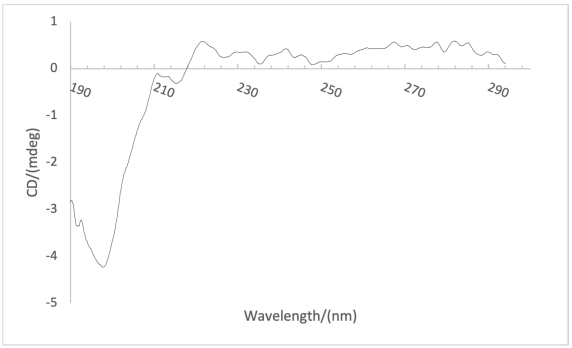
(m) 7HBD-mod8 in DPC



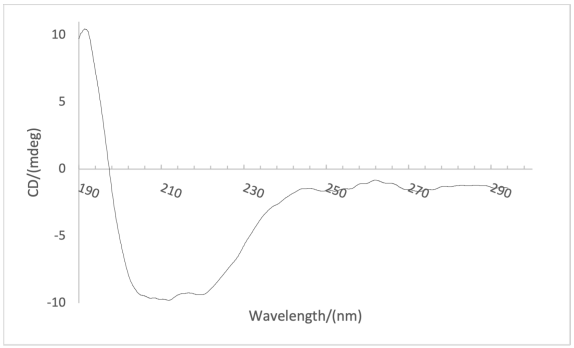
(n) 7HBD-mod8 in LPS



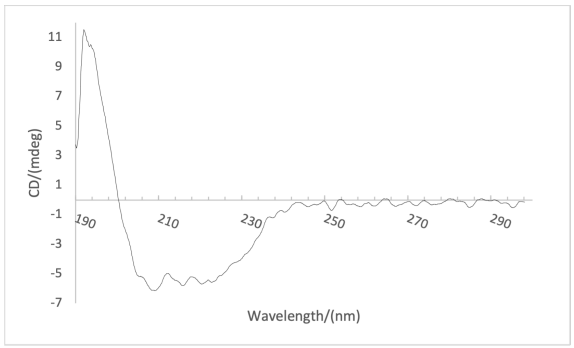
(o) 7HBD-mod8 in LTA



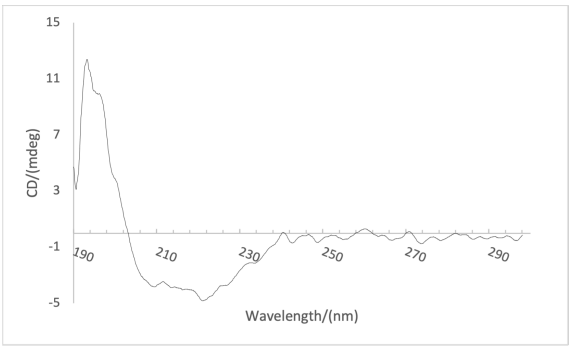
(p) 8HBD-mod8 in PBS



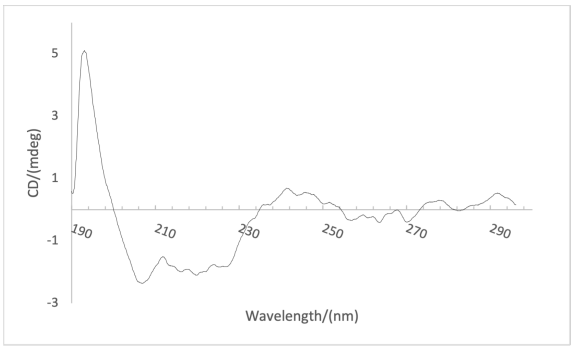
(q) 8HBD-mod8 in SDS



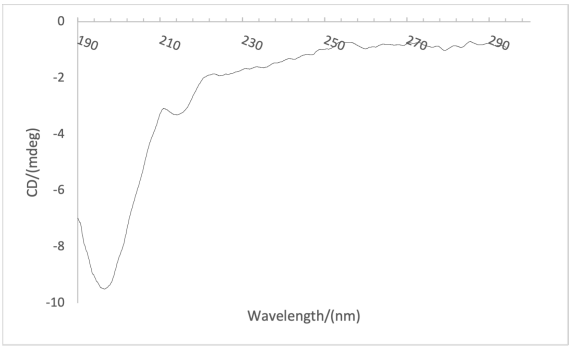
(r) 8HBD-mod8 in DPC



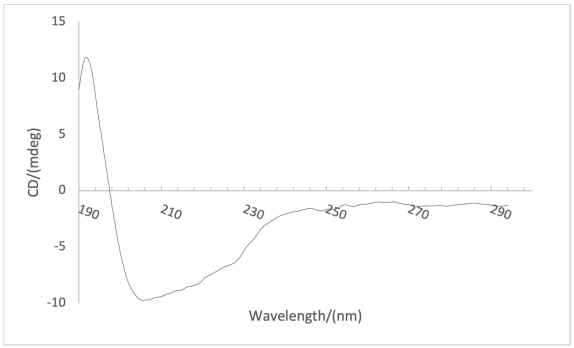
(s) 8HBD-mod8 in LPS



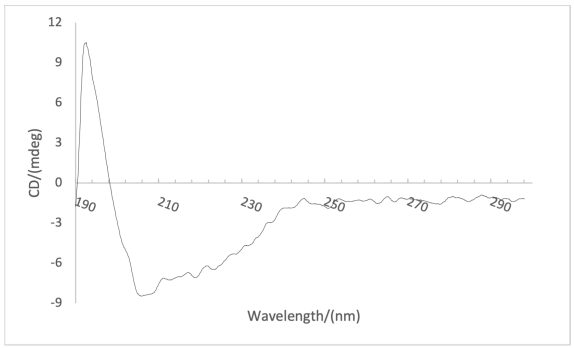
(t) 8HBD-mod8 in LTA



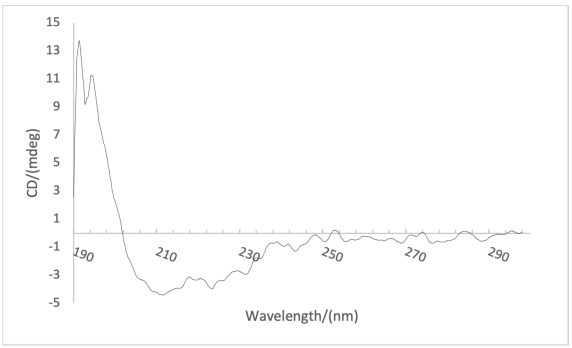
(u) 9HBD-mod8 in PBS



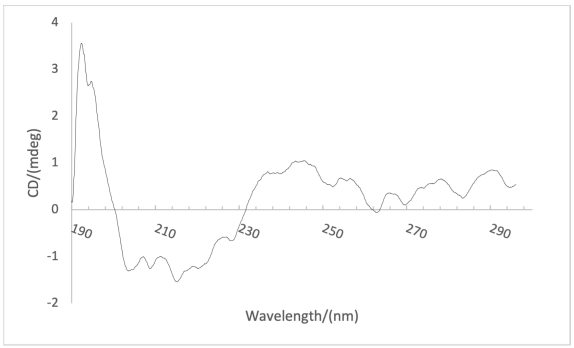
(v) 9HBD-mod8 in SDS



(w) 9HBD-mod8 in DPC

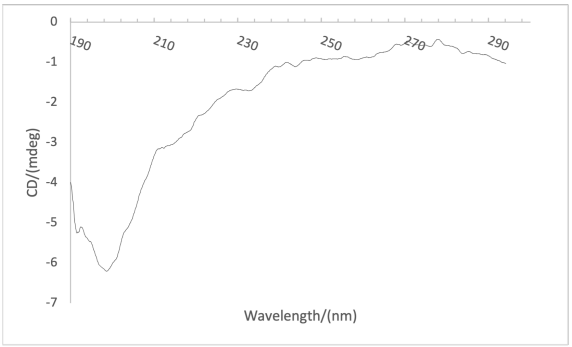


(x) 9HBD-mod8 in LPS

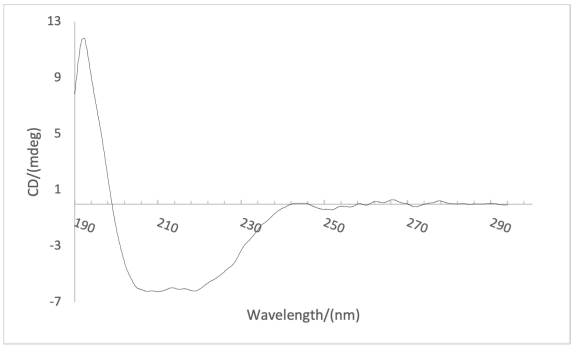


(y) 9HBD-mod8 in LTA

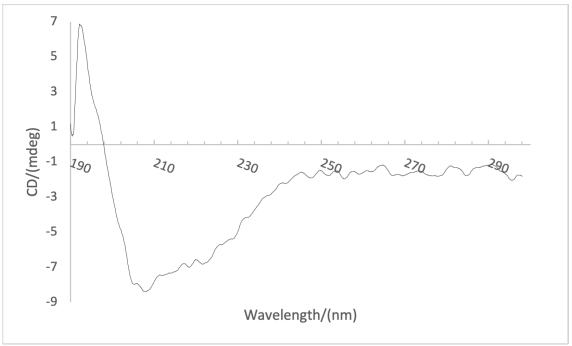
Figure B.5: Showing the secondary structure of peptides based on alanine scan of HBD-mod8 (5HBD-mod8-9HBD-mod8) produced from CD in PBS, SDS, LPS, LTA and DPC representing an anionic environments and mimicking bacterial membrane for Gram-negative and -positive bacteria respectively to show the helical conformational change. All graphs were produced from the instrument software by reading the absorbance of the peptide and they are shown in the y-axis and wavelength shown in x-axis.



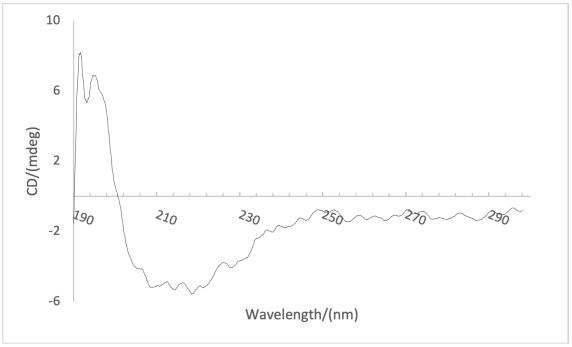
(a) 10HBD-mod8 in PBS



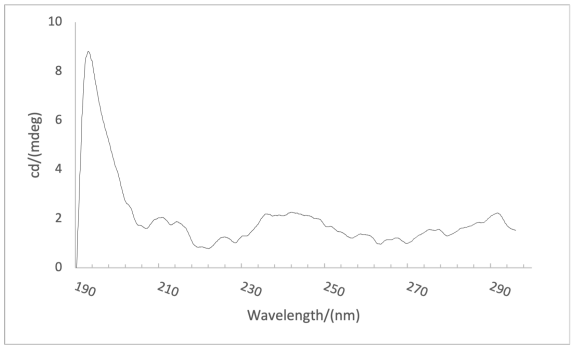
(b) 10HBD-mod8 in SDS



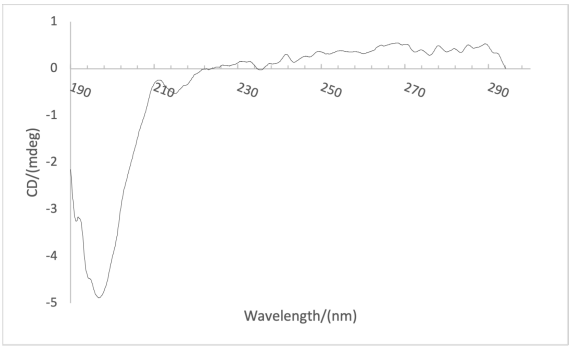
(c) 10HBD-mod8 in DPC



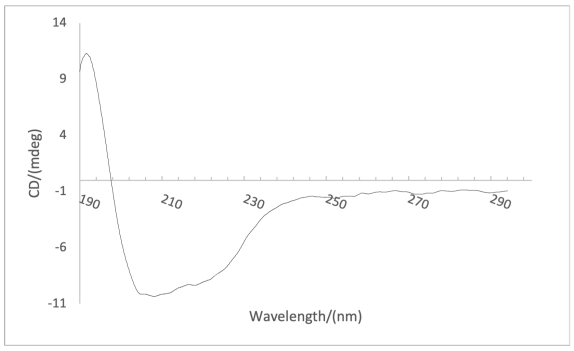
(d) 10HBD-mod8 in LPS



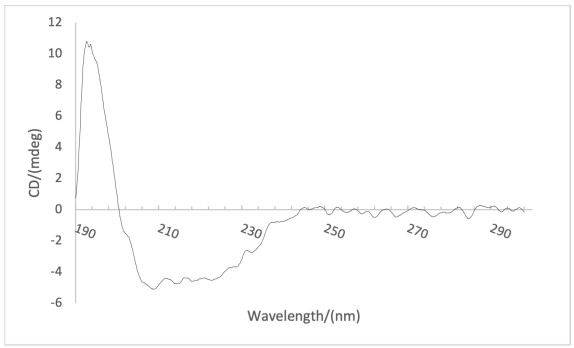
(e) 10HBD-mod8 in LTA



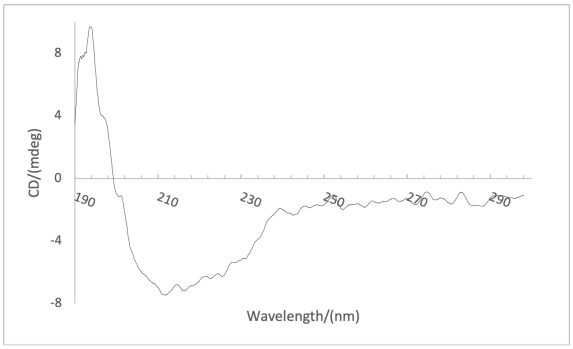
(f) 11HBD-mod8 in PBS



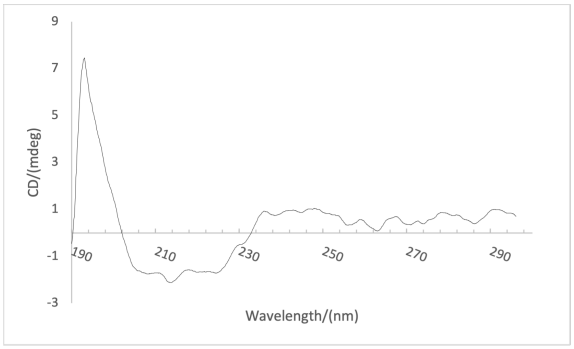
(g) 11HBD-mod8 in SDS



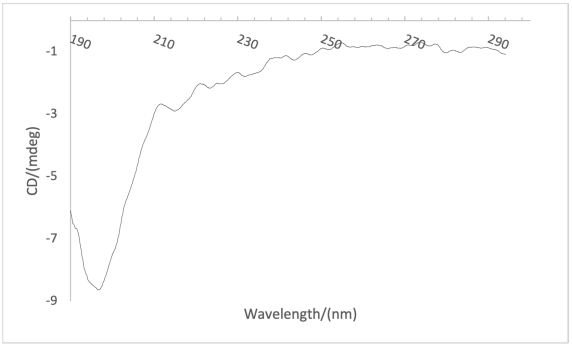
(h) 11HBD-mod8 in DPC



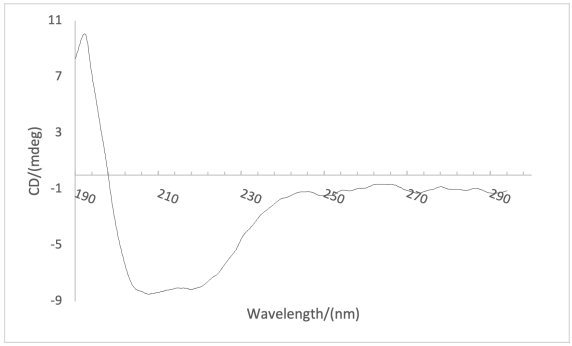
(i) 11HBD-mod8 in LPS



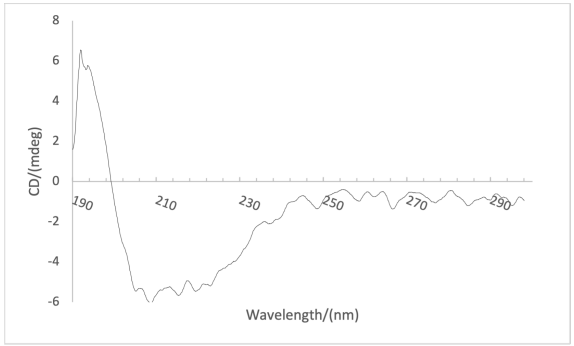
(j) 11HBD-mod8 in LTA



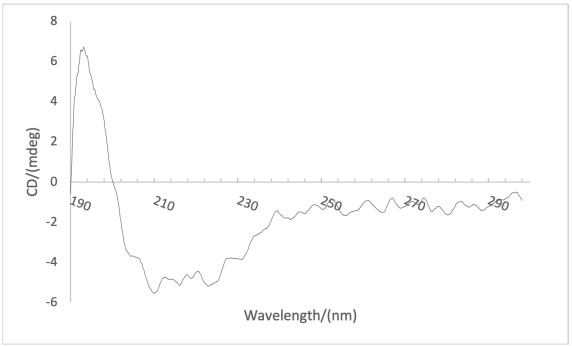
(k) 12HBD-mod8 in PBS



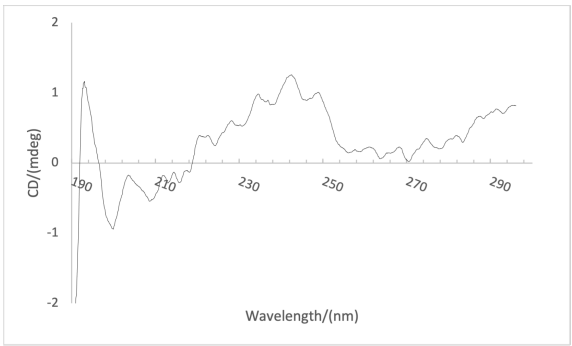
(l) 12HBD-mod8 in SDS



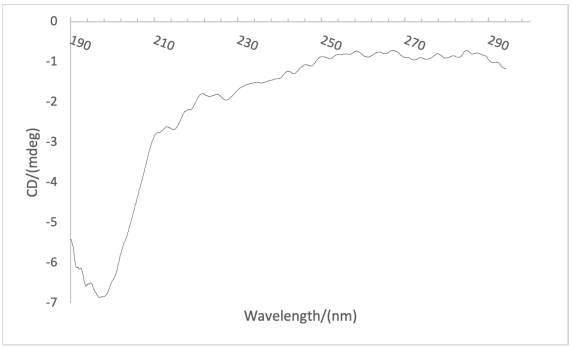
(m) 12HBD-mod8 in DPC



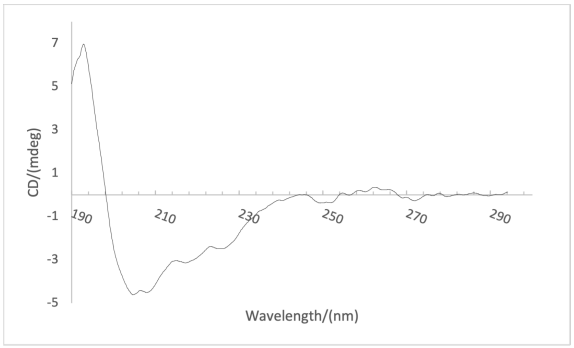
(n) 12HBD-mod8 in LPS



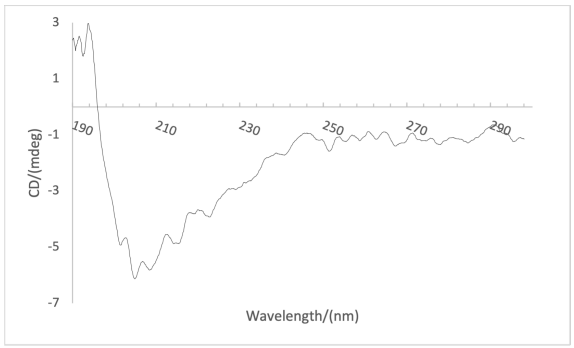
(o) 12HBD-mod8 in LTA



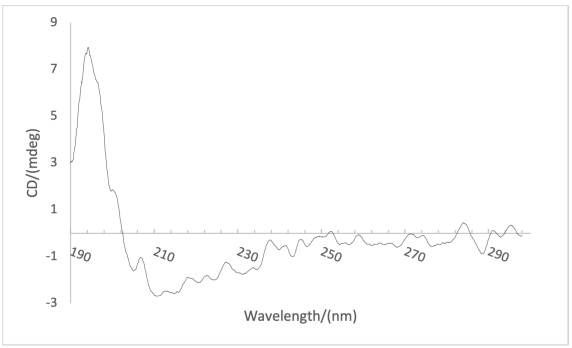
(p) 13HBD-mod8 in PBS



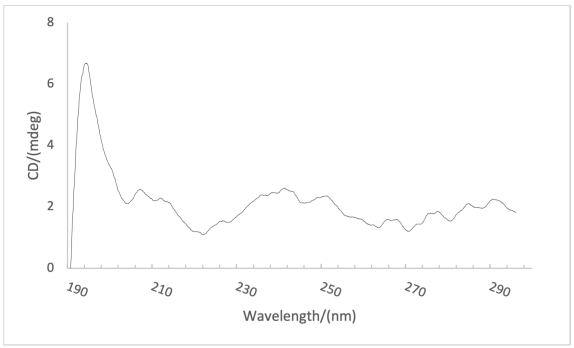
(q) 13HBD-mod8 in SDS



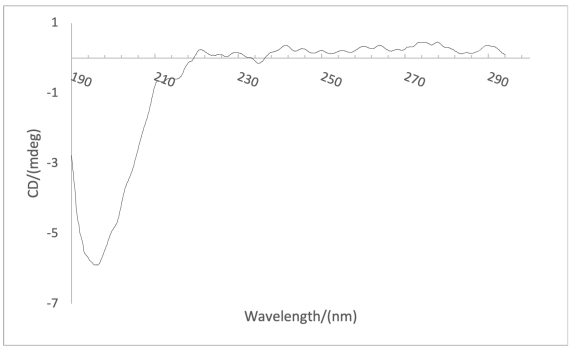
(r) 13HBD-mod8 in DPC



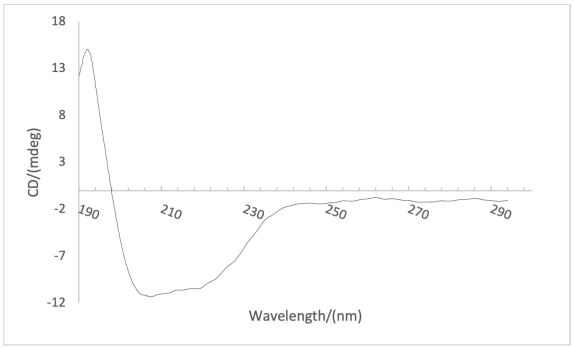
(s) 13HBD-mod8 in LPS



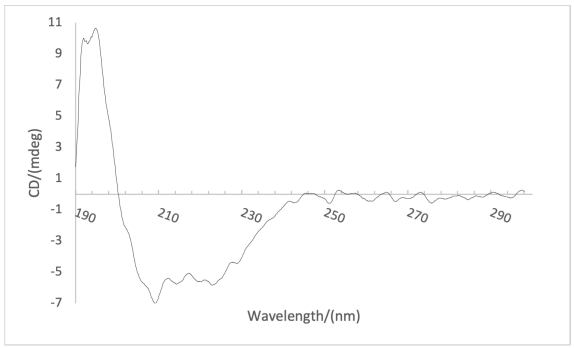
(t) 13HBD-mod8 in LTA



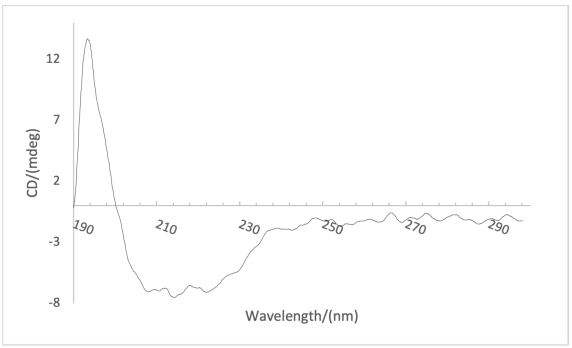
(u) 14HBD-mod8 in PBS



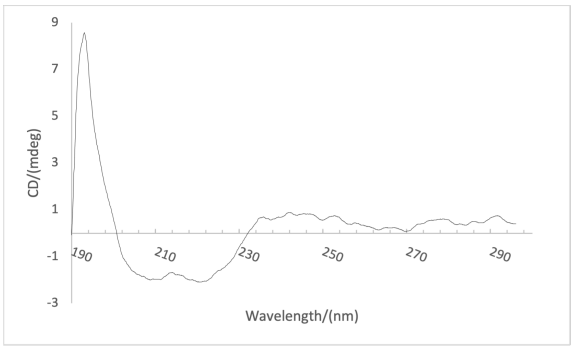
(v) 14HBD-mod8 in SDS



(w) 14HBD-mod8 in DPC

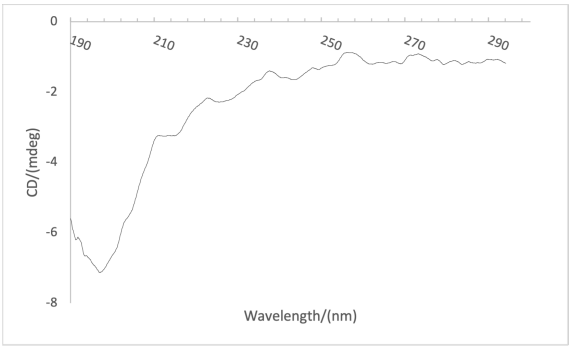


(x) 14HBD-mod8 in LPS

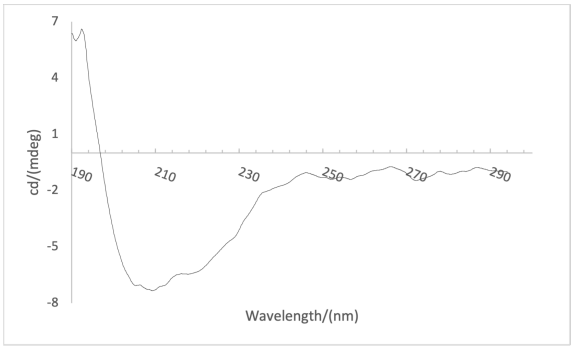


(y) 14BD-mod8 in LTA

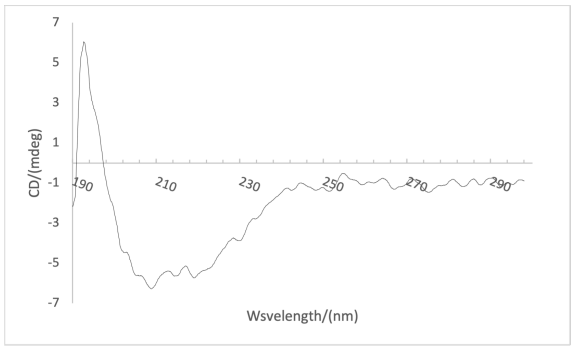
Figure B.6: Showing the secondary structure of peptides based on alanine scan of HBD-mod8 (10HBD-mod8-14HBD-mod8) produced from CD in PBS, SDS, LPS, LTA and DPC representing an anionic environments and mimicking bacterial membrane for Gram-negative and -positive bacteria respectively to show the helical conformational change. All graphs were produced from the instrument software by reading the absorbance of the peptide and they are shown in the y-axis and wavelength shown in x-axis.



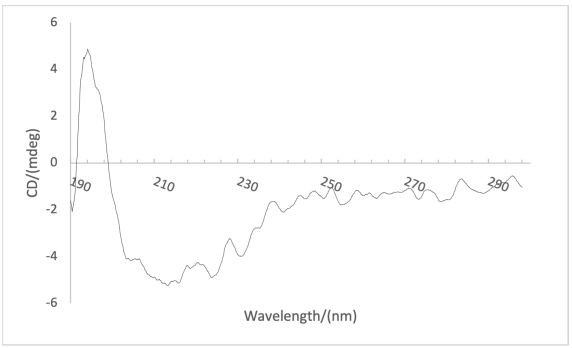
(a) 15HBD-mod8 in PBS



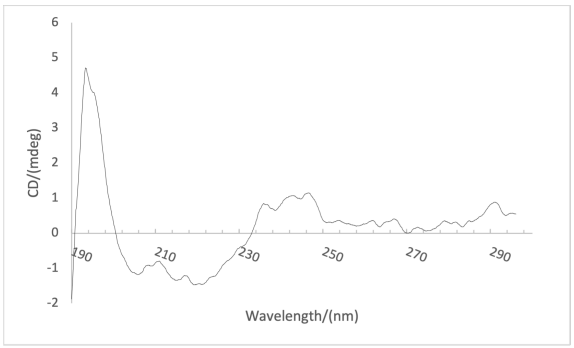
(b) 15HBD-mod8 in SDS



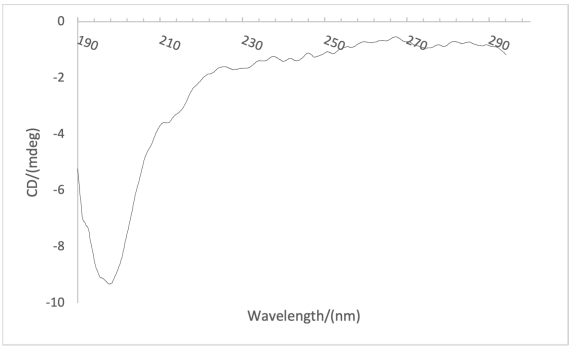
(c) 15HBD-mod8 in DPC



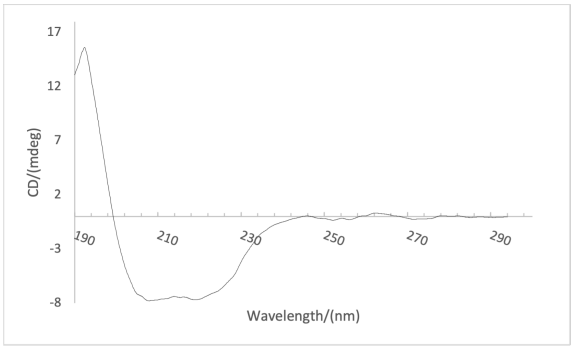
(d) 15HBD-mod8 in LPS



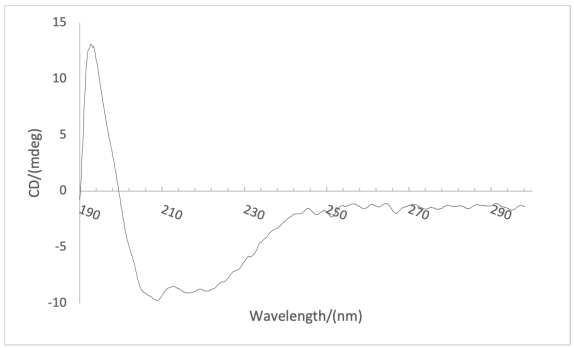
(e) 15BD-mod8 in LTA



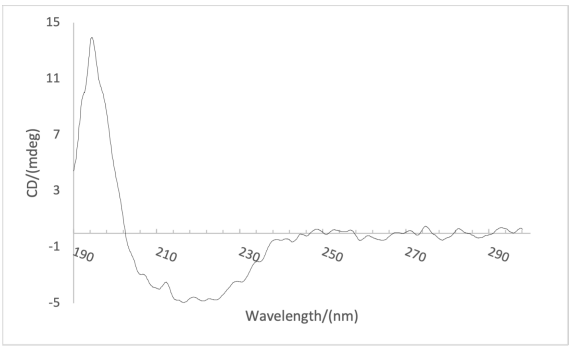
(f) 16HBD-mod8 in PBS



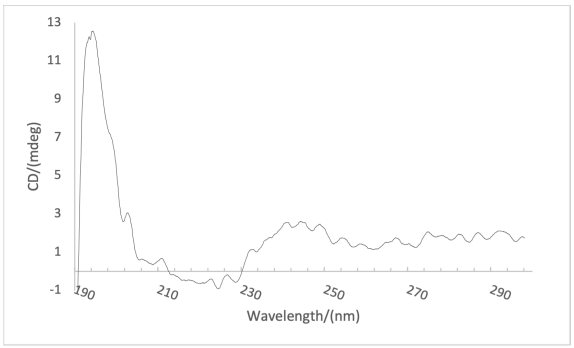
(g) 16HBD-mod8 in SDS



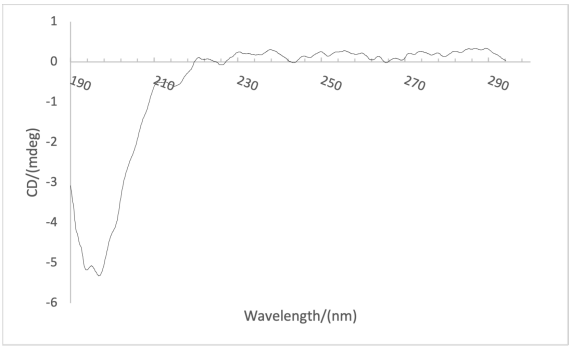
(h) 16HBD-mod8 in DPC



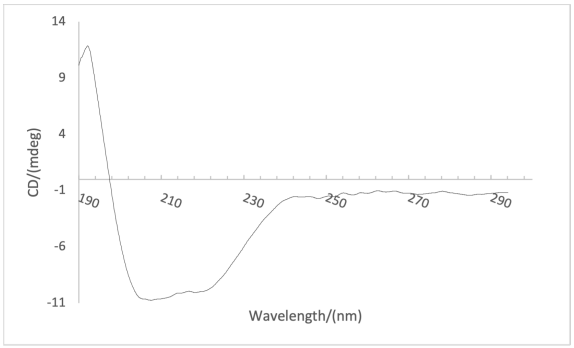
(i) 16HBD-mod8 in LPS



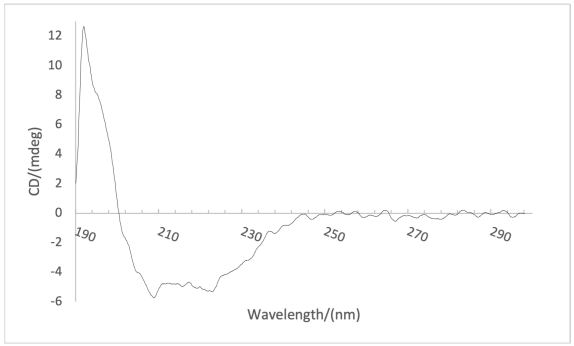
(j) 16BD-mod8 in LTA



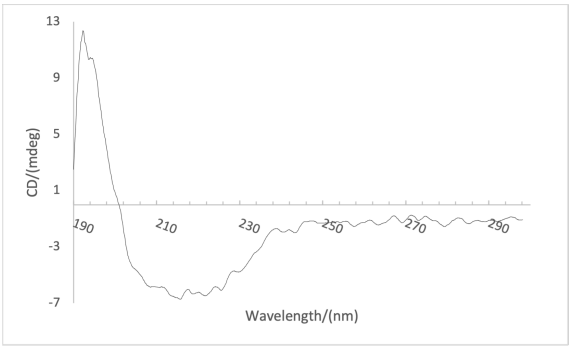
(k) 17HBD-mod8 in PBS



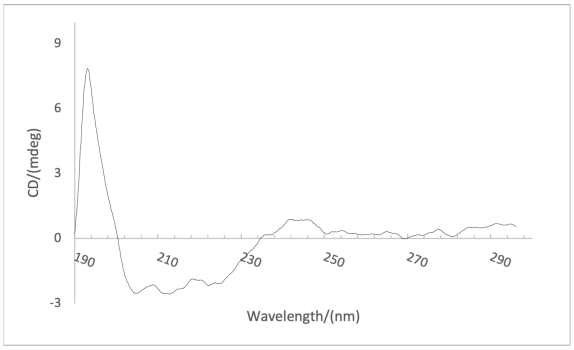
(l) 17HBD-mod8 in SDS



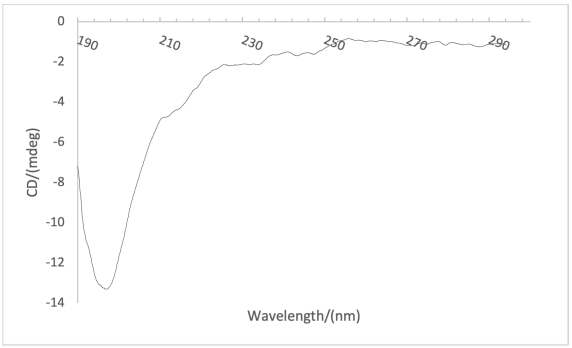
(m) 17HBD-mod8 in DPC



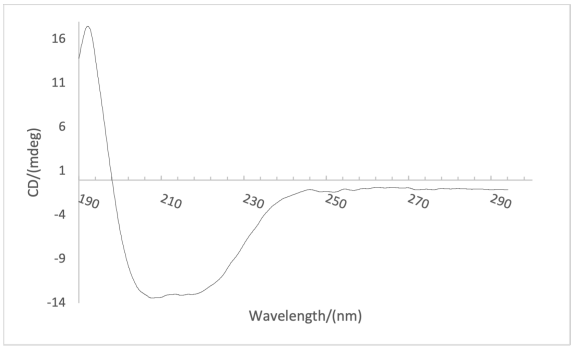
(n) 17HBD-mod8 in LPS



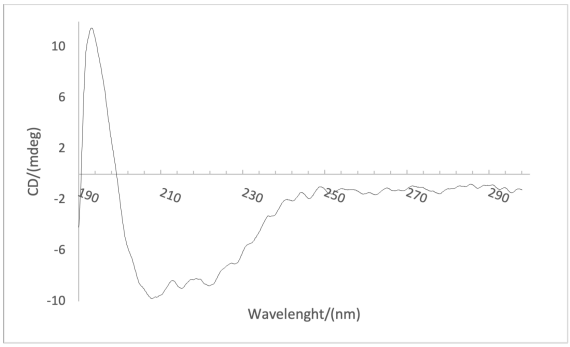
(o) 17BD-mod8 in LTA



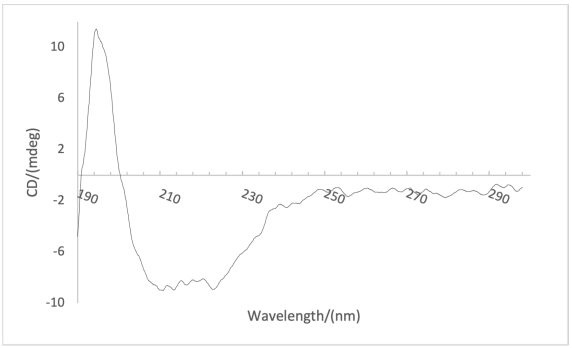
(p) 18HBD-mod8 in PBS



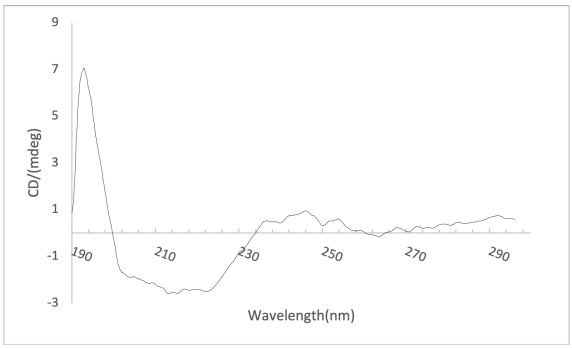
(q) 18HBD-mod8 in SDS



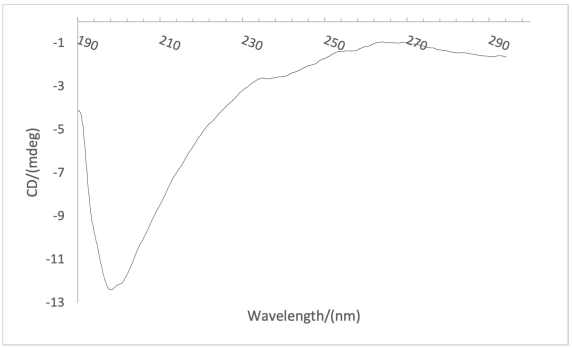
(r) 18HBD-mod8 in DPC



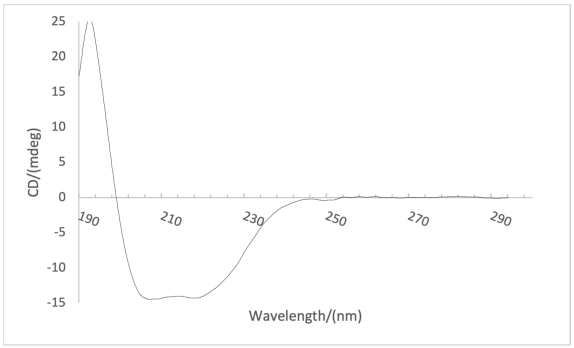
(s) 18HBD-mod8 in LPS



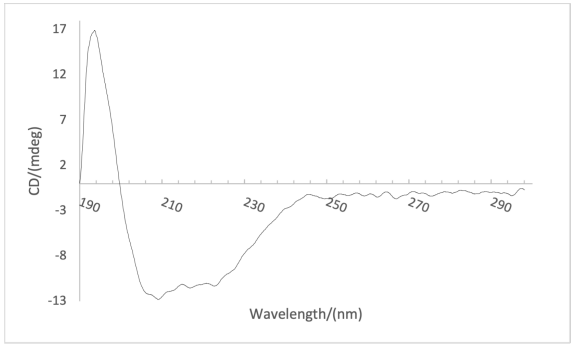
(t) 18BD-mod8 in LTA



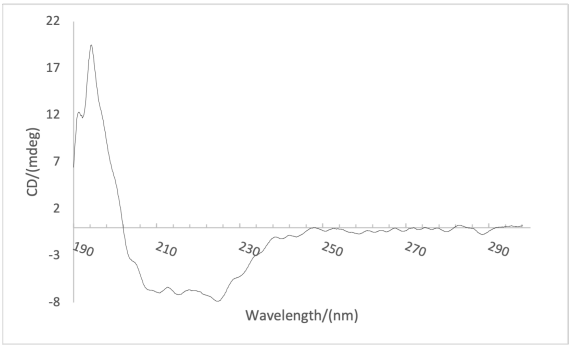
(u) 19HBD-mod8 in PBS



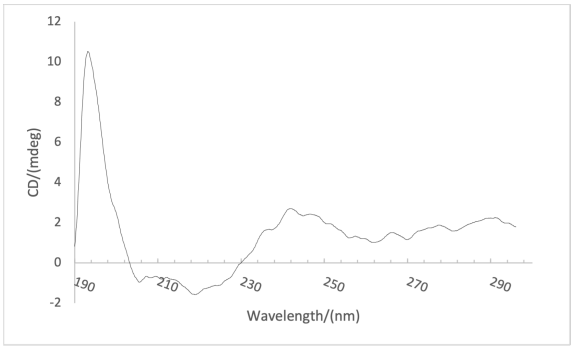
(v) 19HBD-mod8 in SDS



(w) 19HBD-mod8 in DPC



(x) 19HBD-mod8 in LPS

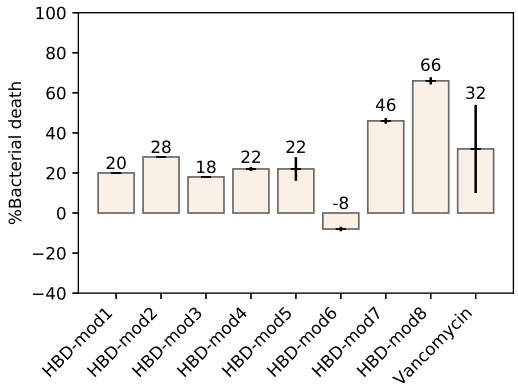


(y) 19BD-mod8 in LTA

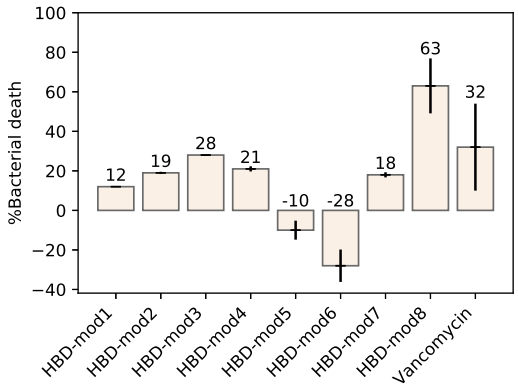
Figure B.7: Showing the secondary structure of peptides based on alanine scan of HBD-mod8 (15HBD-mod8-19HBD-mod8) produced from CD in PBS, SDS, LPS, LTA and DPC representing an anionic environments and mimicking bacterial membrane for Gram-negative and -positive bacteria respectively to show the helical conformational change. All graphs were produced from the instrument software by reading the absorbance of the peptide and they are shown in the y-axis and wavelength shown in x-axis.

Appendix Three

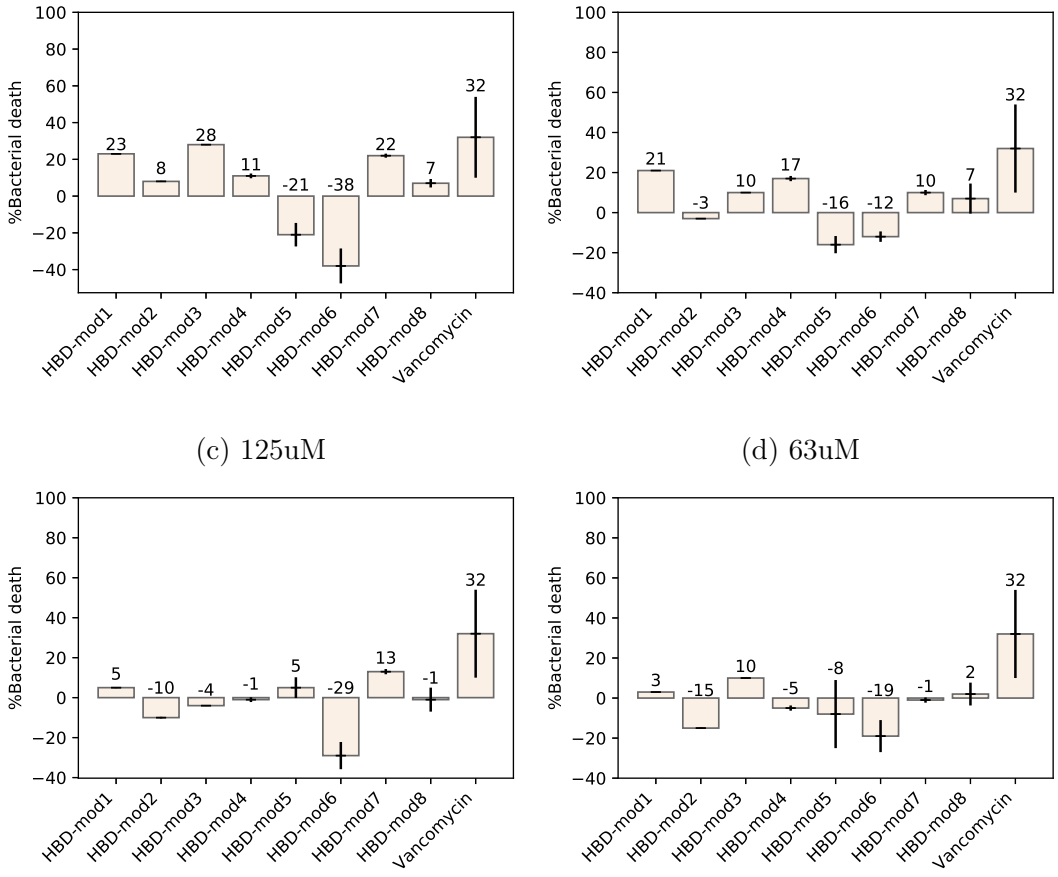
Biological Characterisation



(a) 500uM



(b) 250uM



(c) 125uM

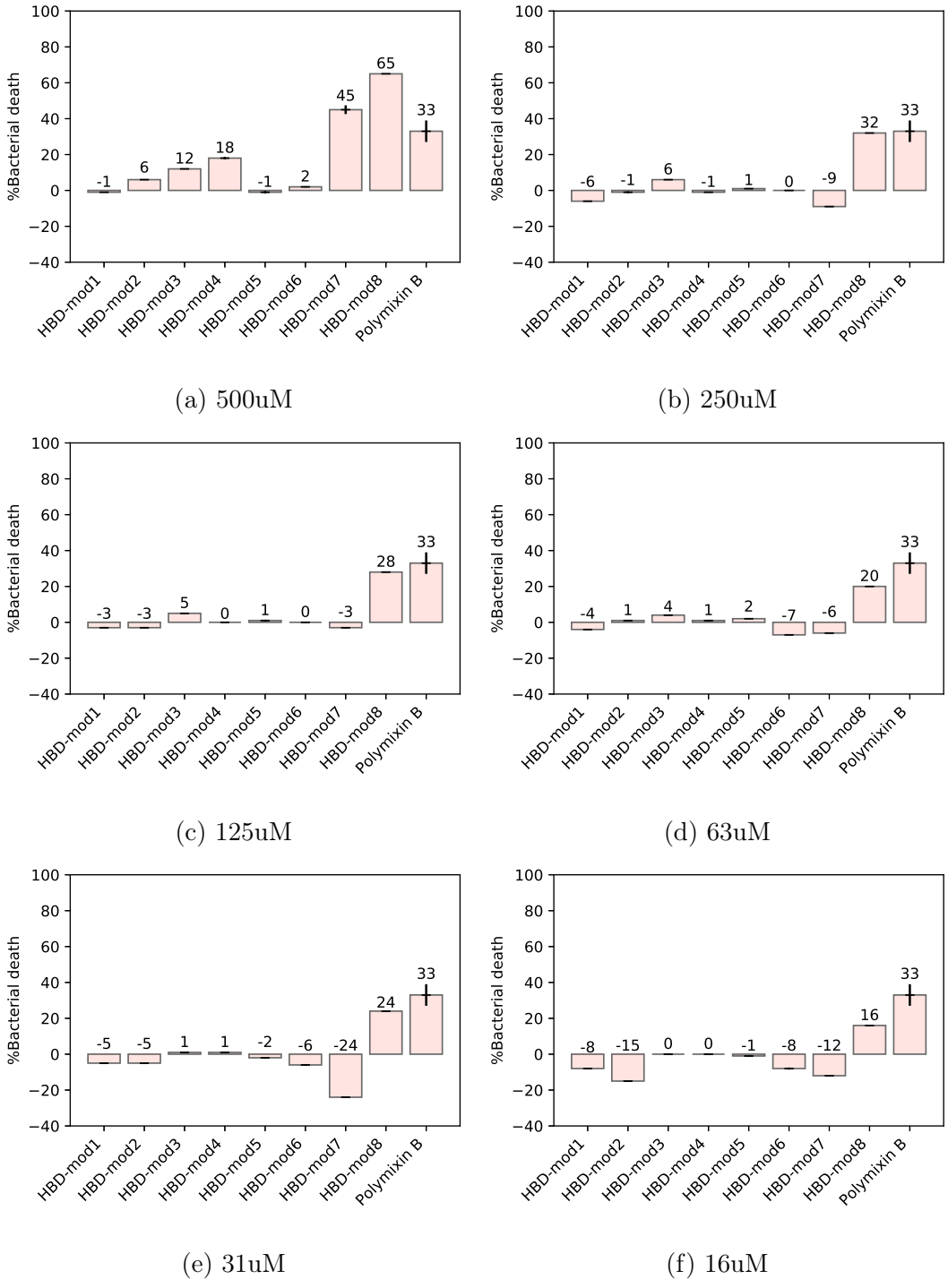
(d) 63uM

(e) 31uM

(f) 16uM

Figure C.1: The effect of peptides as well as their differing concentrations on *S. aureus* survival with its corresponding antibiotics (Vancomycin) as control. (a)-(f) shows the 2-fold dilutions of peptides based on hBD1. The overall mean %bacterial death values for each peptide was used to calculate the p-values are 32, 14, 4, 15, 11, -5, -22, 18 and 24 for antibiotic and HBD-mod1 to HBD-mod8, respectively. The p-value between HBD-mod1, HBD-mod2, HBD-mod3, HBD-mod4, HBD-mod5, HBD-mod6, HBD-mod7, HBD-mod8 and the control is 0.008, 0.000, 0.017, 0.000, 0.000, 0.000, 0.13* and 0.97* respectively. Figure (b): HBD-mod8 at concentration $250\mu M$ has better activity than the antibiotic with higher mean %bacterial death and p-value of 9.9×10^{-5}**.

* shows favourable non significant difference / ** shows favourable significant difference



(a) 500uM

(b) 250uM

(c) 125uM

(d) 63uM

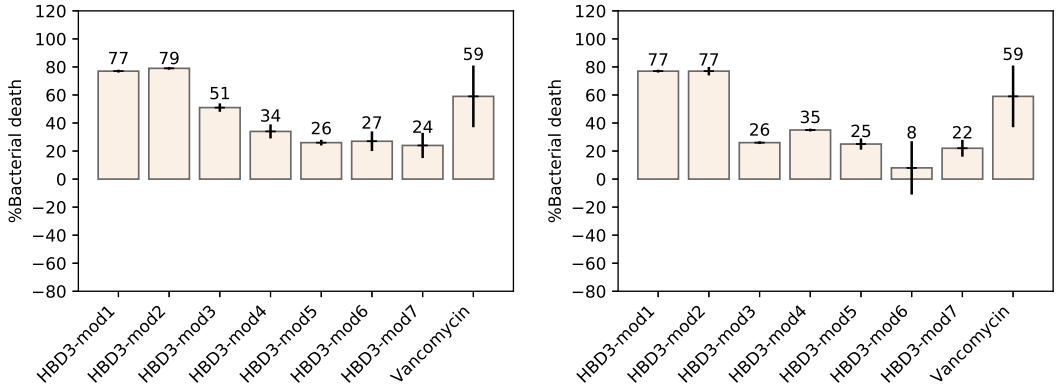
(e) 31uM

(f) 16uM

Figure C.2: The effect of peptides as well as their differing concentrations on *P. aeruginosa* survival with its corresponding antibiotics (Polymixin B) as control. (a)-(f) show the 2-fold dilutions of peptides based on hBD1.

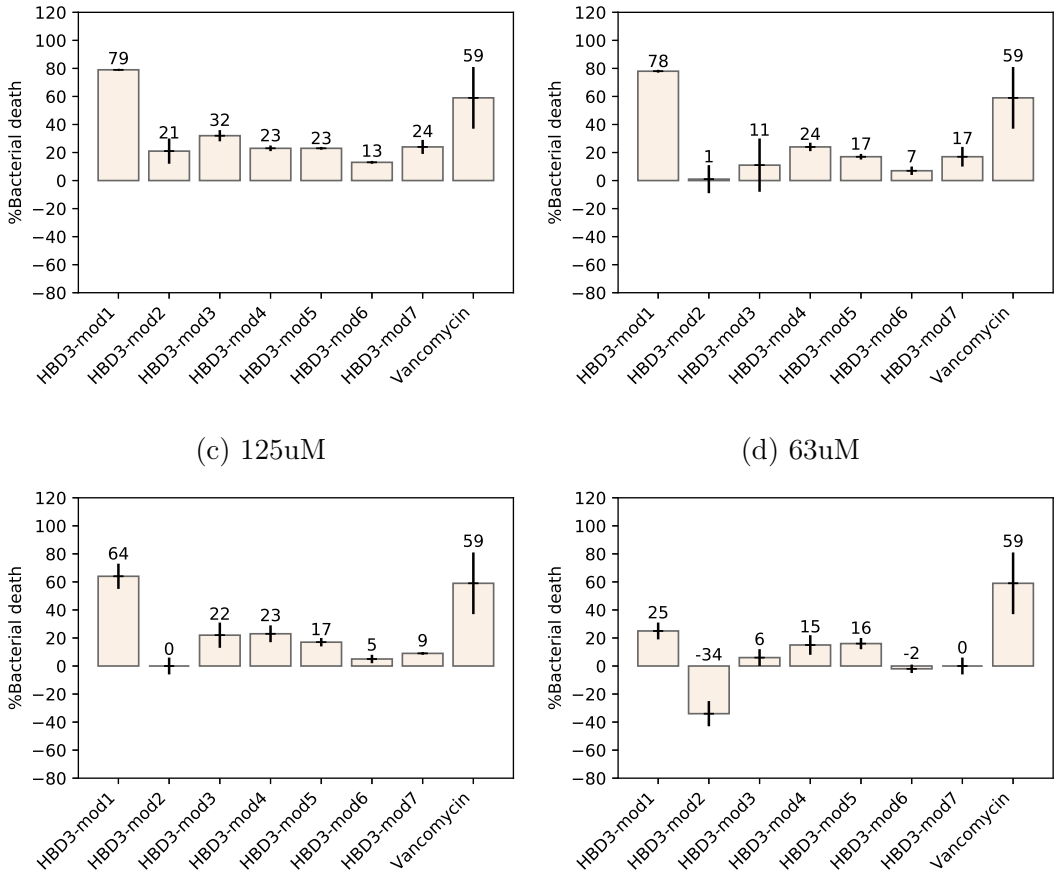
Figure C.2: The mean values for each peptide used to calculate are 33, -5, -3, 5, 3, 0, -3, -2 and 31 for Antibiotic and HBD-mod1 until HBD-mod8, respectively. The p-value between HBD-mod1, HBD-mod2, HBD-mod3, HBD-mod4, HBD-mod5, HBD-mod6, HBD-mod7 and the control is the same value of 1.0×10^{-13} and between HBD-mod8 and the control is the value 1.0*. Figure (a) shows that HBD-mo8 with p-value 7.5×10^{-5} ** shows a better activity than antibiotic and figure (b) shows HBD-mod8 has a similar activity to the antibiotic with p-value of 1.0*.

* shows favourable non significant difference / ** shows favourable significant difference



(a) 500uM

(b) 250uM



(c) 125uM

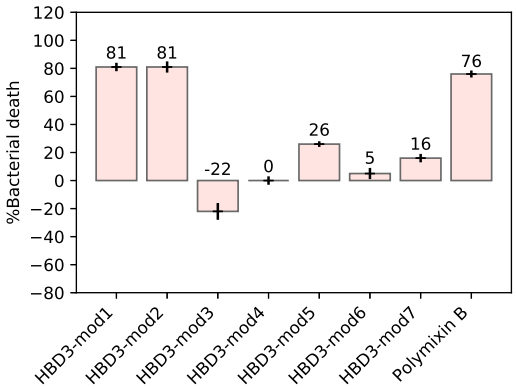
(d) 63uM

(e) 31uM

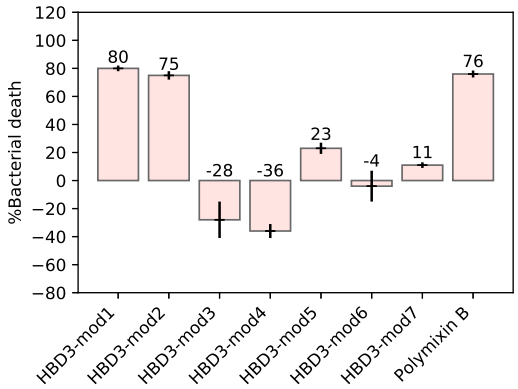
(f) 16uM

Figure C.3: The effect of peptides as well as their differing concentrations on *S. aureus* survival with its corresponding antibiotics (Vancomycin) as control. (a)-(f) show the 2-fold dilutions of peptides based on hBD3. The overall mean %bacterial death values for each peptide used to calculate the p-values are 59, 70, 24, 25, 26, 21, 3 and 16 for Antibiotic and HBD3-mod1 until HBD3-mod7, respectively. The p-value between HBD3-mod1 and the control was 0.06*, between HBD3-mod2, HBD3-mod3, HBD3-mod4, HBD3-mod5, HBD3-mod6, HBD3-mod7 and the control was, 1.2×10^{-13}. Figure (e) shows HBD3-mod1 no significant difference with p-value of 0.9* at $31\mu M$

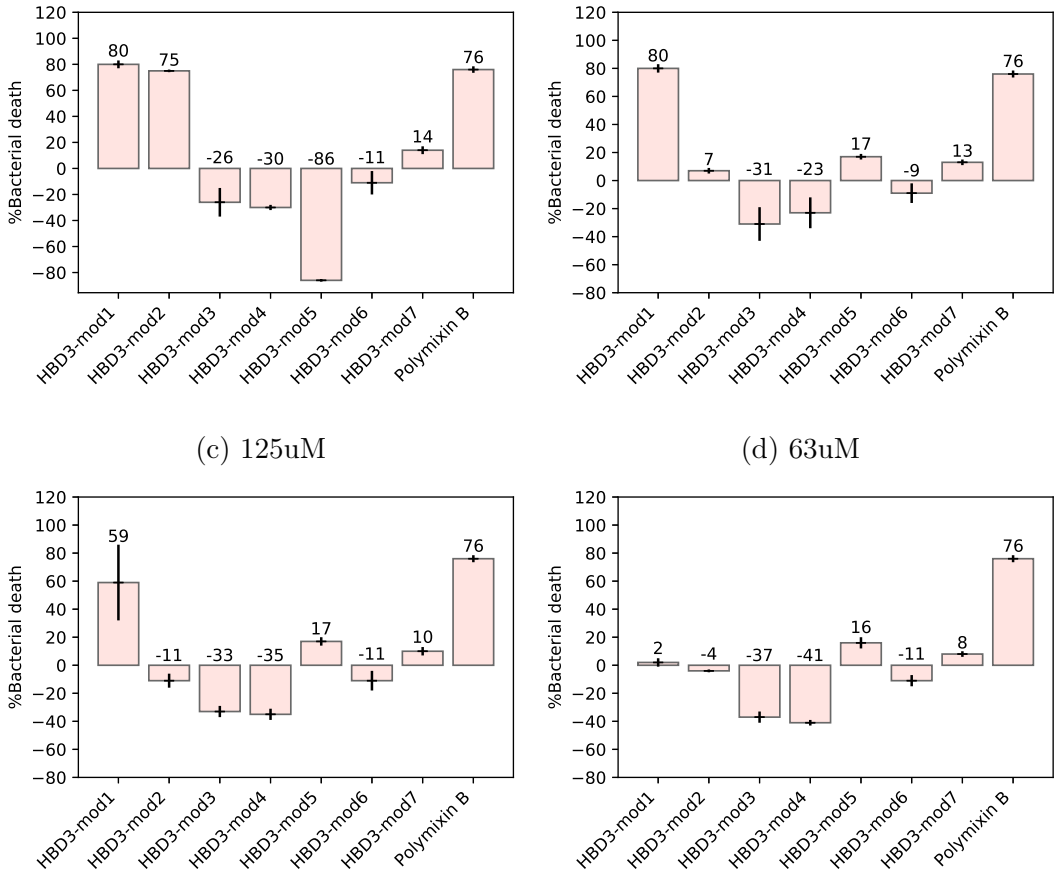
* shows favourable no significant difference.



(a) 500uM



(b) 250uM



(c) 125uM

(d) 63uM

(e) 31uM

(f) 16uM

Figure C.4: The effect of peptides as well as their concentrations on *P. aeruginosa* survival with its corresponding antibiotics (Polymixin B) as control. (a)-(f) shows the 2-fold dilutions of peptides based on hBD3. The mean values for each peptide used to calculate the p-value are 76, 63, 38, -29, -27, 21, -6, 12 for Antibiotic and HBD3-mod1 until HBD3-mod7, respectively. The p-value between HBD3-mod1 and the control is 0.02 and 1.2×10^{-13} between HBD3-mod2, HBD3-mod3, HBD3-mod4, HBD3-mod5, HBD3-mod6, HBD3-mod7 and the control. All values show a significant difference between their activity against *P. aeruginosa* and the peptides meaning none of the peptides show an overall activity similar to the antibiotic tested. Although the antibiotic is included in every graph it was only tested at its critical MIC found in the literature and was not tested at different concentration.

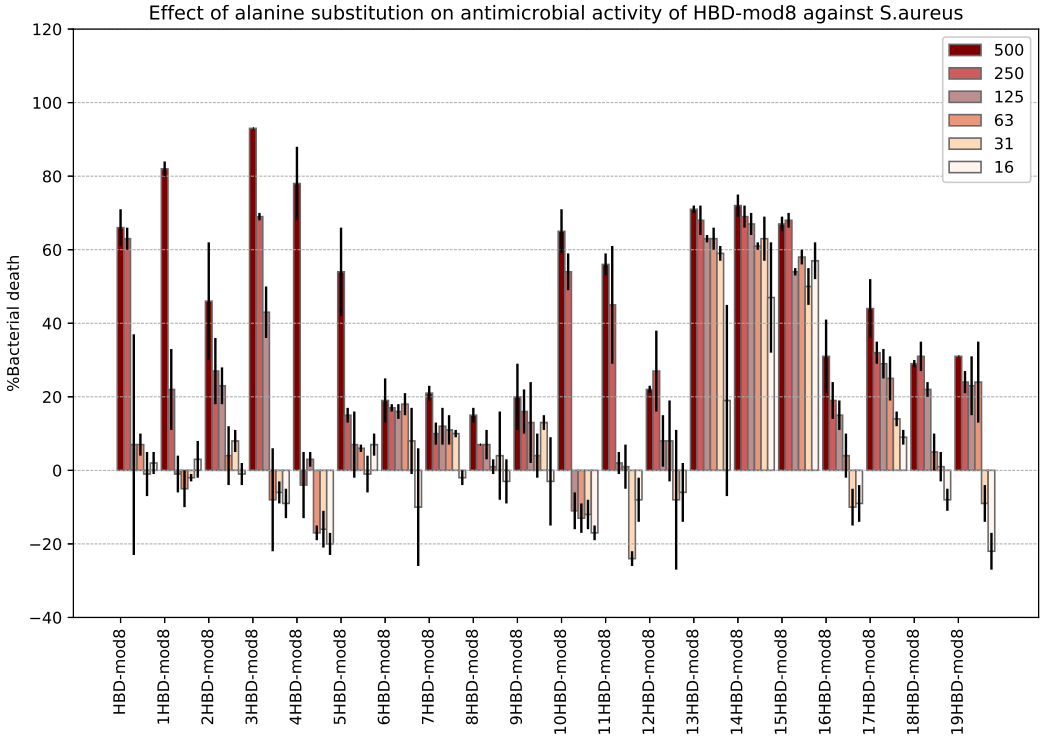


Figure C.5: The effect of alanine substitution on the activity of HBD-mod8 against *S. aureus* at all concentrations.

In this figure the effect of all different concentrations was shown on each substituted peptide and its projected activity on the bacteria. It can be seen that at lower concentrations most of the peptides in the series do not hold their activity. This is not the case with 13HBD-, 14HBD- and 15HBD-mod8 show higher level of activity in the lower concentrations when compared to the rest of the peptide in this series.

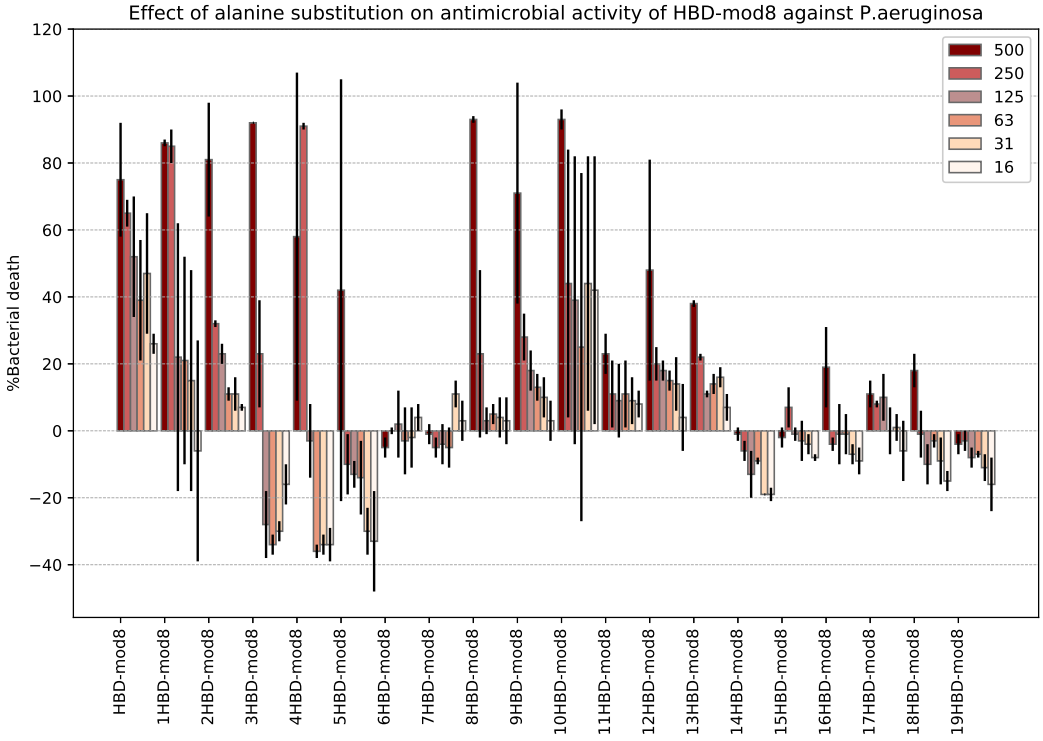


Figure C.6: The effect of alanine substitution on the activity of HBD-mod8 against *P. aeruginosa* at all concentrations.

In this figure the effect of all different concentrations was shown on each substituted peptide and its projected activity on the bacteria. According to this figure HBD-mod8 shows the best activity across the board and it stays active until the concentration of $63\mu M$. 10HBD-mod8 shows large standard deviation bars meaning each time this analysis was performed this peptide showed varying results.

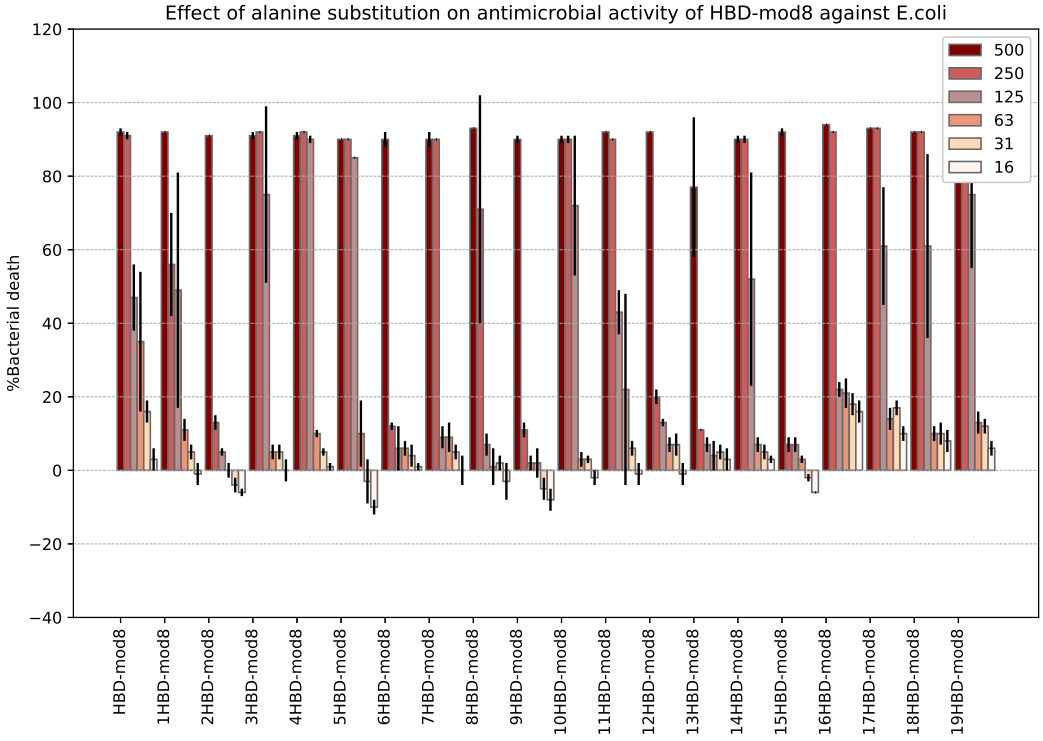


Figure C.7: The effect of alanine substitution on the activity of HBD-mod8 against *E. coli* at all concentrations.

In this figure the effect of all different concentrations was shown on each substituted peptide and its projected activity on the bacteria. The activity of the peptide across the whole series of substitutions is shown to have minimal effect on the activity against *E. coli* where they are mostly equally as active as HBD-mod8. With the expiation of 6HBD-mod that only shows a comparable activity at the highest concentration.

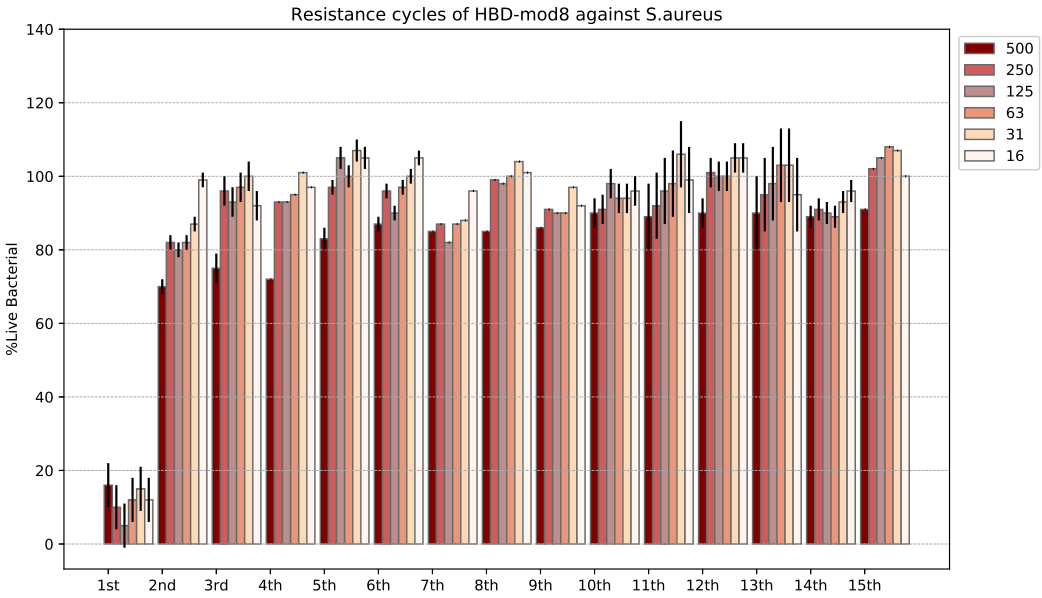


Figure C.8: The resistance pattern of *S. aureus* towards HBD-mod8 at all concentrations.

In this figure the pattern of bacterial resistance was shown for all peptide concentrations. It is evident that this bacteria build resistance towards the peptide immediately after the first cycle however the peptide is still able to remove the bacteria to a certain extent. Until cycle 15 in which the peptide stops being active against the bacteria showing 0% bacterial death at all the concentrations. It was also observed that this peptide works best at its highest concentration.

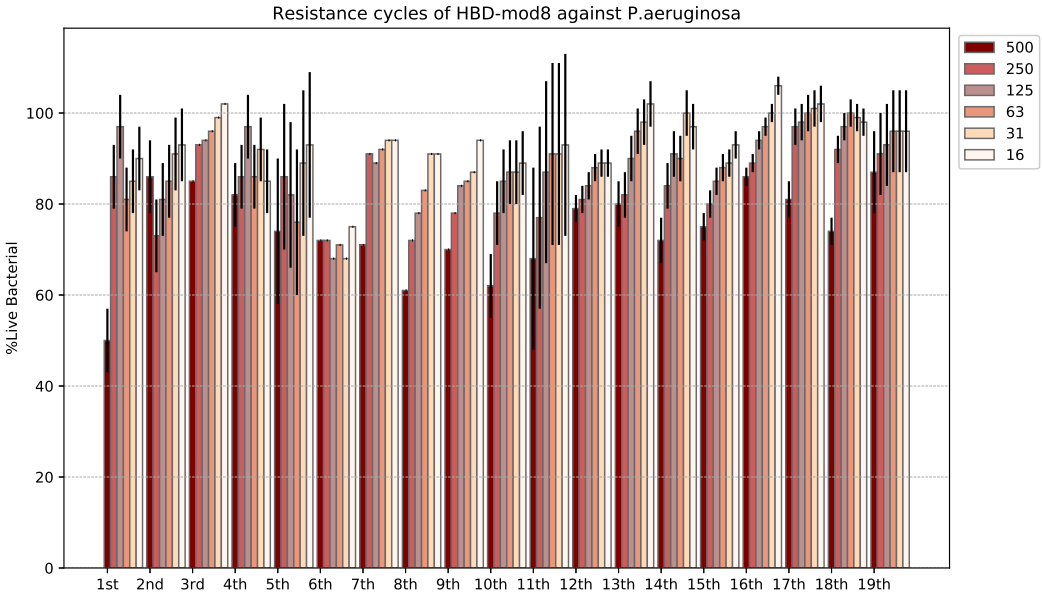


Figure C.9: The resistance pattern of *P. aeruginosa* towards HBD-mod8 at all concentrations.

In this figure the pattern of bacterial resistance was shown for all peptide concentrations. The resistance build up is more uniform with this bacteria showing a more cohesive pattern with a downward trend as the number of cycles increase across all concentrations.

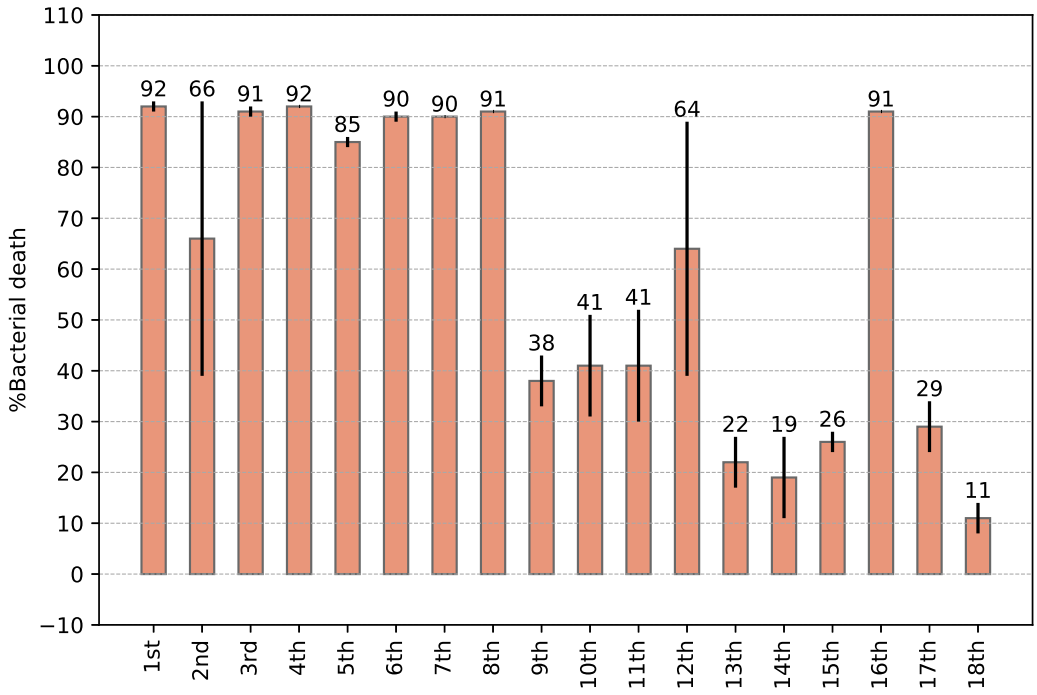


Figure C.10: The resistance pattern of *E. coli* towards HBD-mod8 at all concentrations.

In this figure the pattern of bacterial resistance was shown for all peptide concentrations. Even with the activity of this peptide against *E. coli* being notable the resistance cycles were not so clear in the trends they display. With the highest concentrations showing very little change in activity level as the resistance build up. The lower concentrations for this peptide show very poor activity against the resistance.

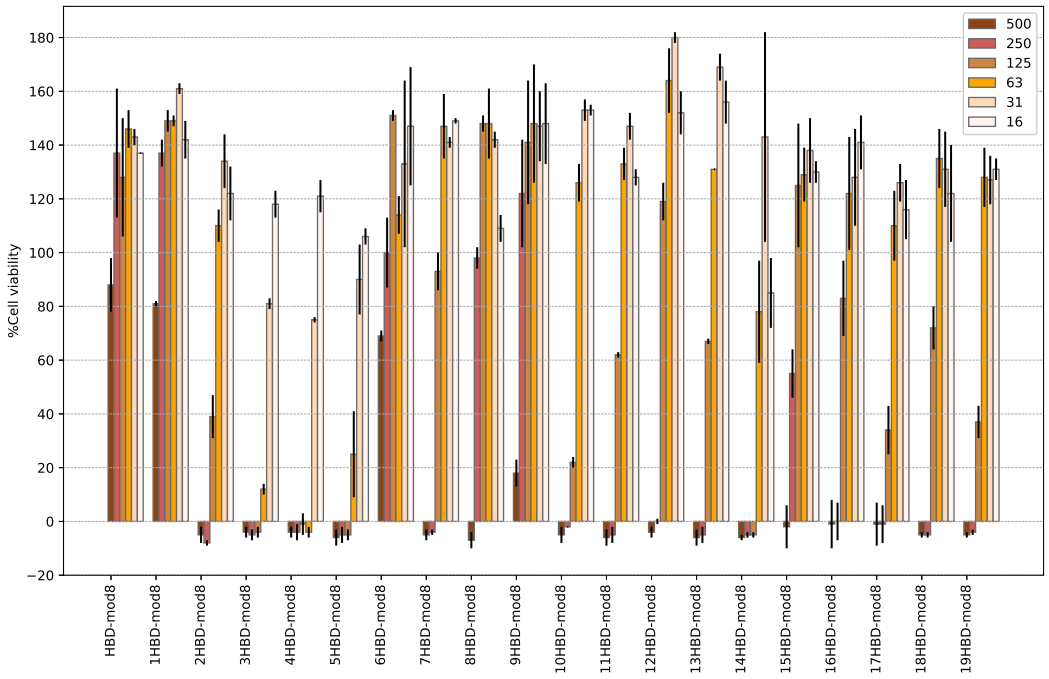


Figure C.11: Bar Chart displaying untouched cell viability data.